DEPARTMENT OF BIOLOGICAL SCIENCES

SELECTIVE ACTIVATION OF TNFR1 AND NF-KB INHIBITION BY A NOVEL BIYOUYANAGIN ANALOGUE PROMOTES APOPTOSIS IN ACUTE LEUKEMIA CELLS

DOCTOR OF PHILOSOPHY DISSERTATION

CHRISTIANA G. SAVVA

Christiana Savva

2016

DEPARTMENT OF BIOLOGICAL SCIENCES

SELECTIVE ACTIVATION OF TNFR1 AND NF-KB INHIBITION BY A NOVEL BIYOUYANAGIN ANALOGUE PROMOTES APOPTOSIS IN ACUTE LEUKEMIA CELLS

CHRISTIANA G. SAVVA

A Dissertation Submitted to the University of Cyprus in Partial Fulfillment of the Requirements for the Degree of Doctor of Philosophy

May 2016

Christiana Savva

Christiana Savva

©CHRISTIANA G. SAVVA, 2016

VALIDATION PAGE

Doctoral Candidate: *Christiana G. Savva*

Doctoral Thesis Title: *Selective activation of TNFR1 and NF-κB inhibition by a novel biyouyanagin analogue promotes apoptosis in acute leukemia cells.*

The present Doctoral Dissertation was submitted in partial fulfillment of the requirements for the Degree of Doctor of Philosophy at the ***Department of Biological Sciences*** *and was approved on the 9th of May by the members of the* ***Examination Committee****.*

Examination Committee:

Research Supervisor: *Andreas Constantinou, Professor, UCY*

[Name, position and signature]

Committee Member: *Vasilis Promponas, Assistant Professor, UCY*

[Name, position and signature]

Committee Member: *Christos Tsatsanis, Professor, UOC*

[Name, position and signature]

Committee Member: *Kyriakos Fellekis, Associate Professor, UNIC*

[Name, position and signature]

Committee Member: *Chrysoula Pitsouli, Assistant Professor, UCY*

[Name, position and signature]

Christiana Savva

DECLARATION OF DOCTORAL CANDIDATE

The present doctoral dissertation was submitted in partial fulfillment of the requirements for the degree of Doctor of Philosophy of the University of Cyprus. It is a product of original work of my own, unless otherwise mentioned through references, notes, or any other statements.

Christiana G. Savva

[Full Name of Doctoral Candidate]

[Signature]

Christiana Savva

Abstract

KC-53 is a novel biyouyanagin analogue with anti-inflammatory and anti-viral activity. Here, we examined the anti-proliferative effects of KC-53 in 13 representative human cancer cell lines, in normal peripheral blood mononuclear cells (PBMCs) and in immortalized cells. With detailed molecular probing we unraveled its molecular mode of action in the two most sensitive cell lines; HL-60 and CCRF/CEM. The novel agent promoted rapidly and irreversibly apoptosis in both leukemic cell lines at relatively low concentrations (with an IC_{50} of ~2.3 μM). Apoptosis was characterized by an increase in membrane-associated TNFR1, activation of Caspase-8 and proteolytic inactivation of the death domain kinase RIP1 indicating that the KC-53 induced mainly the extrinsic/death receptor apoptotic pathway. Induction of the intrinsic/mitochondrial pathway was also achieved by Caspase-8 processing of Bid, activation of Caspase-9 and increased translocation of AIF to the nucleus. FADD protein knockdown restored HL-60 and CCRF/CEM cell viability and completely blocked KC-53-induced apoptosis. These data advocate the close correlation between the FADD/Caspase-8/RIP1 signaling axis and apoptotic effects of KC-53, which suggests being through activation of the TNFR1 death receptor initiated events. Furthermore, KC-53 administration dramatically inhibited TNFα-induced serine phosphorylation on TRAF2 and on IκBα, stabilizing the cytosolic IκBα-p65/NF-κB and hindering p65 translocation to the nucleus. Reduced transcriptional expression of pro-inflammatory and pro-survival target genes, confirmed that the agent functionally inhibited the transcriptional activity of p65. Our findings demonstrate, for the first time, the selective anticancer properties of KC-53 towards leukemic cell lines and provide a detailed understanding of the molecular events underlying its dual anti-proliferative and pro-apoptotic properties. These findings are likely to provide new insights into the development of innovative death receptor-targeted therapies for the treatment of acute leukemia.

Christiana Saiva

Περίληψη

Το KC-53 είναι ένα νεοσυντιθέμενο *biyouyanagin* ανάλογο μόριο με γνωστή ισχυρή αντιφλεγμονώδη και αντιική δράση. Στην παρούσα εργασία, διερευνήσαμε την αντιπολλαπλασιαστική του δράση σε 13 αντιπροσωπευτικές ανθρώπινες καρκινικές σειρές, σε μονοπύρηνα κύτταρα περιφερικού αίματος (PBMCs) καθώς επίσης και σε αθανατοποιημένα κύτταρα. Με τη χρήση αναλυτικών και ποσοτικών τεχνικών αποκαλύψαμε μεθοδικά το μοριακό μηχανισμό δράσης του στις δύο λευχαιμικές σειρές, HL-60 (APL) και CCRF/CEM (ALL), οι οποίες παρουσίασαν τη μεγαλύτερη ευαισθησία στη δράση του μορίου. Η ουσία KC-53 προκάλεσε άμεσα και μη αναστρέψιμα επαγωγή της απόπτωσης και στις δυο κυτταρικές σειρές σε σχετικά χαμηλές συγκεντρώσεις (με IC_{50} ~2.3 μM). Η απόπτωση χαρακτηρίστηκε από αύξηση των μεμβρανικών επιπέδων του υποδοχέα του παράγοντα νέκρωσης όγκων, TNFR1, ενεργοποίηση της κασπάσης 8 και πρωτεολυτική απενεργοποίηση της κινάσης RIP1 υποδηλώνοντας ότι, το KC-53 επάγει την ενεργοποίηση του εξωγενούς μονοπατιού της απόπτωσης. Επιπροσθέτως, το KC-53 προκάλεσε την επαγωγή του ενδογενούς μονοπατιού της απόπτωσης μέσα από την ενεργοποίηση της κυτταροπλασματικής πρωτεΐνης Bid, της κασπάσης 9 και της μετατόπισης του παράγοντα επαγωγής της απόπτωσης, AIF από το κυτταρόπλασμα προς τον πυρήνα. Η καταστολή της έκφρασης του πρωτεϊνικού μορίου FADD στις σειρές HL-60 και CCRF/CEM, προκάλεσε την ανθεκτικότητα των σειρών έναντι της αντιπολλαπλασιαστικής δράσης του KC-53 και ανέστειλε πλήρως την αποπτωτική του δράση. Επιπροσθέτως, η χορήγηση του KC-53 παρεμπόδισε τη δράση του παράγοντα νέκρωσης όγκων, TNFα καταστέλλοντας συγκεκριμένα τη φωσφορυλίωση της πρωτεΐνης, TRAF2 και του αναστολέα του μεταγραφικού παράγοντα NF-κB, IκBα. Σαν αποτέλεσμα, ο NF-κB παραμένει προσδεδεμένος με τον αναστολέα του στο κυτταρόπλασμα και αδυνατεί να μετακινηθεί εντός του πυρήνα. Αυτό υποστηρίζεται και από την παρατηρούμενη μείωση των επιπέδων έκφρασης διαφόρων γονιδίων στόχων του NF-κB μετά από χορήγηση του KC-53. Συγκεντρωτικά, τα πειραματικά μας δεδομένα, παρουσιάζουν για πρώτη φορά, τις αντικαρκινικές ιδιότητες του KC-53 μορίου και παρέχουν λεπτομερή περιγραφή του μοριακού μηχανισμού δράση του. Τα δεδομένα αυτά θα μπορούσαν μελλοντικά να χρησιμοποιηθούν στο σχεδιασμό νέων στοχευμένων θεραπειών για την καταπολέμηση συγκεκριμένων μορφών λευχαιμίας.

Christiana Savva

Acknowledgements

As it is the case for any significant accomplishment, it would be impossible for me to complete this thesis without the contribution of several excessive people.

First and foremost, I would like to thank my supervisor Dr. Andres I. Constantinou who not only initiated my scientific carrier but, was the person from whom I learned the importance of scientific, clear and rational thinking. I greatly appreciate the opportunity he gave me to work in his lab, the inspirational academic freedom he allowed me to have and for constantly sharing his long experience from research. I am deeply grateful for his assistance and patience during all these years.

I own my deepest gratitude to Dr. Kyriakos C. Nicolaou, from RICE University for providing us the KC-53 compound making this thesis possible. For the great collaboration we had and significant co-authorship assistance. I would also like to thank Dr. Sotirios Totokotsopoulos for the compound synthesis and the willingness to answer my questions.

I wish to express my warm and sincere appreciation to my family and friends, for allowing me to study so long, for being proud of me and for all the generous support, love and trust. I cannot thank them enough for all the things they have done for me but I hope I can repay soon.

Last but not least, I would especially like to pay my gratitude to; Dr. Christiana Neophytou for the important contribution on my paper's writing and reviewing, Dr. Paris Scouridis and Dr. Ioanna Antoniade, for providing invaluable assistance and help regarding immunefluorescence experiments, and Dr. Christiana Charalambous, Dr. Panos Papageorgis, Dr. Katia Nicolaou, Dr. Chara Pitta, Dr. Elena Odiatou and Christina Dimitriadou for their daily support and for creating an enjoyable working environment.

Christiana Savva

“The real meaning of enlightenment is to gaze with undimmed eyes of all darkness”

N. Kazantzakis

To my family and

honored friend who lost fight with cancer

Christiana Savva

Table of Contents

Christiana Savva

Christiana Savva

Christiana Savva

List of Figures

Christiana Savva

Christiana Savva

List of Supplementary Figures

Christiana Savva

List of Tables

Christiana Savva

List of Abbreviations

ABL: Abelson murine leukemia viral oncogene homolog
AEL: acute erythroid leukemia
AIF: apoptosis-inducing factor
ALL: acute lymphoblastic leukemia
AMKL: acute megakaryoblastic leukemia
AML: acute myelogenous leukemia
AMMoL: acute myelomonocytic leukemia
AMoL: acute monocytic leukemia
Apaf-1: apoptosis protease activating factor-1
APL: acute promyelocytic leukemia
Ara-C: cytarabine
ATO: arsenic trioxide
ATRA: all-trans retinoic acid
B-ALL: acute B-lymphoblastic leukemia
BCP: B-cell progenitor
BCR: breakpoint cluster region
BH: Bcl-2 homology domain
BIRC: baculoviral IAP repeat containing
BM: bone marrow
CAD: Caspase-activated DNase
CARD: caspase activation and recruitment domain
CD: caspase-dependent
CDKN2A/B: cyclin-dependent kinase inhibitor 2A/B
CD-PCD: caspase-dependent programmed cell death
CEBRA: CCAAT/enhancer binding protein
c-FLIP: cellular-FLICE (FADD-like IL-1β-converting enzyme)-inhibitory protein
CID: caspase-independent
CID-PCD: caspase-independent programmed cell death
CLL: chronic lymphocytic leukemia
CLP: common lymphoid progenitor
CML: chronic myeloid leukemia
CMP: common myeloid progenitor
CPT: circularly permuted TRAIL
CPT1a: carnitine palmitoyl transferase 1a
CR: complete remission
CSC: cancer stem cell
CYLD: cylindromatosis
DCF: 2,7-dichlorodihydrofluorescein
DCFH-DA: 2,7-dichlorodihydrofluorescin
DcR: decoy receptor
DD: death domain
DED: death effector domain
DISC: death-inducing signaling complex
DNMT: DNA methyltransferase
Dox: doxorubicin
DR: death receptor
DUB: deubiquitinases
EBF1: early B-cell factor 1
EndoG: endonuclease G

Christiana Salva

ETO (MTG8): myeloid translocation gene
Eto: etoposide
ETV6: DNA-binding kinase TEL1
FAB: French-American-British cooperative group
FADD: Fas-associated DD
FDA: Food and Drug Administration
FLT3: fms-like tyrosine kinase-3
GATA1: GATA binding protein 1 (globin transcription factor 1)
GMP: granulocyte-monocyte progenitor
H_2O_2: hydrogen peroxide
HBA: hydrogen bond acceptors
HBD: hydrogen bond donors
HDAC: histone deacetylase
HDACI: histone deacetylase inhibitor
HIV: human immunodeficiency virus
HMT: histone methyltransferase
HSCs: hematopoietic stem cells
HSP: heat shock protein
IAP: inhibitor of apoptosis protein
IKK: inhibitor of NF-κB kinase
IKZF1: IKAROS zing finger 1 transcription factor
IL: interleukin
IL-1R: interleukin 1 receptor
ITD: internal tandem duplication
IκB: inhibitor of NF-κB
JAK: Janus kinases
JNK: c-Jun N-terminal kinases
LCMV: lymphocytic choriomeningitis virus
LEF: lymphoid enhancer-binding factor
LLS: Leukemia and Lymphoma Society
LogP: octanol water partition coefficient
LPS: lipopolisaccharides
LSC: leukemic stem cell
MAPK: mitogen-activated protein kinase
MDP: monocyte-dendritic cell progenitor
MEP: megakaryocyte–erythroid progenitor
MIS: mitochondrial intermembrane space
MKL1: megakaryocytic leukemia 1
MLL: myeloid/lymphoid or mixed-lineage leukemia
MOMP: mitochondrial outer membrane permeabilization
MP: 6-mercaptopurine
MTD: maximal tolerated dose
MTT: 3-(4,5-dimethylthiazol-2-yl)-2,5-diphenyltetrazolium bromide
MTX: methotrexate
MW: molecular weight
NEMO: NF-κB essential modulator
NF-κB: nuclear factor kappa B
NGF: neuronal growth factor
NK: natural killer cells
NLS: nuclear localization signal
NPM: nucleophosmin
OS: overall survival
OTT/RBM: RNA-binding motif

Christiana Savva

PAR: poly(ADP-ribose)
PARP-1: poly-ADPribose polymerase-1
PBMCs: peripheral blood mononuclear cells
PCD: programmed cell death
Ph: philadelphia chromosome
PI: propidium iodide
PLZF: promyelocyte leukemia zinc finger
PML: promyelocytic leukemia
poly-ub: polyubiquitin
PPAPs: poly-prenylated-acyl-phloroglucinols
PSA: topological polar surface area
PT: permeability transition
PTEN: phosphatase and tensin homolog gene
RA: retinoic acid
RARE: RA response elements
RARα: retinoic acid receptor α
RB1: Retinoblastoma 1
RHD: REL homology domain
rhTNFα: recombinant human TNF-α
RIP1: receptor interacting protein-1
ROS: reactive oxygen species
RT: room temperature
RUNX: runt-related transcription factor
SAR: structure-activity relationships
Ser: serine
SNP: single nucleotide polymorphism
SP: sodium pyruvate
STAT: signal transducers and activators of transcription
sTNF: soluble TNF
t: translocation
TAB2/3: TAK1 binding protein-2/3
TACE: TNF-α-converting enzyme
TAD: transcriptional activation domain
TAK1: transforming growth factor-activated kinase-1
T-ALL: acute T-cell leukemia
tBid: truncated Bid
TCF3: transcription factor 3
TICAM1: toll-like receptor adaptor molecule 1
TLR4: toll-like receptor 4
TNFR1: tumor necrosis factor receptor-1
TNFRSF: TNFR superfamily
TNF-α: tumor necrosis factor-α
TNK: T-cell and NK-cell progenitor
TRADD: TNF receptor-associated DD
TRAF2/5: TNF receptor associated factor-2/5
TRAIL: TNF-related apoptosis-inducing ligand
WHO: World Health Organization

Christiana Sava

Chapter I: Introduction

Leukemia

Almost twenty years have passed since the cancer stem cell (CSC) model of carcinogenesis was engrafted for first time in immune-deficient mice (Bonnet and Dick, 1997). Nowadays, the stemness of cancer cells tends to become the seventh hallmark of cancer (Hanahan and Weinberg, 2011). The model was demonstrated by *Bonnet D.* and *Dick J.E.* in xenotransplanted blood and bone marrow (BM) samples from patients with acute leukemia. According to this model, a unique clonal and mutated leukemic stem cell (LSC) population was sufficient enough to promote leukemic cells expansion. This model was based on the eminent association of hematopoiesis to the pathogenesis of hematological malignances (Bonnet and Dick, 1997).

Hematopoiesis is one of the main vital process of our body that take place in BM. It is a tightly regulated and highly hierarchical process that balances self-renewal, differentiation, dormancy and proliferation of the progenitor cells. Hematopoiesis, begins with non-differentiated hematopoietic stem cells (HSCs) with self-renewal capacity and finishes with the highly-differentiated cells with no self-renewal and limited proliferative capacity (Weissman et al., 2001, Goldsby et al., 2002). The daughter cells of HSCs, the common myeloid (CMP) and lymphoid (CLP) progenitor cells, are committed to any of the alternative differentiation pathways giving rise to all blood cells (Figure 1) (Mansson et al., 2007). The mature hematopoietic cells are divided into three main lineages, erythrocytes/megakaryocytes, lymphocytes and myelocytes (Goldsby et al., 2002).

Erythroid cells are the oxygen carrying red blood cells and compromise a homogenous entity. Lymphocytes are the cornerstone of the adaptive immune response deriving from CLP. The lymphoid lineage is primarily composed of T-cells and B-cells (white blood cells) and by Natural Killer cells (NK) and dendritic cells. Myelocytes are heterogeneous comprising many cell subsets. All cell types derive from CMP giving rise to the key players of innate immunity (intrinsic or natural immunity) which include granulocytes (basophil, neutrophil, eosinophil) and

Christiana Savva

monocytes. The latter, have the ability to further differentiate into macrophages and dendritic cells in peripheral tissues in response to inflammation signals.

Hematopoiesis regulation involves cellular and environmental cues, including the activity of transcription factors, signaling cascades, and non-coding RNAs. Deregulation of hematopoiesis due to mutations in the regulating genes can result in hematological disorders characterized by impaired differentiation and/or increased proliferation (Rieger and Schroeder, 2012). Leukemia is the most commonly diagnosed hematological malignancy characterized by abnormal

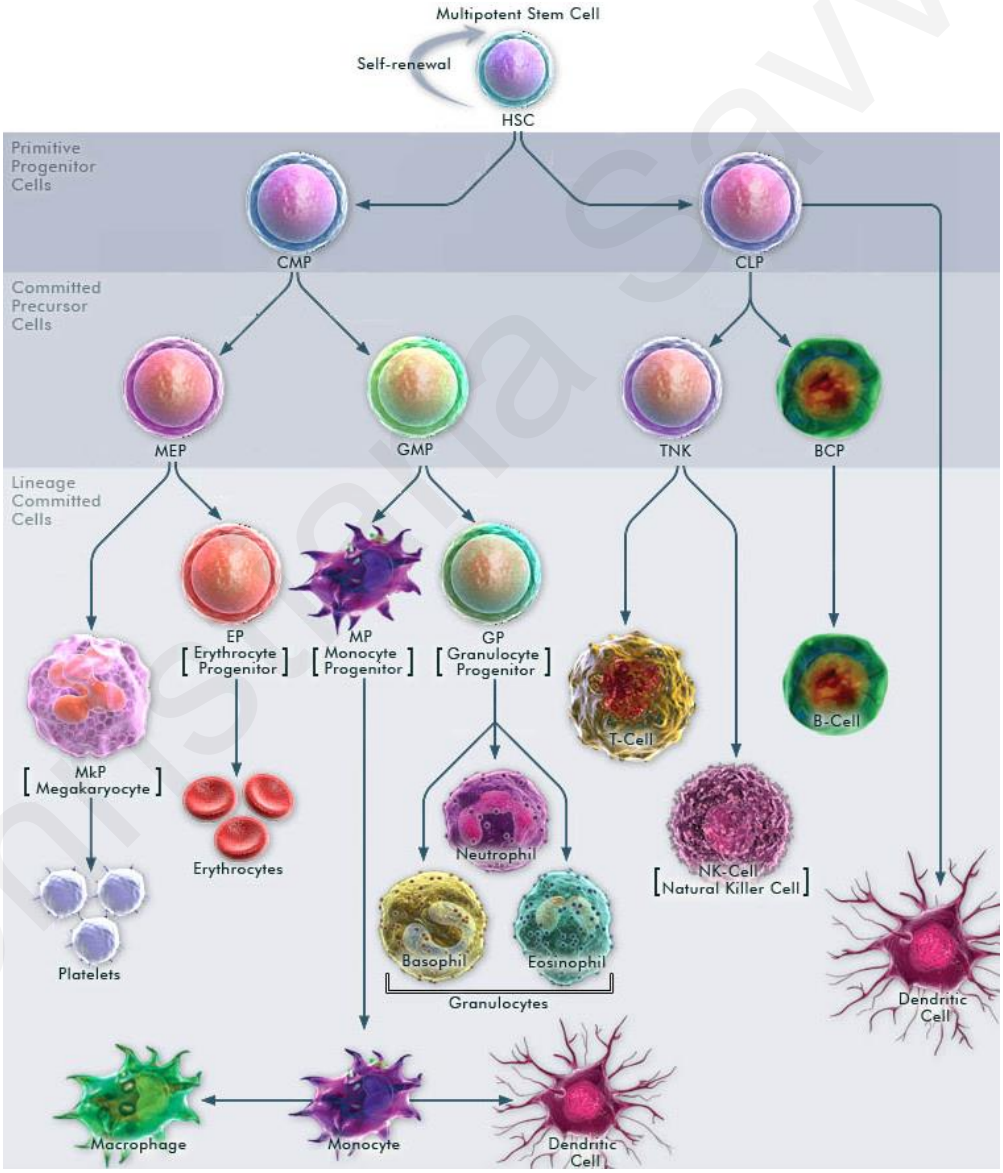

Figure 1. The multiple lineages of human hematopoiesis. HSC, hematopoietic stem cell; CMP, common myeloid progenitor; CLP, common lymphoid progenitor; MEP, megakaryocyte–erythroid progenitor; GMP, granulocyte-monocyte progenitor; TNK, T-cell and Natural Killer cell progenitor; BCP, B-cell progenitor. Modified from *eBioscience.com*.

Christina Savva

neoplastic proliferation of the cells of the immune system. It is consider as a complex group of diseases where the abnormal cells accumulate in the BM, blood and/or lymphatic tissue interfering with the production and functioning of red cells, white cells and platelets. The malignant cells may be HSCs that have become leukemic by accumulating mutations or progenitors that have reacquired the stem cell capability for self-renewal (Ketley et al., 2000, Pui et al., 2008, Riether et al., 2015). Leukemia is a heterogeneous disease in terms of phenotype, prognosis, progression, and response to therapy. The general mechanisms underlying leukemic transformation are starting to be well understood. The abnormal cells can spread to other parts of the body, including the skin, spleen, liver, brain, and spinal cord (Creutzig, 1996, Pui et al., 2008). Progressively the disease can lead to severe anemia, bleeding, an impaired ability to fight infections, or death (Creutzig, 1996, Pui et al., 2008, Coombs et al., 2015).

There are four main types of leukemia: *acute lymphoblastic leukemia (ALL)*, *acute myelogenous leukemia (AML)*, *chronic lymphocytic leukemia (CLL)*, and *chronic myeloid leukemia (CML).* In 2014 it was estimated that approximately 52,380 people were going to be diagnosed with leukemia. Of these, 36% was account to AML and 12% to ALL. The remaining 48% was account for other types of leukemia and lymphoma (data adapted from American Cancer Society; Cancer Facts 2014). Among adults, the most common diagnosed types are CLL (36%) and AML (32%). The reverse is true in children were, ALL accounts for the majority of leukemias. Approximately, three out of four childhood leukemias are ALL and the remaining cases are AML (Hunger et al., 2012, Asselin et al., 2013). ALL occurs most frequently in people under the age of 15 or over the age of 45 while the incidence of AML gradually increases with age and peaks at the age >80 years. ALL it is much more common in white children than among African-American and Asian-American children, and it is more common in boys than in girls. AML occur almost equally in both sexes of all races (data retrieved from Leukemia and Lymphoma Society; Facts 2014-2015).

Despite the fact that the overall survival rate of the patients with leukemia has dramatically increased the past decade, there is a need to discover more effective and specific therapeutic agents. The remarkable improvement in leukemia treatment is largely the result of chemotherapy. Research has led to the growing

Christiana Sawa

understanding of the many subtypes of leukemias and necessity to introduce different therapeutic approaches based on the subtype. The short- or long-term side-effects caused by conventional therapies impose the discovery of new targeted drugs for the complete cure and remission of childhood leukemia.

Acute Myelogenous Leukemia

Acute myeloid leukemia is also called acute myelogenous leukemia, acute myeloblastic leukemia, acute granulocytic leukemia or acute non-lymphocytic leukemia. Is a diverse disease characterized by clonal expansion and/or differentiation of malignant cells arising from genetically altered LSCs or progenitor cells that form granulocytes and monocytes (Jabbour et al., 2006, Estey, 2012). These genetic aberrations lead to excessive proliferation, defective differentiation and resistance to apoptosis of leukemic cells (Ketley et al., 2000). AML is usually found in the BM and blood, but it can also spread to other parts of the body, including the brain and skin (Creutzig, 1996). Occasionally, leukemia cells can form solid tumor named myeloid sarcoma (Byrd et al., 1996).

As a heterogeneous disease, AML might involve one or more differentiation paths and several stages of maturation resulting in many subtypes of the disease. Over the years, two main classification for AML have been defined. The earliest was designed by a French-American-British cooperative group (FAB) (Bennett et al., 1985) and the later by World Health Organization (WHO) (Vardiman et al., 2009). Based on the FAB system classification, AML is classified in eight subtypes, M0 through M7 (Bennett et al., 1976, Jabbour et al., 2006). Development of leukemia is analogous to normal hematopoiesis and leukemic cells can often be described based on their corresponding cell type in normal hematopoiesis (Figure 2).

FAB classes were defined based on the maturation stage and differentiation path of the malignant cells without taking into account chromosomal or sub-chromosomal abnormalities (Bennett et al., 1976). Thus, FAB classification only recognizes the morphologic heterogeneity of AML without reflecting the genetic or clinical diversity of the disease (Hassan et al., 1993). Researches continuous efforts uncovered that many cases of AML were associated with recurring genetic abnormalities that affect cellular pathways of myeloid maturation and proliferation.

Christiana Savva

In order to accommodate the body of new research, the WHO introduced a new classification of tumors of hematopoietic and lymphoid tissues (Sabattini et al., 2010). This classification was designed to include all currently available information, including morphology, cytochemistry, immunophenotype, genetics, and clinical features (Vardiman et al., 2009, Vardiman, 2010).

According to WHO classification AML was divided in four main categories; AML with recurrent genetic abnormalities, AML with multilineage dysplasia, AML with myelodysplastic syndromes and AML not otherwise characterize that is divided in nineteen sub-categories. Table 1 shows in comparison the AML classification based on FAB and WHO system. Nowadays, the extensive use of microarrays, proteomics and next-generation sequencing, allows to scientists to identify undifferentiated acute leukemias or acute leukemia entities expressing simultaneously several antigens (van Dongen, 1995, Casasnovas et al., 2003, Cui et al., 2004).

Table 1. AML classification based on FAB and WHO system

Type	FAB classification	WHO classification
M0	AML minimally differentiated	AML minimally differentiated
M1	AML with minimal maturation	Acute myeloblastic leukemia t(8;21)(q22,q22)
M2	AML with maturation	Acute myeloblastic leukemia t(6;9)
M3	Acute promyelocytic leukemia (APL)	Acute promyelocytic leukemia t(15;17)
M4	Acute myelomonocytic leukemia (AMMoL)	• Acute myelomonocytic leukemia • Myelomonocytic leukemia with bone marrow eosinophilia (M4eo)
M5	Acute monocytic leukemia (AMoL)	• Acute monoblastic leukemia (M5a) • Acute monocytic leukemia (M5b)
M6	Acute erythroid leukemia (AEL)	Acute erythroid leukemias, including • Erythroleukemia (M6a) • Very rare pure erythroid leukemia (M6b)
M7	Acute megakaryoblastic leukemia (AMKL)	Acute megakaryoblastic leukemia
M8	-	Acute basophilic leukemia

Christiana Sawa

Acute Promyelocytic Leukemia

Acute promyelocytic leukemia is the second most frequently diagnosed subtype of AML compromising a distinct entity. Historically, this type of leukemia was considered to be one of the most aggressive forms of leukemia with rapidly fatal progression and high incidence of early hemorrhagic death (Coombs et al., 2015). The APL phenotype is maintained by an increased proliferation of the promyelocytes (see Figure 2), as a result of the concomitant (i) inhibition of differentiation hindering progenitors to reach the post-proliferative stage and subsequently undergo apoptosis and (ii) by an aberrantly activated self-renewal capacity (Fenaux et al., 1997).

What makes APL unique among other types of leukemia is the chromosomal translocation t(15;17) that is consider a specific cytogenetic marker for APL diagnosis (Puccetti and Ruthardt, 2004). The translocation leads to the formation of the *PML* (promyelocytic leukemia gene)-*RARα* (retinoic acid receptor α gene), leading to the formation of *PML-RARα* oncoprotein (Cantu-Rajnoldi et al., 1994). The functional PML is a growth suppressor protein that regulates cell cycle progression and induces programmed cell death. The RARα is a nuclear receptor which can also act as a transcription factor of genes that are important for the differentiation of immature promyelocyte. The RARα protein binds to specific regions of DNA and recruits various repressive proteins suppressing gene expression. In response to specific signals, the repressive proteins are removed and other proteins that induce gene transcription bind to the RARα promoting gene transcription leading to cell differentiation (Pandolfi, 2001).

The activity of *PML-RARα* was thoroughly investigated by numerous research groups in both *in vitro* and *in vivo* models (Grignani et al., 1993, Grisolano et al., 1997). This chimeric transcription factor binds to the RA response elements (RARE) recruiting histone deacetylase (HDAC) and DNA methyltransferases (DNMT) to the promoter regions of target gene through a co-repressor mechanism (Lin et al., 1998, He et al., 1998, Carbone et al., 2006, Villa et al., 2006). The presence of RA causes allosteric modification in the *PML/RARα*, leading to the disassociation of co-repressors and the recruitment of co-activators (Pandolfi, 2001). This results, in the transcriptional activation of genes controlling

Christiana Savva

differentiation and growth arrest. In hematopoietic cell lines this leads to the blockage of apoptosis and to increased differentiation in response to retinoic acid (RA) (Grignani et al., 1993).

Various data have shown that, upon RA administration, *PML-RARα* transgenic mice show a variable percentage of promyelocytes that respond to RA-induced differentiation (Grisolano et al., 1997, He et al., 1997). These data were surprising because based on the RARα protein rearrangement, in APL, one would have expected that RA will not be functional. This paradox was of importance as APL was the first leukemia in which therapies like all-trans retinoic acid (ATRA) and arsenic trioxide (ATO), target the underlying molecular lesion promote the induction of differentiation and apoptosis with promising clinical application (Sun, 1993, Park, 2012). The advent of ATRA therapy has transformed APL from being a disease with a poor outlook to one of with most prognostically advantageous subset of AML.

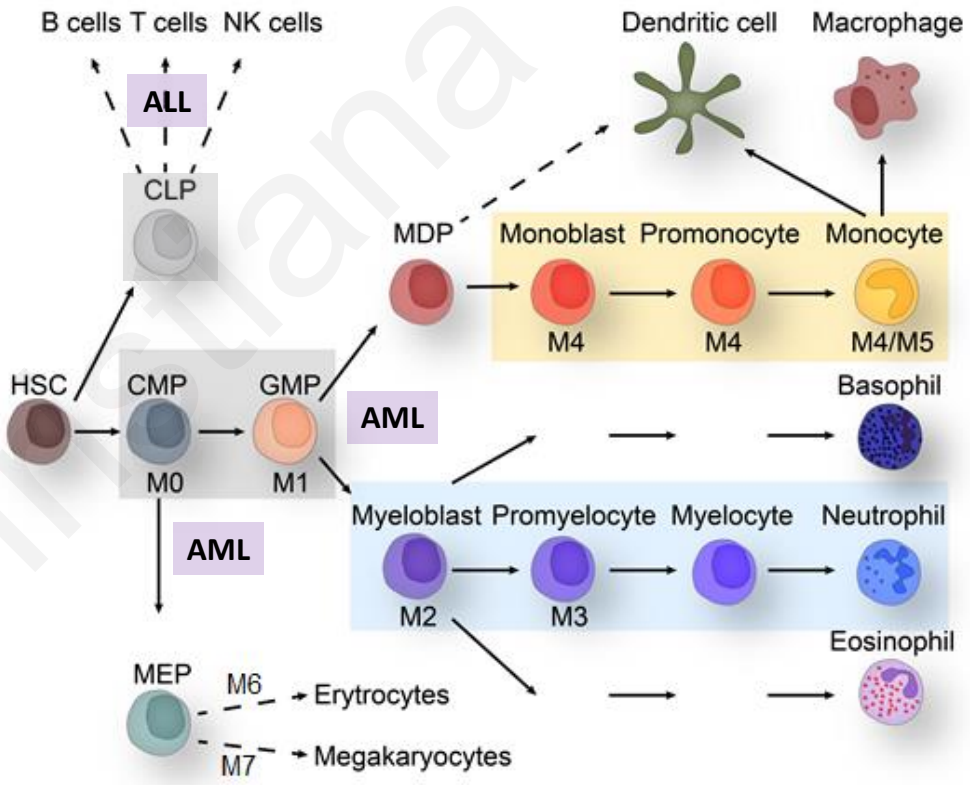

Figure 2. Schematic illustration of human hematopoiesis and the developmental stages of AML and ALL. Grey squares show progenitor cells without established differentiation. Blue and yellow squares indicate granulocytic and monocytic differentiation, respectively. HSC, hematopoietic stem cell; CMP, common myeloid progenitor; CLP, common lymphoid progenitor; GMP, granulocyte-monocyte progenitor; MEP, megakaryocyte-erythroid progenitor; MDP, monocyte-dendritic cell progenitor.

Christiana Savva

Other cytogenetics alterations that may be found in APL are the translocations t(11;17)(q23;21) which juxtaposes promyelocyte leukemia zinc finger gene, *PLZF* to *RARα* (*PLZF-RARα*) (Jansen and Lowenberg, 2001), the t(5;17) variant that fuses the genes for nucleophosmin, *NPM* and the *RARα* (*NPM-PARα*) (Hummel et al., 2002), or sporadic translocations that affect the *RARα* locus (Hummel et al., 2002, Puccetti and Ruthardt, 2004). The biological activities of these fusion proteins have not been completely elucidated.

Acute Lymphoblastic Leukemia

Acute lymphoblastic leukemia, also called acute lymphocytic leukemia or acute lymphoid leukemia, is a blood cancer that results when abnormal white blood cells accumulate in the BM (Pui et al., 2008). It originates from progenitor cells that are committed to differentiate in the T-cell or B-cell pathway by mutations that impair the capacity for unlimited self-renewal leading to precise stage developmental arrest (Pui et al., 2008) (Figure 2). The cells implicated in ALL commonly have rearrangements in their immunoglobulin genes and express differentiation-linked cell-surface glycoproteins that largely found in immature lymphoid progenitor cells within the early developmental stages of normal T and B lymphocytes (Pui et al., 2008). ALL progresses rapidly, replacing healthy cells that produce functional lymphocytes with malignant cells (Pieters and Carroll, 2010, Advani, 2013).

Table 2. ALL classification based on WHO system

Type
Acute B-lymphoblastic leukemia (B-ALL) • Acute precusor B-cell leukemia • Pre B-cell lymphoblastic leukemia
Acute T-cell leukemia (T-ALL) • Pre-T cell leukemia • T-cell ALL
Burkitt's lymphoma

ALL, as AML, is classified according to the maturation of the leukemic and by the type of lymphocyte (Amaki, 1982, Khalidi et al., 1999). Prior to 2008, subtyping of ALL was based on FAB classification in which, ALL was classified as: ALL-L1, ALL-L2 and ALL-L3 (Bennett et al., 1976). In 2008, the WHO divided ALL into three distinct categories based on the surface markers and recurrent genetic abnormalities of the atypical lymphocytes: Acute B lymphoblastic leukemia, Acute T cell leukemia and Burkitt's lymphoma (Vardiman et al., 2009, Harris et al., 1999, Jaffe et al., 1999) (Table 2). The two main ALL subtypes, B lymphoblastic and T-

Christiana Savva

cell, were earlier found within ALL-L1 and -L2 of the FAB classification (Bennett et al., 1976). Most people with ALL have the B-cell type and especially, precursor B-cell. An additional form of ALL is a unique biphenotypic leukemia in which the blasts have features of both myeloid and lymphoid cells or of both B and T lineages (Mikulic et al., 2008).

Pathogenesis

For most types of leukemia, as for most types of solid tumors, the precise pathogenetic molecular events are still unknown. Only a few cases are associated with inherited genetic syndromes such as Down syndrome (Pastorczak et al., 2011, Buitenkamp et al., 2014), or with excess exposure to ionizing radiation (Wakeford et al., 2010) or to specific chemotherapeutic drugs like alkylating agents (Davies, 2001) and topoisomerase II inhibitors (Ross, 1998) (therapy-related leukemia). During the past years, several models have been proposed regarding the origin of leukemia cells and the hierarchical nature of the disease has been generally established (Greaves, 2006, Roboz and Guzman, 2009, Huang and Zhu, 2012). The common axis in these models is that, LCSs cells must first regain their stem cell capability before becoming tumorigenic. Once this has been accomplished, the LSCs or progenitor cells can be further transformed by accumulating genetic and epigenetic alterations (secondary or cooperating mutations). These alterations impair the normal function of specific genes resulting in the loss of programmed cell death and differentiation ultimately leading to the progression of fully malignant diseases (Figure 3).

The constant and retrospective identification of leukemia-specific fused genes, mono- or hyper-diploids or rearrangements in the genome, established chromosomal abnormalities as a hallmark of leukemia pathogenesis (Machnicki and Bloomfield, 1990, Robinson, 2001, Cervera et al., 2010). Apart from chromosomal deviations, the molecular detection of gene mutations plays an increasingly important role in the classification, risk stratification, and management of leukemias (Mullighan, 2012, Hatzimichael et al., 2013, Wang et al., 2015). The following paragraphs describe the main cytogenetics and molecular genetics abnormalities found in ALL and AML leukemias.

Christiana Sawa

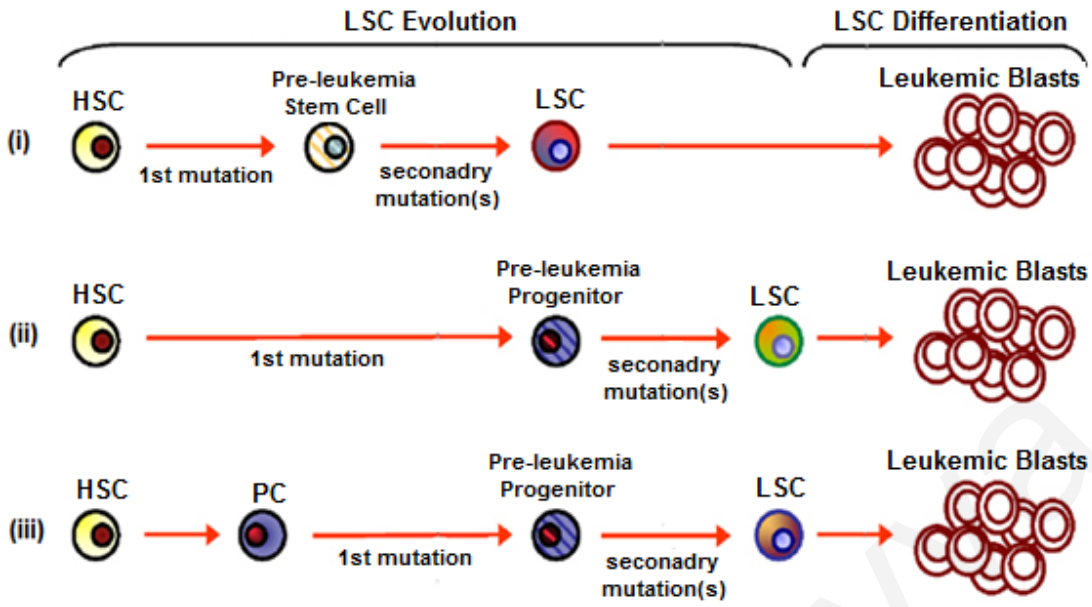

Figure 3. Possible models of leukemogenesis. Despite the extremely heterogeneous nature of AML and less complex nature of ALL, the various subtypes seem to share common pathways leading to leukemogenesis. Both HSCs and progenitors cells (PC) are susceptible to genetic alterations that regulate self-renewal and differentiation. Precursor cells with a single mutation are called "pre-leukemic". Upon secondary mutation(s) or epigenetic alterations precursor cells give rise to LSCs which gain the ability to differentiate generating leukemias. Modified by (Jordan and Guzman, 2004).

Cytogenetics

Chromosomal translocations (t) usually activate genes that are responsible for the expression of transcription factors (Tamai and Inokuchi, 2015). These transcription factors can exert negative or positive effects leading to aberrant expression of single gene products or unique fusion proteins (Pui et al., 2008, Tamai and Inokuchi, 2015). The leukemia-related fusion proteins function as aberrantly activated signaling mechanisms that directly interfere with the hematopoietic differentiation program (Zhu and Emerson, 2002). The t(8;21), is among the commonest rearrangements found in AML (Downing et al., 2000). This translocation involves the *RUNX1* (Runt-related transcription factor 1, also known as *AML1*) on chromosome 21 and the *ETO* (or MTG8; myeloid translocation) ononcogene on chromosome 8 generating an *RUNX1-ETO* (formerly *AML1-ETO*) fusion transcription factor (Miyoshi et al., 1991, Tighe et al., 1993). The fusion protein *RUNX1-ETO* has been shown to directly up-regulate the expression of *Bcl-2* pro-apoptotic gene by binding to its promoter elements (Klampfer et al., 1996).

Christiana Savva

Less common translocations in AML include the 11q23/*MLL* (myeloid/lymphoid or mixed-lineage leukemia) rearrangements, the t(1;22) and the t(15;17) that generates the *PML-RARA* fusion protein. Chromosomal rearrangements involving the MLL gene are associated with aggressive AML and ALL in infants and therapy-related leukemia (Sachdev et al., 2015). The gene encodes a histone methyltransferase (HMT) and up to now, more than 100 different 11q23 rearrangements have been reported and more than 60 MLL fusion partners genes have been cloned (Zangrando et al., 2009). The t(1;22) translocation results in the fusion of the *OTT* (or *RBM15*; RNA-binding motif protein 15) on chromosome 1 and *MKL1* (megakaryocytic leukemia 1, also known as *MAL*) on chromosome 22 (Bernard et al., 2009). The *OTT-MAL* fusion gene was predicted to play important role in chromosomal organization, Hox-induced differentiation, and Ras signaling (Hsiao et al., 2005). This translocation is associated closely, if not exclusively, with AMKL and has been detected in up to one third of such childhood cases and occasionally in adult AML (Hsiao et al., 2005, Ravid, 2009).

Chromosomal abnormalities, like monosomies 5 and 7 or 5q deletions, are present in only approximately 2% to 4% of AML casesin adults (Matsumoto et al., 2009, Wawrzyniak et al., 2013). The deletions in 5q have been associated with *p53* tumor suppressor gene loss or mutations and with poor prognosis (Hattori et al., 2011, Sebaa et al., 2012). Genome-wide microarray studies have also identified novel sub-karyotypic abnormalities such is, the acquired uniparental disomy with high percentage rate (Gupta et al., 2008).

Similar to AML, many of the chromosomal abnormalities in ALL result in alteration of the function of transcription factors critical for normal hematopoiesis. The most frequent cytogenetic abnormalities diagnosed in ALL are the *ETV6-RUNX1* (formerly known as *TEL-AML1*) and the *BCR-ABL1* translocations (Mullighan et al., 2007, Mullighan, 2012). About 25% of cases of B-ALL, harbor the *ETV6-RUNX1* fusion gene generated by the t(12;21)(p13;q22) chromosomal translocation. This translocation leads to the formation of *ETV6-RUNX1* fusion protein with transcriptional activity. Specifically, the ETV6 (DNA-binding protein kinase TEL1) moiety of the chimeric protein converts RUNX1 from an activator to a repressor transcription factor (Fenrick et al., 1999). This lead to the expansion of

Christiana Savva

B-cell precursors with altered self-renewal capacity, enhanced survival properties and impaired differentiation stages (Fischer et al., 2005, Torrano et al., 2011).

The reciprocal translocation t(9;22)(q34;q11) is the most frequent chromosomal translocation identified in adult ALL. It links the *ABL1* (Abelson murine leukemia viral oncogene homolog 1) gene to a part of *BCR* (breakpoint cluster region) gene producing the Philadelphia chromosome (Ph) (Li et al., 2014). The *BCR-ABL1* fusion protein differs from the normal ABL1 in its preferential location in the cytoplasm and its constitutively elevated serine/threonine kinase activity and GTPase-activating tyrosine activity leading to aberrant cell differentiation, proliferation, and survival (Klein et al., 2004b, Lucas et al., 2010). Albeit, Ph translocation is most commonly associated with CML (Aliano et al., 2013, Li et al., 2014), it can also be found in ALL (Klein et al., 2004a, Nacheva et al., 2013) and sporadic in AML (Klein et al., 2004a, Tirado et al., 2010).

In approximately 80% of Ph^+-ALL the *IKZF1* (Ikaros zing finger 1 transcription factor) gene is deleted of the cases (Mullighan et al., 2008). Interestingly, there is a high-risk subgroup of Ph^--ALL that is characterized by *IKZF1* deletion and has a genetic profile similar to that of cases with Ph^+-ALL (Jia et al., 2014). *Mullighan et. al.,* in search of activated tyrosine kinase signaling in these subtypes of ALL, managed to identify activating alterations in the Janus kinases (JAK1, JAK2, and JAK3) in approximately 10% of high-risk Ph^--ALL cases (Mullighan et al., 2009). The expression of *BCR-ABL1* further results in the activation of multiple signal transduction pathways including the Ras-Raf-MAPK (mitogen activated protein kinase), leading to growth factor independent cellular proliferation (Piccaluga et al., 2007). It also enhances the survival of leukemic cells through the modulation of pro- and anti-apoptotic molecules (Piccaluga et al., 2007, An et al., 2010).

Molecular genetics

Currently, various somatic genetic abnormalities exert important roles in leukemogenesis, and also have important prognostic and therapeutic implications (Breit et al., 2006, Mullighan et al., 2007, Gutierrez et al., 2009, Mullighan et al., 2009). The excessive assessments of high-resolution analyses have led to the

Christiana Savva

detection of many novel genetic abnormalities (Mullighan et al., 2007, Toujani et al., 2009, Harvey et al., 2010, Fujiwara et al., 2014). The *CEBRA* (CCAAT/enhancer binding protein) and *GATA2* genes are the two most well-known genes found to be associated in leukemogenesis. Currently, these mutations have valuable diagnostic implications in the hereditary predisposition to AML and the related myelodysplastic syndromes (Godley, 2014). Mutations in the *CEBPA* gene are present in 7 - 10% of human patients with AML (Kirstetter et al., 2008). CEBPA is a key transcription factor regulating differentiation of several cell types, including myeloid precursors (Kirstetter et al., 2008, Ho et al., 2009). The end result of double or single allele mutations is that of a null phenotype or, loss of function (Kirstetter et al., 2008). Even so, no genetic models have been found explaining the etiological relevance of CEBPA with AML. *GATA1* gene is critical in regulating the differentiation of hematopoiesis, particularly for the erythroid and megakaryocyte lineages (Ferreira et al., 2005, Crispino, 2005). Although mutations leading to truncated forms of GATA1 are not sufficient by themselves in causing leukemia, they have been established as a first genetic hit in the development of AML and particular AMKL (Crispino, 2005)

In many leukemias activating mutations of several cytokine receptors have been shown to result in altered signal transduction, increased cell proliferation and chemoresistance (Kojima et al., 2010, Singh et al., 2011). The fms-like tyrosine kinase-3 (FLT3) is expressed in a large majority of ALLs, including 94% of B-lineage and 32% of T-lineage ALL. The FLT3-internal tandem duplication (*FLT3-ITD*) leads to constitutive receptor activation (Choudhary et al., 2005). *FLT3-ITD* is found in the 20% of young adult and over 35% of older AML patients (Meshinchi et al., 2006). Both, co-expression and activating, mutations on the *FLT3* gene can constitutively activate downstream targets, including STAT (signal transducers and activators of transcription) (Mizuki et al., 2000) and Src non-receptor tyrosine kinases (Robinson et al., 2005) that regulate proliferation, differentiation, and survival. Small GTPases have also been found to be abnormally expressed in AML. *N-Ras* has been reported to be mutated in approximately 10% of children and up to 30% of adults with AML (Shih et al., 2008). These activating mutations most frequently involve single-base changes resulting in inhibition of GTPase activity.

Christiana Savva

Commonly detect mutations are also found in genes relating to cell survival and self-renewal molecular pathways including Notch signalling. Activating mutations that encompass *Notch1* are widely expressed in T-ALL (Ferrando, 2009) through mechanism that remain unclear. Experimental data obtained by *in vivo* studies suggest that the c-Myc oncoprotein is an important downstream mediator of the pro-growth effects of Notch signalling in thymocytes development (Sharma et al., 2006, Weng et al., 2006, Herranz et al., 2014). The association of *Notch1* gain-of-function mutations in more than 50% of T-ALL with sustained c-Myc levels has led to functional screening for Notch1 inhibitors (Weng et al., 2004).

Using SNPs arrays and other genome-wide platforms many novel genomic alterations have recently been identified. An example is the biallelic deletion or epigenetic silencing of the *CDKN2A* whose inactivation neutralizes p53 pathway in many cases of T- and B-ALL (Krieger et al., 2010). In pediatric ALL, deletions amplifications, point mutations, and other structural rearrangements have similarly been reported. These genes mainly encode regulators of B-lymphocyte development with *Pax5* gene somatic mutations having the higher frequency (Mullighan et al., 2007). Deletions were also detected in other developmental genes, such as T*CF3* (Transcription factor 3), *EBF1* (Early B-cell factor 1), *LEF1* (Lymphoid enhancer-binding factor 1), *PTEN* (phosphatase and tensin homolog gene) and, *RB1* (Retinoblastoma 1) (Mullighan et al., 2007).

Hypermethylation of densely clustered cytosines (CpG islands) within the promoter region of silenced gene have been also identified in acute leukemias (Wouters et al., 2007). Few of the many examples include hypermethylation of the *CEBPA* gene, the tumor suppressor gene *FHIT* (fragile histidine triad) (Zheng et al., 2004), and cell-cycle regulatory genes, *p73*, *p15*, and *p57* (Bueso-Ramos et al., 2005). These altered CpG methylation profiles seem to be associated with distinct subsets of adult AML (Marcucci et al., 2014). Presently, scientists are also focusing on microRNAs in an attempt to identify specific microRNA signatures associated with leukemia development, relapse and therapy (Velu et al., 2014, Sanghvi et al., 2014, Sakamoto, 2014, Pan et al., 2014, Nemes et al., 2015). Much attention is also given in xenobiotic metabolism and DNA repair pathways (Reikvam et al., 2015). Although the number of investigations and sample sizes are limited, data exist to support, among others, a possible causal role for

Christiana Savva

polymorphisms in genes encoding carnitine palmitoyl transferase 1a (CPT1a) (Ricciardi et al., 2015), cytochrome P450 (Su et al., 2015), glutathione S-transferases (Das et al., 2009, Kassogue et al., 2014), XRCCs and XPD DNA repair enzymes (Sorour et al., 2013, Dincer et al., 2015).

Treatment and therapy

A common chemotherapy treatment for acute leukemias begins with induction (remission induction) followed by consolidation (post-remission) chemotherapy. Induction therapy involves treatment with a combination of drugs in order to eliminate the number of blasts in the blood and BM. Consolidation therapy is used to destroy any remaining malignant cells through either, additional chemotherapies or, stem cell transplantation (SCT).

Cytarabine (Ara-C), a cytosine nucleoside analogue in combination with anthracyclines, doxorubicin (Dox) and daunorubicin has been an important part of AML treatment for many decades (Seval and Ozcan, 2015). Even after 40 years, no other therapy has replaced this combination, as it offers a 64 % complete remission (CR) rate (Hamadani and Awan, 2010, Dohner et al., 2010). Dose escalation (Pabst et al., 2012, Larson et al., 2012, Jin et al., 2015) and combinatorial studies of Ara-C with other chemotherapeutic agents like idarubicin, aclarubicin, and methotrexate (MTX) (Larson et al., 2012, Holowiecki et al., 2012, Zhang et al., 2015) have been accomplished demonstrating significant improvement of CR and overall survival (OS) but with extensive hematological side effects. Allogeneic SCT is preferred for patients with adverse risk factors for relapse (Suciu et al., 2003, Shimoni and Nagler, 2005, Meijer and Cornelissen, 2008).

As previously stated, targeted chemotherapy is exclusive by applied in APL. Current standard induction therapy for APL is the vitamin A derivative all-trans retinoic acid (ATRA) in combination with anthracycline and/or cytarabine followed by consolidation and maintenance therapy with ATRA and MTX plus 6-mercaptopurine (MP) (Avvisati et al., 2011). Clinical trials show CR rates of 90 – 95% and ten years OS of up to 80% (Ades et al., 2010, Avvisati et al., 2011). Nonetheless, APL remains associated with a significant incidence of early death

Christiana Savva

caused primarily by severe bleeding. Early death, rather than resistant disease has emerged as the major cause of treatment failure (Coombs et al., 2015).

Multidrug chemotherapy regimens including cyclophosphamide, Ara-C, vincristine, anthracyclines, steroids, asparaginase, MTX and MP are cornerstones in pediatric ALL therapy since the 80s. A different treatment regimen, named “HyperCVAD”, composed of hyperfractionated cyclophosphamide, vincristine, Dox and dexamethasone is typically used in adults, resulting in 40% long-term survival (Kantarjian et al., 2004). Remarkably, recent studies indicate a better outcome among adolescents and young adults when treated on pediatric protocols instead of adult protocols (Dombret et al., 2014). These studies have changed the current ALL treatment in adults, excluding older patients who are treated with less intense regimens. Allogeneic SCT is used only for ALL patients with high risk of relapse.

In the recent future, the most promising treatment approaches for leukemia will be targeted molecular therapies similar to that of ARA. Investigations are focusing in the discovery of small inhibitory molecules of kinases FLT3 (Li et al., 2012, Ma et al., 2014) and mTOR (Chiarini et al., 2012, Daver et al., 2015), CDK inhibitors (Baumer et al., 2014), heat shock protein (HSP) antagonists (Walker et al., 2013), inhibitors of γ-secretase (Okuhashi et al., 2010) or, proteasome inhibitors like Bortezomib (PS-341) that is currently approved as remedy for mantle lymphoma (Don and Zheng, 2011). Histone deacetylase inhibitors (HDACIs) like Vorinostat (SAHA) (Nimmanapalli et al., 2003, Song et al., 2014) and DNA demethylating agents including Decitabine (5-aza) (He et al., 2015, Kadia et al., 2015) are also under pre-clinical and clinical investigations for the treatment of AML and ALL. At present, both Vorinostat and Decitabine have been approved by the U.S. Food and Drug Administration (FDA) for the treatment of cutaneous T-cell lymphoma and myelodysplastic syndromes (MDS) correspondingly.

Christiana Savva

Programmed Cell Death – Apoptosis

Apoptosis is the main form of programmed cell death (PCD) and has proven to be an evolutionarily conserved mechanism (Huang et al., 2000, Ouyang et al., 2012). It plays a multivital role in developmental biology, immunology, normal growth and homeostasis, ageing, and degenerative processes (Renehan et al., 2001). It can be easily distinguished by specific morphological and energy-dependent biochemical characteristics of dying cells including, cell shrinkage, extensive plasma membrane blebbing, phosphatidylserine externalization, nuclear condensation, chromosomal DNA fragmentation, and a number of intracellular substrate cleavages (Cohen, 1997, Renehan et al., 2001, Ouyang et al., 2012).

Apoptosis occurs in three non-distinctive phases: *induction*, *execution* and *degradation* (Cohen, 1997, Renehan et al., 2001). The induction phase involves the initiation of pro-caspase cascades in response to several stimuli such as, DNA damage, physiological stress and inflammation, leading to exert production of pro-apoptotic molecules. The execution phase is characterized by the mitochondrial outer membrane permeabilization (MOMP), cytochrome *c* and mitochondrial proteins release, and activation of proteases into the cytosol. The critical result of degradation phase is the various morphological changes that demonstrate the commitment to cell death (Takahashi and Earnshaw, 1996, Cohen, 1997). The final outcome of the apoptotic machinery culminates in the cleavage and fragmentation of DNA and the formation of apoptotic bodies (Savill and Fadok, 2000).

Molecular regulators of apoptosis

Caspases are the key mediators of apoptosis. Once caspases are activated, there is an irreversible commitment towards cell death. Caspases, consist a family of cysteine aspartyl-specific proteases (Nunez et al., 1998). Thus far, in human, they have been identified ten major caspases. Based on their function and on which phase of apoptosis they are activated, caspases are categorized into: *initiator* (Caspases 2, 8, 9 and 10), *effector or executioner* (Caspases 3, 6, and 7) and *inflammatory* caspases (Caspases 1, 4 and 5) (Tait and Green, 2010). Other caspases that have been recognized are, Caspase-11, which is reported to

Christiana Savva

contribute to lethality in mouse models of sepsis (Jimenez Fernandez and Lamkanfi, 2015), Caspase-12, which can mediate endoplasmic-specific apoptosis (Szegezdi et al., 2003), Caspase-13, which has been found to be expressed only in cattle (Koenig et al., 2001), and Caspase-14, which is highly expressed in embryonic tissues and appears to be important for keratinocyte terminal differentiation (Eckhart et al., 2000).

Caspases are synthesized as inactive pro-enzyme (zymoge/pro-caspase) containing an N-terminal prodomain followed by a C-terminal catalytic domain (Thornberry, 1998). The catalytic domain is a heterodimer compromised by a large subunit of 17 - 21 kDa and a smaller subunit of 10 - 13 kDa (Figure 4) (Thornberry, 1998, Tait and Green, 2010). Initiator caspases have longer prodomain than effector caspases and their activation depends on conserved motifs within this domain. Caspases -9 and -2 have a caspase activation and recruitment domain (CARD) while, Caspase-8 has a death effector domain (DED) both of which, enable the interaction with molecules that regulate their activity (Thornberry, 1998). Initiator caspase activation involves dimerization of the inactive monomers followed by interdomain cleavage (autoproteolysis) (Tait and Green, 2010). Executioner caspases are present as inactive dimers in cells and are becoming enzymatically active upon cleavage by active initiator caspases (Figure 4).

All caspases can cleave substrates in a highly specific manner after the Asp residue in short tetrapeptide motifs (Thornberry et al., 1997). The collection of initiator caspase substrates is limited and includes self-cleavage, BCL-2 homology 3 (BH3)-interacting domain death agonist (BID) and executioner caspases. By contrast, executioner caspases cleave hundreds of diverse substrates that ultimately cause the morphological and biochemical changes observed during apoptosis (Degterev et al., 2003). Initiator caspases, also respond to distinct stimulus. Caspases, -2 and -9 respond to changes in mitochondrial potential, whereas Caspase, -8 and -10 sense activation of death receptors (DRs).

The executor Caspase-3, is considered to be the most active effector caspase where it is processed and activated by any of the initiator caspases. Caspase-7 can be activated only by Caspase-9 while Caspase-6 is a downstream substrate of Caspase-3 (Cullen and Martin, 2009). Cleavage of specific substrates by

Christiana Savva

Caspases -3, -6 and -7 has the effect of either, activating effector molecules or, triggering characteristic structural changes observed in apoptotic cells (Porter and Janicke, 1999). For instance, Caspase-3 can specifically activates the endonuclease CAD (caspase-activated DNase) that cleave DNA promoting DNA degradation and chromatin condensation (Sakahira et al., 1998, Porter and Janicke, 1999). Other substrates of effector caspases include PARP-1 (poly-ADPribose polymerase-1), alpha-Fodrin, nuclear protein NUMA and cytokeratins (Slee et al., 2001).

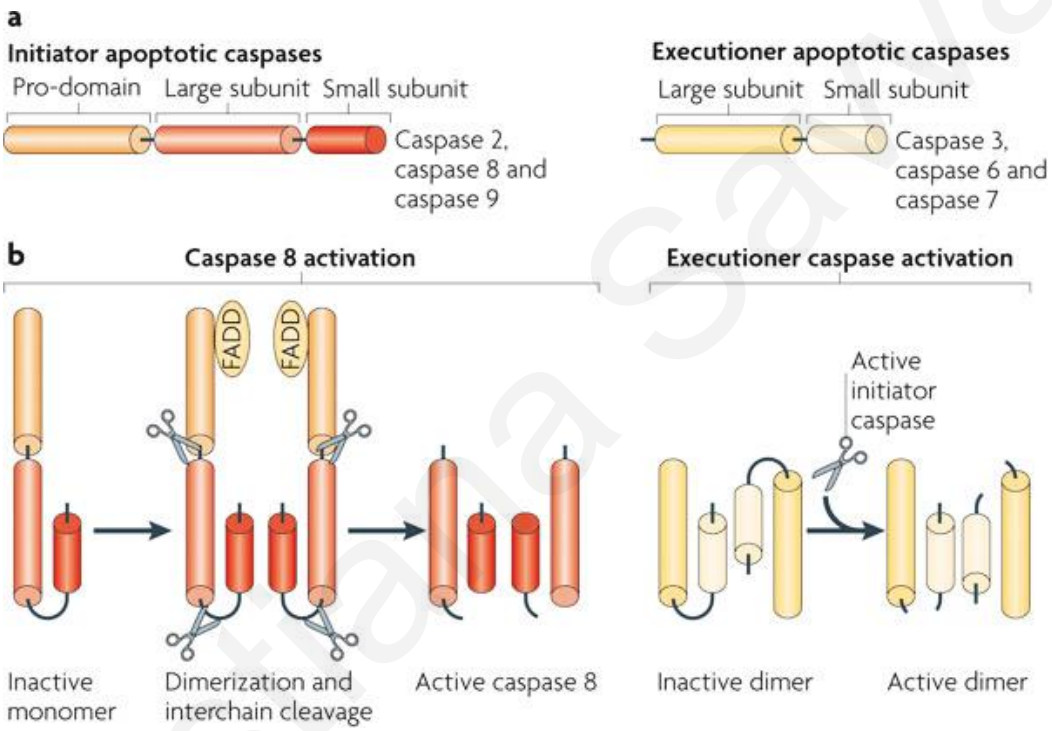

Figure 4. The initiator and executor caspases of apoptosis. (a) Inactive caspases (pro-caspases) composed of an N-terminal prodomain and a C-terminal catalytic domain that is comprised by a p20 large subunit and a p10 small subunit. **(b)** The prodomain of the initiator caspases contains motifs that enable the interaction with other regulatory molecules (i.e. Fas-associated death domain, FADD). These molecules respond to stimuli that cause the clustering of the initiator caspase and their autoproteolysis, so that they can proceed to activate the effector caspases. Adapted from (Tait and Green, 2010).

PARP-1 is one of the first substrates cleaved by Caspase-3 and Caspase-7 during the early stages of apoptosis (Kaufmann et al., 1993). It is an abundant nuclear protein essential for initiating various DNA repair mechanisms (Langelier et al., 2012). PARP-1 is a 116 kDa protein that contains three main functional domains; an amino-terminal DNA-binding domain, a central automodification domain and

Cristiana Sava

the C-terminal catalytic domain. DNA single-strand and double-strand breaks in cells are recognized by PARP-1 enzymes which are rapidly recruited to the damage site to regulate the process of autoPARylation. PARP-1 activation results in the synthesis of PAR (poly(ADP-ribose) polymers and enrolment of other repair enzymes (i.e. histones, DNA polymerases, topoisomerases, DNA-ligases) that bind to DNA strand breaks and reseal or repair the damage (Ko and Ren, 2012). Through this process, PARP-1 does not only regulates DNA cellular repair but also other cellular activities including gene transcription, DNA replication, protein degradation, cytoskeleton organization and many others (Ko and Ren, 2012). During the execution phase of apoptosis, PARP-1 is proteolytical inactivated by Caspase-3 and -7 by cleavage into a 25 kDa N-terminal and 89 kDa C-terminal fragment (Soldani and Scovassi, 2002). This eliminates PARP-1 activation in response to DNA damage-fragmentation during the early stages of apoptosis and helps commit cell to the apoptotic pathway.

Apart from caspase-dependent programmed cell death (CD-PCD), researchers have discovered a specific type of apoptosis independent of caspases activation (CID-PCD). This type of programmed cell death is triggered by the involvement of specific mitochondrial factors that are released from the mitochondrial intermembrane space (MIS) to the cytoplasm. Apoptosis-inducing factor (AIF) (Cande et al., 2002) and Endonuclease G (EndoG) (van Loo et al., 2001) are two of the well-known mediators of CID-PCD. Reactive oxygen species (ROS), have also been reported to contribute to CID-PCD (Circu and Aw, 2010). ROS can induce irreversible and intensive oxidative modifications of lipid, protein, or DNA promoting cell death (Zong and Thompson, 2006). The excess mitochondrial ROS production is a result of extensive mitochondrial electron transport and is a feature commonly observed in dying cells (Zong and Thompson, 2006).

AIF is a flavoprotein with NADPH oxidase and NADH reductase activities (Cande et al., 2002). It is synthesized as a non-apoptogenic precursor in the cytosol and efficiently imported into the MIS. During apoptosis, the mature form of AIF (57 kDa) is generated by removal of the amino-terminal mitochondrial targeting sequence by Calpains (calcium-activated cysteine proteases) and Cathepsins (lysosomal proteases) and becomes potentially apoptogenic (Susin et al., 1999, Lorenzo and Susin, 2007). Following MOMP, AIF is released form the MIS and

Christiana Sawa

translocates to the nucleus, where it induces peripheral chromatin condensation and large-scale (50 kbp) DNA fragmentation through mechanisms that remain to be clarified (Daugas et al., 2000). Although AIF is a CID death effector, evidence shows a crosstalk between AIF and caspase cascade at several levels. Particularly, it has been shown that, when caspase activation occurs early during apoptosis, the release of AIF is secondary to the activation of Caspases-2 (Lassus et al., 2002), or Caspase-8 (Susin et al., 1999), or to cytochrome *c* release (Susin et al., 1999). Therefore, AIF and caspases may cooperate in apoptosis execution depending on the specific apoptosis-inducing stimulus (Cande et al., 2002). EndoG, is another important mitochondrion-specific nuclease that translocates to the nucleus during apoptosis. Once released from mitochondria, EndoG cleaves chromatin DNA into nucleosomal fragments (180 kbp) independently of caspases (Li et al., 2001). In addition, EndoG was found to play important role in mitochondrial DNA replication and was proven to be released along with cytochrome *c* (Cote and Ruiz-Carrillo, 1993).

The Bcl-2 family is comprised of evolutionary related proteins and important regulators of apoptosis. These proteins govern MOMP and can be either pro-apoptotic or anti-apoptotic. Some of the anti-apoptotic proteins include Bcl-2, Bcl-x, Bcl-xL, Bcl-XS, Bcl-w, BAG, and some of the pro-apoptotic proteins include Bcl-10, Bax, Bak, Bid, Bad, Bim, Bik, and Blk (Ola et al., 2011). These members are classified on the basis of structural similarity to the Bcl-2 homology (BH) domains (BH1, BH2, BH3 and BH4), and a transmembrane domain. The BH3 domain exist in all members and is essential for their heterodimerization while is the minimum domain required for the pro-apoptotic function (Hosseini et al., 2013).

The balance between anti- and pro-apoptotic members is important because it determines whether the cell will commit to apoptosis or will abort the process. Following a death signal, pro-apoptotic proteins are activated through post-translational modifications (i.e. phosphorylation, dephosphorylation, cleavage) leading to their translocation to mitochondria, from which apoptosis can be initiated (Shamas-Din et al., 2011). It is believed that, the main mechanism of action of the Bcl-2 family of proteins is the regulation of cytochrome *c* release from the mitochondria via alteration of MOMP and secondly mitochondria derived activator of caspases including initiator Caspase-9 (Engel and Henshall, 2009, Ola et al.,

Christiana Saiya

2011). Specifically, it has been shown that Bcl-2 and Bax interact with proteins of the mitochondrial permeability transition (PT) pore complex (Narita et al., 1998). The opening of the PT pore or translocation of Bax-like proteins from the cytosol to the mitochondrion cause the release of IMS proteins. Several studies have demonstrated that these proteins can interact with each other and these interactions can neutralize their pro- or anti-apoptotic functions. For instance, Bid and Bim are termed activator BH3-only proteins, as they directly induce Bax/Bak-dependent MOMP (Kim et al., 2006).

The tumor suppressor protein p53 (TP53) is an important pro-apoptotic factor. Under normal conditions p53 is a short-lived protein sequestered in the cytoplasm in complex with its inhibitor, HDM2 (Moll and Petrenko, 2003). In response to genotoxic damage, p53 translocates from the cytoplasm to the nucleus and arrests progression of the cell cycle in G1 and/or G2M phase (Jin and Levine, 2001). If the DNA damage cannot be repaired, the cell undergoes apoptosis. Even though the exact apoptotic mechanisms of p53 have not been completely clarified, p53 appears to govern apoptotic signals received by the mitochondrial (Schuler and Green, 2001). Interestingly, p53 was found to interact with the Bcl-xL and Bcl-2 proteins promoting MOMP, and therefore cytochrome *c* release (Mihara et al., 2003). p53, also promotes the expression of pro-apoptotic regulators such as members of the Bcl-2 family (i.e. Bid, Bax, PUMA, Noxa) (Moll and Petrenko, 2003, Day et al., 2008), the TNF-related apoptosis-inducing ligand (TRAIL) (Wu et al., 1997) and the apoptotic peptidase activating factor 1, Apaf-1 promoting the formation of apoptosome (Fortin et al., 2001, Schuler and Green, 2001). Interestingly it has been proven that, p53 can boost the activation of the caspase cascade by both transcription-dependent (MacLachlan and El-Deiry, 2002) and –independent (Ding et al., 1998, Varfolomeev et al., 1998) mechanism.

Apoptotic pathways

The mechanisms of apoptosis are highly complex and sophisticated, involving a sequence of molecular events. The two major cellular death pathways that transduce the effects of various death inducers are the *extrinsic or death receptor* pathway and the *intrinsic or mitochondrial pathway* (Elmore, 2007). Both the

Christiana Savva

extrinsic and intrinsic pathways converge on the same terminal, the execution phase.

Extrinsic pathway

The extrinsic signaling pathway involves death receptors (DRs) that are members of the tumor necrosis factor receptor (TNFR) gene superfamily (Locksley et al., 2001, Wiens and Glenney, 2011). The members of this family share similar cystein-rich extracellular domains and are uniquely characterized by the presence of an 80 amino acid motif in their cytoplasmic C-terminal region, namely death domain (DD) (Ashkenazi and Dixit, 1998). DD is crucial for transmitting apoptotic or other signals from the cell surface to the intracellular signaling pathways. The most well-characterized human DRs and their cognate ligands include; Fas/FasL, TNFR1/TNFα, DR3/TL1A, DR4/Apo2L (TRAIL), and DR5/Apo2L (TRAIL) (Ashkenazi and Dixit, 1998, Gonzalvez and Ashkenazi, 2010) (Figure 5). They have also been identified three 'decoy' receptors that are unable to transmit apoptotic signals, namely, DcR1, DcR2 and DcR3 (Liu et al., 2003, Rizzardi et al., 2009). DcR1 is anchored to the plasma membrane through a glycophospholipid moiety and lacks an intracellular domain, DcR2 is a transmembrane protein harboring a truncated, nonfunctional DD, whereas DcR3 is a soluble protein which contains no transmembrane domain (Yu et al., 1999, Gonzalvez and Ashkenazi, 2010). Decoy receptors were found to inhibit apoptosis by compete for binding to other DRs. More specifically, DcR -1 and -2 compete with DR4 and DR5 for binding to TRAIL whereas, DcR3 compete with Fas and DR3 for the binding of TLI1A (Yu et al., 1999, Gonzalvez and Ashkenazi, 2010).

Upon ligand binding, adapter proteins with corresponding DD are recruited to the cytoplasmic domain of the receptors. Ligand engagement typically causes the association of adaptors proteins such as Fas-associated DD protein (FADD) (Wajant, 2002, Villa-Morales and Fernandez-Piqueras, 2012). FADD then associates with inactive procaspase-8 via a shared DED leading to the formation of the death-inducing signaling complex (DISC) and resulting in the auto-catalytic activation of procaspase-8 (Kischkel et al., 1995). Once Caspase-8 is activated, the execution phase of apoptosis is triggered (Figure 6).

Christiana Savva

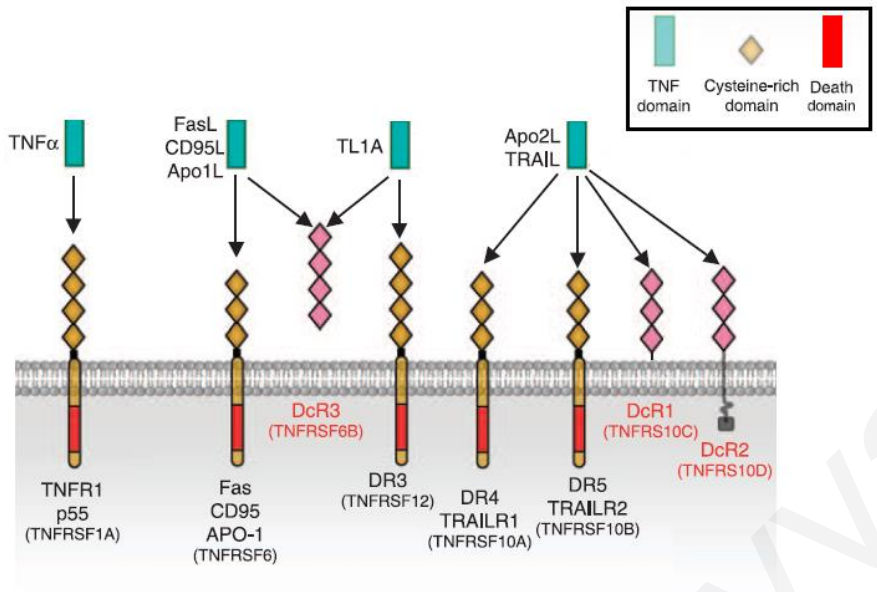

Figure 5. Death receptors and their ligands. DRs belong to the TNFR superfamily. They contain cyteine-rich extracellular domains and have a cytoplasmic domain of about 80 amino acids called death domain (DD). The best-characterized ligands and corresponding death receptors include; FasL/Fas, TNFα/TNFR1, TL1A/DR3, Apo2L/DR4 and Apo2L/DR5. The decoy receptors (DcRs) are non-signaling members of the TNFR superfamily that compete with DRs for ligand binding. Modified by (Gonzalvez and Ashkenazi, 2010).

Intrinsic pathway

The intrinsic signaling pathway involves a diverse array of non-receptor-mediated stimuli. These stimuli produce intracellular signals that may act in either a positive or negative way. Negative signals involve growth-factor deprivation, hormone and cytokines that suppress death programs. Stimuli that act in a positive manner include UV radiation, hypoxia, toxins, viral infections, DNA-damage and free radicals. The intrinsic pathway is regulated by Bcl-2 family proteins. The anti-apoptotic Bcl-2 proteins are inhibited by the pro-apoptotic members of the family like PUMA and Bid in response to an intrinsic signal. This results in Bax and Bak oligomerization, leading to MOMP and the release of second mitochondria-derived activator proteins from the IMS into the cytosol (Saelens et al., 2004, Ouyang et al., 2012). These proteins include the cytochrome *c*, Smac/DIABLO, and the serine protease HtrA2/Omi (Garrido et al., 2006, Moffitt et al., 2010). The released of cytochrome *c*, along with apoptosis protease activating factor-1 (APAF-1) and procaspase-9, form the apoptosome. Within the apoptosome, clustered

Cristiana Sava

procaspase-9 gets activated and cleaves downstream effector caspases, leading to the hallmark of apoptosis (Brunelle and Letai, 2009, Moffitt et al., 2010) (Figure 6). The release of Smac/DIABLO from the mitochondria promotes apoptosis by binding to and neutralizing members of the family of inhibitor of apoptosis proteins (IAPs) (Schimmer, 2004).

The crosstalk between the extrinsic and intrinsic pathways

The crosstalk between the two pathways can be observed at both the execution and initiation level, facilitating in the enhancement of the apoptotic outcome of the two pathways. Agents or stress-inducers can sensitize cells to DR-induced apoptosis or the opposite, death signals may enhance cells sensitivity to mitochondrial-mediated apoptosis (Soderstrom et al., 2002, Metkar et al., 2003, Shankar and Srivastava, 2004, Cuello et al., 2004). Based on the requirement of the intrinsic pathway for apoptosis induced by DRs, cells can be divided into type I and type II cells (Scaffidi et al., 1998, Abdulghani and El-Deiry, 2010). In type I cells, activated Caspase-8 is sufficient enough to direct activate the effector caspases and lead to the execution of apoptosis. In type II cells, only a small amount of FADD and Caspase-8 are recruited to DISC and, as a result, activated Caspase-8 is insufficient and requires the involvement of mitochondria to finally induce apoptosis. Under these circumstances, the BH3-only protein, Bid, is cleaved by Caspase-8 which results in its activation - truncated Bid (tBid), and mitochondrial translocation (Figure 6) (Luo et al., 1998, Li et al., 1998). tBid, then interacts with Bax/Bak proteins increasing the release of cytochrome *c* from the mitochondria (Gonzalvez et al., 2010, Schug et al., 2011).

The cellular-FLICE (FADD-like IL-1β-converting enzyme)-inhibitory protein (c-FLIP) was found to play an important role in the classification of type I or II cells. c-FLIP is a protein that is homologous to caspase-8 that is recruited to the DISC and inhibits the processing and activation of procaspase-8 (Safa, 2012). When the long isoform (c-FLIP$_L$) of the protein exists in high levels, c-FLIP exerts anti-apoptotic effects at the DISC while, when present in low levels, promoting apoptosis (Krueger et al., 2001, Chang et al., 2002).

Christiana Savva

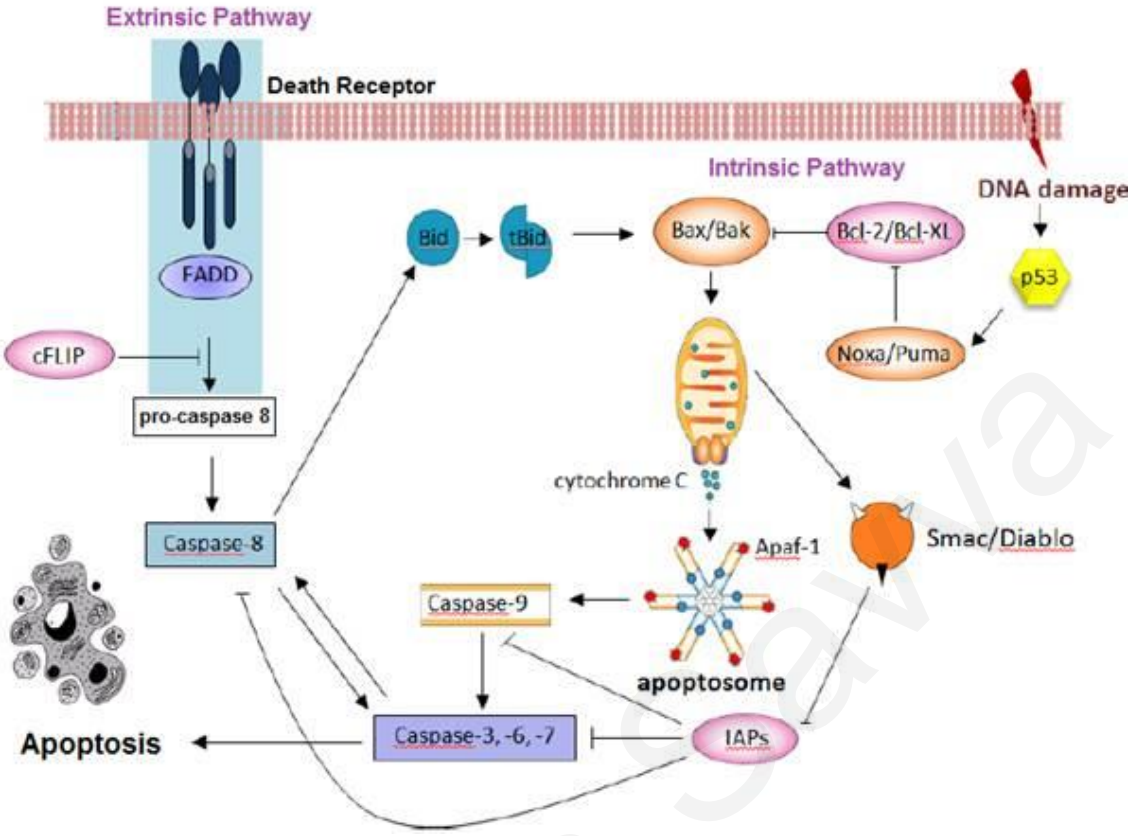

Figure 6. An overview of the extrinsic and intrinsic apoptotic pathways. In the extrinsic pathway, binding of ligands to DRs leads to the recruitment of FADD. Procaspase-8 binds to FADD leading to DISC formation. Activated Caspase-8 directly activates executioner caspases (Caspase, -3, -6, and -7) (type I cells) and/or cleaves Bid (type II cells). Translocation of the tBid to the mitochondria promotes the assembly of Bax/Bak that further enhances apoptosis. When c-FLIP levels are elevated in cells, Caspase-8 recruits c-FLIP to form a Caspase-8/c-FLIP heterodimer which does not trigger apoptosis. In the intrinsic pathway, Bax/Bak translocation to the mitochondria promotes MOMP. This induces the release of proteins Smac/DIABLO which promotes apoptosis by binding to and antagonizing IAPs. Cytochrome *c* is released into cytosol and, in combination with Apaf-1 and Caspase-9, forms the apoptosome. Active Caspase-9 initiates a proteolytic cascade of effector caspases activation that leads to morphological hallmarks of apoptosis. DNA damage can also promote activation and expression of p53-dependent genes such as PUMA and Noxa, which can bind to anti-apoptotic proteins Bcl-2/Bcl-xL, thereby opposing their effect. Modified by (Goncharenko-Khaider et al., 2013).

Christiana Saliva

Deregulation of apoptosis in leukemia

The hematopoietic system is particularly sensitive to deregulation of apoptosis as LSCs go through a high turnover rate. Therefore, these cells have to sustain a tight balance between cell apoptosis and proliferation. Alterations in gene expression or protein activation affect this balance, leading to accumulation of leukemic cells. Consistent with this notion, over-expression of Bcl-2 (Nuessler et al., 1999, Mehta et al., 2013) and deletions or mutations of p53 (Wattel et al., 1994, Melo et al., 2002) common in AML and ALL, resulting in resistance to drugs that induce apoptosis through the intrinsic pathway.

Deregulation of Bcl-2 family members plays an important role for the transformation of myeloid cells. *Bcl-2* gene can accumulate somatic mutations in one or both alleles, and is also involved in chromosomal translocation that result in elevated levels of Bcl-2 mRNA and protein production (Kitada et al., 2002). Activating mutations by retroviral integration in the Bcl-xL gene have also been reported in AML and T-ALL (Noronha et al., 2003, Addeo et al., 2005). Experimental results from these studies suggest that elevated levels of Bcl-2 protein expression may be associated with adverse clinical outcome; reduced rates of CR and shorter disease OS for some groups of patients with CLL and AML (Nuessler et al., 1999, Kitada et al., 2002, Mehta et al., 2013). In addition to the BCL-2 family proteins, apoptosis is often disturbed through upregulation of IAPs. Changes in expression levels of IAPs are due to chromosomal translocation, mutations, amplifications, or loss of endogenous inhibitors (Smolewski and Robak, 2011). Gene expression signatures that included c-IAP2 were correlated with poor OS in newly diagnosed AML patients while, in childhood *de novo* AML, high XIAP expression was found to be an unfavorable prognostic factor and was also associated with poor response to chemotherapy in pediatric T-ALL (Fulda, 2012, Fulda, 2014) .

Although p53 mutations occur in only 10 - 15% of AML cases, they are associated with the most aggressive disease courses and drug resistance (Abdel Hamid et al., 2015, Weisberg et al., 2015). The translocations that fuse MLL with the ELL (eleven nineteen lysin rich leukemia) gene and CBFb (core-binding factor subunit beta) overexpression were found to be associated with p53 suppressed

Christiana Savva

transcriptional activity and subsequent chemoresistance in AML (Wattel et al., 1994, Kitada et al., 2002, Melo et al., 2002). In overall, *p53* depletion promotes AML by enabling aberrant self-renewal typically by activating Ras signaling pathways and impair terminal myeloid differentiation, while *p53* point mutations are associated with drug resistance and adverse outcome (Gilliland et al., 2004, Zhao et al., 2010).

Christiana Savva

TNFR1: a Key Modulator of Life and Death

The TNFR superfamily (TNFRSF) in humans consist of at least 27 members with unique structural features that couple them directly to signaling pathways for cellular activities in cells such as proliferation, inflammation, apoptosis and differentiation (Locksley et al., 2001, Biswas and Ferrarini, 2012). The capacity to induce cell death is a special property with great adaptive value that only few members of the family possess. Among the 6 homologous receptors able to stimulate apoptosis (for details see § Extrinsic pathway), tumor necrosis factor receptor 1, TNFR1 (TNFRSF1A) owns a distinct and superior position. The interesting feature of TNFR1 is that, depending on the cellular context, it can promote equally and efficiently either pro-inflammatory and pro-survival signaling pathways or apoptosis (Schrofelbauer and Hoffmann, 2011, Mak and Yeh, 2002).

TNFR1 is a single transmembrane glycoproteins with a cysteine rich-extracellular domain (Grell et al., 1994) and an extracellular pre-ligand-binding assembly domain, PLAD that enables receptor trimerization upon activation by its ligand, TNFα (Chan et al., 2000). TNF-α is a cytokine that has been shown to play many important physiologic roles. It is expressed as a 26 kDa transmembrane protein that can be cleaved by the metalloprotease TACE (TNFα-converting enzyme) to release a 17 kDa soluble TNFα form (Idriss and Naismith, 2000). TNFα forms non-covalently-bound homotrimers which are capable of becoming a secreted form.

Following activation, TNFR1 initiates signaling by recruiting one of two death domain (DD)-containing platform adaptor molecules: **(i)** *TRADD* (TNF receptor-associated DD) that engages both apoptotic and nonapoptotic signaling pathways and **(ii)** *FADD* that generally mediates apoptosis (Kischkel et al., 1995). TRADD adaptor protein recruits a DD-containing kinase termed receptor interacting protein-1 (RIP1). RIP1 in turn recruits TNF receptor associated factor-2, TRAF2 and/or TRAF5, as well as c-IAP1 and c-IAP2 that are TRAF2-associating ubiquitin ligases (Figure 7) (Chen and Goeddel, 2002). These adaptor proteins act in concert with RIP1 to engage downstream phosphorylation cascades to activate nuclear factor kappa B (NF-κB) or c-Jun N-terminal kinases (JNK) or p38 (MAPK) pathways, which promote proinflammatory and prosurvival transcriptional responses (Figure 7) (Hayden and Ghosh, 2008, Varfolomeev and Vucic, 2008).

Christina Sawa

The formation of TRADD/RIP1/TRAF2 prosurvival complex (Complex I) at the level of the plasma membrane is temporary since a large portion of this complex dissociates from TNFR1 within an hour and forms a second proapoptotic complex in the cytosol (Micheau and Tschopp, 2003). Specifically, when RIP1 polyubiquitin (poly-ub) chain is removed, RIP1 dissociates from TRAF2 and binds to TRADD/FADD/Caspase-8 (Complex II). Shortly after that, procaspase-8 is proteolytically cleaved to active Caspase-8 which in turns cleaves and inactivates RIP1 and RIP3, promoting apoptosis (Hitomi et al., 2008) (Figure 7). The switch between cell survival and death is very complicated and is believed that cell content and microenvironmental factors are responsible for the TNFR1 fine-tuning (Baker and Reddy, 1998).

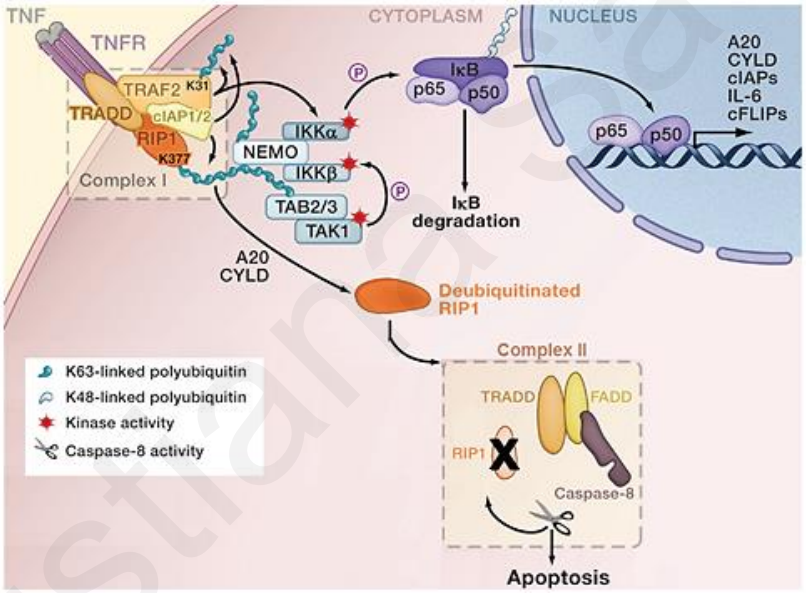

Figure 7. TNFR1 apoptotic and survival signaling. Once TNFR1 is stimulated by its ligand (TNFα), two complexes with opposing effects on cell fate can be formed: a pro-survival and a pro-apoptotic complex. TRADD adaptor protein provides a scaffold for the assembly of prosurvival complex I by binding RIP1, TRAF2 and c-IAPs. TRAF2 and c-IAPs direct the formation of polyubiquitin chains linked through lysine 63 (K63) of ubiquitin on RIP1, thereby allowing it to interact with the TAK1/TAB2/3 complex. K63-linked polyubiquitination on TRAF2 can also recruit the TAK1/TAB2/3 complex. TAK1 activates the IKK complex that in turn phosphorylates the NF-κB (p65/p50) inhibitor IκB to induce its K48 polyubiquitination and proteasomal degradation. Once freed from its inhibitor, NF-κB translocates to the nucleus to activate transcription. A20 and CYLD remove K63-linked polyubiquitin chains from RIP1 and abolish its ability to activate NF-κB. The proapoptotic complex II formation involves FADD-mediated recruitment and activation of caspase-8 for RIP1 cleavage. Modified by (Declercq et al., 2009).

Christiana Savva

The route of survival

TRADD recruitment to activated TNFR1 organizes the assembly of the Complex I proteins: RIP1, TRAF2 and/or TRAF5 and cIAP1/2. TRAF proteins are cytoplasmic proteins that directly interact with the intracellular domains of TNFR1 and serve as the signal transducers of the TNFR1 pathway. Experiments aimed at the identification and characterization of these proteins resulted in the isolation of six total, distinct TRAF proteins (termed TRAF-1 through 6) (Arch et al., 1998). The members of TRAF family share several structural motifs. The C-terminal portion of the TRAFs domain is highly conserved while the N- terminal domain is less conserved and conforms a coiled-coil α-helix motif, and is accountable of the oligomeric qualities of TRAFs (Arch et al., 1998, Lee and Lee, 2002). TRAFs, either as homodimers or heterodimers, can associate with the C-terminal signal transducing component of the TNFR1, playing a central role in the regulation of cell survival and apoptosis (Lee and Lee, 2002).

TRAF2 has E3 ubiquitin-protein ligase activity and catalyzes the formation of K63-linked poly-ub chains on itself, as well as on its substrates, RIP1, IKK (inhibitor of NF-κB kinase), BIRC3 (baculoviral IAP repeat containing 3) and TICAM1 (Wertz and Dixit, 2010). The K63-linked poly-ub chain of TRAF2 acts as scaffold for the recruitment of TAK1 (transforming growth factor- activated kinase-1) and its partner proteins TAB2/3 (TAK1 binding protein-2/3), as well as the apoptotic adaptor proteins c-IAP1 and c-IAP2 (Figure 7) (Rothe et al., 1995). These ubiquitination events are essential for TNFα-induced NF-κB and JNK pathways activation (Chen, 2005, Ea et al., 2006). In particular, it has been shown that TRAF, -2, -5 and -6 overexpression can activate the NF-κB, JNK and p38 cascades (Lee and Lee, 2002). *Yeh. et. al*., also observed that TRAF2-deficient mice failed to activate JNK in response to TNFα (Yeh et al., 1997), while more recent studies showed that inactivating mutations of TRAF2 is a dominant-negative event, neutralizing TNFα-induced NF-κB activation (Blackwell et al., 2009, Zhang et al., 2011).

The mechanisms by which TRAF2 activates NF-κB remains unknown, while still remaining undefined in the membrane-proximal events of TRAF2 activation. TRAF2 has been reported to be phosphorylated at serine (Ser) residues

Christiana Sawa

(Chaudhuri et al., 1999). Particularly, following TNFα administration TRAF2 is phosphorylated at residues Ser11 and Ser55 (Blackwell et al., 2009, Thomas et al., 2009). These phosphorylation are essential TNFα-induced secondary and prolonged IKK activation and for the expression of a subset of NF-κB target genes. Thus, TRAF2 Ser phosphorylation inhibits apoptosis and promotes cell survival.

RIP1 kinase, is a multifunctional protein that contains an N-terminal serine/threonine kinase and a C-terminal DD. When TNFα stimulates TNFR1, RIP1 regulates whether the cell lives by activating NF-κB or dies by apoptosis or necroptosis (programmed necrosis) (Declercq et al., 2009, Weinlich et al., 2011). The kinase domain of RIP1 is involved in regulating necroptosis while the DD regulates RIP1 recruitment to the intracellular domain of TNFR1. Within Complex I, RIP1 is modified by polyubiquitination mediated through cIAPs and TRAF2 E3 ubiquitin ligase activity.

RIP1 decorated with K63-linked poly-ub chains promotes the assembly of downstream signaling components including TAK1 and TAB2/3. In addition, the IKK complex is also anchored to RIP1 via binding of NEMO (NFκB essential modulator) to K63-linked poly-ub chains (Figure 7). The poly-ub of RIP1 and recruitment of NEMO functions as the first pro-survival checkpoint at early after TNFR1 stimulation because this restrains the apoptosis-inducing property of RIP1 by sequestering it from procaspase-8. The ub chains can be removed by the deubiquitinases (DUB), A20 and protease, cylindromatosis (CYLD) (Wertz et al., 2004, Wilson et al., 2009). When K63 polyubiquitination of RIP1 is reduced by the action of deubiquitinases or by cIAPs (Mahoney et al., 2008) or TRAF2 depletion (Lee et al., 2004, Wertz et al., 2004), RIP1 loses its ub-binding proteins and switches its function to that of promoting cell death.

Signaling to NF-κB activation

NF-κB family of transcription factors regulate the expression of various genes implicated in many physiological processes, including immunity, inflammation and cell survival (Oeckinghaus and Ghosh, 2009). The role of NF-κB in these processes is to recruit and activate various immune cells by inducing the transcription of proinflammatory mediators like chemokines, cytokines such as

Christiana Savva

TNF-α and interleukins (IL), -1, -6, and 8, and anti-apoptotic factors including c-IAP1/2 and c-FLIP (Grivennikov et al., 2010). Nevertheless, in the end NF-κB activity is down-regulated in order to prevent chronic inflammation. Uncontrolled inflammation can be accompanied by several autoimmune diseases and can have critical role in the development and pathogenesis of cancer and leukemias (Grivennikov et al., 2010, Gasparini et al., 2014).

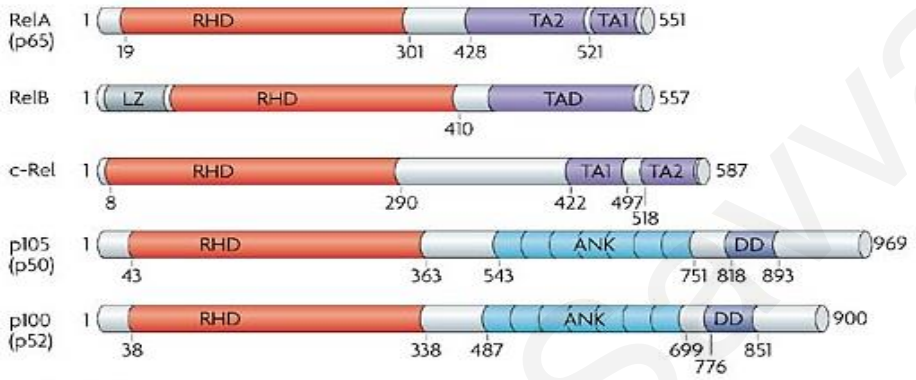

Figure 8. The NF-κB family of transcription factors. The five members of NF-κB family, RelA (p65), RelB, c-Rel, p50/p105 (NF-κB1) and p52/p100 (NF-κB2). p50 and p52 are derived from the longer precursor proteins p105 and p100, respectively. All members have an N-terminal REL homology domain (RHD). Rel members have a transcriptional activation domain (TAD) at the C-terminus. TA1 and TA2 are subdomains of the TAD. Ankyrin-repeat motifs (ANK) are found only in the C-terminus of precursors proteins. DD, death domain; LZ, RelB-transactivation domain containing putative leucine-zipper-like motif. Adapted from (Perkins, 2007).

The NF-κB family comprises five members: RelA (p65), RelB, c-Rel, p50/p105 (NF-κB1), and p52/p100 (NF-κB2) (Figure 8) (Napetschnig and Wu, 2013). Both p105 and p100 are synthesized as precursor proteins that are processed to the smaller active forms of p50 and p52. All members share an N-terminal REL homology domain (RHD) (Perkins, 2007, Hayden and Ghosh, 2008). This domain is essential for NF-κB dimerization, interaction with inhibitors of κB (IκBs), nuclear translocation and binding to DNA. RelA, c-Rel and RelB proteins also have a transcriptional activation domain (TAD) at the C-terminus, which is important for the transcription of NF-κB target genes (Perkins, 2007, Hayden and Ghosh, 2008). The TAD is absent in the NF-κB subunits p50 and p52, therefore they may repress transcription unless associated with a TAD-containing NF-κB family member or other proteins capable of co-activator recruitment (Ghosh et al., 1998, Hayden and

Cristiana Savva

Ghosh, 2008). In most cells, the most prominent form of NF-κB is the p65/p50 heterodimer followed by the p50/50 and p65/p65 homodimer complexes (Mankan et al., 2009).

NF-κB signaling can be activated by canonical (or classic) or non-canonical (or alternative) pathway. The canonical pathway is activated by a wide range of stimuli, such as the cytokines, TNF-α, and the bacterial endotoxin, lipopolysaccharide (LPS). These stimuli activate the NF-κB dimer p50/p65 through TNFR1 and TNFR2, interleukin 1 receptor (IL-1R) and the toll-like receptor 4 (TLR4) (McCool and Miyamoto, 2012). The non-canonical pathway is activated by lymphotoxin beta, B cell activating factor, or CD40 ligand and induces the processing of p100 that result in RelB/p52 mediated transcription. From a therapeutic point of view, only inhibition of canonical NF-κB signaling was shown to impair leukemic cell growth for reasons partially understood (Dos Santos et al., 2010).

Activation of NF-κB is a complex process that is governed mainly by members of the IκB kinase (IKK) complex, which are upstream of another set of regulator proteins called inhibitor of NF-κB (IκB). The IKK complex consists of two catalytic subunits with kinase activity, IKKα and IKKβ and a regulatory subunit, IKKγ, also known as NEMO, which serves as an adaptor protein connecting both catalytic domains with upstream activators (Napetschnig and Wu, 2013). The IKK complex is recruited to TNFR1, where it becomes activated within minutes of TNF-α treatment through a TRAF2/RIP1-dependent manner. As described above, poly-ub chains of TRAF2 and RIP1 serve as platforms for the assembly of NEMO and TAK1/TAB2 in IKK (Figure 7). NEMO oligomerization and TAK1/TAB2 phosphorylation lead to a subsequent autophosphorylation of IKK proteins and ultimately to the inactivation of IκBs (Delhase et al., 1999). The precise mechanism of IKK activation remains until now unclear.

In the canonical pathway, NF-κB dimers p50/65 are sequestered in the cytosol by their inhibitory protein, IκB consisting of three proteins, namely IκBα, IκBβ and IκBε (Senftleben and Karin, 2002). These proteins maintain NF-κB dimers in the cytosol by masking their nuclear localization signal (NLS) and thus prevent NF-κB translocation to the nucleus (Ghosh and Karin, 2002). Downstream of TNFR1, IKK

Christiana Savva

complex is necessary for the phosphorylation of IκBα on Ser32 and Ser36, allowing targeting of IκBα by ubiquitin-proteasomal system (Karin, 1999, Senftleben and Karin, 2002). Upon phosphorylation, IκBα is subsequently ubiquitinated (K48 poly-ub) and rapidly degraded by proteasome (Figure 7) (Wertz and Dixit, 2010). Degradation of IκBα alters the dynamic balance between cytosolic and nuclear localization signals to favor nuclear localization of NF-κB (Hayden and Ghosh, 2008). The released dimeric combinations of RelA (p65) bind to κB sites (9-10 base pair DNA sites) within the promoters of target genes and regulate transcription through the recruitment of coactivators and corepressors (Hayden and Ghosh, 2008, Mankan et al., 2009). Upon NF-κB activation, the expression of IκBα and DUB A20 and CYLD is also induced as a negative feedback loop mechanism (Figure 7) (Hoffmann et al., 2002, Shembade and Harhaj, 2012). The newly synthesized IκBα enters the nucleus and promotes the disassociation of NF-κB from the DNA leading to its exportation from the nucleus. The enzymatic activity of A20 and CYLD promotes K48-ubiquitin-mediated RIP1 and IKK regulators degradation resulting in the downregulation of the canonical NF-κB signaling cascades.

The route of apoptosis

Micheau and Tschopp were the first to report the existence of two distinct complexes with opposing arms within the TNFR1 pathway (Micheau and Tschopp, 2003). The signaling steps that are unique to FADD-mediated TNFR1 signaling are limited as TRADD-mediated TNFR1 signaling pathways feed in at a proximal step. Thus, ligand/DR binding, recruitment of FADD to DR, and recruitment of caspase-8/10 with subsequent formation of DISC are the only signaling steps that are unique.

FADD, is 28 kDa protein with bipartite architecture; is comprised of a C-terminal DD and an N-terminal death effector domain (DED). The DD of FADD recognizes and binds to TNFR1 (or other DRs) at the plasma membrane whereas, DED enables recruitment of the zymogen forms of initiator Caspase, -8 and/or -10 (Barnhart and Peter, 2003). It supported that upon ligand binding (to TNFR1), FADD undergoes conformational changes that enable the interaction of its DED to one of the two DEDs of procaspase-8 (Cohen, 1997). This results to

Christiana Saiya

oligomerization of procaspase-8, activation of its autoproteolytic activity and ultimately the generation of enzymatically active Caspase-8. Activated Caspase-8 thereby activates downstream effector caspases including resulting in the cleavage of death substrates and subsequent rapid demise of the cell.

The complex of TNFR1/FADD/Caspase-8/10 is referred as DISC. A critical regulator of the DISC that determines the degree of activation of Caspase-8 is the decoy molecule $cFLIP_{L,}$ DISC is negatively regulated by $cFLIP_L$ whose expression is regulated by the NF-κB transcriptional activity. Through a negative loop, NF-κB upregulates $cFLIP_L$ in order to inhibit Caspase-8-mediated apoptosis, whereas the E3 ubiquitin ligase, ITCH promotes $c\text{-}FLIP_L$ degradation stimulating DISC formation and cell death (Chang et al., 2006). (For details see §The crosstalk between the extrinsic and intrinsic pathways)

Thus, FADD is an essential adaptor protein that links DRs with Caspase-8 and is considered to be critical for DRs-induced apoptosis. In support of this, FADD-deficient mouse, thymocytes as well as, in leukemic cells present resistant to DRs-induced apoptosis (Zhang et al., 1998, Kuang et al., 2000, Zhang et al., 2001, Kabra et al., 2001). Since FADD is required for full activation of caspase-8, both FADD and caspase-8 are required for apoptosis. Consistent with this idea, TNF-induced apoptosis was abrogated by FADD deficiency. FADD also regulates necroptosis by directly regulating the RIP1-RIP3 interaction. It has been reported that siRNA- or shRNA-mediated knockdown of FADD in L929 mouse fibroblast and HT-29 human colon cells resulted in an increase in necroptosis, whereas FADD overexpression in L929 cells delayed RIP1-RIP3 necrosome formation and necroptosis (Lee et al., 2012). This is probably due to the fact that, since FADD is required for the activation of caspase-8, which is able to suppress necroptosis, FADD-deficient cells facilitate necroptotic cell death by abrogating caspase-8 function.

Therapeutic implications

NF-κB possess a distinct role in leukemogenesis, leukemia progression, chemoresistance and relapse (Dos Santos et al., 2010, Rushworth et al., 2012, Kornblau et al., 2013, Kapelko-Slowik et al., 2013, Jacamo et al., 2014). Aberrant

activation of nuclear factor has been observed in primitive stages of AML and ALL, whereas almost 40% of patients have shown increased activity of NF-κB, mostly due to alterations in regulatory proteins of the NF-κB (Guzman et al., 2001, Dos Santos et al., 2010, Kapelko-Slowik et al., 2013). Other genetic alterations associated with dysregulation of NF-κB include missense mutations in IκBα (Oh and Ghosh, 2013) and chromosomal translocations involving the IκB family member, Bcl-3 (Collins et al., 2014, Schlette et al., 2005). NF-κB directly binds the promoters and induces expression of several anti-apoptotic genes, including the Bcl-2 family members Bcl-xL, the IAP-family member c-IAP2, and the gene c-FLIP (Mora et al., 2003, Benayoun et al., 2008, Varfolomeev et al., 2015). Thus, elevations in NF-κB activity can increase cellular resistance to apoptosis, affecting both the intrinsic and extrinsic pathway. Blocking the NF-κB signaling with the use of degradation-resistant IκB proteins (Adekoya et al., 2001, Poligone and Baldwin, 2001), IKK inhibitors (Cilloni et al., 2006, Carvalho et al., 2007) or by the use of proteasome inhibitors (Saito et al., 2013, Koyama et al., 2014, Nishioka et al., 2014), could enhance the sensitivity of cells to apoptosis inducing stimuli.

The extrinsic pathway of apoptosis is a promising target for anticancer drug development as it induces cell death independent of p53 and hence, is active in p53-mutated cells. Targeting the activation of the extrinsic pathway will therefore bypass mutations in the intrinsic pathway. Clinical trials aiming to evaluate the anticancer efficacy of TNF family members originated with the use of human TNFα mainly in advanced solid cancers (Lejeune et al., 2006, Roberts et al., 2011). Recombinant human TNFα (rhTNFα) has been tested as a systemic treatment in several phase I and phase II clinical trials and used as both a single agent and in combination with chemotherapeutics (Balkwill, 2002). Even though rhTNFα was proven as an effective anticancer agent in preclinical studies, these attempts were disappointing as clinical activity was rarely obtained; rhTNFα was unable to trigger apoptosis via TNFR1 unless the initial NF-κB pathway was blocked (Micheau et al., 2001). In addition, rhTNFα was highly cytotoxic towards hepatocytes causing severe side effects and lacked of evidence for therapeutic benefit (Roberts et al., 2011). Therefore, for the development of rational death receptor-targeted therapy it is important to discover agents able to activate death receptor without triggering the NF-κB cascade and furthermore, be able to overcome mitochondrial block.

Christiana Savva

Agents that target TNFR1 efficiently and inhibit leukemic cell growth have not yet been identified.

Nevertheless, use of soluble TNF (sTNF) α in combination with the chemotherapeutic drug melphalan yields impressive clinical responses (Eggermont et al., 2003, Rothbarth et al., 2004). In these applications, sTNF was infused at over 50 times the maximal tolerated dose (MTD) as identified during systemic sTNF therapy. This high dose of TNF induced endothelial cell apoptosis, whereas normal blood vasculature was not influenced. Apart from TNFR1, TNFR2 signaling was shown to be required to sensitize tumor vasculature to apoptotic TNFR1 signaling supporting that, the combined use of a low dose of sTNF with a TNFR2 agonists may optimize therapeutic effects on tumor vasculature and minimize toxicity. Of interest in this respect is the development of TNF-based fusion proteins like the TNC-scTNFR2 (Bueno et al., 2011), that specifically activate TNFR2 sensitizing cancer cells to TNFR1 mediated apoptosis. It is hence clear that TNFR1 is deemed as target for inclusion in cancer targeted strategies. At the present, researchers are focus on the development of TNFR1-targeted cancer immunotherapies with very promising and encouraging preliminary results (Bremer, 2013, Moran et al., 2013).

Christiana Savva

Hypericum Plant Genus

Hypericum is a plant genus including about 490 species in the family **Hypericaceae** (Clusiaceae). The name Hypericum derives from the Greek name of the plant Hyperikon. The word roots are “hyper” meaning over and “eikon” meaning image. The common name for the plants of this genus is *Saint John's wort*, a name given by early Christians in honor of John the Baptist. In Cyprus and Greece, these plants are acknowledged as balsam or sedge.

Plants of this genus have been used medicinally for at least 2000 years. Many of their therapeutic applications including their uses as antiviral and vulnerary, stem from traditional Greek medicine, originally documented by the ancient Greek medical herbalists Hippocrates, Theophrastus, Dioscorides, and Galen (Bombardelli and Morazzoni, 1995). As practical folk-remedies, they had been widely used for the treatment of cold, chest congestion, burns, asthma, skin problems, menstrual disorders and to alleviate nervous disorders (Bombardelli and Morazzoni, 1995, Wurglics and Schubert-Zsilavecz, 2006).

Nowadays, the species of Hypericum have attract the interest of many chemist because of their well-documented anti-depressive (Wurglics and Schubert-Zsilavecz, 2006, Crupi et al., 2013), anti-tumoral (Masuda et al., 2003b, Tanaka et al., 2009a, Pia Schiavone et al., 2014) and anti-microbial activities (Huang et al., 2013, Pia Schiavone et al., 2014). Furthermore, due to their strong antiviral (Nicolaou et al., 2008, Nicolaou et al., 2011, Chang et al., 2012, Esposito et al., 2013) properties they are under preclinical investigations for the treatment of human immunodeficiency virus (HIV). Of the total species, six species namely *H. chinense*, *H. choisianum*, *H. cordifolium*, *H. monanthemum*, *H. podocarpoides* and *H. trigonum* were identified as rare (Robson, 1985) and four species, *H. choisanum*, *H. oblongifolium*, *H. perforatum* and *H. sampsonii* were recorded as multipurpose species used in pharmaceutical, cosmetics, energy and food industry (Wang et al., 2002).

Christiana Savva

Hypericum chinense (Chinese St. John's wort)

Hypericum chinense (biyouyanagi in Japanese) although is a well-known species of the Hypericum genus, has not been extensively studied. Its formal scientific name is ***Hypericum monogynum*** and it has a list of various comprehensive synonyms including *H. monogynum salicifolium*, *H. salicifolium, H. chinense L. var. salicifolium*, *H. chinense latifolium*, *H. chinense obtusifolium*, *H. chinense salicifolium*, *Komana salicifolia*, and *Norysca chinensis* (Robson, 1985).

Plant description

Hypericum chinense

H. chinense is a perennial, woody, evergreen member of the Hypericum genus. It is an upright plant, about 0.5-1.3 m high with branchy stems in the upper part and irregular twigs. Leaves are simple, narrow, elliptic and oval, with glandular dots containing essential oils. Branched clusters of golden yellow flowers with, long stamens and dark roseate seeds are blossom from June to August (Hsi-wen et al., 2007). It is widely cultivated in China and Japan and is native to North and West Europe, Africa, Asia, Central America and Australia. It can be found in a range of habitats and plant communities, including forest, woodland, rangeland, and prairie communities.

Pharmacology and bioactive constituents

Extracts from *H. chinense* have a long tradition. As folk medicine in Eastern Asia they have being applied in the treatment of hepatitis, acute laryngopharyngitis, conjunctivitis, sepsis, fever and snakebite (Reviewed in (Xu et al., 2015)). In Japan, the plant was prominently used for the treatment of female disorders such as abnormal uterine bleeding, dysmenorrhea and depression-related syndromes (Pinarosa A., 2005).

The pharmacological effects of this herb are related to the active ingredients contained in the plant, some of them are primary metabolites and others are secondary metabolites. The first phytochemical studies on *H. chinense* dates back

Christiana Savva

on 1987, when *Nagai M. & Tada M.* discovered and isolated the antimicrobial phloroglucinols compounds chinesin I and II from the plant's flowers (Nagai and Tada, 1987). Two years later, *Matsuzaki T.* research group came across with a novel spiro-lactone molecule isolated from the stems and leaves of the plant (Tada et al., 1989). Currently, more than ten classes of bioactive compounds, namely polycyclic polyprenylated acylphloroglucinols (PPAPs) (Tanaka et al., 2009a), naphthodianthrones (hypericin), flavonoids (quercetin, quercitrin, hyperoside, rutin, epicatechin) (Wang et al., 2002), procyanidines, phenylpropanes, xanthones, shikimic, and oleanoic acid (Wang et al., 2002) and, essential oils and tannins (Masuda et al., 2003a) have been identified form different parts of the plant. Some of these secondary metabolites exhibit highly interesting biological properties, including antimicrobial activities, cytotoxicity against human tumor cell lines, as well as selective inhibition of HIV-replication. The plant also contains compounds with radical scavenging abilities and strong antioxidant activities (Masuda et al., 2003a).

Notable attention has been given to PPAPs as this special class of complex products it can only be found in the plants of the genus Hypericum (Ciochina and Grossman, 2006). PPAPs display a spectrum of biological activities such as antimicrobial, antioxidant, inhibition of lipid peroxidation, cytotoxic, and anti-HIV activities (Ciochina and Grossman, 2006). Nowadays, hyperforin and adhyperforin, two of the major PPAPs are considered as the main bioactive compounds responsible for the antidepressant effects of *St. John's wort* (Medina et al., 2006, Wurglics and Schubert-Zsilavecz, 2006). Both known (Tanaka et al., 2009a) and unique PPAPs (hypermongones A−J) (Xu et al., 2015) have been isolated and identified in *H. chinense*.

Compare to the others members of its genus, *H. chinense* roots extracts contain unusually high quantities of xanthones, prenylated xanthones and biyouxanthones (Tanaka and Takaishi, 2006, Tanaka and Takaishi, 2007, Tanaka N. et al., 2010) exhibiting significant antidepressant (Muruganandam et al., 2000) and anti-proliferative (Tanaka et al., 2009b) activities. Further investigation of this species has resulted in the isolation of three novel meroterpenoids with a unique dilactone structure, biyoulactones A, B and C (Tanaka et al., 2011). In 2010, *Wang W. et. al*., reported the isolation of a series of novel metabolites from the leaves of the

Christiana Sawa

plant. Among them were two norlignans, hyperiones A-B, and three new acylphloroglucinols, aspidinol C and hyperaspidinols A-B (Wang et al., 2010). Recently, extensive phytochemical analysis of the plant brought up numerous constituents with novel structurally intriguing skeletal motifs. This includes chipericumins A, B, C and D (Abe et al., 2012), tricyclic meroterpenoids, and biyoulactones (Tanaka N. et al., 2012) and rare hypermongones A-J with inhibitory effects on nitric oxide (NO) production (Xu et al., 2015).

Biyouyanagins A and B

As previously mentioned, spiro-lactone-related derivatives were the first compounds to be isolated and characterized in *H. chinense*. Among them, biyouyanagins have attracted much scientific interest because of their fascinating chemical structures and intriguing biological activities. Thus far, two main biyouyanagins were found pure in nature, biyouyanagin A and biyouyanagin B (Figure 9). Worth mentioning here is that *H. chinense* is the only source of biyouyanagins in nature. Biyouyanagins are structural derivatives of terpene, are hydrophobic molecules and contain sesquiterpene (zingiberene), cyclobutane, and spiro-lactone (hyperolactone C) moieties (Figure 9).

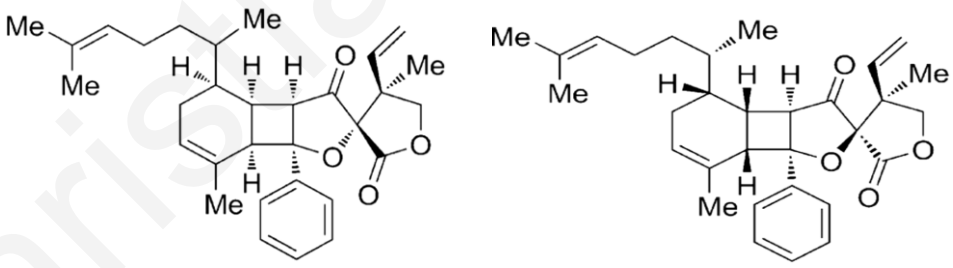

biyouyanagin A **biyouyanagin B**

Figure 9. Chemical structure of biyouyanagin A and B isomeric molecules. The molecules contain sesquiterpene, cyclobutane, and spiro-lactone moieties. Adapted from (Nicolaou et al., 2011).

Biyouyanagin A was first isolated by *Tanaka N.* and co-workers in 2005 while investigating the methanol (MeOH) extract from the leaves of *H. chinense* for new bioactive natural products (Tanaka et al., 2005). This natural molecule showed to possess selective inhibitory activity against HIV replication and lipopolysaccharide

Christiana Savva

(LPS)-induced cytokine production (Tanaka et al., 2005). More specific, the molecule inhibited the HIV replication in H9 lymphocytes with an EC_{50}† value of 0.79 μg/ml, whereas at 10 μg/ml it inhibited the LPS-induced production of interleukins IL-10, IL-12 and TNFα.

Few years later, *Nicolaou K.C.* achieved biyouyanagin A total synthesis, establishing a 24-epimer absolute configuration (Nicolaou et al., 2007), as well as revision and determination of its stereochemistry and synthesis of several analogues (Nicolaou et al., 2008). Comparison studies of the newly synthesized biyouyanagin A analogues with hyperolactone C analogues, brought to the light significant information regarding the structure-activity relationships (SAR) of the molecule (Nicolaou et al., 2008, Tanaka et al., 2009a). Researchers observed that, hyperolactone C and some of its analogues displayed comparable, and in some cases more potent, anti-HIV activities (IC_{50}‡ = 12 - 29 μM) than biyouyanagin A and its analogues (IC_{50} = 19 - 31 μM) (Nicolaou et al., 2008). Moreover, biyouyanagin A was evaluated for its cytotoxicity against human cancer cell lines including multiply drug-resistant (MDR) cell lines; KB-C2 (colchicine resistant skin carcinoma) and K-562/Adr (doxorubicin resistant CML) (Tanaka et al., 2009a). The compound displayed a moderate cytotoxicity in all cell lines tested with an IC_{50} between 16.6 and 38.8 μM. Similar results against MDR cancer cell lines were evident in hyperolactones A, C and D and in 4-hydroxyhperolactone (Tanaka et al., 2009a). Conclusively, the above findings argue that, biyouyanagins biological activities might reside in their spiro-lactone (hyperolactone C) structural domain.

Following *Nicolaou K.C.* photocycloaddition§ synthesis of biyouyanagin A, *Tanaka N.* achieved the isolation of a second biyouyanagin molecule named, biyouyanagin B (Tanaka et al., 2009a) (Figure 9). This new molecule, proved to be a stereoisomer of biyouyanagin A. It has identical molecular formula ($C_{31}H_{38}O_4$) and sequence of atoms to that of biyouyanagin A but differs in the three-dimensional positioning of atoms in space (Figure 9). The structure of biyouyanagin B was

† Half maximal effective concentration

‡ Half maximal inhibitory concentration

§ Cycloaddition-type reaction that entails the formation of new molecules by the reaction of two unsaturated molecules via two atoms from each molecules ([2+2]). In the thermal process a form of light is used.

further revised and several new biyouyanagins, including biyouyanagin C, were synthesized (Nicolaou et al., 2010). The novel biyouyanagins have not yet been discovered in nature but are believed to physically exist based on biosynthetic considerations.

Been recently discovered, there is limited information about the biological properties of biyouyanagins B and C apart, from their anti-HIV activity. Both isomers were found to evoke prominent activity against HIV with IC_{50} values of 42.9 μM and 83.9 μM, respectively (Nicolaou et al., 2011, Chang et al., 2012). What is more important, the two isomers were more effective than biyouyanagin A which, in the same bioassay exhibited an IC_{50} near to 123.4 μM (Nicolaou et al., 2011, Chang et al., 2012). Biyouyanagin B along with biyouyanagin A, were also examined for their potential against LCMV (lymphocytic choriomeningitis virus), the prototype member of the arenavirus family that includes several causative agents of deadly hemorrhagic fever disease. The two molecules exhibited significant activity against LCMV by preventing its replication and gene expression in the middle micromolar range (~50 μM) (Nicolaou et al., 2011). Both the anti-HIV and anti-LCMV mechanisms of action of biyouyanagins remain to be elucidated.

Biyouyanagin analogue 53 (KC-53)

With such unique molecular architecture and important biological properties, biyouyanagin A received notoriety as prominent synthetic target. Our collaborator *Nicolaou K.C.,* once he had completed synthesizing the molecular framework of biyouyanagin structure (Nicolaou et al., 2007, Nicolaou et al., 2008), he moved towards exploring the molecular space around this structure in an attempt of discovering simpler structures with enhanced biological activities (Nicolaou et al., 2011, Chang et al., 2012). By applying developed synthetic technology he companied a variety of different building blocks achieving the design of a library consisting of 64 novel molecules; 22 biyouyanagins, 14 hyperolactone C analogues and 28 biyouyanagin analogues molecules.

The members of the newly-synthesized compound library were subjected for their anti-viral and anti-inflammatory properties through a series of experiments. The comprehensive results of this study revealed a promising new lead molecule; the

Christiana Saiya

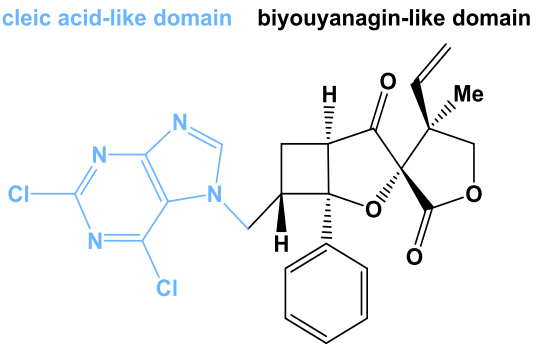

Figure 10. Chemical structure of biyouyanagin analogue 53 (KC-53). The compound consists of a biyouyanagin- and a nucleic acid-like moieties.

post-photocycloaddition modified biyouyanagin analogue 53, hence KC-53 (Figure 10). KC-53 exposed higher anti-HIV potencies than biyouyanagins A and B, and was the most active compound from the entire library (Nicolaou and Kannas, 2011, Nicolaou et al., 2011, Chang et al., 2012). However, in comparison to the well-known HIV drug AZT (Zidovudine), KC-53 was less efficacious as AZT exhibited an IC_{50} of 0.056 μM whereas KC-53 an IC_{50} of 7 μM. On the contrary, in the anti-inflammatory tests, KC-53 proved to be equally potent as the commercially available products. In the LPS-induced cytokine assay, the agent elicited selective effects on the production of specific anti-inflammatory cytokines (Chang et al., 2012). Precisely, in THP-1 human macrophage cells, KC-53 at 10 μM inhibited the production and secretion of cytokines IL-6, IL-1β, and TNFα by 90 - 96%. In addition, no effect on the production of cytokines IL-1α and IL-8 was observed. Up until now, the agent has not been evaluated for any other biological properties. The investigation of this novel agent and the further examination of its anti-tumor properties are especially appealing and challenging.

KC-53 was obtained from biyouyanagin analogue 37 after post [2+2] photocycloaddition modifications (Figure 11). The one side of its structure, is principally the same as that of a natural biyouyanagin (biyouyanagin-like domain), while the other side, is a structural motif like the nitrogenous bases found in DNA (nucleic acid-like domain) (Figure 10). Whether its biological properties are primarily derived from its dichloronucleobase- or its biyouyanagin-like domain or both remains an open issue at the present.

Christiana Sawa

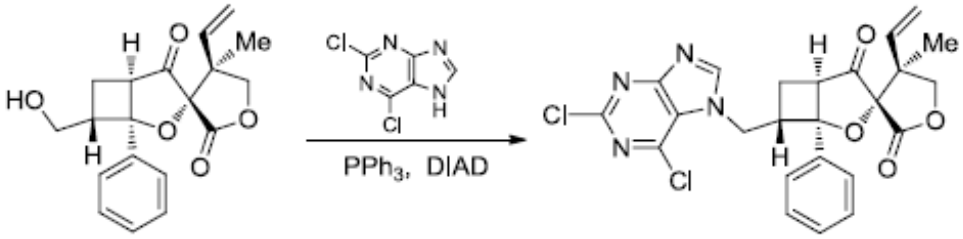

analogue 37 **KC-53**

Figure 11. Preparation of post [2+2] modified biyouyanagin analogue 53 (KC-53). PPh3; Triphenylphosphine, DIAD; Diisopropyl azodicarboxylate. Adapted from (Nicolaou et al., 2011).

Without literature available information concerning the physicochemical properties of the agent, we followed an *in silico*-based approach in order to define some of its basic characteristics. Our previous experience in computer-aided drug discovery techniques and in predictive models design[**] (Kannas et al., 2015), enabled us to estimate the druglikeness of KC-53. With the use of LiSIs predictive tool[††] which was developed based on the *Lipinski's rule of five* for oral drugs, we achieve to determine the drug-like properties of KC-53 (Table 3) (unpublished data). According to the *Lipinski's rules* (Lipinski, 2004) a compound is more likely to be membrane permeable if it meets the following criteria:

- a molecular weight less than 500 daltons
- no more than 5 hydrogen bond donors (nitrogen or oxygen atoms with one or more hydrogen atoms)
- not more than 10 hydrogen bond acceptors (nitrogen or oxygen atoms)
- a polar surface area no greater than 140 Å^2
- a lipophilicity (expressed as logP) less than 5

As was proven, KC-53 matches all the above physicochemical criteria (Table 3) especially those of lipophilicity as is the most important physical property of a drug in relation to its absorption, distribution, potency, and bioavailability. What is more, these findings are signifying the potential pharmacological use of this lead compound and may be valuable for the future development of drugs. Therefore,

[**] GRANATUM Platform (*http://www.granatum.org/pub/)*

[††] Galaxy Platform; Life Sciences Informatics Systems (LiSIs) Tools (*http://lisis.cs.ucy.ac.cy/root*)

pharmacokinetic and metabolism studies are necessary to be performed and define the pharmaceutical importance and prospects of this novel agent.

Table 3. KC-53 drug-like properties

Property	Value
Molecular Weight (MW)	498
Hydrogen Bond Donors (HBD)	0
Hydrogen Bond Acceptors (HBA)	7
Topological Polar Surface Area (PSA)	74.64 A^2
Octanol Water Partition coefficient (LogP)	3.52

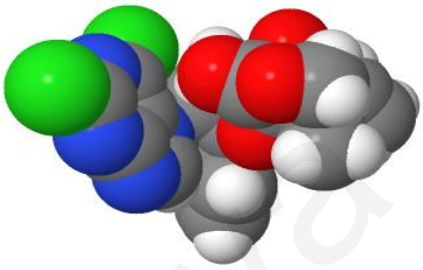

3D Structure of KC-53

The drug-like properties of KC-53 were estimated with the use of LiSIs predictive tool. The three-dimensional (3D) structure of the molecule was generated using CORINA online software[‡‡] (green; Cl, blue; N, white; H, red; O, gray; C).

Christiana Savva

[‡‡] *https://www.molecular-networks.com*

Project Hypothesis and Aims

Apoptosis evasion is a hallmark of cancer and has been connected to cancer pathogenesis, progression and chemoresistance (Gerl and Vaux, 2005). Elimination of cells bearing activated oncogenes or stimulation of tumor suppressor mediators may provide a selection pressure to overcome resistance. TNFR1 fine-tuning might be of significant importance in cancer treatment, as switching the balance between the TNFR1 pro-survival/NF-κB and pro-apoptotic/Caspase-8 axis in support of the latter, can restore the apoptotic defense mechanism (Bremer, 2013). Based on the above literature information and considering the key role of NF-κB in the inflammatory response (Xiao and Ghosh, 2005), we **hypothesized** that, KC-53 with documented anti-inflammatory properties (Nicolaou et al., 2011) may exhibit pro-apoptotic efficacy mediated through its interference with the TNFR1/NF-κB pathway. In this study we used a panel of human cancer cell lines in order to examine the antitumor activity of KC-53 and unravel its underlying mechanism of action. Following extensive and systematic investigation, we report for first time the anticancer efficacy of KC-53 and the mechanism of its dual anti-proliferative and pro-apoptotic action in cancer cells. To examine our hypothesis we evaluated the following specific aims:

Specific Aim 1: To investigate the anti-proliferative potency of KC-53 in normal and cancer human cell lines

Evaluation of KC-53 cytotoxic effects

The effects of KC-53 on cell viability have not been investigated in any cancer type. In this study we assessed the anti-proliferative effect of KC-53 by using a panel of human cancer cell lines and normal or immortalized cells. In particular we determined (i) the most sensitive and most resistant cell lines and (ii) the optimal concentration of the agent that is selectively cytotoxic to cancer cells but not in normal cells. The two most sensitive cell lines were selected to further investigate the anticancer mode of action of KC-53.

Identification of KC-53 cytostatic activity

Decrease in cell viability can be caused either by delayed cell cycle progression or by increased cellular death, or both. To investigate this, we implemented cell cycle

Christiana Savva

analysis after administration of KC-53 to HL-60 and CCRF/CEM acute leukemia cells as well as in normal PBMC cells.

Specific Aim 2: To examine the mechanism by which KC-53 induces apoptosis

Quantification of apoptotic effect induced by KC-53 in acute leukemia and normal cells

The apoptotic potency of the agent was quantified in leukemic cells by assessing DNA fragmentation, as well as Annexin V and Propidium Iodide (PI) staining which serve as molecular markers of apoptosis for the quantification of early and late apoptotic cells correspondingly. Apoptosis quantification was also determined by the COMET assay, a method that enables the measurement of DNA strand breaks and DCFH-DA assay for the detection of reactive oxygen species (ROS) which cause DNA oxidative damage.

Evaluation of the expression, activity and sub-cellular distribution of proteins involved in apoptotic signaling pathways

The two major pathways that are involved in apoptosis are the intrinsic/mitochondrial pathway and the extrinsic/death receptor pathway. To investigate which apoptotic pathway is activated by KC-53, we determined the effect of KC-53 on the activation of initiator and effector Caspases, as well as, on the membrane and cytosolic levels of death receptors (DRs) and their adaptor molecules. In addition, we examined the effect of the agent on the levels of activated Caspase-8 and on its substrate Bid. The sub-cellular distribution of AIF endonuclease, which translocates from mitochondria to the cytosol and therefore to the nucleus during CI-PCD, was also investigated in the presence of KC-53.

Specific Aim 3: To evaluate the effect of KC-53 on TNFR1 signaling pathways

Investigation of the mechanism by which KC-53 hinders the NF-κB cascade

Based on the results of Specific Aim 2 where we evaluated the effect of KC-53 on the activation of the extrinsic apoptotic pathway, we further investigated the TNFR downstream events. Activation of NF-κB signaling is initiated by extracellular stimuli including TNFα. These stimuli are recognized by TNFR1 and transmitted

Christiana Savva

into the cell, where adaptor signaling proteins initiate the signalling cascade. In order to examine these pathways, we initially determined the expression levels of FADD and RIP1, and therefore the phosphorylation and total levels of TRAF2 and IκBα proteins.

Evaluation of the NF-κB sub-cellular localization and transcriptional activity

The sub-cellular localization of p65/NF-κB was investigated by immunoblotting and immunofluorescence while its transcriptional activity was evaluated by determining the mRNA levels of selected p65 target genes using RT-PCR methodology.

Specific Aim 4: To investigate the effect of KC-53 on molecules involved in apoptosis

As a final point, we performed loss- of function studies in order to evaluate the proposed molecular mechanism of action of KC-53. For this purpose, we generated transiently transfected cell lines in order to manipulate the expression levels of candidate proteins.

Christiana Savva

Chapter II: Materials and Methods

Synthesis of KC-53

KC-53 was prepared by *Nicolaou K.C.* laboratory as previously described (Nicolaou et al., 2011).

Chemicals and Reagents

Fetal bovine serum (FBS), horse serum (HS), antibiotic/antimycotic, epidermal growth factor (EGF), insulin, cholera toxin, hydrocortizone, L-glutamine, HEPES, Sodium Pyruvate and media used in cell culture were purchased from Gibco, Invitrogen (Carlsbad, California, USA). Etoposide and doxorubicin were purchased from Tocris (Bristol, UK). The pan caspase inhibitor, z.vad.fmk was purchased from Sigma (St. Louis, Missouri, USA). TNFα, and PS-341 (Bortezomib) were purchased from Merck Millipore (Darmstadt, Germany). Protease inhibitor cocktail was obtained from Roche (Indianapolis, IN). Caspase -3, -7, -8, -9, PARP1, RIP1, Bid, AIF, TNFR1, TNFR2, Fas, DR3, DR5, DcR3, TRADD, FADD, p-IκBα, p-TRAF2, NF-κB/p65 and α-Tubulin antibodies were purchased from Cell Signaling Technology (Danvers, Massachusetts, USA). Total TRAF2, total IκBα, Bax, Bcl-2, total and p-p53, total and p-JNK, EGFR, Histone H3 and GAPDH antibodies were obtained from Santa Cruz Biotechnology (Heidelberg, Germany). All other reagents were purchased from Sigma (St. Louis, Missouri, USA).

Cell Culture

MCF-7, MDA-MB-231-TXSA, MCF-12F, A-549, PC-3, LoVo, Ishikawa, KHOS, STSA, Jurkat, HL-60, CCRF/CEM, Raji and Daudi were obtained from the American Type Culture Collection (ATCC) (Manassas, VA). PBMCs were isolated from the blood of healthy, non-smokers volunteers based on the Cyprus National Bioethics Committee (CNBC) regulations.

MCF-7, MDA-MB-231-TXSA, STSA, LoVo, Ishikawa and KHOS cells were cultured in DMEM supplemented with 10% FBS, 1% antibiotic/antimycotic and 4

Christiana Savva

mM L-glutamine, PC-3, A-549, Jurkat, HL-60, CCRF/CEM, Raji and Daudi in RPMI supplemented with 10% FBS, 1% antibiotic/antimycotic and 4 mM L-glutamine, and MCF-12F in DMEM-F12 supplemented with 20 ng/ml EGF, 100 ng/ml cholera toxin, 500 ng/ml hydrocortizone, 10 µg/ml insulin, 5% HS and 1% antibiotic/antimycotic. All cells were cultured in 95% air, 5% CO_2, 37 °C. For cryopreservation cells were suspended in freeze medium comprising by complete growth medium supplement with 5% (v/v) dimethyl sulfoxide (DMSO) and stored in liquid nitrogen.

Isolation of Human Peripheral Blood Mononuclear Cells (PBMCs)

Human normal PBMCs were isolated from heparinised venous blood samples of healthy, nonsmoker volunteers by density gradient centrifugation method using Ficol-Histopaque (Sigma). The heparinised blood was layered on Histopaque in the ratio of 1:1 and subjected to centrifugation at 2,000 rpm, for 30 min at room temperature (RT). The white layer representing PBMCs was collected with the use of an 18G syringe and transferred to new tube. The suspension of cells was washed twice with 1X PBS followed by centrifugation at 2,000 rpm, for 10 min at RT. Cell pellet (PBMCs) was cultured in RPMI supplemented with 10% FBS, 1% antibiotic/antimycotic and 4 mM L-glutamine. After 24 h incubation (95% air, 5% CO_2, 37 °C) non adherent cells (B- and T-cells) were collected and maintained in RPMI supplemented with 10% FBS, 1% antibiotic/antimycotic, 4 mM L-glutamine and 100 ng/mL TNFα.

Proliferation Assay

A total of $1x10^4$ cells were seeded per well of a 96-well plate in 200 µl medium supplemented with the appropriate agent(s) or vehicle control(s) as described in the figure legends. At the end of each incubation period, 3-(4,5-dimethylthiazol-2-yl)-2,5-diphenyltetrazolium bromide (MTT) at a final concentration of 0.5 mg/ml was added to the medium and left to be metabolized for 3 h. Following that, plates were centrifuged at 1,500 rpm, for 5 min. The medium was removed and 150 µl of DMSO were added in each well and incubated on a microplate shaker under gently shaking (250 rpm) for 20 min at RT. The absorbance measured at 570 nm, was proportional to the number of viable cells per well.

Christiana Sava

Table 4. **Features of the cell lines used**

Cell Line	Tissue	Morphology	p53[§§]	Disease
Hl-60	PB	promyeloblast	-/-	Leukemia (APL)
CCRF/CEM	PB	T lymphoblast	+/+	Leukemia (T-ALL)
LoVo	Colon (metastatic)	E	wt	Colorectal Adenocarcinoma
Jurkat	PB	T lymphoblast	+/+	Leukemia (T-ALL)
Daudi	PB	B lymphoblast	wt/+	Burkitt's Lymphoma
KHOS	BM	F, E	wt/+	Osteosarcoma
MDA-MB-231-TXSA	Breast (metastatic site)	E	wt/+	Breast Adenocarcinoma
STSA	Stomach	E	n/a	Gastric Adenocarcinoma
MCF-12F	Breast	E	wt/+	Normal
Raji	BM	B lymphoblast	+/+	Burkitt's Lymphoma
A549	Lung	E	wt	Lung Carcinoma
Ishikawa	Uterus (metastatic site)	E	wt/+	Endometrial Adenocarcinoma
PC-3	Prostate (metastatic site)	E	-/+	Prostate Adenocarcinoma
MCF-7	Breast	E	-/+	Breast Adenocarcinoma
PBMCs	PB	B and T lymphocytes	wt	Normal

PB, peripheral blood; BM, bone marrow; E, epithelial; F, fibroblast; wt, wild type; -, deletion or rearrangement; +, mutation; n/a, not available

[§§] Data adapted from UMD TP53 mutation database (*http://p53.free.fr*)

Cristiana Sava

Cell Cycle Analysis

Cells were seeded at a concentration of $1x10^6$ per a 100 mm plate and treated with KC-53 for the indicated concentrations and times at 37 ^oC. Following incubation, samples were harvested by centrifugation at 1,500 rpm, for 5 min at 4 ^oC and washed with ice cold PBS. Cells resuspended in ice cold PBS were fixed in 70% ethanol and stored at 4 ^oC. After 24 h, cells were harvested by centrifugation at 1,500 rpm, for 5 min at 4 ^oC and washed with ice cold PBS followed by centrifugation at 1,500 rpm, for 10 min at 4 ^oC. Afterward, cells were stained with 300 µl of propidium iodide (PI) staining solution (0.2 mg/ml RNase A, 0.01 mg/ml PI in PBS) and incubated for 15 min at 37 ^oC. Samples were analyzed for DNA content using the Guava EasyCyte™ flow cytometer and the GuavaSoft analysis software (Millipore, Watford, UK).

Annexin-V/PI Staining

Cells were seeded at a concentration of $1x10^6$ cells per a 100 mm plate and treated with KC-53 or doxorubicin (Dox) as indicated. Following incubation cells were harvested by centrifugation at 1,500 rpm, for 5 min at 4 ^oC. Subsequently, cells were washed with ice cold PBS followed by centrifugation at 1,500 rpm, for 5 min and stained using Annexin-V Alexa Fluor® 488/PI, as described by the Tali™ apoptosis kit (Life Technologies, Carlsbad, CA). In brief, cells were resuspended in Annexin binding buffer (ABB), so that there is at least 100 µl of cells per individual assay at a concentration of approximately $5x10^5$ -$5x10^6$ cells/ml. Then, 5 µl of Annexin-V was added to each sample and incubated in the dark, for 20 min at RT. Cells were then centrifuged at 1,000 rpm, for 15 min and resuspended in 100 µl of ABB. To each sample, 1 µl of PI was added and incubated in the dark, for 1-5 min at RT. Cell viability, death and apoptosis were evaluated using the Tali™ Image-based Cytometer (Life Technologies, Carlsbad, CA). The Annexin-V(+)/PI(-) cells were recognized as early apoptotic cells by the cytometer software whereas, the Annexin-V(+)/PI(+) cells were identified as late apoptotic/dead cells. Similarly, the Annexin-V(-)/PI(-) cells were identified as viable cells.

Christiana Savva

Cell Death/DNA Fragmentation Detection Analysis

Cells were added at a concentration of $1x10^4$ cells per well of a 96-well plate and treated with KC-53 in the present or absence of pan-caspase inhibitor, z.vad.fmk as indicated. The quantification of mono- and oligo-nucleosomes present in the cytoplasm of apoptotic cells was performed using the Cell Death ElisaPLUS Apoptosis Kit according to the manufacturer's instructions (Roche). Briefly, after incubation plate was centrifuged at 1,500 rpm, for 8 min and cells were resuspended in 200 µl Lysis buffer and incubated for 30 min at RT. Lysates were then centrifuged at 200 g, for 10 min and 20 µl of the supernatant (cytosolic fraction) were transferred into streptavidin coated wells. Following that, 80 µl of Immunoreagent (Anti-histone-biotin, Anti-DNA-peroxidase in Incubation buffer) were added to each sample and incubated on a microplate shaker under gently shaking (300 rpm), for 2 h at RT. Afterwards, solution was removed and each well was washed with 300 µl of Incubation buffer. Peroxidase substrate was then added and incubated under gently shaking (250 rpm), for 20 min at RT. After incubation, 100 µl of Stop solution were added and absorbance was measured at 405 nm (against substrate) and 490 nm (against Stop solution) wavelengths. The background value was subtracted (Oncubation buffer + Stop solution) and the specific enrichment of mono- and oligo-nucleosomes was cexpressed as absorbance of treated cells to absorbance of corresponding negative control using the formula:

$$Enrichement\ Factor = \frac{mU\ of the\ sample}{mU\ of\ the\ corresponding\ negative\ control}$$

mU = absorbance

Measurement of Intracellular ROS Generation

Reactive oxygen species (ROS) generation was determined by performing 2,7-dichlorodihydrofluorescin (DCFH-DA) assay. The generation of ROS promotes the conversion of the non-fluorescent DCFH to the highly fluorescent 2,7-dichlorodihydrofluorescein (DCF). The fluorescence intensity (F.I.) is proportional to the ROS levels within the cytosol. Cells were seeded at a concentration of $4x10^4$ per well of a 12-well plate and DCFH-DA at a concentration of 100 µM was added and incubated for 1 h at 37 ºC. Following that, plates were centrifuged at 1,500

Christiana Sawa

rpm, for 5 min. The medium was removed and fresh medium containing KC-53 was added to the cells. Sodium pyruvate (SP) at 1 mM was used as negative control while, H_2O_2 at 100 µM was used as positive control. Cells were incubated for various interval time points (0-24 h) at 37 ºC and fluorescence was measured in a fluorometric plate reader (Infinite 200, Tecan Systems Inc., CA, USA) at 485 nm excitation/535 nm emission wavelengths.

DNA Damage Analysis - Comet Assay

Cells ($1x10^{5)}$ were seeded in a 60 mm plate and treated with KC-53 for the indicated time points. Cells were also treated with 100 µM hydrogen peroxide (H_2O_2) for 30 min as a positive control. Following incubation, samples were harvested by centrifugation at 1,500 rpm, for 5 min at 4 °C. Cells were washed and re-suspended in 100-200 µl ice cold PBS. Using 50 µl of cell suspension, cells were mixed with low melting point agarose in a ratio of 1:10, applied to a CometSlide (Trevigen Inc., Gaithersburg, MD) and allowed to set for 30 min at 4 ºC. Slides were immersed in a gentle Lysis solution (Trevigen Inc.) for 1 h at 4 ºC., washed with ice cold ddH_2O, and submerged in alkaline electrophoresis buffer (1 mM EDTA, 300 mM NaOH, pH>13) at RT for 40 min. Following that, slides were electrophoresed in alkaline solution at 1 V/cm (30V), 300-350 mA, for 30 min at 4 ºC. After electrophoresis, slides were rinsed in ice cold ddH_2O and submerged in 70% ice cold ethanol for 5 min and allowed to completely air dry. Samples were stained with 50 µl of 1XSYBR Green I (Invitrogen), and data was visualized by epifluorescence microscopy (excitation 494 nm, emission 521 nm). Cells were given a qualitative score between 0 and 4 based on the overall size of their tail. DNA damage score was calculated based on the equation:

$$\frac{\Sigma(0 * n0 + 1 * n1 + 2 * n2 + 3 * n3 + 4 * n4)}{N} \times 100$$

Where, n0 was the number of cells with a score of 0, n1 was the number of cells with a score of 1, and so on, and N was the total number of cells counted. Duplicate samples were prepared for each treatment, and at least 200 cells were scored for each sample.

Chrisdana Saiya

Caspase-8 Enzymatic Activity

Caspase-8 activity was measured using the fluorogenic substrate IETD-AFC (KHZ0052) according to the manufacturer's instructions (Invitrogen). In brief, a total of $2x10^6$ cells were treated as indicated in figures legends. Following incubation, cells were harvested by centrifugation at 1,200 rpm, for 5 min at 4 ^oC and washed with ice cold PBS followed by centrifugation at 1,200 rpm, for 5 min at 4 ^oC. Cell pellets were resuspended in Lysis buffer and incubated on ice for 10 min. Lysates were centrifuged at 11,000 rpm, for 5 min at 4 ^oC. The supernatant (cytosolic fraction) was collected to new tubes and protein concentration was determined for each extract using Bradford reagent. Afterward, 50 µg of protein per 50 µl of each sample were added in the wells of a black 96-well plate already containing 50 µl of the Reaction buffer. IETD-AFC substrate was added to the extract at 50 µM final concentration followed by incubation in the dark, for 1.5 h at 37 °C. Caspase enzymatic activity was measured by monitoring the release of fluorigenic 7-amino-4-trifluoromethylcoumarin (AFC) using an auto-microplate reader (Infinite 200, Tecan Systems Inc., CA, USA) at 400 nm excitation/505 nm emission wavelengths, slit width 15. Fold-increase in Caspase-8 activity was determined by direct comparison to the level of the uninduced control.

Immunofluorescence Cell Staining

Cells were seeded on glass coverslips (charged with HCl and 0.01% poly-L-lysine solution), washed 3 times with PBS and incubated as descripted in figure legends. Following incubation, cells were washed with PBS, fixed for 10 min in 4% paraformaldehyde (PFA), 10 min in 50 mM glycine solution and permeabilized with 0.1% Triton X-100 for 10 min. Fixation was followed by blocking using 10% normal horse serum (Gibco) in PBS for 30 min. Cells were incubated with NF-κB/p65 (D14E12) (Cell Signaling Technology) primary antibody at a dilution 1:400 in PBS containing 10% horse serum at RT for 1.5 h. Following several washes with PBS, fluorescein isothiocyanate-conjugated secondary antibody, Cy3 anti-rabbit (Jackson ImmunoResearch, West Grove, PA, USA) in blocking solution was added and incubated at RT for 1 h. Actin labeling was performed using Alexa Fluor Phalloidin 488 (Invitrogen). The slides were then with PBS and nuclei was counterstained using 0.1 µg/ml of 4',6-diamidino-2-phenylindole (DAPI) (Tocris) at

Christiana Savva

RT for 15 min. Subsequently, the stained samples were washed with PBS, mounted using one drop of ProLong Gold Antifade Mountant (Invitrogen) and stored at 4 ºC overnight. Images were acquired using a Zeiss AxioImager Z1 fluorescence microscope (Germany) equipped with a Zeiss Axiocam MR3 and using the Axiovision 4.8 software.

RNA Isolation

Total RNA was extracted with Trizol reagent (Invitrogen). Approximately $1x10^5$ cells were plated in 60 mm dishes and treated as described in figure legend. After treatment, cells were harvest by centrifugation at 1,500 rpm, for 5 min at 4 °C, washed with ice cold PBS and re-centrifuged under the same conditions. PBS was removed and Trizol was added and incubated at RT for 5 min. Next, 200 ul of chloroform were added and samples were incubated at RT for 2-3 min. Samples were then centrifuged at 12,000 rcf, for 15 min at 4 ºC. Following centrifugation the upper aqueous phase (containing the RNA) was transferred into clean tubes, mixed with 500 µl of isopropanol and allowed to incubate at RT for 10 min. Following that, samples were centrifuged at 12,000 rcf, for 10 min at 4 ºC. Formed RNA pellet was washed with 75% ethanol and centrifuged at 7.500 g, for 5 min at 4 ºC. RNA pellet was then air-dried, dissolved in 20 µl DNase/RNase-free H_2O and stored at -80 ºC. Total RNA concentration was determined using NanoDrop 2000 spectrophotometer. The ratio of absorbance at 260 nm and 280 nm was used to assess the purity of RNA ($A_{260/280}$ ~2.0).

cDNA Synthesis

Complementary DNA (cDNA) was synthesized with random and oligo(dT) primers using the PrimeScript Reverse Transcriptase (2680A) according to the manufacturer's instructions (TaKaRa Bio. Inc, Dalian, China). In brief, 1 µg of total RNA was mixed with random and oligo(dT) primers (50 pmol each), dNTP mixture (10 mM each) and DNase/RNase free H_2O. Samples were incubated at 65°C for 5 min and then on ice for at least 1 min. Reaction was prepared by adding to the RNA mixture 1XFirst Strand buffer, 5 mM DTT, 20 units RNase Inhibitor and 200 units PrimerScript Reverse Transcriptase. The standard reaction volume was 20 µl. Reverse transcription reaction was performed under the following condition:

Christiana Sava

incubation at 30 ºC for 10 min, incubation at 50 ºC for 60 min and incubation at 70 ºC for 15 min. cDNA was stored at -20 ºC and total concentration was estimated by measuring the absorbance at 260 nm.

Quantitative Real-Time PCR (RT-qPCR)

Primer sequences were designed using Primer3 and are shown in Table 5.Real-time RT-PCR was performed using the BioRad CFX96 Real-Time System and the SYBR Green PCR Master Mix (Kapa Biosystems, Massachusetts, USA) according to the manufacturer's instructions. The standard reaction volume was 10 μl and contained 1 μl of primers pool mix (40 ng/μl each), 1 μl of cDNA (100 ng), 5 μl of SYBR Green PCR Master Mix and 3 μl DNase/RNase free H_2O. The reaction was performed in optical 96-well fast thermal cycling plates and all reactions were performed in duplicates. The thermal-cycling conditions were the following: incubation at 95 ºC for 10 min, followed by 40 cycles of amplification. Each cycle consisted of 15 sec melt at 95 ºC, followed by 30 sec annealing/extension at 60ºC. The PCR products were normalized to those obtained from GAPDH mRNA amplification and cDNA was quantified using the following equations:

$$\Delta\mathrm{CT} = \mathrm{CT1} - \mathrm{CT2}$$

Where, CT1 refers to the gene of interest and CT2 to the reference gene

$$\Delta\Delta\mathrm{CT} = \Delta\mathrm{CT1} - \Delta\mathrm{CT2}$$

Where, ΔCT1 refers to the treated cells and ΔCT2 to the untreated vehicle control

$$\text{Fold change in cDNA levels} = 2 - (\Delta\Delta\mathrm{CT})$$

RNA Interference

FADD siRNA (sc-35352) and negative control siRNA (sc-37007) were purchased from Santa Cruz Biotechnology. For the transfection procedure, HL-60 and CCRF/CEM cells were seeded at a concentration of $4x10^5$/ml per well of a 12-well plate and FADD siRNA or control siRNA were transfected with the use of LipofetamineTM 2000 (Invitrogen) and siRNA Transfection Reagent (sc-29528) (Santa Cruz Biotechnology) correspondingly. The final concentration of siRNA in each well was 100 nM.

Christiana Savva

Table 5. Nucleotide sequences of PCR primers

Gene	Forward Primer	Reverse Primer
IL-1β	$^{5'}$TCCAGCTACGAATCTCCGAC$_{3'}$	$^{5'}$ACCAGCATCTTCCTCAGCTT$_{3'}$
IL-6	$^{5'}$AGTCCTGATCCAGTTCCTGC$_{3'}$	$^{5'}$CATTTGTGGTTGGGTCAGGG$_{3'}$
IL-8	$^{5'}$CAGTTTTGCCAAGGAGTGCT$_{3'}$	$^{5'}$TTGGGGTGGAAAGGTTTGGA$_{3'}$
BCL-xL	$^{5'}$TAAACTGGGGTCGCATTGT$_{3'}$	$^{5'}$TGGATCCAAGGCTCTAGGTG$_{3'}$
BCL-2	$^{5'}$CAGCCCAGACTCACATCACC$_{3'}$	$^{5'}$CATGTGTGTGGAGAGCGTCA$_{3'}$
BCL-3	$^{5'}$AAGAAACCGTGCAGCTCTTG$_{3'}$	$^{5'}$CCGCTCTTAATGTCCACTGC$_{3'}$
MCL-1	$^{5'}$ATGCCAAACCAGCTCCTACT$_{3'}$	$^{5'}$GCTGCATCGAACCATTAGCA$_{3'}$
XIAP	$^{5'}$TGGGGTTCAGTTTCAAGGAC$_{3'}$	$^{5'}$TGCAACCAGAACCTCAAGTG$_{3'}$
cIAP1	$^{5'}$GCATTTTCCCAACTGTCCAT$_{3'}$	$^{5'}$ATTCGAGCTGCATGTGTCTG$_{3'}$
cIAP2	$^{5'}$GCATTTTCCCAACTGTCCAT$_{3'}$	$^{5'}$ATTTTCCACCACAGGCAAAG$_{3'}$
cFLIP	$^{5'}$TGTGCCGGGATGTTGCTATA$_{3'}$	$^{5'}$CCGACAGACAGCTTACCTCT$_{3'}$
Survivin	$^{5'}$GACGACCCCATAGAGGAACA$_{3'}$	$^{5'}$GACAGAAAGGAAAGCGCAAC$_{3'}$
FADD	$^{5'}$ACACAGAGAAGGAGAACGCA$_{3'}$	$^{5'}$GCCTGCTGAACCTCTTGTAC$_{3'}$
GAPDH	$^{5'}$CTGACTTCAACAGCGACACC$_{3'}$	$^{5'}$AAAGTGGTCGTTGAGGGCA$_{3'}$

LipofetamineTM 2000 Protocol

For each transfection sample oligomer-Lipofectamine complexes were prepared as follows: (a) siRNA was diluted in 100 µl Opti-MEM (or RPMI serum/antibiotics free) (b) 2 µl Lipofectamine reagent were diluted in 100 µl Opti-MEM (or RPMI serum/antibiotics free), mix gently and incubated for 20 min at RT. The siRNA and Lipofectamine reagent were then combined and the mixture was incubated for 30 minutes at RT. The oligomer-Lipofectamine complexes were transferred on wells already containing 800 µl cells (suspended in RPMI supplement with 1% FBS and free of antibiotics) and incubated for 24 hours.

siRNA Transfection Reagent Protocol

For each transfection sample the following solutions were prepared as follows: (a) siRNA was diluted in 100 µl siRNA Transfection Medium (or RPMI serum/antibiotics free) (b) 6 µl siRNA Transfection Reagent were diluted into 100 µl siRNA Transfection Medium (or RPMI serum and antibiotics free). The two solutions were combined and the mixture was incubated for 30 min at RT. The siRNA-Transfection Reagent mixture was then transferred on wells and 800 µl cells (suspended in RPMI supplement with 1% FBS and antibiotics free) were added (reverse transfection). Cells were incubated for 24 hours and then assayed with the appropriate protocol.

Christiana Sava

Preparation of Whole Cell Extract

A total of $2x10^6$ cells were treated as indicated. After incubation cells were harvested by centrifugation at 1,500 rpm, for 5 min at 4 °C and washed with ice cold PBS. Cells were lysed with ice cold RIPA buffer (150 mM NaCl, 50 mM Tris, 50 mM EDTA, 1% (v/v) Triton X-100, 0.1% (w/v) SDS, protease inhibitors, phosphatase inhibitors; 5 mM NaF, 1 mM Na_3VO_4) and incubated at 4 °C for 10 min. Following that, samples were centrifuged at 10,000 rpm for 10 min at 4 °C and supernatant (whole cell extract) was collected and stored at -80 °C.

Preparation of Membrane and Cytosolic Extracts

For preparation of membrane and cytosolic extracts, the Subcellular Protein Fractionation Kit for Cultured Cells (PI-78840) was used according to the manufacturer's instructions (Thermo Scientific, Rockford, USA) with slight modifications. A total of $2x10^6$ cells were treated as indicated. After incubation cells were harvested by centrifugation at 2,000 rpm, for 5 min at 4 °C, washed with ice cold PBS and pellet again by centrifugation at 2,000 rpm, for 5 min at 4 °C. Following that, supernatant was removed and cell pellet was resuspended in 50 µl ice cold Cytosolic Elution buffer (CEB) containing protease inhibitors. Samples were incubated at 4 °C, for 10 min. After that, lysates were centrifuged at 2,000 rpm, for 10 min at 4 °C and supernatant (cytosolic extract) was collected to clean tubes. Cytosolic fraction was further cleaned up by additional centrifugation at 10,000 rpm, for 10 min at 4 °C. Supernatant was recollected and stored at -80 °C. Pellet was washed twice with PBS and resuspended in 40 µl ice cold Membrane Elution buffer (MEB) containing protease inhibitors and incubated at 4 °C, for 10 min. Lysate was centrifuge at 12,500 rpm, for 5 min at 4 °C and supernatant (membrane extract) was transferred to clean tubes and stored at -80 °C.

Preparation of Nuclear and Cytosolic Extracts

A total of $2x10^7$ cells were treated as indicated. After incubation, cells were harvested by centrifugation at 1,500 rpm for 5 min at 4 °C and washed with ice cold PBS. Cells were resuspended in ice cold Lysis buffer (10 mM HEPES, 1 mM EDTA, 60 mM KCl, 0.5% (v/v) NP-40, 1 mM DTT, 1 mM PMSF, protease

Christiana Sava

inhibitors, pH 7.9) and incubated at 4 °C for 10 min. Following that, samples were centrifuged at 12,000 rcf for 10 min at 4 °C and supernatant (cytosolic extract) was collected. Cytosolic fraction was further clarified by centrifugation at 14,000 rcf, for 10 min at 4 °C. Supernatant was recollected and stored at -80 °C. Pellet was washed with Washing buffer (10 mM HEPES, 1 mM EDTA, 60 mM KCl, 1 mM DTT, 1 mM PMSF, protease inhibitors, pH 7.9) and Nuclear suspension buffer (250 mM Tris-Hydrochloride, 60 mM KCl, 1 mM DTT, 1 mM PMSF, protease inhibitors, pH 7.8) was added to each sample. Nucleus lysis was achieved by sonication (4 bursts, at amplitude 4, for 4 sec with 2 min cooling between bursts) with the use of an ultrasonic microprocessor and clarified by centrifugation at 10,000 rcf for 15 min at 4 °C. Supernatant (nuclear extract) was collected and stored at -80 °C.

Bradford Protein Assay

Protein concentration was determined using Bradford reagent (Sigma) as follow: A total of 1 μl of each sample was transferred to a well of a 96-well plate already containing 19 μl NaCl. Bradford reagent at 200 μl volume was then added to each well and mixed on a horizontal shaker for 5 min. The absorbance was measured at 595 nm. The protein concentration of the unknown samples was determined by comparing samples A595 values against a standard curve. The protein standards (ranging from 0.25-5 μg) were prepared using bovine serum albumin (BSA).

Immunoblotting

Western blotting was performed with the use of Mini-PROTEAN® Tetra Cell system according to the manufacturer's instructions (BIO-RAD, California, USA). In brief, protein extracts were mixed with SDS Sample buffer containing mercaptoethanol, boiled for 5 min and subjected to SDS-PAGE. 50 μg of total protein was loaded in each lane of 8 - 12% SDS polyacrylamide gel. After electrophoresis, proteins were transferred to Polyvinylidene fluoride (PVDF) membrane and blocked with 5% non-fat dry milk or BSA in TBS-Tween buffer for 1 h. Following that, membranes were incubated with the appropriate primary antibodies in blocking solution at 4 °C overnight, and then washed with TBS-Tween buffer. Westerns blots were probed with the specific secondary antibody in

Christiana Savva

5% non-fat dry milk in TBS-Tween for 1 h, at RT and protein bands were detected by enhcaned chemiluminescence. Anti-GAPDH, anti-Histone H3, anti-α-Tubulin and anti-EGFR monoclonal antibodies were used as loading controls. The buffers used in Western blotting are listed in Table 6. The intensity values from the densitometry analysis of Western blots were normalized against corresponding loading control using ImageJ analysis software (NIH). Intensity values were expressed as fold change compared to control.

Table 6. Western Blotting buffers

Buffer	Composition
4X Tris Separating buffer	1.5 M Tris-HCl, 0.4% (w/v) SDS, pH 8.8
4X Tris Stacking buffer	0.5 M Tris-HCl, 0.4% (w/v) SDS, pH 6.8
1X Running buffer	0.025 M Tris-base, 0.19 M glycine, 0.1% (w/v) SDS, pH 8.3 - 8.8
1X TBS-Tween	0.01 M Tris-base, 0.1 M NaCl, 0.1% (v/v) Tween-20, pH 7.5
1X Transfer buffer	25 mM Tris-base, 0.19 M glycine, 10% (v/v) methanol
2X SDS Sample buffer	25 % (v/v) 4X Tris Stacking buffer, 20% (v/v) glycerol, 4% (w/v) SDS, 2% (v/v) mercaptoethanol, 0.001% (w/v) bromophenol blue

Statistical Analysis

Results for continuous variables were presented as Mean ± Standard Error. Two-group differences in continuous variables were assessed by the unpaired t-test. P-values are two-tailed with confidence intervals 95%. Statistical analysis was performed by comparing treated samples with untreated control. All statistical tests were conducted using Prism software version 5.0 (Graphpad, San Diego, California, USA).

Christian Sava

Chapter III: Results

KC-53 elicits strong anti-proliferative effect in human cancer cell lines but not in normal PBMCs

The effect of KC-53 on tumor cell viability was initially determined in a series of human cancer cell lines to identify those that are the most sensitive to the agent. Thus, we have determined the effects of KC-53 on the viability of human breast (MCF-7, MDA-MB-231-TXSA), lung (A-549), prostate (PC-3), colon (LoVo), endometrial (Ishikawa), osteosarcoma (KHOS), gastric (STSA), leukemia (Jurkat, HL-60, CRF/CEM) and lymphoma (Raji, Daudi) tumorigenic cells. Human normal peripheral blood mononuclear cells (PBMCs) and "normal" immortalized MCF-12F breast cells were used as control cell lines. KC-53 reduced cancer cell viability in a dose-depended manner in all cell lines with a maximum effect on the most sensitive cell lines ranging from 5-10 μM (Figure 12).

KC-53 exhibited the highest cytotoxicity activity towards HL-60 (AML/APL) and CCR/CEM (ALL) leukemic cell lines with IC_{50} values of 2.3 and 2.4 μM respectively (Table 7). In particular, when HL-60 and CCRF/CEM cells were treated with 5 μM of KC-53 for 48 hours, the reduction in cell viability reached the 74% in both cell lines (Figure 13). Lesser sensitive to the antiproliferative effects of the KC-53 were the Jurkat (ATL) leukemic cells (IC_{50} = 3.4 μM) and Daudi lymphoma cells (IC_{50} = 3.8 μM) while, the Raji lymphoma cells exhibited moderate levels of resistance with an IC_{50} value of 16.3 μM (Figure 13 & Table 7). Remarkably, the normal PBMCs and the immortalized MCF-12F cells were relatively resistant to the anti-proliferative effects of the compound eliciting the IC_{50} values of 60 and 16 μM correspondingly (Table 7). Specifically, KC-53 at 5 μM reduced PBMCs and MCF-12F cell viability by 15% and 12% respectively (Figure 13). These results clearly suggested that the KC-53 inhibitory effects were selective against cancer cells.

Since HL-60 and CCRF/CEM cells displayed the highest sensitivity in the presence of KC-53, these cell lines were used to further investigate the underline antiproliferative mechanism(s) of KC-53. In all subsequent experiments, KC-53 was used at a final concentration of 5 μM, unless otherwise indicated.

Christiana Savva

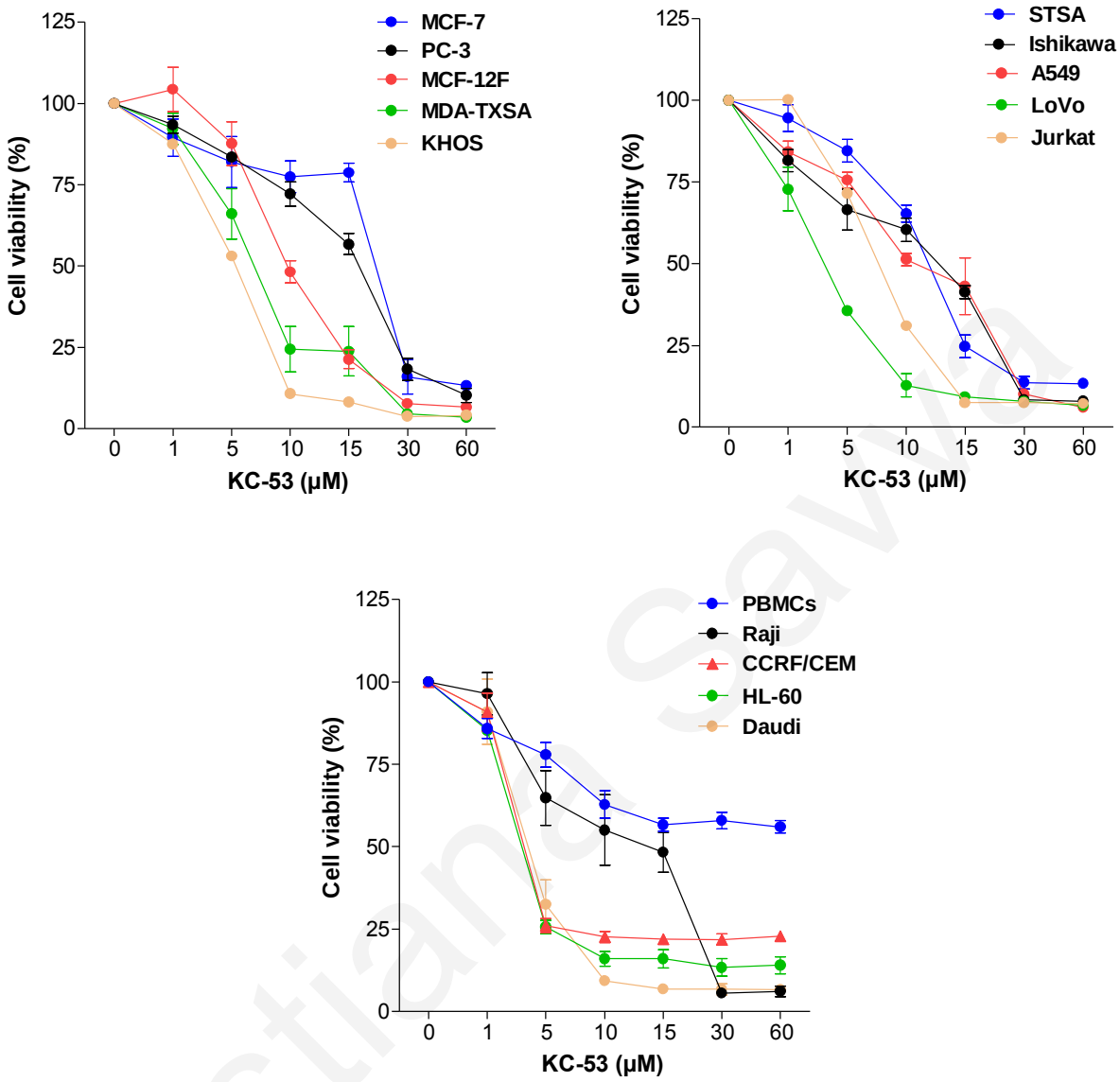

Figure 12. The effect of KC-53 on the survival of various human cancer cell lines, on normal PBMCs and on immortalized cell line, MCF-12F. Cells were exposed to increasing concentrations (0-60 μM) of KC-53 for 48 h. Cell survival was determined with the MTT cell viability assay and is expressed as percentage of survival in comparison to vehicle treated cells. The results represent the mean ± SEM of three replicates and are representative of at least three different experiments.

Christiana Savva

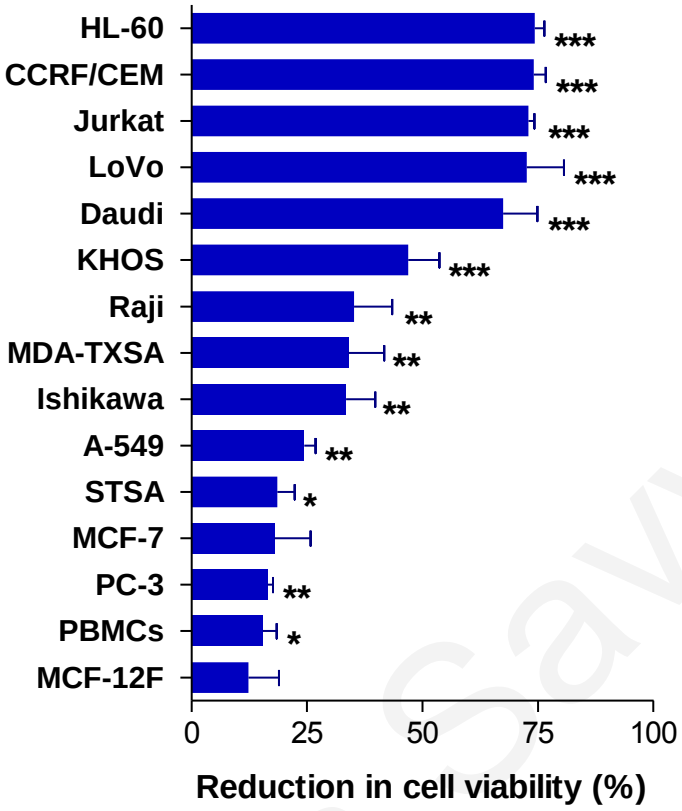

Figure 13. KC-53 reduces human cancer cell viability but not PBMCs and MCF-12F cells. Cells were incubated with 5 μM KC-53 for 48 h. Cell survival was determined with the MTT cell viability assay and is expressed as reduction in cell viability compare to the vehicle control cells. The results represent the mean ± SEM of three replicates and are representative of at least three different experiments. (*p value < 0.05, **p value < 0.01, ***p value < 0.001)

Christiana Savva

Table 7. **IC_{50} values of KC-53 in vitro antiproliferative activity in human cell lines**

Cell Line	IC_{50} (μM) 48 h
Hl-60 (APL)	2.3 ± 1.0
CCRF/CEM (T-ALL)	2.4 ± 1.0
LoVo (Colon carcinoma)	2.5 ± 1.6
Jurkat (T-ALL)	3.4 ± 1.7
Daudi (Burkitt's Lymphoma)	3.8 ± 1.9
KHOS (Osteosarcoma)	5.0 ± 2.0
MDA-MB-231-TXSA (Breast Adenocarcinoma)	8.0 ± 3.5
STSA (Gastric Adenocarcinoma)	15.4 ± 5.2
MCF-12F (Non-tumorigenic breast cells)	15.5 ± 5.5
MCF-7 (Breast Adenocarcinoma)	16.0 ± 3.5
Raji (Burkitt's Lymphoma)	16.3 ± 6.1
A549 (Lung Adenocarcinoma)	19.1 ± 10
Ishikawa (Endometrial Adenocarcinoma)	21.1 ± 10
PC-3 (Prostate Adenocarcinoma)	33.6 ± 9.7
PBMCs (Peripheral blood mononuclear cells; mainly B- & T- cells)	>60

Cells were incubated with increasing concentrations of KC-53 (0-60 μM) for 48 h. The IC_{50} values were calculated from MTT viability curves. The data are expressed as the mean ± SD of three independent experiments performed in triplicates.

Christina Sawa

KC-53 inhibits APL and ALL leukemia cell lines growth in a dose- and time- depended manner

KC-53 was found to reduce HL-60 and CCRF/CEM cell growth in a dose- and time- depended manner producing maximum reduction in cell viability at 10 μM in HL-60 and at 5 μM in CCRF/CEM (Figure 14). Similar results were also observed in the Jurkat leukemic cell line (Figure S1). It became apparent from these growth response curves that the effect of the agent was almost immediate. To follow-up on this observation, we examined the possibility that the effects of KC-53 were irreversible. Towards this objective, we exposed the cells to KC-53 for 1, 3, 6 and 12 hours followed by a post-treatment recovery period in agent-free medium for 24 h up to 72 hours. In both cell lines viability was only partially restored when KC-53 was removed after 1 or 3 hours of treatment (Figure 15). Treatments for 6 and 12 hours produced a similar effect to that of continuous exposure. Thus, after 6 hours of treatment the compound produced an irreversible inhibition of cell growth. We also examined if the compound renewal will contributed to any further decrease in cell viability. As shown in Figure 16, in both cell lines KC-53 renewal produced a similar effect to that where the agent was not removed. The above results showed that, a single administrative dose of 5 μM KC-53 is sufficient for continuous inhibition of cell growth.

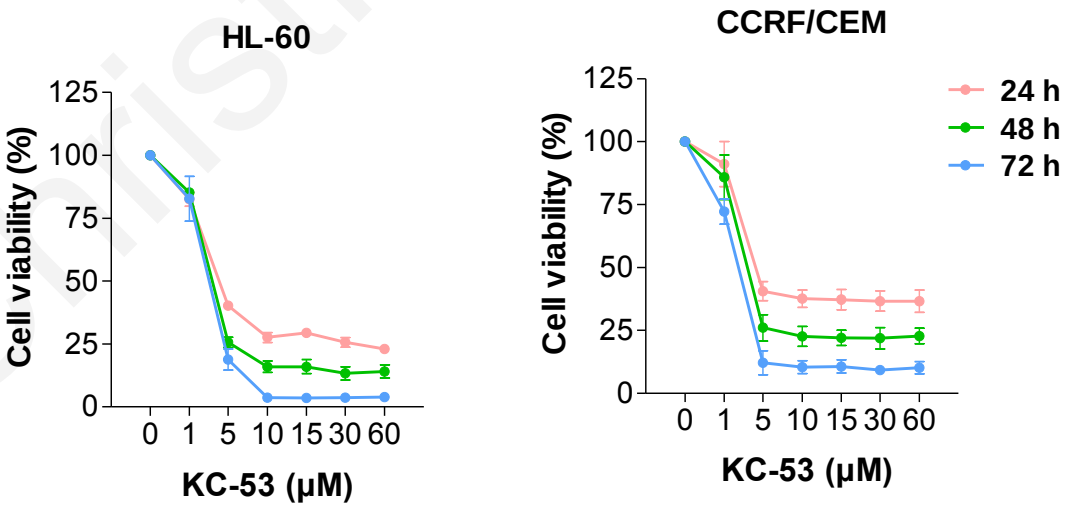

Figure 14. KC-53-induced growth inhibition of leukemic cells is dose- and time-dependent. Cells were treated with increasing concentrations of KC-53 for the times indicated. Cell viability determined by the MTT assay is expressed as percentage of survival in comparison to vehicle treated controls.

Christiana Saiya

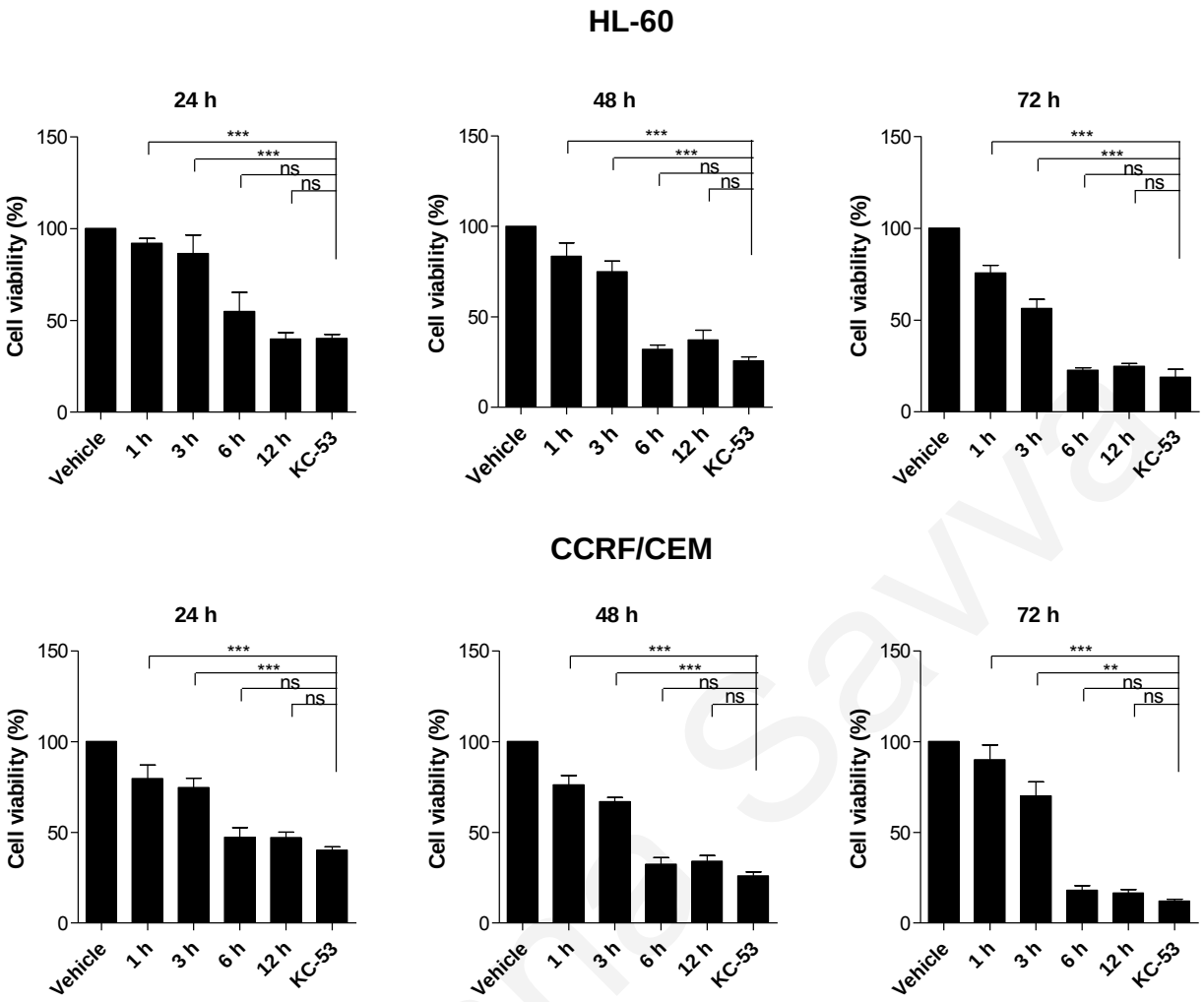

Figure 15. The effects of KC-53 are irreversible after 6 hours of treatment. Cells were exposed to vehicle control or 5 μM of KC-53 followed by removal of the agent after 1, 3, 6 or 12 h, and a recovery period in drug free medium for 48 h. A positive control, where KC-53 was not removed, is shown for comparison. Cell survival was determined with the MTT assay. The results represent the mean ± SEM of two replicates and are representative of at least three different experiments. (***p value < 0.001 significant difference, ns; no significant difference)

Christian Savva

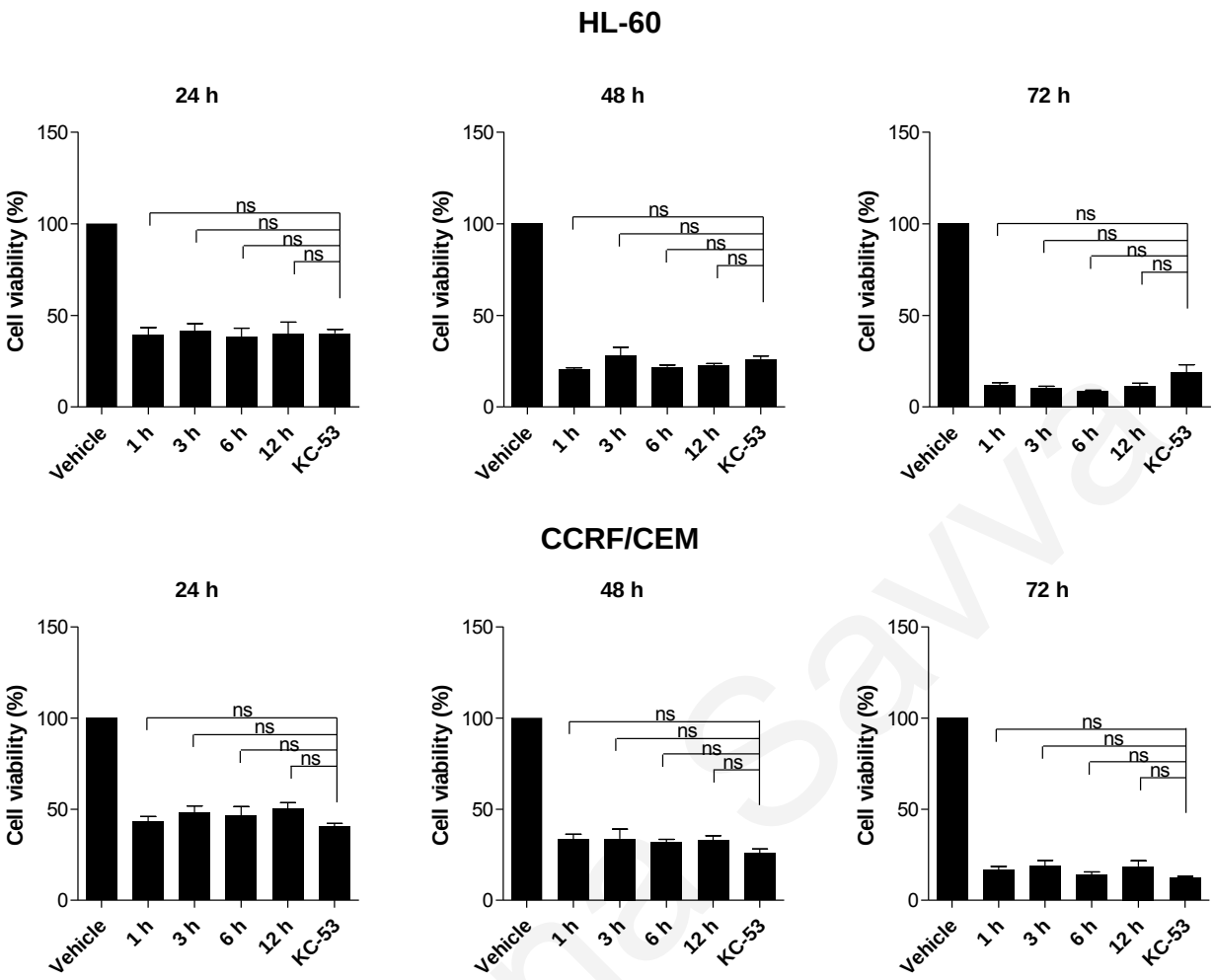

Figure 16. The renewal of KC-53 in medium does not contribute in further decrease in cell viability. Cells were exposed to 0 or 5 μM of KC-53 followed by renewal of the agent after 1, 3, 6 or 12 h, and allowed to grow for 24, 48 and 72 h. A positive control, where KC-53 was not renewed is shown for comparison. Cell survival was determined with the MTT assay. The results represent the mean ± SEM of three different replicates and are representative of at least three different experiments.

Christiana Savva

To further investigate and compare the anticancer activity of KC-53 to its parental molecule, Biy-A HL-60 and CCRF/CEM cells were incubated at various concentration for up to 72 hours. As it can be observed in Figure 17, KC-53 exerts a stronger antiproliferative effect than its parental molecule.

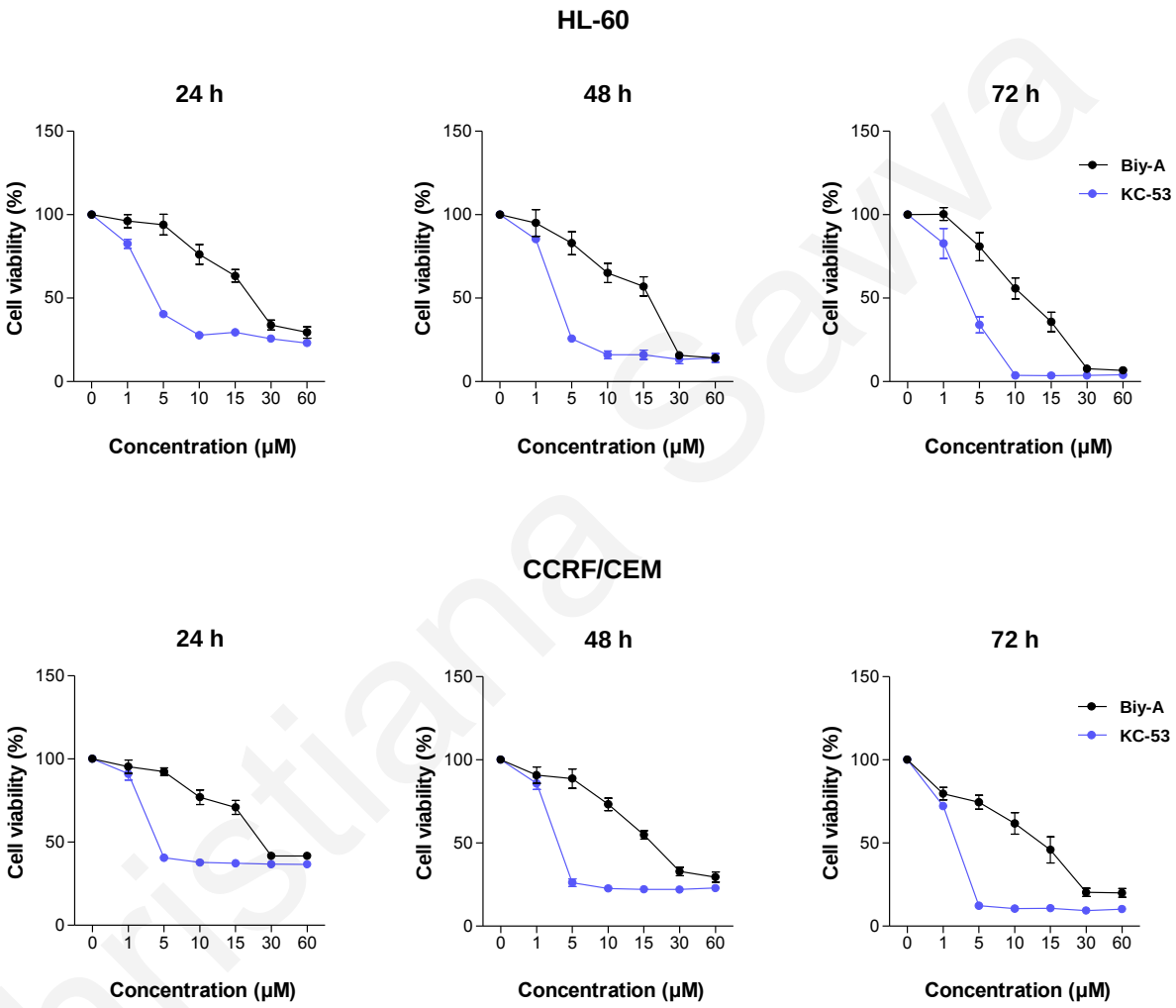

Figure 17. KC-53 exerts stronger antiproliferative activity than its parental molecule, Biy-A. HL-60 and CCRF/CEM cells were treated with increasing concentrations of KC-53 and Biy-A for the times indicated. Cell viability determined by the MTT assay is expressed as percentage of survival in comparison to vehicle treated cells. The results represent the mean ± SEM of three different replicates and are representative of at least three different experiments.

Christiana Savva

KC-53 does not affect cell cycle progression neither of acute leukemic nor of normal PBMC cells

Cancer is considered as a disease of cell cycle deregulation. Alteration in the expression of positive or negative regulators of cell cycle machinery lead to the abnormal proliferation of cancer cells (Pucci et al., 2000). Therefore, induction of cell cycle arrest in cancer cells is considered to be a promising therapeutic approach. To determine whether the growth inhibitory effect of KC-53 is accompanied by cell cycle arrest, we incubated HL-60 and CCRF/CEM cells with 5 μM KC-53 for 3, 6, 12 and 24 h and performed flow cytometry analysis.

By DNA content analysis it became obvious that the growth inhibitory effect of KC-53 in acute leukemia cells was exclusive due to increased cell death, as no significant changes in the distribution of cell cycle phases were observed (Figure 18). A time-depended increase in SubG1 phase was evidenced in both cell lines, indicative of apoptosis. Specifically, after 12 and 24 hours of treatment with 5 μM KC-53 there was a significant increase in SubG1 phase by 14% and 31% in HL-60 cells (Figure 18A) and by 16% and 33% in CCRF/CEM cells (Figure 18B) respectively. Similar results under the same conditions were observed in KC-53-treated Jurkat cells (Figure S2). Notably, the cell cycle profile of normal PBMCs was not affected when treated with KC-53 (Figure 18C). Thus, the apoptotic effects of KC-53 are specific towards leukemic cells impaling normal cells.

Christiana Savva

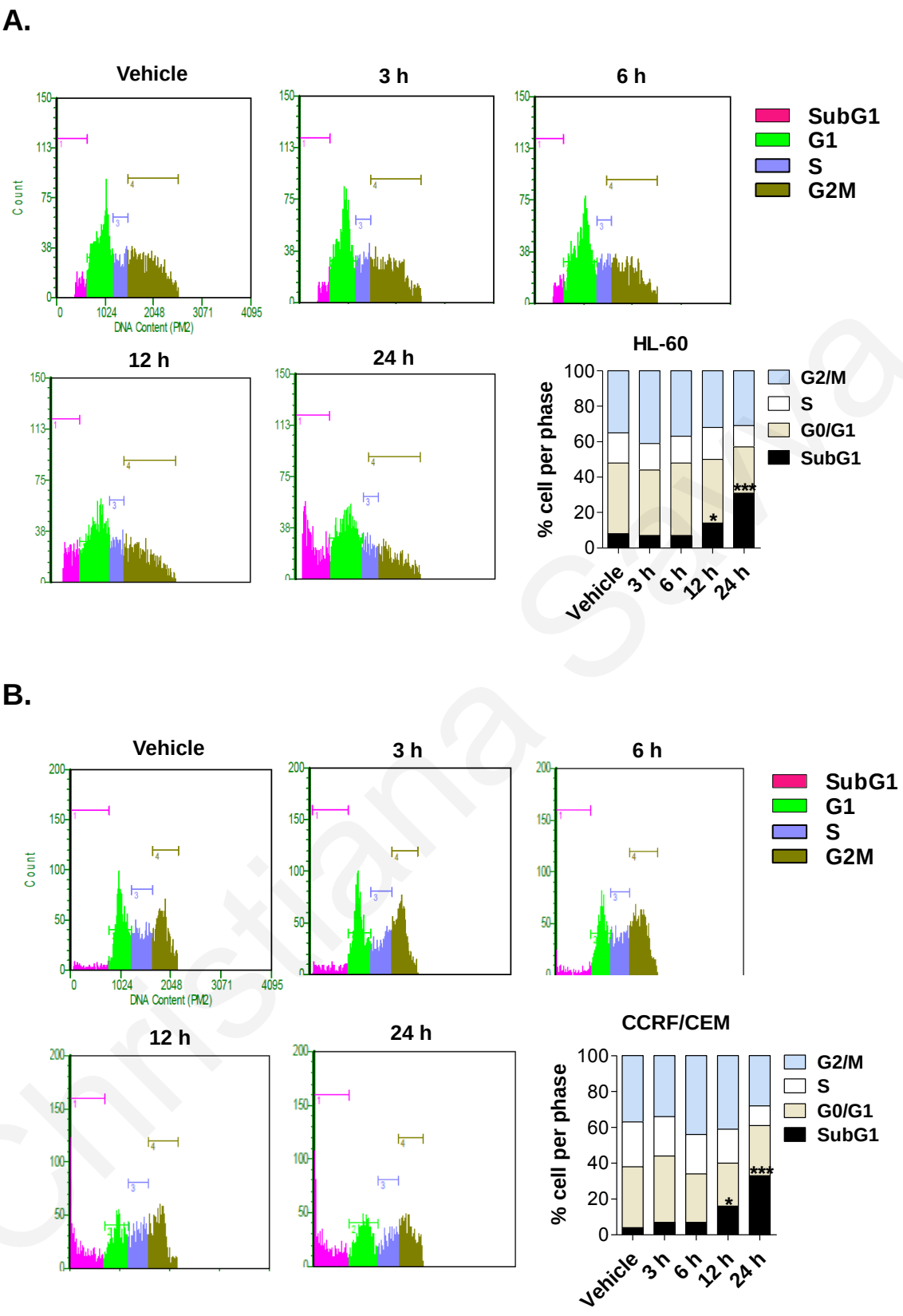

Figure 18. KC-53 increases SubG1 fraction in leukemic but not in normal cells. (A) HL-60, **(B)** CCRF/CEM and **(C)** PBMCs cells were treated with 0 or 5 μM KC-53 for 0-24 h prior to cell cycle analysis. The treatments were performed in duplicate and represent the mean ± SEM of three different experiments. (*p value < 0.05, ***p value < 0.001) (Figure continued in the next page)

Christiana Serra

C.

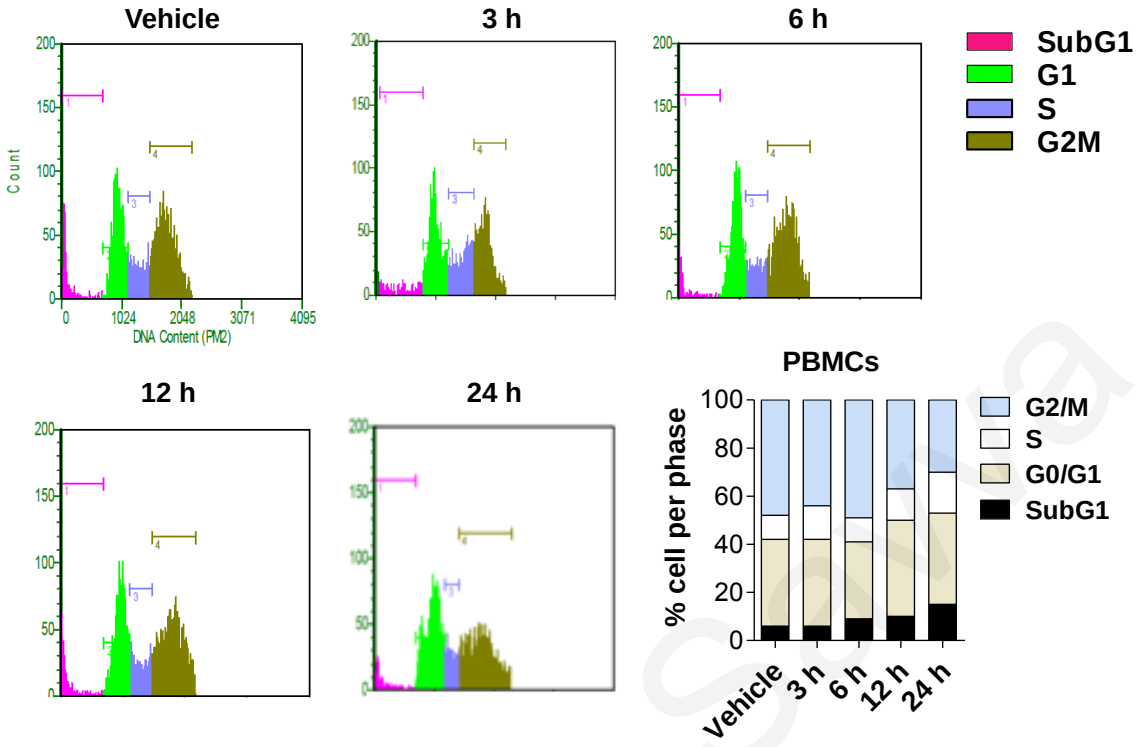

Figure 18 (Continued)

Christiana Soria

KC-53 induces programmed cell death in acute leukemia cell lines but not in PBMCs

The induction of apoptosis in target cells is a key mechanism for anti-cancer therapy. Energy-dependent biochemical pathways and distinct morphological features are the main characteristics of apoptosis. The morphological changes in apoptotic cells are accompanied by various biochemical changes, including protein cross-linking and DNA breakdown. One such biochemical modification is the expression of cell surface markers such as phosphatidylserine (PS) which translocates to the outer side of plasma membrane during the early apoptosis. The process of late apoptosis is accompanied by extensive blebbing of plasma membrane with tightly packed organelles. To further investigate whether the enchantment of cell growth inhibition induced by KC-53 is associated with increased of apoptosis we investigated the externalization of PS by Annexin-V-FITC/PI assay. Annexin-V as a PS-binding protein with high affinity for externalized PS was used for the detection of early and late apoptosis while PI was used for detection of the late apoptosis and necrosis.

Accordingly, to evaluate whether HL-60 and CCRF/CEM cells undergo apoptosis, untreated and KC-53 treated cells were stained with Annexin-V and PI. The analysis of stained cells can distinguish the cells into three categories, namely viable (Annexin-V and PI negative), early apoptotic (Annexin-V positive, PI negative) and late apoptotic/necrotic (Annexin-V negative, PI positive). As illustrated in Figure 19, KC-53 treatment at different time periods resulted in a time-depended increase of early apoptotic and late apoptotic fragments. In more details, within 12 hours of KC-53 treatment, there was a significant increase in the early apoptotic fraction in both HL-60 and CCRF/CEM cells which peaked at 26.5% and 27.5% respectively after 24 h treatment (Figure 19). In addition, 15% of cells from both cell lines were in the late apoptotic stage. The increase in late apoptotic fraction further confirms the observed SubG1 increase in the cell cycle findings. Apoptotic induction was also analyzed in PBMCs. As was expected, the agent did not affect the distribution of early and late apoptotic PBMC cells (Figure 19). However, when normal cells were treated with the chemotherapeutic agent Doxorubicin (Dox) for 24 h, the increase in the early and late apoptotic fraction touched the 25% and 20%, correspondingly signify that an amount of more than

Christiana Savva

50% of the total cell population is undergoing apoptosis (Figure 19). In contrast, the apoptotic effects of Doxorubicin in HL-60 and CCRF/CEM were not as robust, affecting only 27% of the total population of both cell lines. The above data suggest that KC-53 apoptotic activity is specific for acute leukemia cells and it might be more efficacious and less toxic than Doxorubicin.

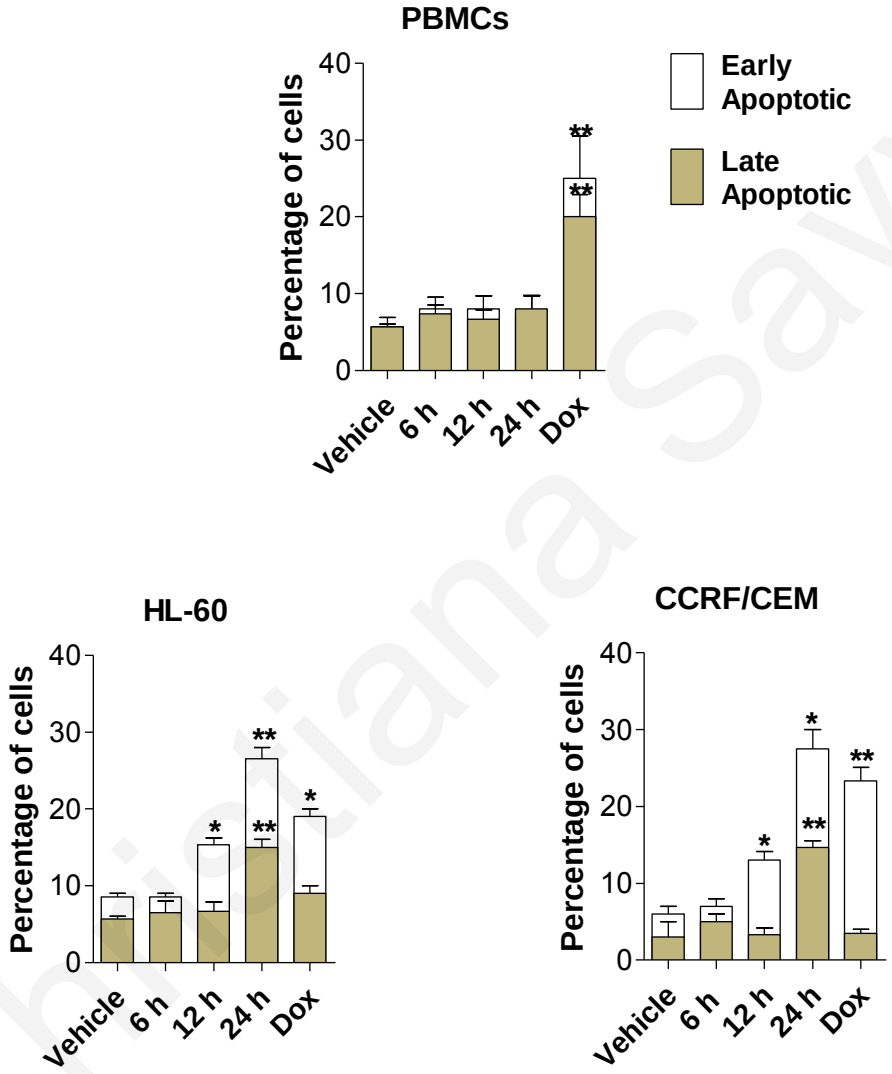

Figure 19. KC-53 induces apoptosis in HL-60 and CCRF/CEM cells but not in normal PBMCs. Cells were treated with vehicle control or 5 μM KC-53 for the indicated time points and apoptosis was assessed with Annexin-V/PI staining. Statistical significance was evaluated by comparing each cell population of the treated samples with the corresponding population of the untreated control. Doxorubicin (Dox) at 0.5 μM was used as positive control. The results represent the mean ± SEM of two different replicates and are representative of at least three independent experiments. (*p value < 0.05, **p value < 0.01)

Chiediana Savva

As mentioned formerly, DNA breakdown is one of the typical biochemical characteristics occurring in apoptosis. During apoptosis, cell cytosol is enriched by mono- and oligo-nucleosomes due to DNA fragmentation. For the detection of fragmented DNA, we used the ELISA Cell death detection kit. KC-53 induced substantial DNA fragmentation in HL-60 cells (7.4 fold increase compared to the control) and in CCRF/CEM cells (6.4 fold increase compared to the control) as shown in Figure 20A. In the presence of the caspase inhibitor, z.vad.fmk, DNA fragmentation was significantly reduced in HL-60 cells and it was fully abolished in CCRF/CEM cells (Figure 20A). These data suggest that activation of caspase cascades is predominantly involved in KC-53-induced apoptosis. Even though co-incubation of KC-53 with z.vad.fmk restored DNA fragmentation it did not restore the viability of cells (Figure 20B). HL-60 viability increased from 43% to 60% in the presence of z.vad.fmk while no alterations were observed in the viability of CCRF/CEM. These findings indicate that inhibition of cell proliferation by KC-53 might be mediated by both caspase-dependent (CD) and caspase-independent (CID) pathways in a cell-context-specific manner.

DNA analysis was additionally performed with the Comet assay, also known as single-cell gel electrophoresis assay. KC-53-induced DNA damage was evident within 9 hours of treatment in both cell lines (Figure 21 & 22) and was exclusively attributed to apoptosis as no cellular ROS production was detected (Figure 23). ROS are known to be involved in CID apoptosis by promoting DNA and lipids oxidative damage (Circu and Aw, 2010). The addition of sodium pyruvate (SP) in media has been found to diminish H_2O_2 levels thereby producing artifacts that may be mistaken as a specific anticancer activity (Odiatou et al., 2013). In order to investigate whether the effects of KC-53 may be attributed to the production of H_2O_2 and its subsequent elimination by SP, we performed time DCFH-DA assays with or without the SP presence in the cell growth media. Our results clearly showed that KC-53 cell death effects are independent by ROS production and/or SP which indicate that are not due to oxidative damage (Figure 23). Additionally, these results support that KC-53-CID apoptotic effects are not mediated by ROS suggesting that other mediators of CID apoptosis might be activated. Moreover, ROS are one of the main mediators of non-programmed cell death, necrosis. It is obvious therefore, that KC-53-induced cell death is not caused by necrosis but

Christiana Savva

exclusively by apoptosis. Preliminary results in Jurkat cells show a similar pattern of KC-53-induced-apoptosis (Figure S3 & S4).

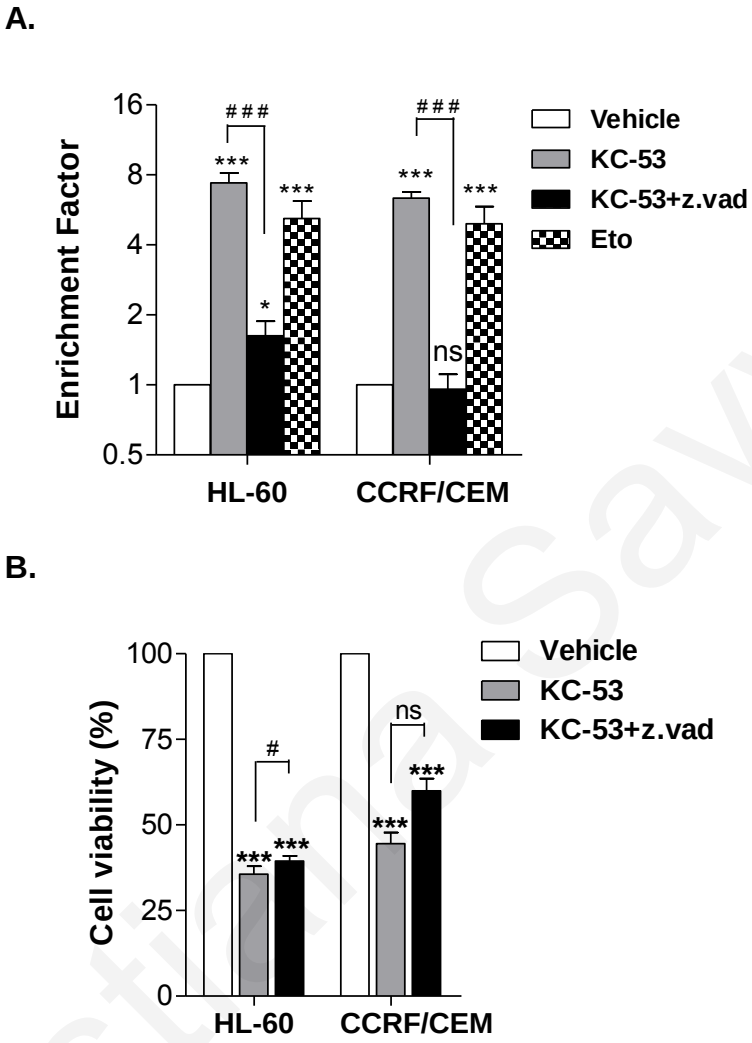

Figure 20. KC-53-induced apoptosis is mainly attributed to caspases activation. Cells were treated with 0 or 5 μM KC-53 in the presence or absence of 20 μM z.vad.fmk for 24 h. Following incubation **(A)** the presence of nucleosomes in the cytoplasm was determined with ELISA cell death detection kit and **(B)** cell viability was assessed with the MTT assay. Etoposide (Eto) at 5 μM concentration was used as positive control. The results represent the mean ± SEM of two different replicates and are representative of at least three independent experiments. (*p value < 0.05, ***p value < 0.001, #p value < 0.05, ###p value < 0.001)

Christina Savva

(i)

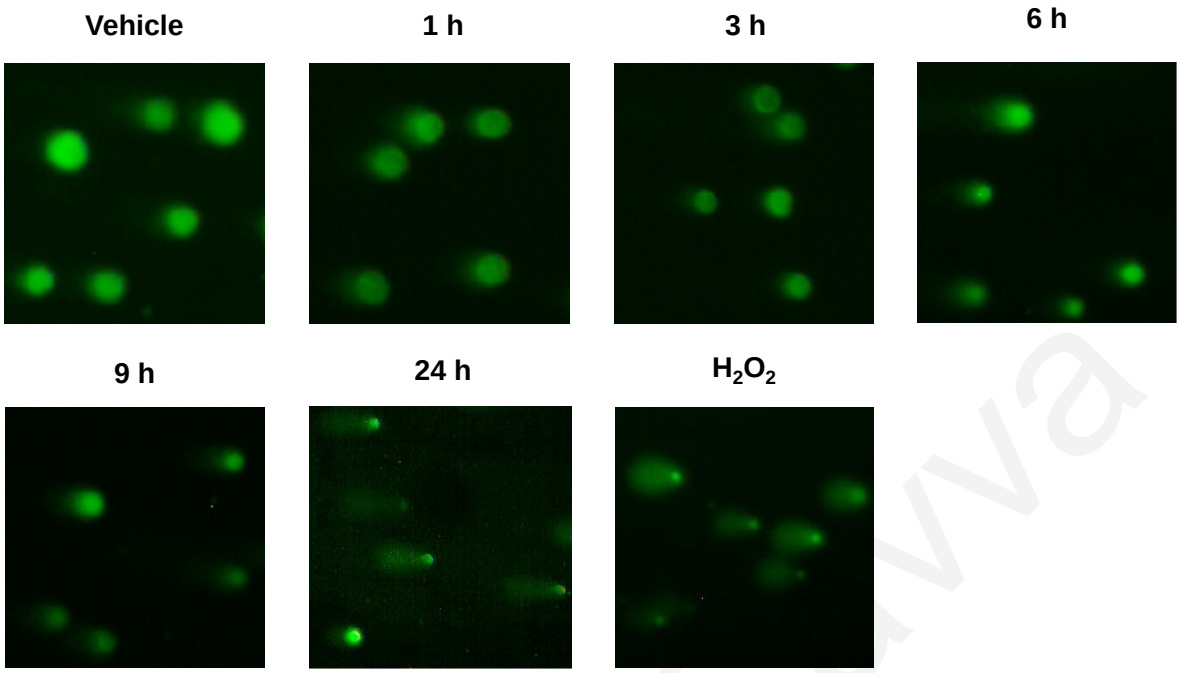

(ii)

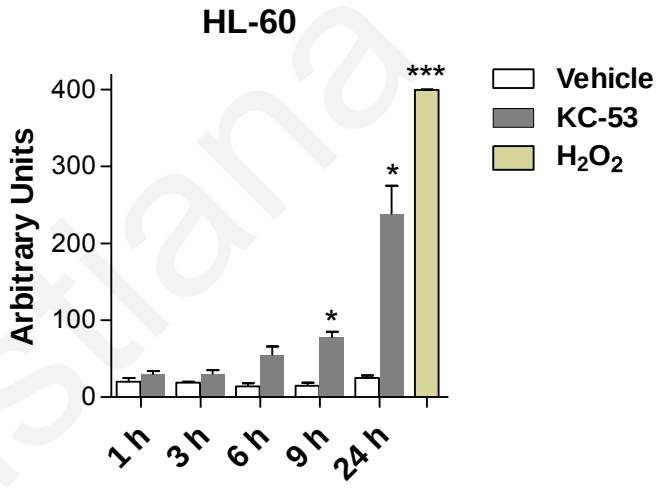

Figure 21. KC-53 induces DNA damage in HL-60 cells. Cells were treated with vehicle control or 5 μM of KC-53 for the times indicated and DNA damage was evaluated with the Comet assay. For comparison, cell samples were treated with 100 μM H_2O_2 for 30 min which is known to produces oxidative DNA damage (positive control). **(i)** Images were obtained by fluorescence microscopy and show comet fields after SYBR Green I staining. **(ii)** The DNA damage was quantified based on the comet tail length. More than 200 cells were inspected per experiment, and cells with typical morphology were presented. The results are representative of three independent experiments. (*p value < 0.05, ***p value < 0.001)

Christiana Salva

(i)

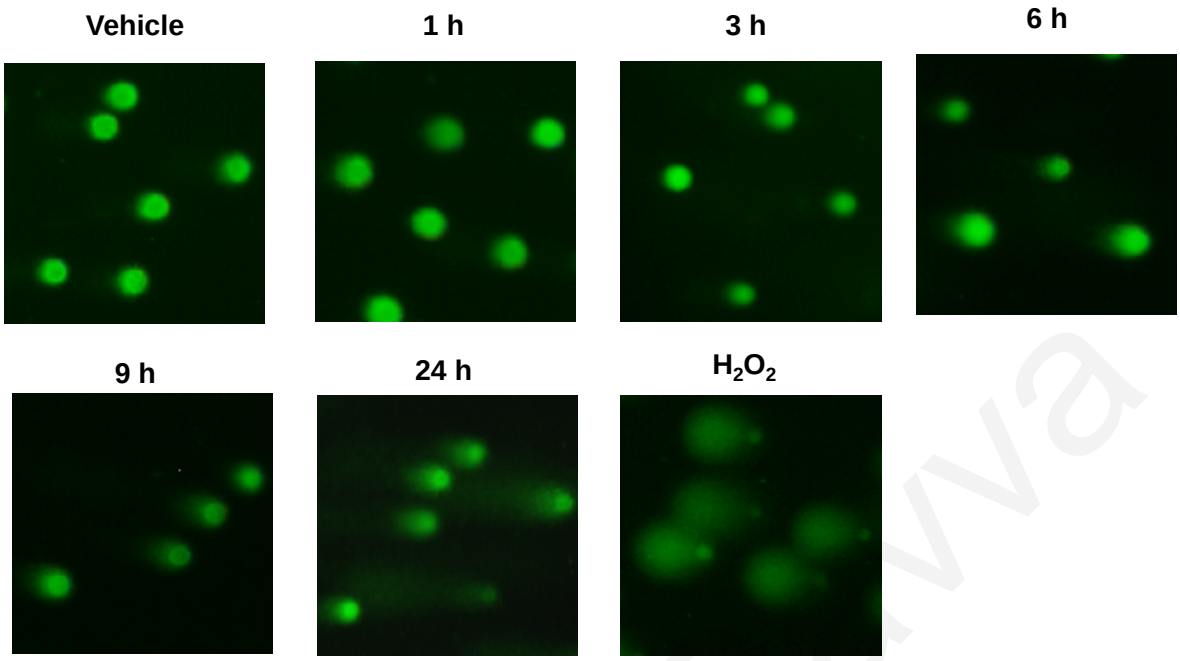

(ii)

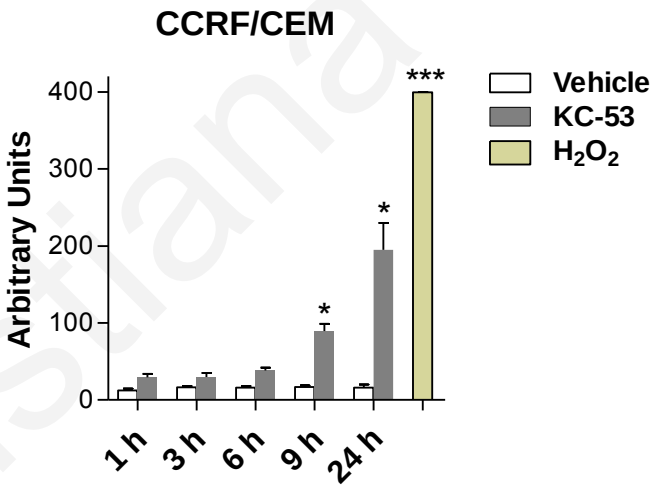

Figure 22. KC-53 induces DNA damage in CCRF/CEM cells. Cells were treated with vehicle control or 5 μM of KC-53 for the times indicated and DNA damage was evaluated with the Comet assay. For comparison, cell samples were treated with 100 μM H_2O_2 for 30 min which is known to produces oxidative DNA damage (positive control). **(i)** Images were obtained by fluorescence microscopy and show comet fields after SYBR Green I staining. **(ii)** The DNA damage was quantified based on the comet tail length. More than 200 cells were inspected per experiment, and cells with typical morphology were presented. The results are representative of three independent experiments. (*p value < 0.05, ***p value < 0.001)

Christiana Salva

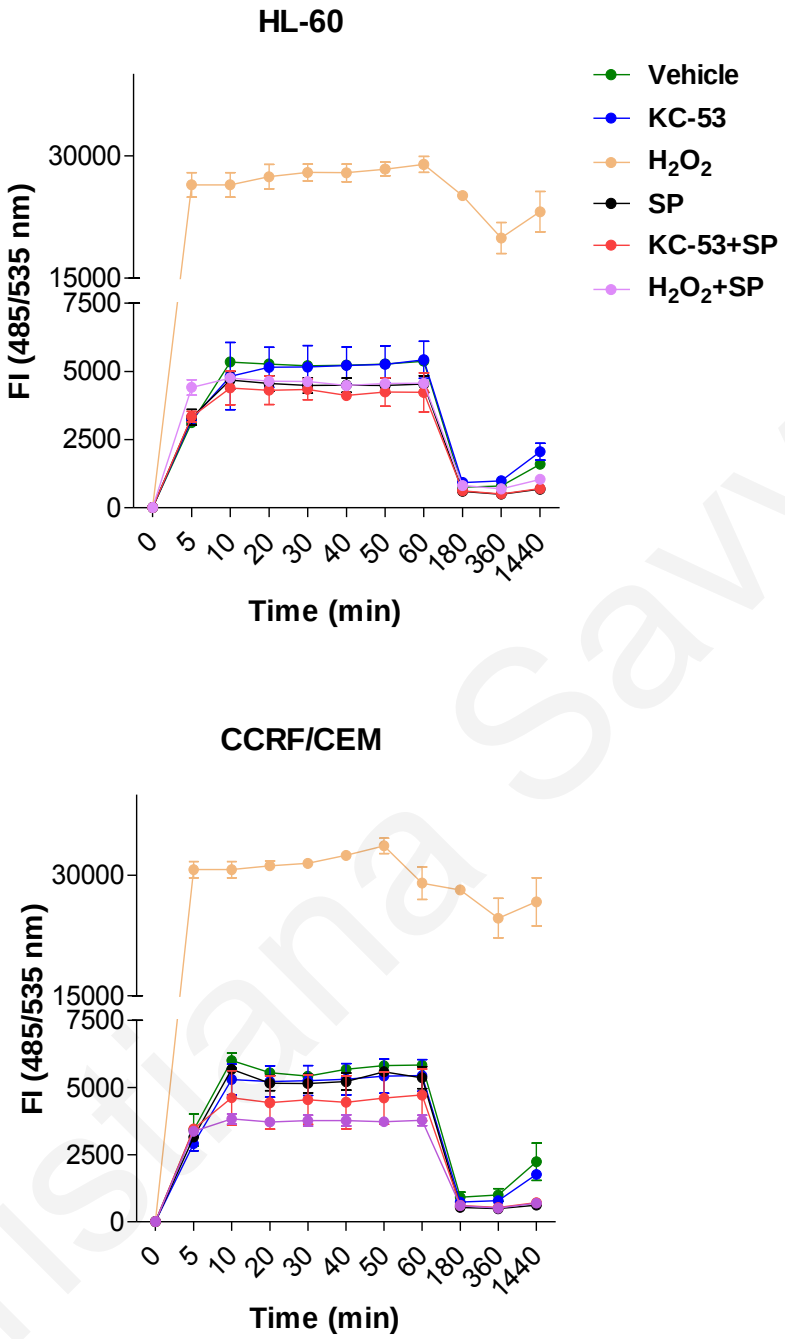

Figure 23. KC-53-induced cell death is not caused by ROS-mediated necrotic cell death. HL-60 and CCRF/CEM cells were treated with vehicle control or 5 μM of KC-53 in the presence or absence of 1 mM Sodium Pyruvate (SP) for the indicated time points. Cells were also treated with 100 μM Hydrogen Peroxide (H_2O_2) in the presence or absence of 1 mM SP as controls. ROS production was determined with the DCFH-DA assay. Fluorescence Intensity (F.I.) was measured in 485/535 nm and is proportional to the ROS levels within the cell cytosol. Statistical significance was evaluated by comparing treated samples with corresponding DMSO vehicle control group. The treatments were performed in duplicate and represent the mean ± SEM of three independent experiments.

Christiana Savva

KC-53 activates the TNFR1-extrinsic pathway of apoptosis with subsequent activation of the mitochondrial-intrinsic pathway

Apoptosis is the predominant pathway for programmed cell death. The two major pathways that are involved in apoptosis are the intrinsic, or mitochondrial, pathway and the extrinsic, or death receptor pathway. Intrinsic and extrinsic pathways are activated by their own initiator caspases, namely Caspase-9 and -8, respectively. The activation of initiator caspases will, in turn, lead to activation of executioner caspases like Caspase-3 and -7. To fully characterize the apoptotic pathway being induced by KC-53, we monitored the potential activation of caspases and any changes in the membrane death receptor levels.

In both HL-60 and CCRF/CEM cell lines, an increase in membrane-associated TNFR1 was evident with KC-53 treatment for 6 to 24 hours (Figure 24). The corresponding protein levels of TNFR2 were not significantly affected by the treatment (Figure 24). Densitometric analysis data can be seen in (Figure S5). The levels of death receptors FAS, DR3 and DR5, decoy receptor DcR3, as well as those of adaptor proteins FADD and TRADD, remained relatively unaffected by the treatment (Figure 25). The increase in TNFR1 levels was accompanied by strong activation and detection of the cleaved 43/41 kDa forms of Caspase-8 (C-Casp8) and proteolytic inactivation of RIP1 (C-RIP1) (Figure 26A) indicating that the extrinsic pathway of apoptosis is triggered.

Although mitochondria are the starting point for the intrinsic pathway, damages to these organelles may be the result of the extrinsic pathway. The crosstalk between the extrinsic and the intrinsic pathways is well established and occurs though Caspase-8 cleavage and activation of the pro-apoptotic protein Bid (Luo et al., 1998, Schug et al., 2011). To investigate this scenario we determined the expression levels of cleaved/truncated Bid (tBid). KC-53 administration resulted in the detection of the 15 kDa tBid, fragment in both cell lines (Figure 26A). The cleavage of Bid occurred in the early stage of apoptosis (6 h) and paralleled Caspase-8 activation. In both cell lines the amount of the 15 kDa peptide was constant during the time course of apoptosis and became undetectable after 24 hours, possibly due to further degradation to smaller fragments. The tBid translocation from the cytosol to the mitochondrial was also examined and data

Christiana Savva

are illustrated in Figure 27. Caspase-8 enzymatic activity was verified with the use of fluorometric protease assay kit, in the presence or absence of z.vad.fmk. KC-53 produced a significant increase of Caspase-8 activity within 4 hours of treatment, and after 12 hours there was a 6.6 fold increase of Caspase-8 activity in HL-60 cells and an 8 fold increase in CCRF/CEM cells (Figure 26B). The effects of KC-53 on Caspase-8 activity were fully reversed by z.vad.fmk in both cell lines. Data here signify the major involvement of initiator Caspase-8 in KC-53-mediated apoptosis.

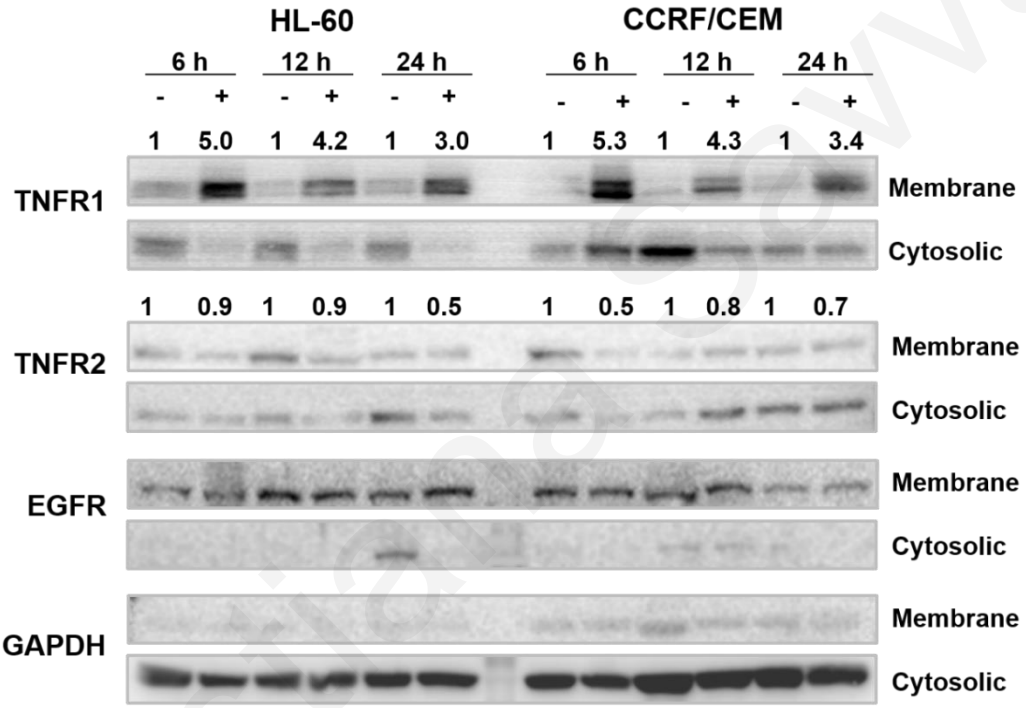

Figure 24. TNFR1 membrane expression levels are increased upon KC-53 administration. HL-60 and CCRF/CEM cells were treated with vehicle control or 5 μM KC-53 for the indicated time points prior protein extraction. TNFRs membrane and cytosolic expression levels were analyzed by immunoblotting. EGFR levels were determined as a loading control and the GAPDH levels as an indicator of cytosolic contamination. Numbers represents intensity values and are expressed as fold change compared to control. The results are representative of three repetitions.

Christiana Sowa

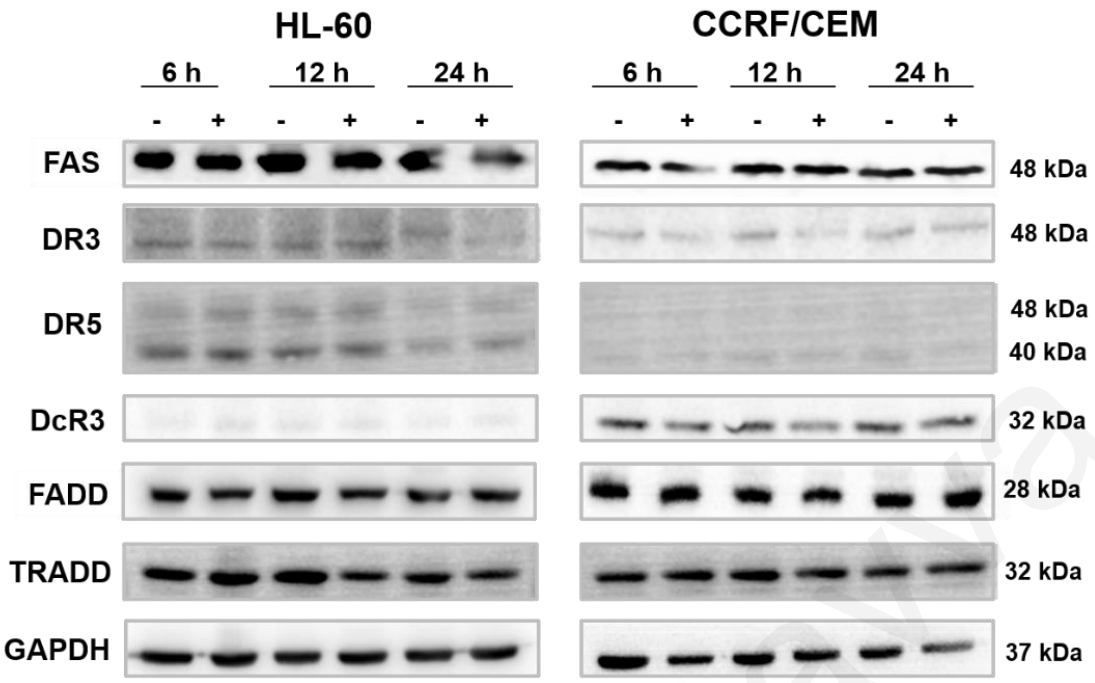

Figure 25. The expression levels of DRs and their adaptor proteins TRADD and FADD are not affected by KC-53 activity. Cells were treated with vehicle control or 5 μM KC-53 for the indicated time points prior protein extraction. Whole cell protein lysates were run by SDS-PAGE and immunoblotted with the indicated antibodies. The results are representative of three repetitions.

Christiana Saiva

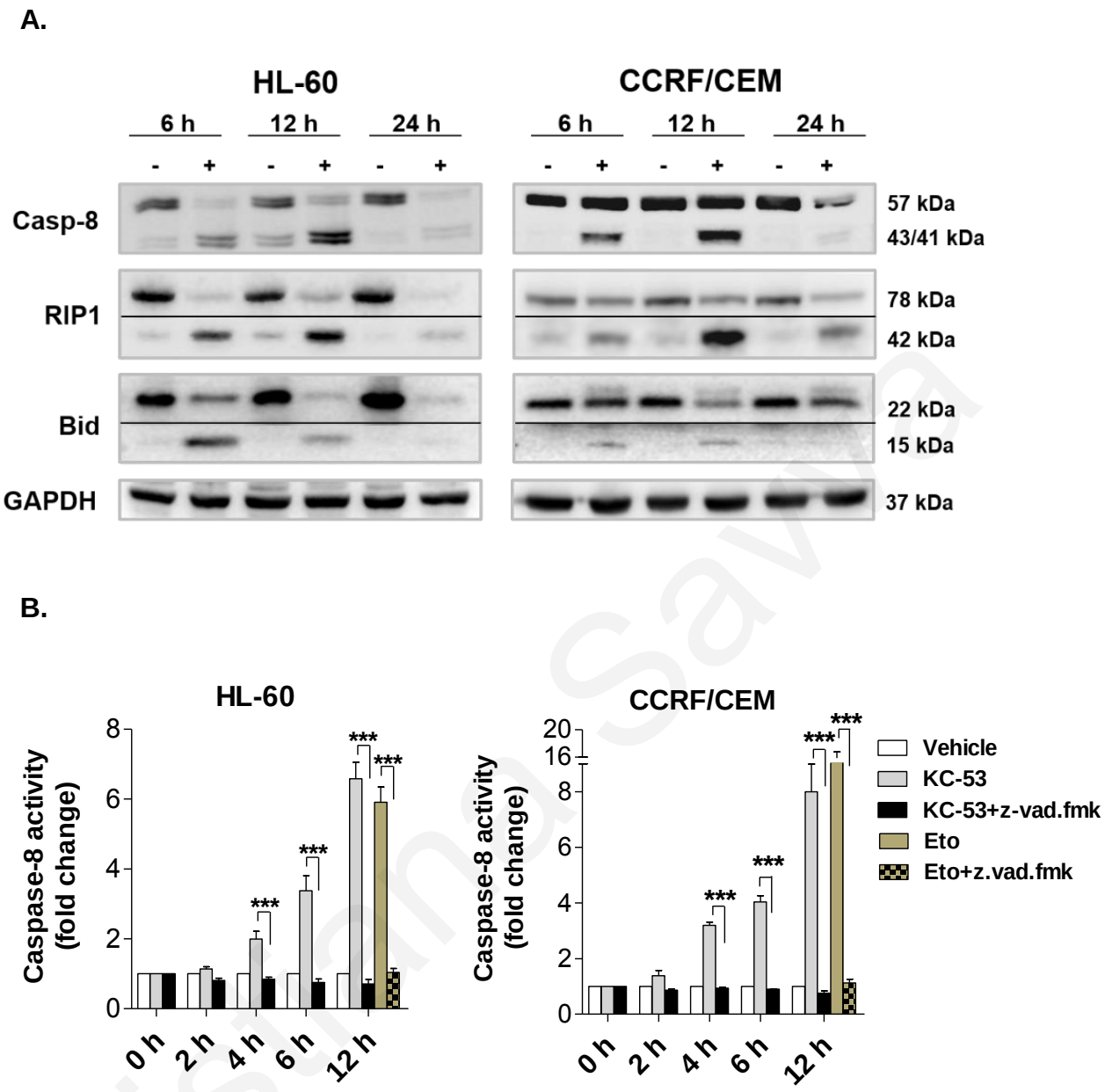

Figure 26. KC-53 promotes the proteolytic activation of Capsase-8. (A) Cells were treated with vehicle control or 5 μM KC-53 for the indicated time points prior protein extraction. Samples were run by SDS-PAGE and immunoblotted with the indicated antibodies. **(B)** Cells were treated with vehicle control or 5 μM KC-53 in the presence or absence of 20 μM z.vad.fmk. Caspase-8 enzymatic activity was determined as described in Methods. Etoposide (Eto) added at 5 μM was used as a positive control. The results in panel A are representative of three repetitions. The results in B panel represent the mean ± SEM of two different replicates and are representative of at least three independent experiments. (***p value < 0.001)

Christina Savva

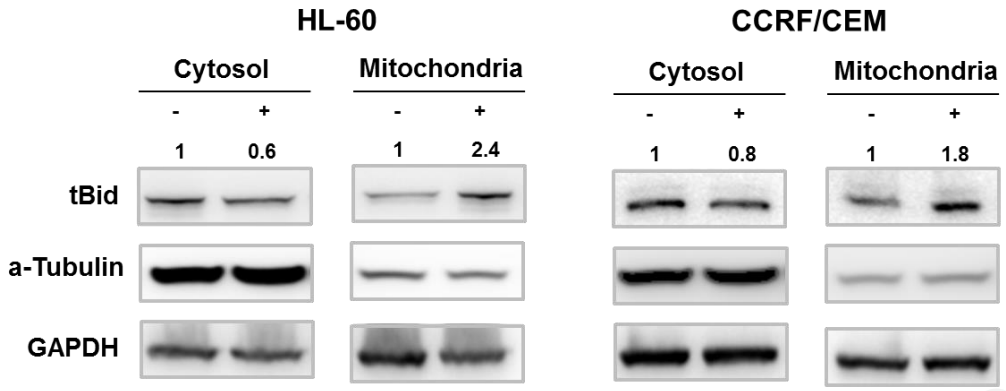

Figure 27. KC-53 induces the translocation of tBid from the cytosol to the mitochondrial. Cells were incubated with 5 μM KC-53 for 6 h and cytosolic and mitochondrial protein extracts were prepared. Numbers represents intensity values and are expressed as fold change compared to control. The results are representative of at least three independent experiments.

To further evaluate the apoptotic effect of KC-53, we monitored the expression of the executor Caspases, -3 and -7 and their substrate PARP1 in both cell lines. KC-53 decidedly increased the active cleaved forms of Caspase-3 (C-Casp3; 19/17 kDa) and Casapse-7 (C-Casp7; 20 kDa), which was evident within 6 hours of treatment and persisted 24 hours post-treatment (Figure 28A). The low levels of full-length or cleaved forms of some caspases (i.e. Caspase-3 in HL-60 cells) after 24 hours of treatment may be attributed to prolonged activation. Caspase activation was accompanied by a decrease in the levels of the full length 116 kDa PARP1 and appearance of the cleaved 89 kDa form (C-PARP1) (Figure 28A). Similar results for Caspase-8 and -3 as well as for PARP1 were obtained in Jurkat cells (Figure S6).

KC-53 equally induced activation of the initiator Caspase-9 (C-Casp9; 37/35 kDa) (Figure 28A) and release of apoptosis inducing factor (AIF) from the cytosol to the nucleus (Figure 28B). Both Caspase-9 activation and AIF release are characteristics of mitochondria outer membrane permeabilization (MOMP) apparently induced by tBid. In HL-60 cells, the nuclear levels of AIF increased up to 2-fold and in CCRF/CEM up to 2.8 -fold following 6 hours of treatment (Figure 28B). Densitometric analysis data are available in Figure S7. As AIF is a mediator of CID, its nuclear increase provides further support to the possible involvement of CID mechanisms in the apoptotic pathways induced by KC-53. Similarly,

Christiana Savva

unaffected remained the levels of the pro-apoptotic mediator, Bax, and the pro-survival mediator, Bcl-2 (Figure 29). Overall, the results here suggest the involvement of the mitochondrial/intrinsic pathway in the induction of apoptosis by KC-53.

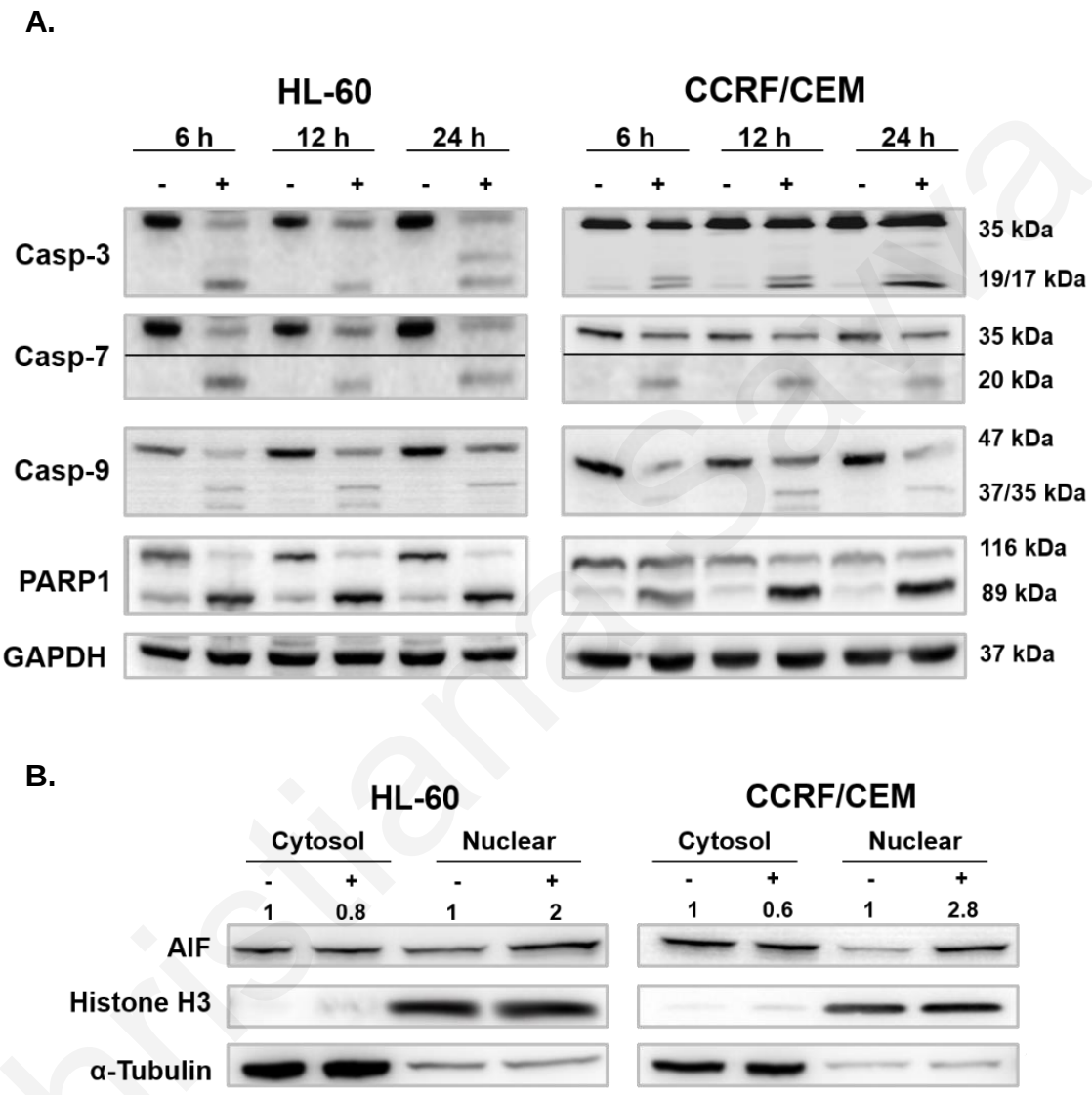

Figure 28. KC-53 promotes the activation of apoptosis executor molecules. (A) Cells were treated with vehicle control or 5 μM KC-53 for indicated times and cell protein lysates were immunoblotted with indicated antibodies. **(B)** Cells were incubated with 5 μM KC-53 for 6 h and cytosolic and nuclear protein extracts were prepared. Histone H3 levels were determined as a loading control and the α-Tubulin levels as an indicator of cytosolic contamination. Numbers represents intensity values and are expressed as fold change compared to control. The results are representative of at least three independent experiments.

Christiane Sana

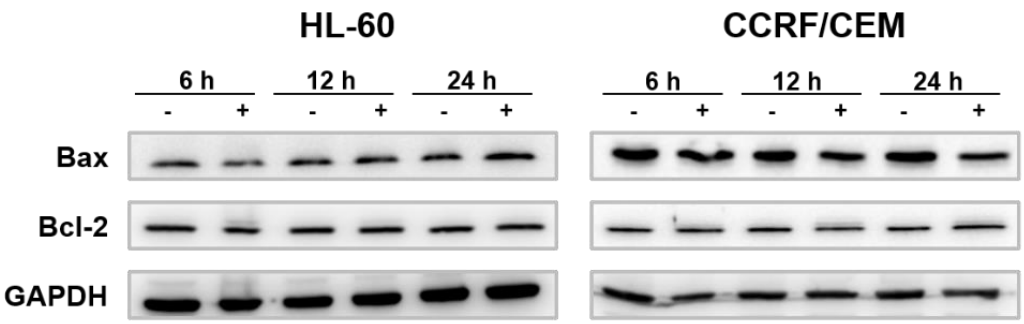

Figure 29. Effect of KC-53 on the expression levels of Bax and Bcl-2. Cells were treated with 0 or 5 μM KC-53 for the indicated time points. Samples were run by SDS-PAGE and immunoblotted with the indicated antibodies. The results are representative of three repetitions.

Concluding, the above findings revealed that KC-53 induced apoptosis mainly through the TNFR1-mediated extrinsic pathway. Once TNFR1 is stimulated, two complexes with opposing effects on cell fate can be formed; a pro-survival and a pro-apoptotic complex. In the presence of phosphorylated TRAF2, pro-survival NF-κB activation dominates over pro-apoptotic Caspase-8 activation. TRAF2 promotes RIP1 ubiquitination, facilitating the recruitment and activation of the downstream kinases. This leads to NF-κB activation preventing RIP1 from interacting with FADD. Under pro-apoptotic conditions, RIP1 dissociates from TRAF2 and binds to the FADD/Caspase-8 complex. Active Caspase-8 cleaves and inactivates RIP1 initiating therefore the extrinsic pathway of apoptosis. The detection of the cleaved, inactive form of the RIP1 kinase indicated that KC-53 acts in favor of the pro-apoptotic complex formation and opposed to the pro-survival complex assembly.

Christiana Savva

KC-53 inhibits the activation of the TNFR1/NF-κB pro-survival axis

NF-κB is sequestered in the cytosol by IκB proteins and it is released through specific signaling cascades that lead to the phosphorylation of IκBs, and degradation of IκBs by the proteasome. The released NF-κB is then transported into the nucleus where it binds to its target sequence and activates gene transcription. Since the recruitment of TRAF2 in TNFR1 is required for the assembly of kinases regulating the phosphorylation, and therefore the degradation of IκBα (Lee and Lee, 2002, Micheau and Tschopp, 2003), we investigated whether KC-53 affects the downstream molecular events of the TNFR1 signaling as well as the NF-κB translocation to the nucleus. This was evaluated by monitoring the phosphorylation status and protein levels of TRAF2 and IκBα following induction by TNFα in the absence or presence of KC-53.

We found that TNFα increased the phosphorylation levels of TRAF2 (Ser11) by 3.5 fold in HL-60 cells and by 2.2 fold in CCRF/CEM cells (compared to the control levels) while KC-53 fully attenuated these effects (Figure 30). Furthermore, pre-treatment with KC-53 fully abolished the phosphorylation of IκBα on Ser32/36 that was induced by TNFα, without affecting the overall IκBα levels in both cell lines (Figure 30). Densitometric analysis data are available in Figure S8. Furthermore, the TNFR1-associated pathways JNK and MEKK were not affected by the inhibitory effects of KC-53 as determined by the detection of the total and phosphorylated levels of JNK and p38 (Figure 31).

Nuclear extraction and immunoblotting against the NF-κB subunit p65 showed a time-dependent decrease in the nuclear levels of p65 in response to KC-53 in both cell lines (Figure 32). An impressive 71% and 82% decrease in the p65 nuclear levels in HL-60 and CCRF/CEM cells, respectively, was noted after 6 h of treatment; apparently due to decreased translocation. Densitometric analysis charts are available in Figure S9. The KC-53-induced decrease in p65 nuclear expression observed by protein gel blotting was confirmed by significant reduction in nuclear immunostaining of p65 (Figure 33). As expected, TNFα treatment resulted in enhanced p65 staining in the nucleus, while co-treatment with KC-53 decreased p65 staining (Figure 33). The present findings show that the NF-κB

Christiana Savva

translocation can be suppressed by KC-53, which suggests the involvement of an NF-κB inhibition mechanism in apoptosis.

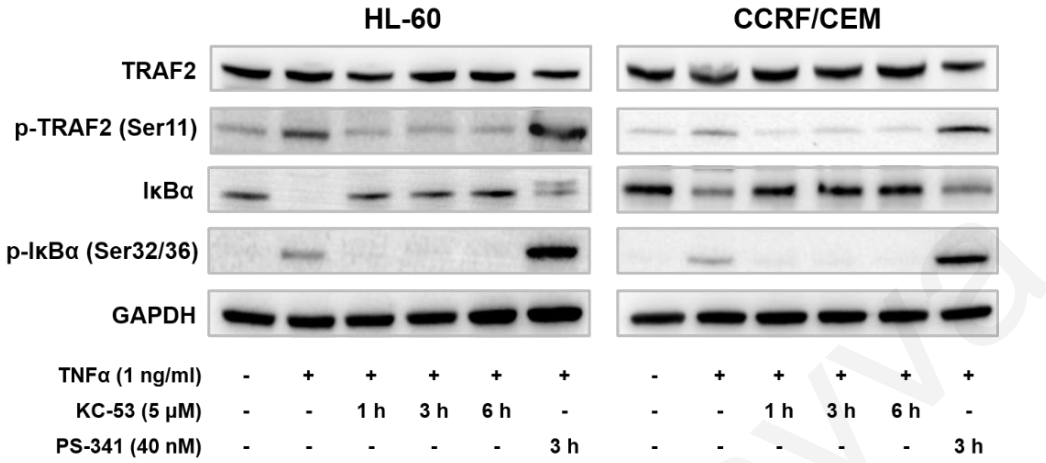

Figure 30. KC-53 diminishes TRAF2 phosphorylation and stabilizes IκBα. HL-60 and CCRF/CEM cells were incubated with vehicle, KC-53 or PS-34 for the times indicate followed by incubation with TNFα for 20 min. Whole cell protein lysates were analyzed by immunoblotting. The results are representative of three repetitions.

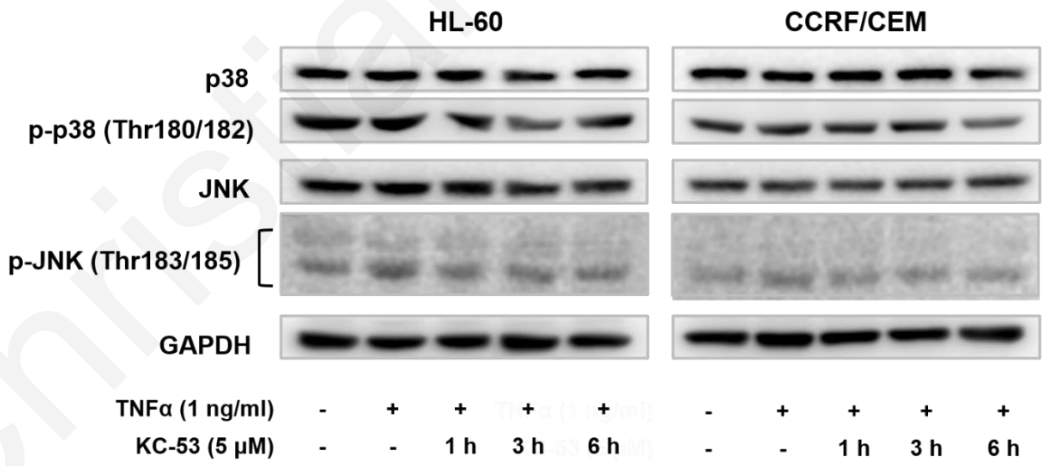

Figure 31. KC-53 does not affect p38 or JNK phosphorylated levels. HL-60 and CCRF/CEM cells were incubated with vehicle control, TNFα for 20 min or KC-53 for the times indicated followed by incubation with TNFα for 20 min. Whole cell protein lysates were analyzed by immunoblotting. The results are representative of three repetitions.

Christiana Sawa

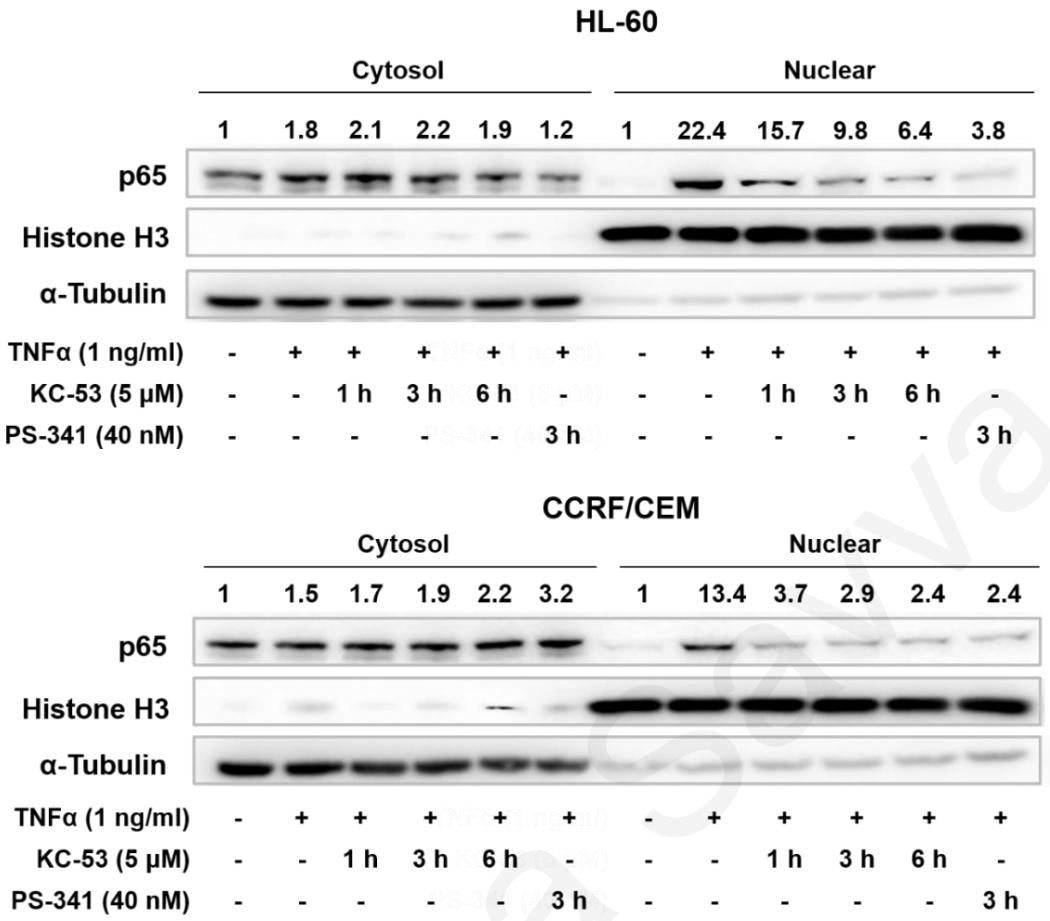

Figure 32. KC-53 hinders p65 translocation to the nucleus. Cells were incubated to either vehicle, KC-53 or PS-341 for the times indicated followed by the addition of TNFα for 20 min. The nuclear localization of p65 was examined by immunoblotting. The results are representative of three repetitions. Histone H3 levels were determined as a loading control and the α-Tubulin levels as an indicator of cytosolic contamination.

Christiana Sava

(ii)

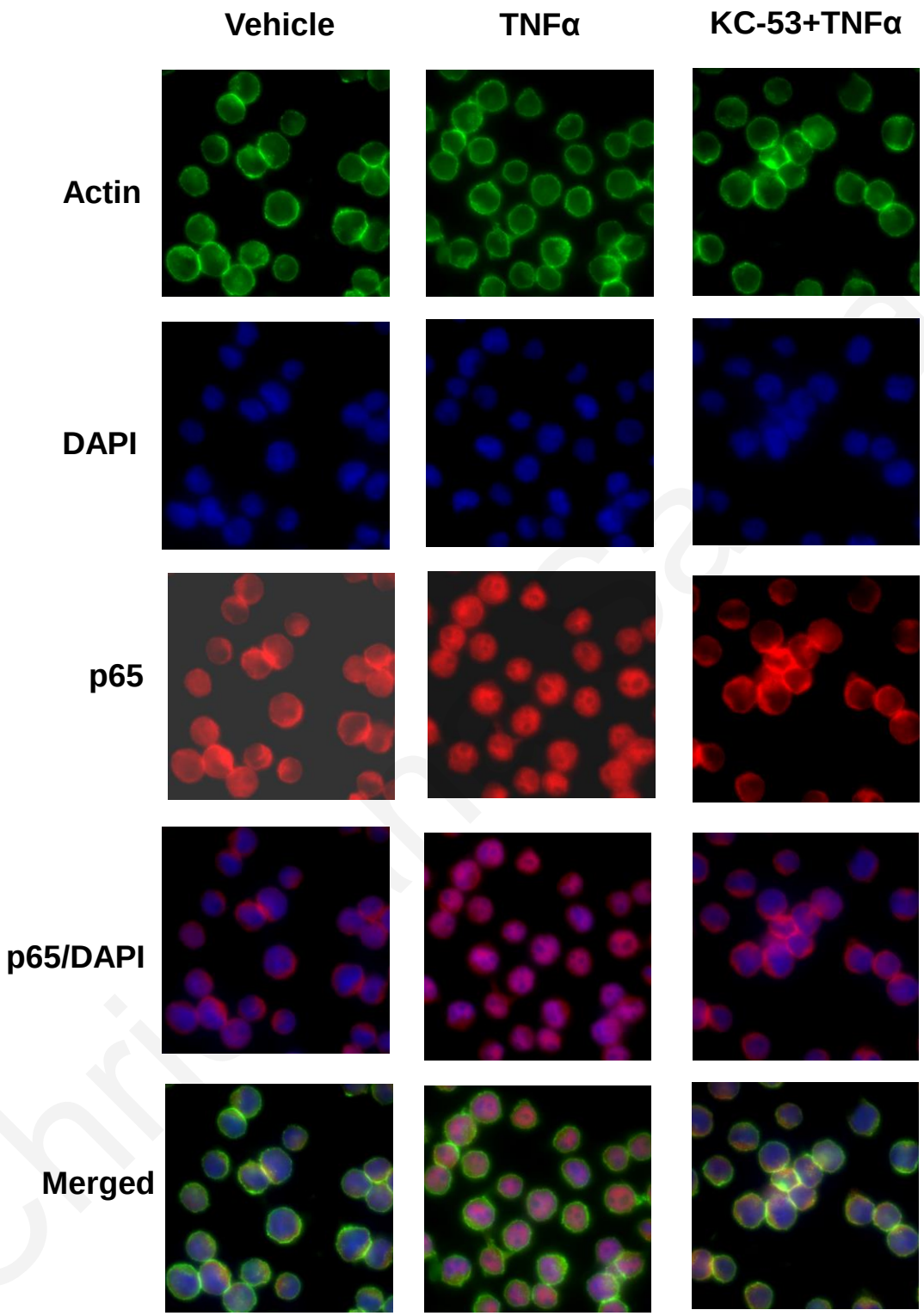

Figure 33. KC-53 hinders p65 translocation to the nucleus. (i) HL-60 and **(ii)** CCRF/CEM were treated with vehicle control, TNFα (1 ng/ml) for 20 min, or KC-53 (5 μM) for 1 h followed by incubation with TNFα (1 ng/ml) for 20 min. The subcellular localization of p65 was examined using fluorescence microscopy. More than 100 cells were inspected per experiment, and cells with typical morphology were presented. The results are representative of three repetitions. (Figure continued in the next page)

(ii)

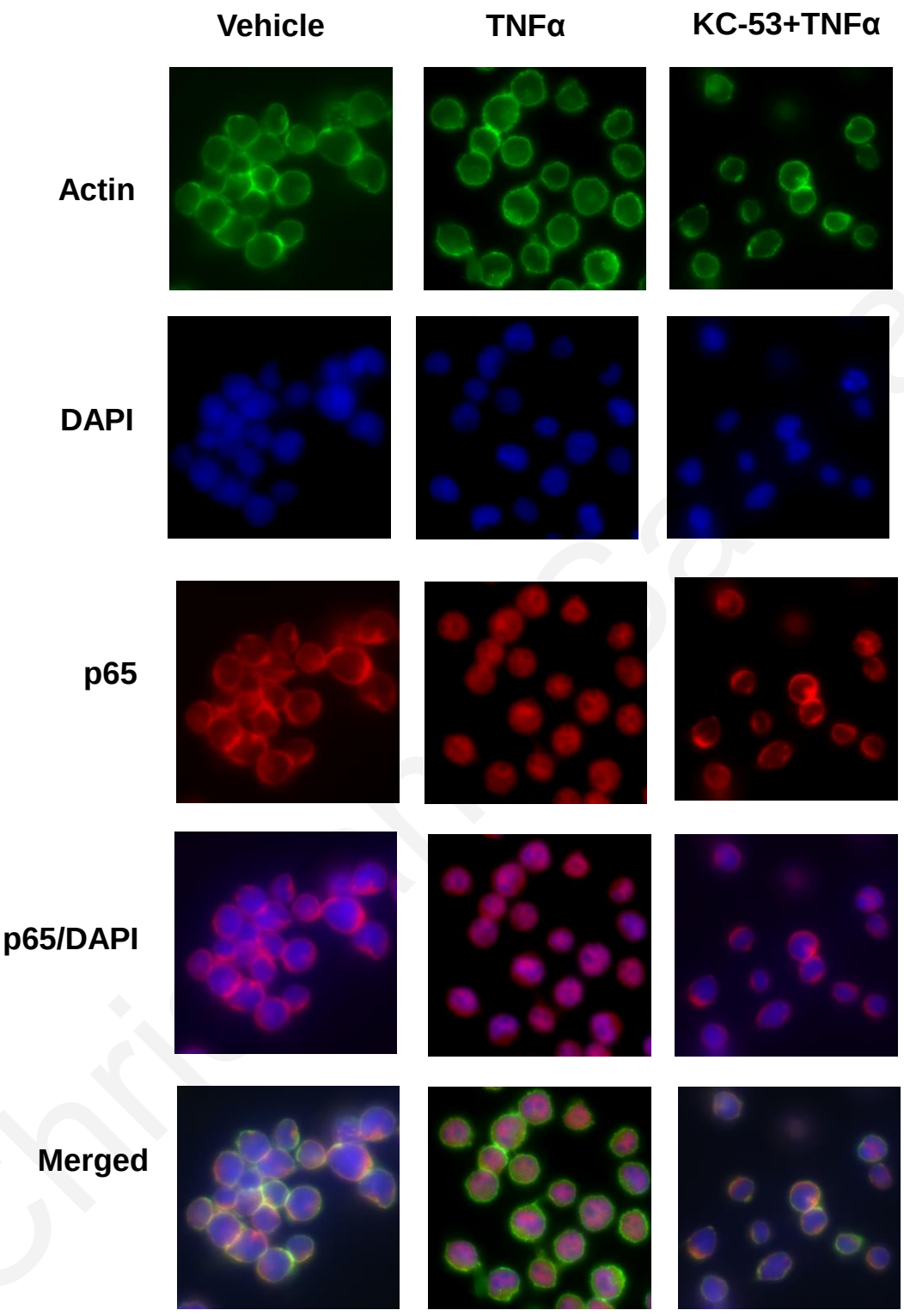

Figure 33 (Continued)

The efficiency of KC-53 in inhibiting TRAF2 and IκBα phosphorylation and/or p65 translocation was also compared with the established proteasome inhibitor, Bortezomib (PS-341). The inhibitor disrupts various cell signaling pathways including NFκ-B, leading to cell cycle arrest, apoptosis, and inhibition of angiogenesis. As was expected, PS-341 maintained the IκBα levels without abolishing the phosphorylation on Ser32/36, nor that of TRAF2 on Ser11 (Figure 30). Nonetheless, PS-341 reduced p65 nuclear levels by 83% compared to the TNFα-treated samples (Figure 32). Thus, the effects of KC-53 on the nuclear levels of p65 are similar to those of PS-341, although the mechanism by which this is achieved is different between the two compounds. In addition, we compared KC-53 and PS-341 leukemia cell sensitivity by using the effective concentrations of the compounds. As expected from our former results (Figure 12, 13 and Table 7) KC-53 decreased the viability of leukemia cell lines affecting moderately the normal PBMCs cells (Figure 34). Contrary to that, PS-341 decrease almost equally PBMCs, HL-60 and CCRF/CEM cell viability (Figure 34).

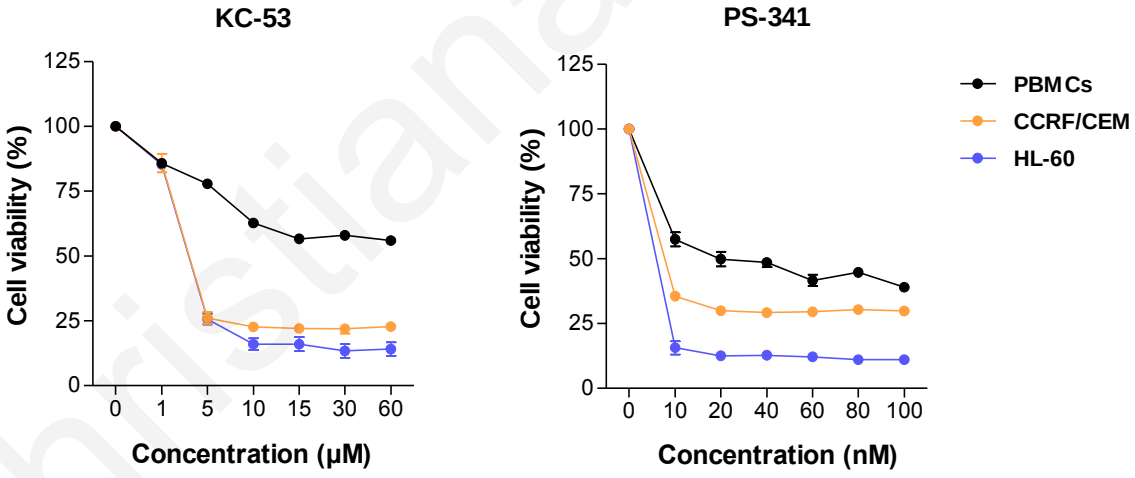

Figure 34. The effect of KC-53 against leukemia cell viability is more selective viability compared to PS-341. HL-60 and CCRF/CEM cells were treated with increasing concentrations of KC-53 (0-60 μM) or PS-341 (0-100 nM) or for 48 h. Cell viability determined by the MTT assay is expressed as percentage of survival in vehicle treated cells. The results represent the mean ±SEM of three different replicates and are representative of at least three different experiments.

Christiana Savva

Having observed the suppression of NF-κB translocation, we investigated the effects KC-53 on pro-survival and pro-inflammatory gene products. To address this, we determined the transcriptional levels of genes known to be transcriptionally activated by p65. Thus, cells were treated with TNFα alone (4 h) or with KC-53 (6 h) plus TNFα or vehicle. TNFα produced a substantial increase in all transcripts while KC-53 was found to significantly inhibit the expression of the pro-inflammatory cytokines; *IL -1β, -6 and -8* and the pro-survival mediators; *c-FLIP, cIAP-1, cIAP-2, BCL-xL* and *XIAP,* whereas *MCL-1*, *BCL-2* and *Survivin* mRNA levels were not significantly affected (Figure 35). From these results it can be concluded that KC-53 represses the TNFR1 pro-survival axis in favor of pro-apoptotic axis, blocking in this manner the activation of NF-κB signaling pathway in both cell lines.

Christiana Savva

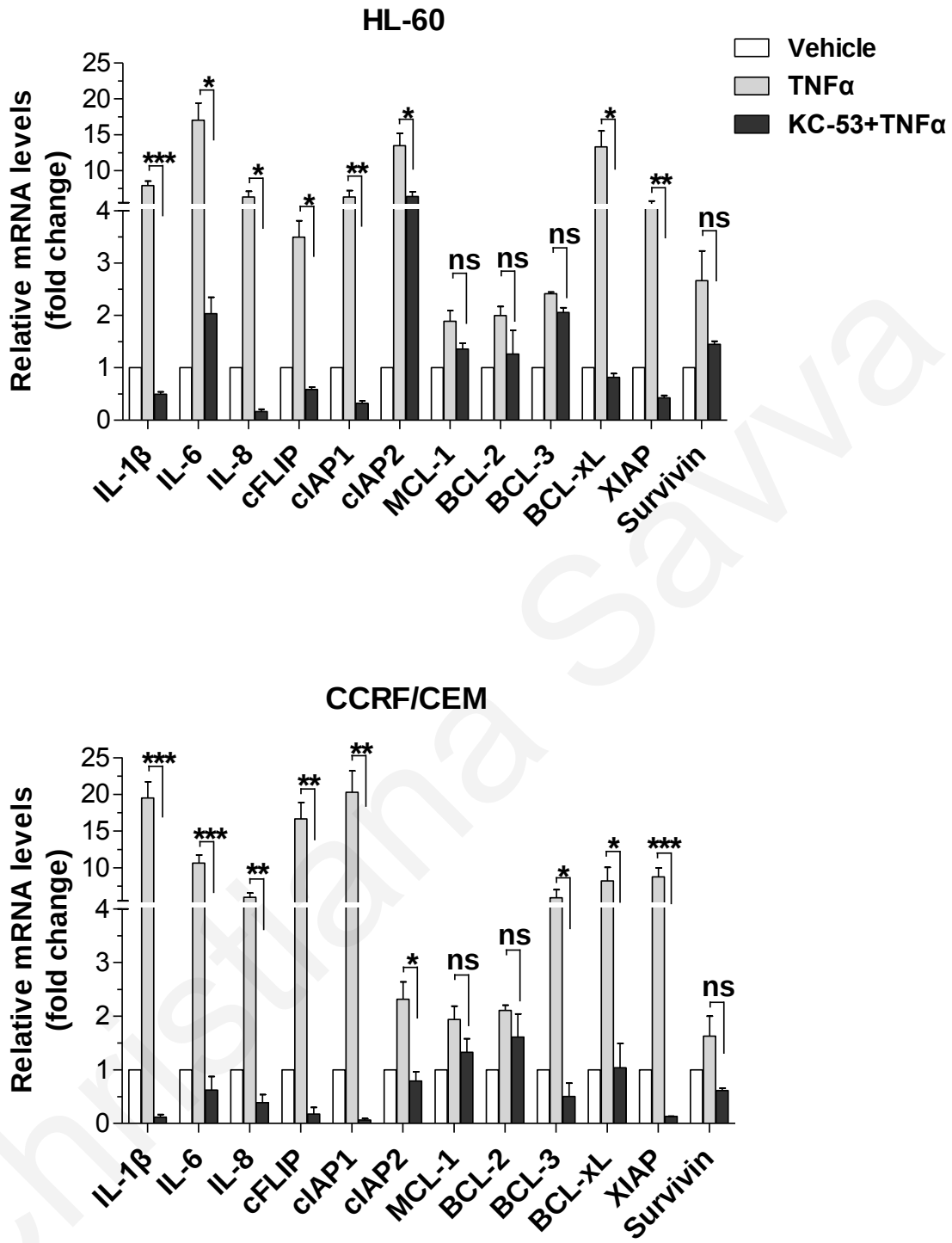

Figure 35. KC-53 downregulates the expression of p65 pro-inflammatory and pro-survival mediators. Cells were subjected to treatments either with the vehicle or TNFα (1 ng/ml) for 4 h, or KC-53 (5 μM) for 6 h plus TNFα for 4 h. The PCR products were normalized to those obtained from GAPDH mRNA amplification. The results represent the mean ± SEM of two different replicates and are representative of at least three independent experiments. (*p value < 0.05, **p value < 0.01, ***p value <0.001)

Christiana Savva

Silencing of FADD protects leukemic cells from KC-53 pro-apoptotic effects

This set of experiments was designed to further evaluate the above conclusions. FADD is a core protein of the pro-apoptotic complex facilitating Caspase-8 activation soon after TNFR1 activation (Tourneur and Chiocchia, 2010). In order to investigate whether apoptosis induction is directly linked to FADD, we used small interfering RNA (siRNA) to induce transient knockdown of FADD in HL-60 and CCRF/CEM cells (Figure 36). As shown in Figure 37A, specific targeting of FADD significantly restored cell viability by up to 81% and 90% in HL-60 and CCRF/CEM respectively. FADD knockdown was accompanied by KC-53 failure to activate Caspase-8, and to promote the proteolytic inactivation of RIP1 and PARP1 (Figure 37B). Consequently, FADD-deficient cells developed resistance to the anti-proliferative and apoptotic effects of KC-53. These data advocate the close correlation between the FADD/Caspase-8/RIP1 signaling axis and apoptotic effects of KC-53, which suggests being through activation of the TNFR1 death receptor initiated events.

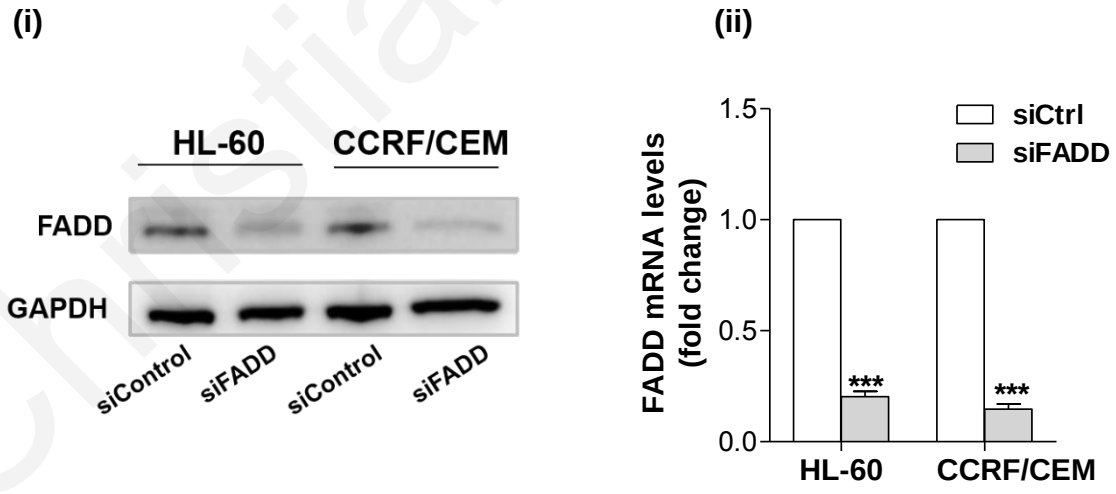

Figure 36. Translational silencing of FADD in HL-60 and CCRF/CEM cells. Cells were transiently transfected with siRNA control or siRNA FADD followed by **(i)** immunoblotting for the detection of FADD protein levels and **(ii)** qPCR in order to measure FADD mRNA levels. The results in (ii) panel represent the mean ± SEM of four different replicates and are representative of two separate experiments. (***p value < 0.001 compare to the vehicle siCtr)

Christiana Savva

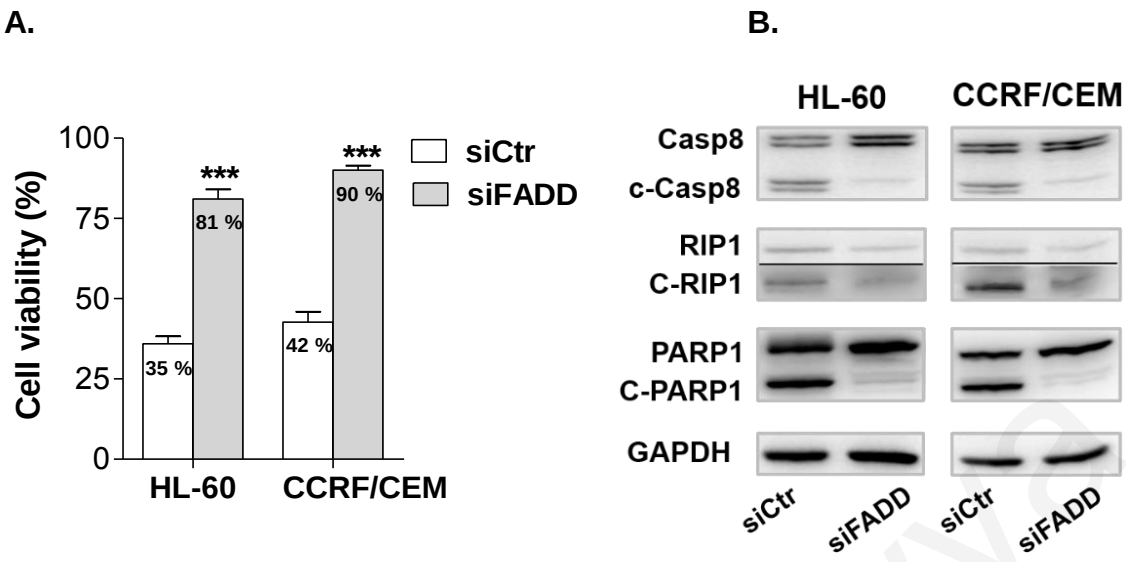

Figure 37. FADD silencing inhibits KC-53 induced apoptosis. (A) Transient transfected cells were treated with 0 or 5 μM KC-53 for 24 h and cell viability was determined with MTT assay. **(B)** Transiently transfected cells were treated with 5 μM KC-53 for 6 h and protein levels were determined by immunoblotting. The results in panel A represent the mean ± SEM of four different replicates and are representative of two separate experiments. The results in panel B are representative of three repetitions. (***p value < 0.001 compare to the vehicle siCtr)

Christiana Sawa

Chapter IV: Discussion

Even though the overall survival rate of patients with leukemia has dramatically increased in the past decade, there is still a strong need for discovering new therapeutic agents with higher specificity and milder side-effects (Reismuller et al., 2009, Horton et al., 2010, Schmiegelow et al., 2013). A large part of these studies is focused on natural products that play a crucial role in the emergence and advancement of organic synthesis.

Biyouyanagins A and B are sesquiterpene spiro-lactones isolated from the plant *Hypericum chinense.* They have a unique structural frame and a prominent activity against HIV replication and LPS-induced cytokine production (Tanaka et al., 2005, Nicolaou et al., 2008, Tanaka et al., 2009a, Nicolaou et al., 2011). KC-53 is a small, newly-synthetic analogue of biyouyanagin molecule poorly characterized for its biological properties apart from data supporting its anti-HIV activity and strong anti-inflammatory action. In the present study we investigate for the first time the anticancer efficacy of this novel compound and we examine its potential as a new anti-leukemic agent. Importantly, we discovered that, KC-53 reduces cancer cell viability and exhibits the highest cytotoxicity towards leukemic cell lines. Significantly, the novel agent promotes the activation of the death receptor TNFR1 and switches pro-survival to pro-apoptotic response. In leukemia cells, KC-53 effectively triggers primarily the extrinsic pathway of apoptosis, bypassing the p53-mitochondrial block and hindering the p65/NF-κB survival cascade.

Initially, the effects of KC-53 were evaluated in various human cancer cell lines in order to explore the role that the cellular microenvironment may affect the response to the agent. We have found that KC-53 reduces cancer cell viability in a dose-depended manner in all cancer cell lines and exhibits the highest cytotoxicity activity towards HL-60 (AML/APL) and CCR/CEM (ALL) leukemic cell lines. Remarkably, the normal PBMCs and the immortalized MCF-12F cells were relatively resistant to the anti-proliferative effects of the compound, suggesting that the KC-53 effects are selective against cancer cells. The observed decrease in cell viability is exclusive attributed to increase cell death as, the novel agent promoted rapidly and irreversibly apoptosis in both leukemic cell lines without affecting cell cycle progression neither in HL-60 nor in CCRF/CEM acute leukemia cells.

Christiana Sava

In order to examine the molecular mechanism(s) of induction of apoptosis we investigated whether KC-53 promotes the activation of death receptors and caspases in HL-60 and CCRF/CEM cells. Our results show that KC-53 upregulates the membrane-associated levels of TNFR1, promoting the activation of initiator Caspase-8 and therefore executor Caspases, -3 and -7. Thus, KC-53 activates the caspase-mediated apoptotic pathway in both cell lines. However, cell viability is not completely restored in the presence of the pan-caspase inhibitor, z.vad.fmk suggesting that CID mechanisms may also be involved in the mode of action of KC-53. This prediction is supported by the release and translocation of AIF from the mitochondrial to the nucleus (Figure 28B) which is commonly induced by Calpains and Cathepsins (Norberg et al., 2010). Interestingly, it has been previously shown that when Caspase-8 activity is blocked, the cell uses necroptosis as an alternative cell death pathway (Vandenabeele et al., 2010).

Necroptosis is a form of cell death controlled by death receptors, including TNFR1 that does not involve the activation of caspases. It is possible that following activation of the TNFR1 by KC-53, treatment with z.vad.fmk led to the inactivation of Caspase-8 preventing the degradation of RIP1 kinase. Various earlier studies reported that following inhibition of Caspase-8 by pharmacological interventions, RIP1 and RIP3 become phosphorylated and engage the effector mechanisms of necroptosis (Reviewed in (Vanden Berghe et al., 2010)). Based on our results, the ability of KC-53 to induce necroptosis cannot be excluded and requires further investigation. An issue that also remains open is how KC-53 promotes the stimulation of TNFR1 and whether this is the outcome of a direct or indirect interaction with the receptor.

It is supported by findings in the literature that ROS are also involved in CID apoptosis by promoting DNA and lipids oxidative damage (Circu and Aw, 2010). Furthermore, ROS are considered as one of the main mediators of non-programmed cell death, necrosis. ROS are formed as byproducts during various cellular mechanisms including the enzymatic conversion of H_2O_2 to water and oxygen. Recently published work from our laboratory has demonstrated that media containing sodium pyruvate (SP) in their formulations produce little or no H_2O_2 in comparison to media that do not contain it (Odiatou et al., 2013). In order to investigate the effects of the different culture conditions on the ability to KC-53 to

Christiana Savva

promote ROS generation in cancer cells, we treated HL-60 and CCRF/CEM cells with KC-53 in the presence or absence of SP in the media. Our results showed that KC-53 cell death is independent of ROS production and SP presence in cell culture media (Figure 22). Thus, it is obvious that KC-53-induced cell death is not caused by necrosis but exclusively by apoptosis. Consequently, the observed DNA damage in cells exposed to KC-53 is attributable to apoptosis and not oxidative damage.

Despite the fact that TNFR1 is required for induction of apoptosis, the main signaling outcome of induced TNFR1 is the activation of NF-κB (Micheau and Tschopp, 2003). NF-κB signaling cascade has been well-documented in AML and ALL, and several preclinical studies indicate that inhibition of this pathway could be an effective treatment for targeted therapy of leukemia (Lo Nigro, 2013, Bertacchini et al., 2014, Hsieh and Van Etten, 2014). Elevated NF-κB activity in cancer cells provides a survival mechanism by up-regulating anti-apoptotic genes, thereby representing a major causative factor for drug resistance. Further on this, NF-κB modulates the expression of inflammatory cytokines linking chronic inflammation to cancer development (Hoesel and Schmid, 2013).

TNFR1 pathway became a focus for anticancer therapeutics after the discovery that TNFα induces cell suicide. This discovery led to various attempts to stimulate apoptosis in cancer cells by activating TNFR1 signaling. However, initial attempts to activate the pathway by designing agents that activate through TNFα met with failure because of the inflammatory response induced by activation of the NF-κB pathway (Micheau et al., 2001). Anti-TNF antibodies (Song et al., 2002), IKK inhibitors (Cilloni et al., 2006, Carvalho et al., 2007) and proteasome inhibitors (Saito et al., 2013, Koyama et al., 2014, Nishioka et al., 2014) have been used to block the NF-κB pathway and to enhance the sensitivity of cancer cells to apoptosis. For instance, the proteasome inhibitor, Bortezomib is currently approved for the treatment of mantle cell lymphoma (Don and Zheng, 2011, Attar et al., 2013, Vasu and Blum, 2013, Walker et al., 2013). However, due to low specificity for cancer cells versus normal cells, it causes severe side-effects (Attar et al., 2013, Vasu and Blum, 2013, Walker et al., 2013). In particular, in a phase I clinical study in relapsed/refractory ALL, Bortezomib demonstrated significant dose-limiting toxicities (Cortes et al., 2004), whereas in a more resent phase I/II

Christiana Saliva

trial in combination with HyperCVAD, chemotherapy showed healthy tolerance but moderate effectiveness in patients complete remission (CR) and overall survival (OS) (Daver et al., 2015).

In order to investigate the potential use of KC-53 as a chemotherapeutic agent we compared its effects to those of Bortezomib (PS-341). Even though the proteasome inhibitor PS-341 is more potent than KC-53, PS-341 does not show selectivity between normal PBMCs and leukemia cells. What is more, our data revealed that KC-53 elicits effects comparable to Bortezomib's, regarding p65 nuclear translocation and IκBα inhibition though the mechanism by which this is achieved is different. These findings strongly propose a potential of KC-53 in cancer therapy without significant side-effects. However, evaluation of KC-53 in preclinical animal studies is required for assessing its potential as an effective and specific agent.

Proteasome, which is responsible for IκBα degradation, has many other vital cellular functions and it is also not feasible to block it for prolonged periods. Therefore, hindering NF-κB indirectly by controlling upstream regulatory molecules, like RIP1 or TRAF2, might be a more efficient and less cytotoxic approach for the treatment of leukemia and other types of cancers. Preclinical evidence for the importance of TRAF2 and RIP1 as targets for anticancer drugs is based on two observations: (i) that inactivating mutations of TRAF2 is a dominant-negative event, neutralizing TNFα-induced NF-κB activation (Zhang et al., 2011, Blackwell et al., 2009) and, (ii) RIP1-null cells or mice do not undergo TNFα-induced cell death (Reviewed in (O'Donnell and Ting, 2012, Weinlich et al., 2011)). In addition, more recent data supports that the E3 ubiquitin ligase activity of TRAF2 contributes to TNFα resistance in FLT3-ITD-positive AML cells (Schnetzke et al., 2013) and in IKKε-mediated tumorigenesis (Zhou et al., 2013), through NF-κB activation. Emerging events also support the oncogenic properties of TRAF2 in epithelial cancers. Aberrant TRAF2 expression or phosphorylation at Ser11 residues contribute to malignant transformation and resistance to apoptosis (Sharma et al., 2014, Shen et al., 2015, Sorokin et al., 2015). This phosphorylation is essential for TNF-α-induced secondary and prolonged IKK activation and NF-κB translocation. Thus, TRAF2 Ser phosphorylation inhibits apoptosis and promotes cell survival.

Christiana Savva

In the current study, KC-53 dramatically inhibits the TNFα-induced phosphorylation on Ser11 of TRAF2 as well as on Ser32/36 of IκBα. As a result, KC-53 stabilizes the cytoplasmic IκBα-p65/NF-κB complex and hinders p65 translocation to the nucleus. The agent also promotes a robust degradation of RIP1 as a consequence of Caspase-8 aberrant activation. As such, the absence of RIP1 and phospho-TRAF2, from the pro-survival complex blocked the downstream phosphorylation events leading to NF-κB activation. The above findings are further supported by knockdown experiments performed in HL-60 and CCRF/CEM cells. The participation of FADD in a complex with Caspase-8 and RIP1 is known to be required for the activation of the extrinsic pathway through TNFR1 (Lee et al., 2012). Silencing of FADD unleashed the pro-apoptotic effects of KC-53 rescuing RIP1 proteolytic inactivation and contributing to resistance of HL-60 and CCRF/CEM to KC-53. These results strongly suggest that, following TNFR1 activation, one of the primary apoptotic effects of KC-53 is the formation of the FADD/Caspsase-8/RIP1 pro-apoptotic complex. Since TRAF2 and RIP1 regulate several downstream regulatory molecules of the NF-κB cascade, the ability of KC-53 to affect molecules such as, TAK1, A20, IKKs must be further investigated.

Elevated NF-κB activity in cancer cells provides a survival mechanism by up-regulating anti-apoptotic genes such as cFLIP (Benayoun et al., 2008), cIAP1/2 and BCL-xL (Pahl, 1999). Besides, NF-κB modulates the expression of inflammatory cytokines linking chronic inflammation to cancer development (Hoesel and Schmid, 2013). In the current study, KC-53 reduces TNFα-stimulated gene expression of both pro-survival and pro-inflammatory p65-mediators at the basal levels (Figure 35). These findings could potentially shed light in the earlier report that KC-53 provokes strong anti-inflammatory activity (Nicolaou and Kannas, 2011, Nicolaou et al., 2011, Chang et al., 2012). It is worth noting that the genes evaluated in this study, have NF-κB binding sites in their promoter regions (Prasad et al., 2010). Subsequently, the effect of KC-53 on NF-κB transcriptional activity must be further investigated.

The above data firmly documents that KC-53, by blocking the phosphorylation and/or activation of upstream regulators of NF-κB such as TRAF2 and RIP1, hinders NF-κB survival axis in leukemia cells. In accordance with our results, similar sesquiterpene lactones, such as parthenolide, were found to retain

Christiana Savva

antitumor (Oka et al., 2007) and anti-inflammatory properties by direct (Siedle et al., 2004) or indirect (Hehner et al., 1999) inhibition of the NF-κB. In addition, KC-53 administration could find applications in overcoming resistance and/or increase responsiveness of cancer cells to conventional proteasome inhibitors. Whether KC-53's anticancer and anti-inflammatory activity resides with its dichloronucleobase- or its biyouyanagin-like moiety warrants further investigation.

Unlike most chemotherapeutic drugs, ligands of the TNF family induce apoptosis in a p53-independent manner and are promising alternatives to conventional chemotherapy. Specifically for leukemia, mutational inactivation of the p53 gene which mainly regulates apoptosis via the intrinsic pathway reduces cancer cell sensitivity to conventional treatments (Wattel et al., 1994, Melo et al., 2002). Thus, enabling the crosstalk between the still intact components of apoptotic signaling pathways represents a strong approach for drug development against leukemias (Jacquemin et al., 2010, Droin et al., 2013).

The crosstalk between the extrinsic and intrinsic pathways is well established and can be observed at both the execution and initiation level, enchansing the apoptotic outcome of the two pathways. Agents or stress-inducers can sensitize cells to death receptor-induced apoptosis, or the opposite, death signals may enhance cells sensitivity to mitochondrial-mediated apoptosis (Soderstrom et al., 2002, Metkar et al., 2003, Shankar and Srivastava, 2004, Cuello et al., 2004). In this aspect, KC-53 enables the crosstalk between the extrinsic and intrinsic pathway enabling cell lines with non-functional p53 to bypass the p53-mitochondrial block. Caspase-8-mediated cleavage of Bid provided the link between death receptor stimulation and mitochondrial apoptotic events following KC-53 administration. The tBid has the ability to accumulate at mitochondria and to initiate MOMP by interacting with Bax/Bak (Schug et al., 2011). MOMP in turn results in the release of pro-apoptotic factors from the mitochondrial intermembrane space, including cytochrome *c*, triggering formation of the apoptosome and activation of Caspase-9 (Gonzalvez et al., 2010, Schug et al., 2011). However, we did not observed any significant changes in the expression levels of Bax or Bcl-2 proteins suggesting that other molecules of the Bcl-2 family may be involved in the induction of the intrinsic pathway of apoptosis.

Christiana Savva

Collectively, the above data pinpoints that KC-53-induced apoptosis is attributed to the cross-talk between the extrinsic and intrinsic pathways, and importantly bypasses the p53-mitochondrial block. The engagement of the mitochondrial system amplifies the killing of malignant cells; something that may be of valuable importance in clinical implications, since it may critically reduce the time required for execution of the death program. This also suggests that KC-53 may find applications in leukemia with non-functional p53 that developed resistance to apoptosis.

The idea to specifically target the extrinsic pathway to trigger apoptosis in leukemia cells is attractive for cancer therapy since death receptors have a direct link to the death machinery (Jacquemin et al., 2010, Hegde et al., 2012, Droin et al., 2013). Nowadays, attention is focused on the development of TNFR-targeted cancer immunotherapies with very promising results (Bremer, 2013, Moran et al., 2013). Of interest is the development of TNF-based fusion proteins like the TNC-scTNFR2, which specifically activates TNFR2 and sensitized cancer cells to TNFR1 mediated apoptosis (Bueno et al., 2011). Nevertheless, the potential for systemic administration rhTNF in cancer patients depends on the cancer cells selectivity of the rhTNF-based drug. The effects of KC-53 as shown here are specific towards leukemia cells, as it spares human normal PBMCs, and breast non-tumorigenic cell line MCF-12F. In this respect, the combined use of KC-53 with TNFR2 agonist or rhTNFα in sequential treatment schedules may optimize therapeutic effects and minimize toxicity.

The ligand of death receptors DR4/5, TRAIL remains promising as a cancer therapeutic, despite the fact that many tumors remain refractory towards treatment with TRAIL (Fulda et al., 2002, von Haefen et al., 2004, Riccioni et al., 2005). In most, if not all, clinical studies the lack of efficacy was probably attributed to their inability to overcome the mitochondrial block (Ganten et al., 2004, Morizot et al., 2011, Jacquemin et al., 2012). In addition, the expression of Fas and DR5 (Wu et al., 1997) are mainly depended on p53 transcriptional activity. Consequently, cells that do not express p53 or express nonfunctional p53 they do not respond to therapy. Since KC-53 promotes apoptosis in a p53 independed manner and being a strong candidate for TNFR1 activation it may help to overcome TRAIL resistance and/or increase malignant cell sensitivity to chemotherapy.

Christiana Savva

Based on our findings, we propose a potential molecular mechanism of KC-53 antiproliferative anti apoptotic properties in acute leukemia cells (Figure 38). KC-53 acts by stimulating TNFR1 and inhibiting the phosphorylation of TRAF2, thereby promoting the activation of the FADD pro-apoptotic cascade inhibiting the NF-κB pro-survival axis. Precisely, following TNFR1 stimulation and TRAF2 hypophosphorylation, the death receptor kinase, RIP1 dissociates from TRADD/TRAF2 pro-survival complex and associates with FADD/pro-caspase 8 for the formation of the pro-apoptotic complex. This leads to the activation of the procaspase-8 which in turns cleaves and inactivates RIP1. Activated Caspase-8 thereby activates downstream effector Caspases, -3 and -7 that induce caspase-depended programmed cell death. Caspase-8 also cleaves and activates Bid (tBid), initiating the intrinsic/mitochondrial pathway of apoptosis. tBid leads to Caspase-9 activation and AIF release and translocation to the nucleus. AIF may also be involved in the induction of caspase-independed cell death. The absence of RIP1 and the hypophosphorylated form of TRAF2 diminishes the phosphorylation of IκBα inhibitor by downstream kinases. As a result, IκBα fails to be ubiquitinated and degraded by proteasome. Thus, IκBα remains in complex with NF-κB hindering its translocation to the nucleus and blocking cell survival signaling.

The present study provides compelling evidence that the antileukemic action of KC-53 involves the enrollment of the anticancer TNFR1 characteristics (pro-apoptotic axis) and resignation of the survival TNFR1 characteristics (NF-κB pro-survival axis). Our findings show for the first time that KC-53 effectively triggers apoptosis by facilitating both the extrinsic and intrinsic pathway, bypassing the p53-mitochondrial block and hindering the p65/NF-κB survival cascade in APL and ALL cells. The TNFR1 stimulation and the formation of the FADD/Caspase-8/RIP1 pro-apoptotic complex seems to be responsible for the main apoptotic effects mediated by KC-53 soon after its administration. KC-53-induced alterations in TRAF2 and IκBα phosphorylation may also be an initiating event and an important component of the underlying molecular mechanism blocking NF-κB survival and inflammatory signaling leading to apoptosis.

Because of these qualities, we anticipate that KC-53 is very likely to find applications, either as a single agent, or in combination with other conventional

chemotherapeutic agents in targeted therapeutics against acute leukemias. Our work also represents a new concept in the design of TNFR1-targeted therapies as this is the first time that an agent has been reported to stimulate efficiently TNFR1 inhibiting cancer cell growth and concurrently eliminate the activation of NF-κB.

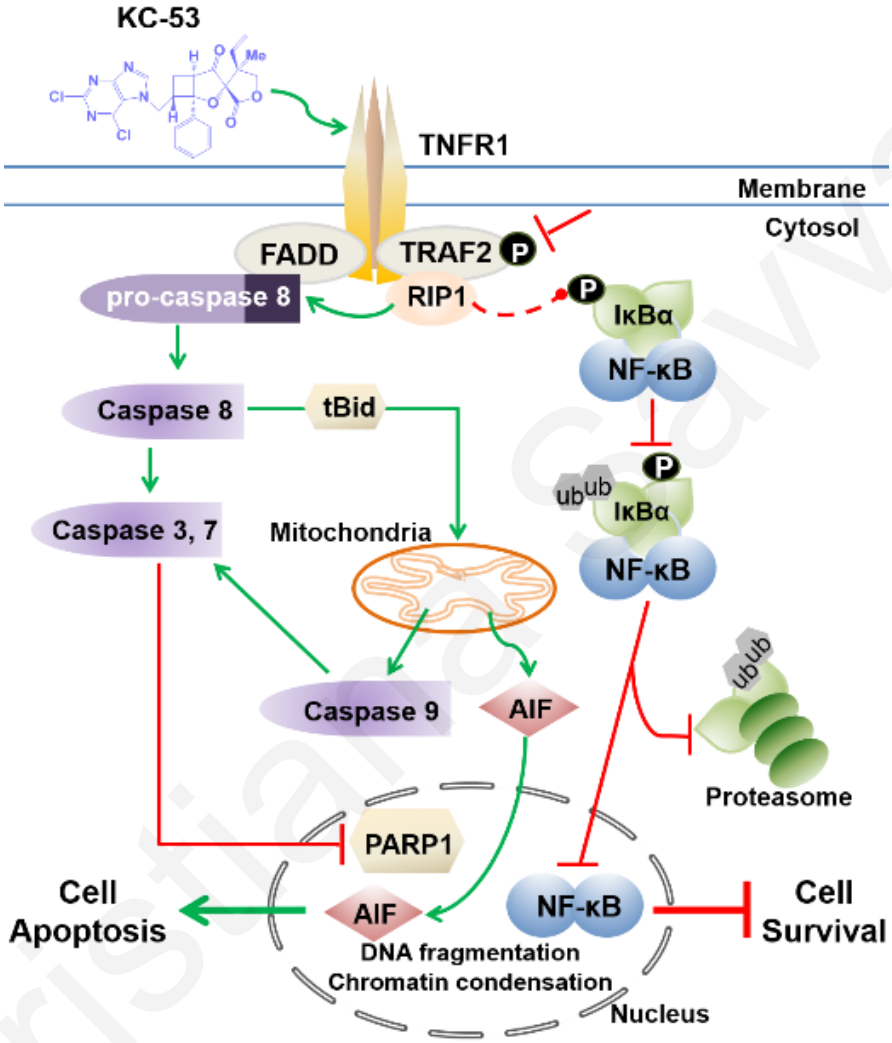

Figure 38. Sequence of molecular events leading to anti-proliferative and pro-apoptotic effects of KC-53 in leukemic cells. KC-53 stimulates TNFR1 and inhibits TRAF2 phosphorylation. RIP1 dissociates from TRAF2 and binds to the FADD/pro-caspase 8 complex. This leads to the activation of the procaspase-8 which in turns cleaves and inactivates RIP1. Caspase-8 triggers Bid cleavage, activation of effectors Caspases, -3 and -7 and inactivation of PARP1 promoting cell apoptosis. tBid leads to Caspase-9 activation and AIF release and translocation to the nucleus. The absence of RIP1 from TRADD/TRAF2 diminishes the phosphorylation of IκBα by downstream kinases. As a result, IκBα is not phosphorylated and fails to be ubiquitinated and degraded by proteasome. Subsequently, NF-κB remains in complex with IκBα and fails to translocate to the nucleus and cell survival signaling is hindered. P; phosphorylation ub; ubiquitination

Cristiana Cava

Chapter V: Future Work

Further investigation of the implication of TNFR1 in the mode of action of KC-53

An issue that remains open is the precise mechanism by which KC-53 stimulates TNFR1. Future experiments must be carried out in order to elucidate whether KC-53 binds (direct effect) or not (in-direct effect) to TNFR1 promoting its oligomerization and therefore activation. For these purpose we will perform affinity chromatography analysis (Rix et al., 2012) in which we will use immobilized KC-53 in order to pull down the protein(s) of interest. If KC-53 indeed binds to TNFR1, we will then use mutant TNFR1 lacking the extracellular or intracellular domain in order to uncover the precise binding site of the KC-53.

Investigation of the early phosphorylation events initiated by KC-53

The data presented in this study, signify that KC-53 can switch on/off signaling pathways of apoptosis and survival by affecting protein kinases networks. To precisely unravel the phosphorylation cascade(s) that are initiated shortly after KC-53 administration, we are planning to use a global quantitative phosphoproteomics approach. In collaboration with Dr. *Garbis D*., whose work is specialized in high-resolution mass spectrometry analysis (LC-MS/MS), we have identified distinguishing signatures between KC-53-treated and untreated HL-60 cells (Figure S10). The preliminary results from this analysis revealed various phosphorylation cellular responses related to apoptosis and survival, including transcription and chromatin modifications, immune responses, endoplasmic reticulum stress response, and organelle organization. The key molecules (kinases and phosphatases) of these series of experiments will be further validated for their importance by gain- and loss- of function studies and kinases assays.

Further investigation of the underlying mechanism(s) involved in NF-κB inhibition

As part of this aim we plan to further investigate the effect of KC-53 on molecules acting upstream of NF-κB (downstream of TNFR1). As previously mentioned, DUB

Christiana Savva

A20 and CYLD remove K63- and K48- linked polyubiquitin chains from RIP1 and IKKs kinases resulting in the downregulation of the canonical NF-κB signaling cascade (Shembade and Harhaj, 2012, Hoffmann et al., 2002). Apart from these proteins, there are several other negative regulators of the NF-κB signaling including ITCH and TAX1BP1. Preliminary experiments in HL-60 and CCRF/CEM cells treated with KC-53 for 6 h, revealed that, the mRNA levels of A20 and CYLD are significantly increased in the treated cells correspondingly (Figure S11). To further explore this possibility, we will determine the effect of KC-53 on the total and phospho- protein levels of the molecules by immunoblotting. We expect that if these proteins are implicated in the NF-κB-inhibitory mechanism induced by KC-53, both the total and phospho- (Ser418) levels of CYLD and total levels of A20 and ITCH will be increased following treatment with the agent.

Another part of this aim is to determine the ability of KC-53 to inhibit the phosphorylation and activation of IKKs. To accomplish this, we will be perform kinetic studies using the IKK-α and -β Assay/Inhibitor Screening kit (Cyclex). The effectiveness of KC-53 in reducing IKK activity will also be compared with the known IKK inhibitor, IKK VII (Calbiochem). CCRF/CEM and HL-60 will be treated with KC-53 for different time points (15 – 60 min) prior IKK-α and IKK-β isolation with specific antibodies. The amount of the phosphorylated substrate (IκBα) will be determined by reading optical intensity at 450 nm. We anticipate that, KC-53- and IKK VII will produce a decrease in the basal activity of IKKs relative to the vehicle controls.

Further evaluation of the effect of KC-53 on the NF-κB activity

Since KC-53 was found to inhibit the translocation of NF-κB to the nucleus and TNFα-induced expression of NF-κB-target genes, the effect of KC-53 on NF-κB activation must be further investigated. For this aim we will use the Luciferase Reporter Assay (Dual-Luciferase Reporter (DLR) Assay, Promega) during which, HL-60 and CCRF/CEM cells will be transfected with Luciferase construct containing three copies of the NF-κB/p65 binding site upstream of the luciferase reporter gene. The firefly luciferase reporter is measured by adding luciferase assay reagent to generate a stabilized luminescent signal. Cells will be incubated with TNF-α followed by treatment with KC-53 and the effect of the compound on

Christiana Savva

the transcriptional activity of the construct will be measured using luminometer. We expect that NF-κB transcriptional activity will be inhibited in the presence of KC-53.

Further investigation of the Caspase-independent pathways induced by KC-53

In the present study, KC-53 was able to induce caspase-independent apoptosis in leukemia cells. Necroptosis is one of the main CID-mechanisms induced by specific groups of proteases namely, Calpains and Cathepsins. In order to further investigate the CID mechanisms of apoptosis, we will determine the effect of KC-53 on the activation of Calpains and Cathepsins in both cell lines by using a Caplain (ab65308) and Cathepsin (ab65300) activity assay kit respectively. We expect that, if Calpains and/or Cathepsins are implicated in the CID-cell death induced by the compound, the activity of these proteases will be elevated following treatment with KC-53. Another alternative CID apoptotic mechanism is autophagy. By our preliminary results using the known autophagy inhibitor, Bafilomycin A1 in combination with KC-53, we found that KC-53 administration does not restore cell viability (Figure S12), suggesting that autophagy is possibly not induced by KC-53. To further exclude this possibility the expression of various Autophagy (Atg)-related genes, as well as, the activity of mTOR kinase need to be exploited.

Investigation of the ability of KC-53 to act synergistically with other compounds

Based on the proposed mechanism of action of KC-53 as derived from the current study, the ability of KC-53 to enhance the effect or act synergistically with compounds affecting the same molecular pathways will be explored. The combined effect of KC-53 and PS-341 which is currently approved for the treatment of specific types of leukemia, on proliferation and survival of leukemia cells will be investigated *in vitro*. Furthermore, the combination of KC-53 with NF-κB inhibitors (CHS 828, BAY-43-9006) which are also being investigated in preclinical studies will also be evaluated using leukemia and normal cell lines.

Christiana Sawa

Evaluation of the in vivo efficacy of KC-53 in acute leukemia treatment

It's critical and very important to shown in *in vivo* follow-up studies that such advanced compound remain effective and can be sufficiently active at the site of the tumor. In order to investigate the effects of KC-53 on leukemia cells *in vivo*, we will use A20-luciferase (*luc*$^{+}$)-expressing leukemia cells that have been previously demonstrated to migrate primarily to the bone marrow with secondary infiltration of spleen and other lymphoid organs when injected intravenously. C57B/6 mice will be injected with A20 cells and then treated with the compound intraperitoneally. Cells growth will be monitored twice a week and after the completion of the experiments lymph nodes and spleens will used for the following *in vitro* experiments: (i) immunostaining analysis and (ii) ELISA assay for quantitation of cytokines expression levels.

Christiana Savva

References

ABDEL HAMID, T. M., EL GAMMAL, M. M., EIBEAD, G. T., SABER, M. M. & ABOL ELAZM, O. M. 2015. Clinical impact of SNP of P53 genes pathway on the adult AML patients. *Hematology,* 20**,** 328-35.

ABDULGHANI, J. & EL-DEIRY, W. S. 2010. TRAIL receptor signaling and therapeutics. *Expert Opin Ther Targets,* 14**,** 1091-108.

ABE, S., TANAKA, N. & KOBAYASHI, J. 2012. Prenylated acylphloroglucinols, chipericumins A-D, from Hypericum chinense. *J Nat Prod,* 75**,** 484-8.

ADDEO, R., CARAGLIA, M., BALDI, A., D'ANGELO, V., CASALE, F., CRISCI, S., ABBRUZZESE, A., VINCENZE, B., CAMPIONI, M., DI TULLIO, M. T. & INDOLFI, P. 2005. Prognostic role of bcl-xL and p53 in childhood acute lymphoblastic leukemia (ALL). *Cancer Biol Ther,* 4**,** 32-8.

ADEKOYA, E., AIT-ZAHRA, M., ALLEN, N., ANDERSON, M., ANDERSON, S., ANUFRIEV, F., AMBRUSTER, J., AYELE, K., BAKER, J., BALDWIN, J., BARNA, N., BASTIEN, V., BATZOGLOU, S., BECKERLY, R., BEDA, F., BERNARD, J., BIRREN, B., BLUMENSTEIL, B., BOGUSLAVSKY, L., BOUKGHALTER, B., BROWN, A., BURKETT, G., CAMARATA, J., CAMPOPIANO, A., CARNEIRO, H., CHEN, Z., CHOEPHAL, Y., COLANGELO, M., COLLINS, S., COLLYMORE, A., COOKE, P., DAVIS, C., DAWOE, T., DEARELLANO, K., DEVON, K., DEWAR, K., DIAZ, J. S., DODGE, S., DONELAN, E., DORJEE, K., DOYLE, M., DUBE, A., DUPES, A., ENDRIZZI, M., FARINA, A., FARO, S., FERGUSON, D., FERRIERA, P., FISCHER, H., FITZHUGH, W., FLAHERTY, K., FOLEY, K., FUNKE, R., GAGE, D., GALAGAN, J., GARDYNA, S., GILBERT, D., GINDE, S., GOMES, A., GOYETTE, M., GRAHAM, J., GRAHAM, L., GRANDBOIS, E., GRAND-PIERRE, N., GRANT, G., GREGOIRE, D., GUERRERO, R., HAGOS, B., HARRIS, K., HART, D., HATCHER, B., HEAFORD, A., HORTON, L., HOSAGE-NORMAN, C., HOWLAND, J., HULME, B., ILIEV, I., JOHNSON, R., JONES, C., JOSEPH, M., JUDD, M., KANN, L., KARATAS, A., KELLEY, D., KELLY, M., LAMA, D., LAMAZARES, J., LANDER, E. S., LANDERS, T., LANE, A., LAROCQUE, K., LEBLANC, H., LEGER, J. P., LEHOCZKY, J., LEVINE, R., LEWIS, D., LEWIS, T., LIEU,

Christiana Savva

C., LINTON, L., LIU, G., et al. 2001. Initial sequencing and analysis of the human genome. *Nature,* 409**,** 860-921.

ADES, L., GUERCI, A., RAFFOUX, E., SANZ, M., CHEVALLIER, P., LAPUSAN, S., RECHER, C., THOMAS, X., RAYON, C., CASTAIGNE, S., TOURNILHAC, O., DE BOTTON, S., IFRAH, N., CAHN, J. Y., SOLARY, E., GARDIN, C., FEGEUX, N., BORDESSOULE, D., FERRANT, A., MEYER-MONARD, S., VEY, N., DOMBRET, H., DEGOS, L., CHEVRET, S. & FENAUX, P. 2010. Very long-term outcome of acute promyelocytic leukemia after treatment with all-trans retinoic acid and chemotherapy: the European APL Group experience. *Blood,* 115**,** 1690-6.

ADVANI, A. S. 2013. Biology and treatment of acute lymphocytic leukemia in adolescents and young adults. *Am Soc Clin Oncol Educ Book***,** 285-9.

ALIANO, S., CIRMENA, G., FUGAZZA, G., BRUZZONE, R., PALERMO, C. & SESSAREGO, M. 2013. Standard and variant Philadelphia translocation in a CML patient with different sensitivity to imatinib therapy. *Leuk Res Rep,* 2**,** 75-8.

AMAKI, K. 1982. [French-American-British (FAB) classification of acute leukemia]. *Rinsho Ketsueki,* 23**,** 988-90.

AMROLIA, P. J., REID, S. D., GAO, L., SCHULTHEIS, B., DOTTI, G., BRENNER, M. K., MELO, J. V., GOLDMAN, J. M. & STAUSS, H. J. 2003. Allorestricted cytotoxic T cells specific for human CD45 show potent antileukemic activity. *Blood,* 101**,** 1007-14.

AN, X., TIWARI, A. K., SUN, Y., DING, P. R., ASHBY, C. R., JR. & CHEN, Z. S. 2010. BCR-ABL tyrosine kinase inhibitors in the treatment of Philadelphia chromosome positive chronic myeloid leukemia: a review. *Leuk Res,* 34**,** 1255-68.

ARATAKE, K., KAMACHI, M., IWANAGA, N., KAWASAKI, E., IZUMI, Y., IDA, H., TANAKA, F., TAMAI, M., ARIMA, K., NAKAMURA, H., ORIGUCHI, T., KAWAKAMI, A. & EGUCHI, K. 2005. A cross-talk between RNA splicing and signaling pathway alters Fas gene expression at post-transcriptional level: alternative splicing of Fas mRNA in the leukemic U937 cells. *J Lab Clin Med,* 146**,** 184-91.

ARCH, R. H., GEDRICH, R. W. & THOMPSON, C. B. 1998. Tumor necrosis factor receptor-associated factors (TRAFs)--a family of adapter proteins that regulates life and death. *Genes Dev,* 12**,** 2821-30.

Christiana Savva

ASHKENAZI, A. & DIXIT, V. M. 1998. Death receptors: signaling and modulation. *Science,* 281**,** 1305-8.

ASSELIN, B. L., GAYNON, P. & WHITLOCK, J. A. 2013. Recent advances in acute lymphoblastic leukemia in children and adolescents: an expert panel discussion. *Curr Opin Oncol,* 25 Suppl 3**,** S1-13; quiz S14-6.

ATTAR, E. C., JOHNSON, J. L., AMREIN, P. C., LOZANSKI, G., WADLEIGH, M., DEANGELO, D. J., KOLITZ, J. E., POWELL, B. L., VOORHEES, P., WANG, E. S., BLUM, W., STONE, R. M., MARCUCCI, G., BLOOMFIELD, C. D., MOSER, B. & LARSON, R. A. 2013. Bortezomib added to daunorubicin and cytarabine during induction therapy and to intermediate-dose cytarabine for consolidation in patients with previously untreated acute myeloid leukemia age 60 to 75 years: CALGB (Alliance) study 10502. *J Clin Oncol,* 31**,** 923-9.

AVVISATI, G., LO-COCO, F., PAOLONI, F. P., PETTI, M. C., DIVERIO, D., VIGNETTI, M., LATAGLIATA, R., SPECCHIA, G., BACCARANI, M., DI BONA, E., FIORITONI, G., MARMONT, F., RAMBALDI, A., DI RAIMONDO, F., KROPP, M. G., PIZZOLO, G., POGLIANI, E. M., ROSSI, G., CANTORE, N., NOBILE, F., GABBAS, A., FERRARA, F., FAZI, P., AMADORI, S. & MANDELLI, F. 2011. AIDA 0493 protocol for newly diagnosed acute promyelocytic leukemia: very long-term results and role of maintenance. *Blood,* 117**,** 4716-25.

BAKER, S. J. & REDDY, E. P. 1998. Modulation of life and death by the TNF receptor superfamily. *Oncogene,* 17**,** 3261-70.

BALKWILL, F. 2002. Tumor necrosis factor or tumor promoting factor? *Cytokine Growth Factor Rev,* 13**,** 135-41.

BARNHART, B. C. & PETER, M. E. 2003. The TNF receptor 1: a split personality complex. *Cell,* 114**,** 148-50.

BAUMER, N., BAUMER, S., BERKENFELD, F., STEHLING, M., KOHLER, G., BERDEL, W. E., MULLER-TIDOW, C. & TSCHANTER, P. 2014. Maintenance of leukemia-initiating cells is regulated by the CDK inhibitor Inca1. *PLoS One,* 9**,** e115578.

BENAYOUN, B., BAGHDIGUIAN, S., LAJMANOVICH, A., BARTOLI, M., DANIELE, N., GICQUEL, E., BOURG, N., RAYNAUD, F., PASQUIER, M. A., SUEL, L., LOCHMULLER, H., LEFRANC, G. & RICHARD, I. 2008. NF-kappaB-dependent expression of the antiapoptotic factor c-FLIP is

regulated by calpain 3, the protein involved in limb-girdle muscular dystrophy type 2A. *FASEB J,* 22**,** 1521-9.

BENNETT, J. M., CATOVSKY, D., DANIEL, M. T., FLANDRIN, G., GALTON, D. A., GRALNICK, H. R. & SULTAN, C. 1976. Proposals for the classification of the acute leukaemias. French-American-British (FAB) co-operative group. *Br J Haematol,* 33**,** 451-8.

BENNETT, J. M., CATOVSKY, D., DANIEL, M. T., FLANDRIN, G., GALTON, D. A., GRALNICK, H. R. & SULTAN, C. 1985. Proposed revised criteria for the classification of acute myeloid leukemia. A report of the French-American-British Cooperative Group. *Ann Intern Med,* 103**,** 620-5.

BERNARD, O. A., GILLILAND, D. G. & MERCHER, T. 2009. [The OTT-MAL fusion oncogene: another Notch in megakaryoblastic leukemia]. *Med Sci (Paris),* 25**,** 676-8.

BERTACCHINI, J., GUIDA, M., ACCORDI, B., MEDIANI, L., MARTELLI, A. M., BAROZZI, P., PETRICOIN, E., 3RD, LIOTTA, L., MILANI, G., GIORDAN, M., LUPPI, M., FORGHIERI, F., DE POL, A., COCCO, L., BASSO, G. & MARMIROLI, S. 2014. Feedbacks and adaptive capabilities of the PI3K/Akt/mTOR axis in acute myeloid leukemia revealed by pathway selective inhibition and phosphoproteome analysis. *Leukemia,* 28**,** 2197-205.

BISWAS, P. & FERRARINI, M. 2012. A matter of life and death: more members of the TNF receptor family join human gammadelta T lymphocytes. *Eur J Immunol,* 42**,** 803-4.

BLACKWELL, K., ZHANG, L., THOMAS, G. S., SUN, S., NAKANO, H. & HABELHAH, H. 2009. TRAF2 phosphorylation modulates tumor necrosis factor alpha-induced gene expression and cell resistance to apoptosis. *Mol Cell Biol,* 29**,** 303-14.

BOMBARDELLI, E. & MORAZZONI, P. 1995. Hypericum perforatum *Fitoterapia,* 66**,** 43-68.

BONNET, D. & DICK, J. E. 1997. Human acute myeloid leukemia is organized as a hierarchy that originates from a primitive hematopoietic cell. *Nat Med,* 3**,** 730-7.

BREIT, S., STANULLA, M., FLOHR, T., SCHRAPPE, M., LUDWIG, W. D., TOLLE, G., HAPPICH, M., MUCKENTHALER, M. U. & KULOZIK, A. E. 2006. Activating NOTCH1 mutations predict favorable early treatment response

Christiana Savva

and long-term outcome in childhood precursor T-cell lymphoblastic leukemia. *Blood,* 108**,** 1151-7.

BREMER, E. 2013. Targeting of the tumor necrosis factor receptor superfamily for cancer immunotherapy. *ISRN Oncol,* 2013**,** 371854.

BRUNELLE, J. K. & LETAI, A. 2009. Control of mitochondrial apoptosis by the Bcl-2 family. *J Cell Sci,* 122**,** 437-41.

BUENO, N. D., DULLEY, F. L., SABOYA, R., AMIGO FILHO, J. U., CORACIN, F. L. & CHAMONE DDE, A. 2011. Busulfan and melphalan as conditioning regimen for allogeneic hematopoietic stem cell transplantation in acute myeloid leukemia in first complete remission. *Rev Bras Hematol Hemoter,* 33**,** 179-84.

BUESO-RAMOS, C., XU, Y., MCDONNELL, T. J., BRISBAY, S., PIERCE, S., KANTARJIAN, H., ROSNER, G. & GARCIA-MANERO, G. 2005. Protein expression of a triad of frequently methylated genes, p73, p57Kip2, and p15, has prognostic value in adult acute lymphocytic leukemia independently of its methylation status. *J Clin Oncol,* 23**,** 3932-9.

BUITENKAMP, T. D., IZRAELI, S., ZIMMERMANN, M., FORESTIER, E., HEEREMA, N. A., VAN DEN HEUVEL-EIBRINK, M. M., PIETERS, R., KORBIJN, C. M., SILVERMAN, L. B., SCHMIEGELOW, K., LIANG, D. C., HORIBE, K., ARICO, M., BIONDI, A., BASSO, G., RABIN, K. R., SCHRAPPE, M., CARIO, G., MANN, G., MORAK, M., PANZER-GRUMAYER, R., MONDELAERS, V., LAMMENS, T., CAVE, H., STARK, B., GANMORE, I., MOORMAN, A. V., VORA, A., HUNGER, S. P., PUI, C. H., MULLIGHAN, C. G., MANABE, A., ESCHERICH, G., KOWALCZYK, J. R., WHITLOCK, J. A. & ZWAAN, C. M. 2014. Acute lymphoblastic leukemia in children with Down syndrome: a retrospective analysis from the Ponte di Legno study group. *Blood,* 123**,** 70-7.

BYRD, J. C., EDENFIELD, W. J., DOW, N. S., AYLESWORTH, C. & DAWSON, N. 1996. Extramedullary myeloid cell tumors in myelodysplastic-syndromes: not a true indication of impending acute myeloid leukemia. *Leuk Lymphoma,* 21**,** 153-9.

CANDE, C., CECCONI, F., DESSEN, P. & KROEMER, G. 2002. Apoptosis-inducing factor (AIF): key to the conserved caspase-independent pathways of cell death? *J Cell Sci,* 115**,** 4727-34.

Christiana Sava

CANTU-RAJNOLDI, A., FEDERICI, A. B., BIONDI, A., CORTELEZZI, A., ROMITTI, L., GORNATI, G., GAIPA, G., GIANOTTI, G. & MANNUCCI, P. 1994. Acute promyelocytic leukemia with unusual morphological features, absence of the t(15,17) and rearranged PML/RAR alpha genes. *Haematologica,* 79**,** 294-6.

CARBONE, R., BOTRUGNO, O. A., RONZONI, S., INSINGA, A., DI CROCE, L., PELICCI, P. G. & MINUCCI, S. 2006. Recruitment of the histone methyltransferase SUV39H1 and its role in the oncogenic properties of the leukemia-associated PML-retinoic acid receptor fusion protein. *Mol Cell Biol,* 26**,** 1288-96.

CARVALHO, G., FABRE, C., BRAUN, T., GROSJEAN, J., ADES, L., AGOU, F., TASDEMIR, E., BOEHRER, S., ISRAEL, A., VERON, M., FENAUX, P. & KROEMER, G. 2007. Inhibition of NEMO, the regulatory subunit of the IKK complex, induces apoptosis in high-risk myelodysplastic syndrome and acute myeloid leukemia. *Oncogene,* 26**,** 2299-307.

CASASNOVAS, R. O., SLIMANE, F. K., GARAND, R., FAURE, G. C., CAMPOS, L., DENEYS, V., BERNIER, M., FALKENRODT, A., LECALVEZ, G., MAYNADIE, M. & BENE, M. C. 2003. Immunological classification of acute myeloblastic leukemias: relevance to patient outcome. *Leukemia,* 17**,** 515-27.

CERVERA, J., MONTESINOS, P., HERNANDEZ-RIVAS, J. M., CALASANZ, M. J., AVENTIN, A., FERRO, M. T., LUNO, E., SANCHEZ, J., VELLENGA, E., RAYON, C., MILONE, G., DE LA SERNA, J., RIVAS, C., GONZALEZ, J. D., TORMO, M., AMUTIO, E., GONZALEZ, M., BRUNET, S., LOWENBERG, B. & SANZ, M. A. 2010. Additional chromosome abnormalities in patients with acute promyelocytic leukemia treated with all-trans retinoic acid and chemotherapy. *Haematologica,* 95**,** 424-31.

CHAN, F. K., CHUN, H. J., ZHENG, L., SIEGEL, R. M., BUI, K. L. & LENARDO, M. J. 2000. A domain in TNF receptors that mediates ligand-independent receptor assembly and signaling. *Science,* 288**,** 2351-4.

CHANG, D. W., XING, Z., PAN, Y., ALGECIRAS-SCHIMNICH, A., BARNHART, B. C., YAISH-OHAD, S., PETER, M. E. & YANG, X. 2002. c-FLIP(L) is a dual function regulator for caspase-8 activation and CD95-mediated apoptosis. *EMBO J,* 21**,** 3704-14.

Christiana Sawa

CHANG, L., KAMATA, H., SOLINAS, G., LUO, J. L., MAEDA, S., VENUPRASAD, K., LIU, Y. C. & KARIN, M. 2006. The E3 ubiquitin ligase itch couples JNK activation to TNFalpha-induced cell death by inducing c-FLIP(L) turnover. *Cell,* 124**,** 601-13.

CHANG, Y. C., HSU, J. D., LIN, W. L., LEE, Y. J. & WANG, C. J. 2012. High incidence of acute promyelocytic leukemia specifically induced by N-nitroso-N-methylurea (NMU) in Sprague-Dawley rats. *Arch Toxicol,* 86**,** 315-27.

CHAUDHURI, A., ORME, S., VO, T., WANG, W. & CHERAYIL, B. J. 1999. Phosphorylation of TRAF2 inhibits binding to the CD40 cytoplasmic domain. *Biochem Biophys Res Commun,* 256**,** 620-5.

CHEN, G. & GOEDDEL, D. V. 2002. TNF-R1 signaling: a beautiful pathway. *Science,* 296**,** 1634-5.

CHEN, Z. J. 2005. Ubiquitin signalling in the NF-kappaB pathway. *Nat Cell Biol,* 7**,** 758-65.

CHIARINI, F., LONETTI, A., TETI, G., ORSINI, E., BRESSANIN, D., CAPPELLINI, A., RICCI, F., TAZZARI, P. L., OGNIBENE, A., FALCONI, M., PAGLIARO, P., IACOBUCCI, I., MARTINELLI, G., AMADORI, S., MCCUBREY, J. A. & MARTELLI, A. M. 2012. A combination of temsirolimus, an allosteric mTOR inhibitor, with clofarabine as a new therapeutic option for patients with acute myeloid leukemia. *Oncotarget,* 3**,** 1615-28.

CHOUDHARY, C., SCHWABLE, J., BRANDTS, C., TICKENBROCK, L., SARGIN, B., KINDLER, T., FISCHER, T., BERDEL, W. E., MULLER-TIDOW, C. & SERVE, H. 2005. AML-associated Flt3 kinase domain mutations show signal transduction differences compared with Flt3 ITD mutations. *Blood,* 106**,** 265-73.

CILLONI, D., MESSA, F., ARRUGA, F., DEFILIPPI, I., MOROTTI, A., MESSA, E., CARTURAN, S., GIUGLIANO, E., PAUTASSO, M., BRACCO, E., ROSSO, V., SEN, A., MARTINELLI, G., BACCARANI, M. & SAGLIO, G. 2006. The NF-kappaB pathway blockade by the IKK inhibitor PS1145 can overcome imatinib resistance. *Leukemia,* 20**,** 61-7.

CIOCHINA, R. & GROSSMAN, R. B. 2006. Polycyclic polyprenylated acylphloroglucinols. *Chem Rev,* 106**,** 3963-86.

CIRCU, M. L. & AW, T. Y. 2010. Reactive oxygen species, cellular redox systems, and apoptosis. *Free Radic Biol Med,* 48**,** 749-62.

Christiana Sava

COHEN, G. M. 1997. Caspases: the executioners of apoptosis. *Biochem J,* 326 (Pt 1)**,** 1-16.

COLLINS, P. E., KIELY, P. A. & CARMODY, R. J. 2014. Inhibition of transcription by B cell Leukemia 3 (Bcl-3) protein requires interaction with nuclear factor kappaB (NF-kappaB) p50. *J Biol Chem,* 289**,** 7059-67.

COOMBS, C. C., TAVAKKOLI, M. & TALLMAN, M. S. 2015. Acute promyelocytic leukemia: where did we start, where are we now, and the future. *Blood Cancer J,* 5**,** e304.

CORTES, J., THOMAS, D., KOLLER, C., GILES, F., ESTEY, E., FADERL, S., GARCIA-MANERO, G., MCCONKEY, D., RUIZ, S. L., GUERCIOLINI, R., WRIGHT, J. & KANTARJIAN, H. 2004. Phase I study of bortezomib in refractory or relapsed acute leukemias. *Clin Cancer Res,* 10**,** 3371-6.

COTE, J. & RUIZ-CARRILLO, A. 1993. Primers for mitochondrial DNA replication generated by endonuclease G. *Science,* 261**,** 765-9.

CREUTZIG, U. 1996. Diagnosis and treatment of acute myelogenous leukemia in childhood. *Crit Rev Oncol Hematol,* 22**,** 183-96.

CRISPINO, J. D. 2005. GATA1 in normal and malignant hematopoiesis. *Semin Cell Dev Biol,* 16**,** 137-47.

CRUPI, R., ABUSAMRA, Y. A., SPINA, E. & CALAPAI, G. 2013. Preclinical data supporting/refuting the use of Hypericum perforatum in the treatment of depression. *CNS Neurol Disord Drug Targets,* 12**,** 474-86.

CUELLO, M., COATS, A. O., DARKO, I., ETTENBERG, S. A., GARDNER, G. J., NAU, M. M., LIU, J. R., BIRRER, M. J. & LIPKOWITZ, S. 2004. N-(4-hydroxyphenyl) retinamide (4HPR) enhances TRAIL-mediated apoptosis through enhancement of a mitochondrial-dependent amplification loop in ovarian cancer cell lines. *Cell Death Differ,* 11**,** 527-41.

CUI, J. W., WANG, J., HE, K., JIN, B. F., WANG, H. X., LI, W., KANG, L. H., HU, M. R., LI, H. Y., YU, M., SHEN, B. F., WANG, G. J. & ZHANG, X. M. 2004. Proteomic analysis of human acute leukemia cells: insight into their classification. *Clin Cancer Res,* 10**,** 6887-96.

CULLEN, S. P. & MARTIN, S. J. 2009. Caspase activation pathways: some recent progress. *Cell Death Differ,* 16**,** 935-8.

DAS, P., SHAIK, A. P. & BAMMIDI, V. K. 2009. Meta-analysis study of glutathione-S-transferases (GSTM1, GSTP1, and GSTT1) gene polymorphisms and risk of acute myeloid leukemia. *Leuk Lymphoma,* 50**,** 1345-51.

Christiana Sawa

DAUGAS, E., SUSIN, S. A., ZAMZAMI, N., FERRI, K. F., IRINOPOULOU, T., LAROCHETTE, N., PREVOST, M. C., LEBER, B., ANDREWS, D., PENNINGER, J. & KROEMER, G. 2000. Mitochondrio-nuclear translocation of AIF in apoptosis and necrosis. *FASEB J,* 14**,** 729-39.

DAVER, N., BOUMBER, Y., KANTARJIAN, H., RAVANDI, F., CORTES, J., RYTTING, M. E., KAWEDIA, J. D., BASNETT, J., CULOTTA, K. S., ZENG, Z., LU, H., RICHIE, M. A., GARRIS, R., XIAO, L., LIU, W., BAGGERLY, K. A., JABBOUR, E., O'BRIEN, S., BURGER, J., BENDALL, L. J., THOMAS, D. & KONOPLEVA, M. 2015. A Phase I/II Study of the mTOR Inhibitor Everolimus in Combination with HyperCVAD Chemotherapy in Patients with Relapsed/Refractory Acute Lymphoblastic Leukemia. *Clin Cancer Res,* 21**,** 2704-14.

DAVIES, S. M. 2001. Therapy-related leukemia associated with alkylating agents. *Med Pediatr Oncol,* 36**,** 536-40.

DAY, C. L., SMITS, C., FAN, F. C., LEE, E. F., FAIRLIE, W. D. & HINDS, M. G. 2008. Structure of the BH3 domains from the p53-inducible BH3-only proteins Noxa and Puma in complex with Mcl-1. *J Mol Biol,* 380**,** 958-71.

DECLERCQ, W., VANDEN BERGHE, T. & VANDENABEELE, P. 2009. RIP kinases at the crossroads of cell death and survival. *Cell,* 138**,** 229-32.

DEGTEREV, A., BOYCE, M. & YUAN, J. 2003. A decade of caspases. *Oncogene,* 22**,** 8543-67.

DELHASE, M., HAYAKAWA, M., CHEN, Y. & KARIN, M. 1999. Positive and negative regulation of IkappaB kinase activity through IKKbeta subunit phosphorylation. *Science,* 284**,** 309-13.

DINCER, Y., YUKSEL, S., BATAR, B., GUVEN, M., ONARAN, I. & CELKAN, T. 2015. DNA Repair Gene Polymorphisms and Their Relation With DNA Damage, DNA Repair, and Total Antioxidant Capacity in Childhood Acute Lymphoblastic Leukemia Survivors. *J Pediatr Hematol Oncol,* 37**,** 344-50.

DING, H. F., MCGILL, G., ROWAN, S., SCHMALTZ, C., SHIMAMURA, A. & FISHER, D. E. 1998. Oncogene-dependent regulation of caspase activation by p53 protein in a cell-free system. *J Biol Chem,* 273**,** 28378-83.

DOHNER, H., ESTEY, E. H., AMADORI, S., APPELBAUM, F. R., BUCHNER, T., BURNETT, A. K., DOMBRET, H., FENAUX, P., GRIMWADE, D., LARSON, R. A., LO-COCO, F., NAOE, T., NIEDERWIESER, D., OSSENKOPPELE, G. J., SANZ, M. A., SIERRA, J., TALLMAN, M. S., LOWENBERG, B. &

BLOOMFIELD, C. D. 2010. Diagnosis and management of acute myeloid leukemia in adults: recommendations from an international expert panel, on behalf of the European LeukemiaNet. *Blood,* 115**,** 453-74.

DOMBRET, H., CLUZEAU, T., HUGUET, F. & BOISSEL, N. 2014. Pediatric-like therapy for adults with ALL. *Curr Hematol Malig Rep,* 9**,** 158-64.

DON, A. S. & ZHENG, X. F. 2011. Recent clinical trials of mTOR-targeted cancer therapies. *Rev Recent Clin Trials,* 6**,** 24-35.

DOS SANTOS, N. R., GHEZZO, M. N., DA SILVA, R. C. & FERNANDES, M. T. 2010. NF-kappaB in T-cell Acute Lymphoblastic Leukemia: Oncogenic Functions in Leukemic and in Microenvironmental Cells. *Cancers (Basel),* 2**,** 1838-60.

DOWNING, J. R., HIGUCHI, M., LENNY, N. & YEOH, A. E. 2000. Alterations of the AML1 transcription factor in human leukemia. *Semin Cell Dev Biol,* 11**,** 347-60.

DROIN, N., GUERY, L., BENIKHLEF, N. & SOLARY, E. 2013. Targeting apoptosis proteins in hematological malignancies. *Cancer Lett,* 332**,** 325-34.

EA, C. K., DENG, L., XIA, Z. P., PINEDA, G. & CHEN, Z. J. 2006. Activation of IKK by TNFalpha requires site-specific ubiquitination of RIP1 and polyubiquitin binding by NEMO. *Mol Cell,* 22**,** 245-57.

ECKHART, L., DECLERCQ, W., BAN, J., RENDL, M., LENGAUER, B., MAYER, C., LIPPENS, S., VANDENABEELE, P. & TSCHACHLER, E. 2000. Terminal differentiation of human keratinocytes and stratum corneum formation is associated with caspase-14 activation. *J Invest Dermatol,* 115**,** 1148-51.

EGGERMONT, A. M., DE WILT, J. H. & TEN HAGEN, T. L. 2003. Current uses of isolated limb perfusion in the clinic and a model system for new strategies. *Lancet Oncol,* 4**,** 429-37.

ELMORE, S. 2007. Apoptosis: a review of programmed cell death. *Toxicol Pathol,* 35**,** 495-516.

ENGEL, T. & HENSHALL, D. C. 2009. Apoptosis, Bcl-2 family proteins and caspases: the ABCs of seizure-damage and epileptogenesis? *Int J Physiol Pathophysiol Pharmacol,* 1**,** 97-115.

ESPOSITO, F., SANNA, C., DEL VECCHIO, C., CANNAS, V., VENDITTI, A., CORONA, A., BIANCO, A., SERRILLI, A. M., GUARCINI, L., PAROLIN, C., BALLERO, M. & TRAMONTANO, E. 2013. Hypericum hircinum L.

Christiana Sava

components as new single-molecule inhibitors of both HIV-1 reverse transcriptase-associated DNA polymerase and ribonuclease H activities. *Pathog Dis,* 68**,** 116-24.

ESTEY, E. H. 2012. Acute myeloid leukemia: 2012 update on diagnosis, risk stratification, and management. *Am J Hematol,* 87**,** 89-99.

FENAUX, P., CHOMIENNE, C. & DEGOS, L. 1997. Acute promyelocytic leukemia: biology and treatment. *Semin Oncol,* 24**,** 92-102.

FENRICK, R., AMANN, J. M., LUTTERBACH, B., WANG, L., WESTENDORF, J. J., DOWNING, J. R. & HIEBERT, S. W. 1999. Both TEL and AML-1 contribute repression domains to the t(12;21) fusion protein. *Mol Cell Biol,* 19**,** 6566-74.

FERRANDO, A. A. 2009. The role of NOTCH1 signaling in T-ALL. *Hematology Am Soc Hematol Educ Program***,** 353-61.

FERREIRA, R., OHNEDA, K., YAMAMOTO, M. & PHILIPSEN, S. 2005. GATA1 function, a paradigm for transcription factors in hematopoiesis. *Mol Cell Biol,* 25**,** 1215-27.

FISCHER, M., SCHWIEGER, M., HORN, S., NIEBUHR, B., FORD, A., ROSCHER, S., BERGHOLZ, U., GREAVES, M., LOHLER, J. & STOCKING, C. 2005. Defining the oncogenic function of the TEL/AML1 (ETV6/RUNX1) fusion protein in a mouse model. *Oncogene,* 24**,** 7579-91.

FORTIN, A., CREGAN, S. P., MACLAURIN, J. G., KUSHWAHA, N., HICKMAN, E. S., THOMPSON, C. S., HAKIM, A., ALBERT, P. R., CECCONI, F., HELIN, K., PARK, D. S. & SLACK, R. S. 2001. APAF1 is a key transcriptional target for p53 in the regulation of neuronal cell death. *J Cell Biol,* 155**,** 207-16.

FUJIWARA, T., FUKUHARA, N., FUNAYAMA, R., NARIAI, N., KAMATA, M., NAGASHIMA, T., KOJIMA, K., ONISHI, Y., SASAHARA, Y., ISHIZAWA, K., NAGASAKI, M., NAKAYAMA, K. & HARIGAE, H. 2014. Identification of acquired mutations by whole-genome sequencing in GATA-2 deficiency evolving into myelodysplasia and acute leukemia. *Ann Hematol,* 93**,** 1515-22.

FULDA, S. 2012. Exploiting inhibitor of apoptosis proteins as therapeutic targets in hematological malignancies. *Leukemia,* 26**,** 1155-65.

FULDA, S. 2014. Inhibitor of Apoptosis (IAP) proteins in hematological malignancies: molecular mechanisms and therapeutic opportunities. *Leukemia,* 28**,** 1414-22.

Christiana Sava

FULDA, S. & DEBATIN, K. M. 2006. Extrinsic versus intrinsic apoptosis pathways in anticancer chemotherapy. *Oncogene,* 25**,** 4798-811.

FULDA, S., MEYER, E. & DEBATIN, K. M. 2002. Inhibition of TRAIL-induced apoptosis by Bcl-2 overexpression. *Oncogene,* 21**,** 2283-94.

GANTEN, T. M., HAAS, T. L., SYKORA, J., STAHL, H., SPRICK, M. R., FAS, S. C., KRUEGER, A., WEIGAND, M. A., GROSSE-WILDE, A., STREMMEL, W., KRAMMER, P. H. & WALCZAK, H. 2004. Enhanced caspase-8 recruitment to and activation at the DISC is critical for sensitisation of human hepatocellular carcinoma cells to TRAIL-induced apoptosis by chemotherapeutic drugs. *Cell Death Differ,* 11 Suppl 1**,** S86-96.

GARRIDO, C., GALLUZZI, L., BRUNET, M., PUIG, P. E., DIDELOT, C. & KROEMER, G. 2006. Mechanisms of cytochrome c release from mitochondria. *Cell Death Differ,* 13**,** 1423-33.

GASPARINI, C., CELEGHINI, C., MONASTA, L. & ZAULI, G. 2014. NF-kappaB pathways in hematological malignancies. *Cell Mol Life Sci,* 71**,** 2083-102.

GERL, R. & VAUX, D. L. 2005. Apoptosis in the development and treatment of cancer. *Carcinogenesis,* 26**,** 263-70.

GHOSH, S. & KARIN, M. 2002. Missing pieces in the NF-kappaB puzzle. *Cell,* 109 Suppl**,** S81-96.

GHOSH, S., MAY, M. J. & KOPP, E. B. 1998. NF-kappa B and Rel proteins: evolutionarily conserved mediators of immune responses. *Annu Rev Immunol,* 16**,** 225-60.

GILLILAND, D. G., JORDAN, C. T. & FELIX, C. A. 2004. The molecular basis of leukemia. *Hematology Am Soc Hematol Educ Program***,** 80-97.

GODLEY, L. A. 2014. Inherited predisposition to acute myeloid leukemia. *Semin Hematol,* 51**,** 306-21.

GOLDSBY, R., KINDT, T., KUBY, J. & OSBORNE, B. 2002. Immunology (Book). *W. H. Freeman; 5th edition*

GONCHARENKO-KHAIDER, N., LANE, D., MATTE, I., RANCOURT, C. & PICHE, A. 2013. Ovarian Cancer - A Clinical and Translational Update (Book). *InTech; 1st edition*.

GONZALVEZ, F. & ASHKENAZI, A. 2010. New insights into apoptosis signaling by Apo2L/TRAIL. *Oncogene,* 29**,** 4752-65.

GONZALVEZ, F., PARISELLI, F., JALMAR, O., DUPAIGNE, P., SUREAU, F., DELLINGER, M., HENDRICKSON, E. A., BERNARD, S. & PETIT, P. X.

Christiana Sawa

2010. Mechanistic issues of the interaction of the hairpin-forming domain of tBid with mitochondrial cardiolipin. *PLoS One,* 5**,** e9342.

GREAVES, M. 2006. Infection, immune responses and the aetiology of childhood leukaemia. *Nat Rev Cancer,* 6**,** 193-203.

GRELL, M., ZIMMERMANN, G., HULSER, D., PFIZENMAIER, K. & SCHEURICH, P. 1994. TNF receptors TR60 and TR80 can mediate apoptosis via induction of distinct signal pathways. *J Immunol,* 153**,** 1963-72.

GRIGNANI, F., FERRUCCI, P. F., TESTA, U., TALAMO, G., FAGIOLI, M., ALCALAY, M., MENCARELLI, A., PESCHLE, C., NICOLETTI, I. & ET AL. 1993. The acute promyelocytic leukemia-specific PML-RAR alpha fusion protein inhibits differentiation and promotes survival of myeloid precursor cells. *Cell,* 74**,** 423-31.

GRISOLANO, J. L., WESSELSCHMIDT, R. L., PELICCI, P. G. & LEY, T. J. 1997. Altered myeloid development and acute leukemia in transgenic mice expressing PML-RAR alpha under control of cathepsin G regulatory sequences. *Blood,* 89**,** 376-87.

GRIVENNIKOV, S. I., GRETEN, F. R. & KARIN, M. 2010. Immunity, inflammation, and cancer. *Cell,* 140**,** 883-99.

GUPTA, M., RAGHAVAN, M., GALE, R. E., CHELALA, C., ALLEN, C., MOLLOY, G., CHAPLIN, T., LINCH, D. C., CAZIER, J. B. & YOUNG, B. D. 2008. Novel regions of acquired uniparental disomy discovered in acute myeloid leukemia. *Genes Chromosomes Cancer,* 47**,** 729-39.

GUTIERREZ, A., SANDA, T., GREBLIUNAITE, R., CARRACEDO, A., SALMENA, L., AHN, Y., DAHLBERG, S., NEUBERG, D., MOREAU, L. A., WINTER, S. S., LARSON, R., ZHANG, J., PROTOPOPOV, A., CHIN, L., PANDOLFI, P. P., SILVERMAN, L. B., HUNGER, S. P., SALLAN, S. E. & LOOK, A. T. 2009. High frequency of PTEN, PI3K, and AKT abnormalities in T-cell acute lymphoblastic leukemia. *Blood,* 114**,** 647-50.

GUZMAN, M. L., NEERING, S. J., UPCHURCH, D., GRIMES, B., HOWARD, D. S., RIZZIERI, D. A., LUGER, S. M. & JORDAN, C. T. 2001. Nuclear factor-kappaB is constitutively activated in primitive human acute myelogenous leukemia cells. *Blood,* 98**,** 2301-7.

HAMADANI, M. & AWAN, F. T. 2010. Remission induction, consolidation and novel agents in development for adults with acute myeloid leukaemia. *Hematol Oncol,* 28**,** 3-12.

Christina Savva

HANAHAN, D. & WEINBERG, R. A. 2011. Hallmarks of cancer: the next generation. *Cell,* 144**,** 646-74.

HARRIS, N. L., JAFFE, E. S., DIEBOLD, J., FLANDRIN, G., MULLER-HERMELINK, H. K., VARDIMAN, J., LISTER, T. A. & BLOOMFIELD, C. D. 1999. World Health Organization classification of neoplastic diseases of the hematopoietic and lymphoid tissues: report of the Clinical Advisory Committee meeting-Airlie House, Virginia, November 1997. *J Clin Oncol,* 17**,** 3835-49.

HARVEY, R. C., MULLIGHAN, C. G., WANG, X., DOBBIN, K. K., DAVIDSON, G. S., BEDRICK, E. J., CHEN, I. M., ATLAS, S. R., KANG, H., AR, K., WILSON, C. S., WHARTON, W., MURPHY, M., DEVIDAS, M., CARROLL, A. J., BOROWITZ, M. J., BOWMAN, W. P., DOWNING, J. R., RELLING, M., YANG, J., BHOJWANI, D., CARROLL, W. L., CAMITTA, B., REAMAN, G. H., SMITH, M., HUNGER, S. P. & WILLMAN, C. L. 2010. Identification of novel cluster groups in pediatric high-risk B-precursor acute lymphoblastic leukemia with gene expression profiling: correlation with genome-wide DNA copy number alterations, clinical characteristics, and outcome. *Blood,* 116**,** 4874-84.

HASSAN, K., QURESHI, M., SHAFI, S., IKRAM, N. & AKHTAR, M. J. 1993. Acute myeloid leukemia-FAB classification and its correlation with clinico-haematological features. *J Pak Med Assoc,* 43**,** 200-3.

HATTORI, N., FUKUCHI, K., NAKAMAKI, T., HOMMA, M., ARIIZUMI, H., NAKASHIMA, H., MAEDA, T., SAITO, B., YAMOCHI-ONIZUKA, T., YANAGISAWA, K., MATSUDA, I., OTA, H. & TOMOYASU, S. 2011. p53 Protein expression in chronic myelomonocytic leukemia-1 correlates with progression to leukemia and a poor prognosis. *Acta Haematol,* 125**,** 242-6.

HATZIMICHAEL, E., GEORGIOU, G., BENETATOS, L. & BRIASOULIS, E. 2013. Gene mutations and molecularly targeted therapies in acute myeloid leukemia. *Am J Blood Res,* 3**,** 29-51.

HAYDEN, M. S. & GHOSH, S. 2008. Shared principles in NF-kappaB signaling. *Cell,* 132**,** 344-62.

HE, J., XIU, L., DE PORRE, P., DASS, R. & THOMAS, X. 2015. Decitabine reduces transfusion dependence in older patients with acute myeloid leukemia: results from a post hoc analysis of a randomized phase III study. *Leuk Lymphoma,* 56**,** 1033-42.

Christiana Silva

HE, L. Z., GUIDEZ, F., TRIBIOLI, C., PERUZZI, D., RUTHARDT, M., ZELENT, A. & PANDOLFI, P. P. 1998. Distinct interactions of PML-RARalpha and PLZF-RARalpha with co-repressors determine differential responses to RA in APL. *Nat Genet,* 18**,** 126-35.

HE, L. Z., TRIBIOLI, C., RIVI, R., PERUZZI, D., PELICCI, P. G., SOARES, V., CATTORETTI, G. & PANDOLFI, P. P. 1997. Acute leukemia with promyelocytic features in PML/RARalpha transgenic mice. *Proc Natl Acad Sci U S A,* 94**,** 5302-7.

HEGDE, M., KARKI, S. S., THOMAS, E., KUMAR, S., PANJAMURTHY, K., RANGANATHA, S. R., RANGAPPA, K. S., CHOUDHARY, B. & RAGHAVAN, S. C. 2012. Novel levamisole derivative induces extrinsic pathway of apoptosis in cancer cells and inhibits tumor progression in mice. *PLoS One,* 7**,** e43632.

HEHNER, S. P., HOFMANN, T. G., DROGE, W. & SCHMITZ, M. L. 1999. The antiinflammatory sesquiterpene lactone parthenolide inhibits NF-kappa B by targeting the I kappa B kinase complex. *J Immunol,* 163**,** 5617-23.

HERRANZ, D., AMBESI-IMPIOMBATO, A., PALOMERO, T., SCHNELL, S. A., BELVER, L., WENDORFF, A. A., XU, L., CASTILLO-MARTIN, M., LLOBET-NAVAS, D., CORDON-CARDO, C., CLAPPIER, E., SOULIER, J. & FERRANDO, A. A. 2014. A NOTCH1-driven MYC enhancer promotes T cell development, transformation and acute lymphoblastic leukemia. *Nat Med,* 20**,** 1130-7.

HITOMI, J., CHRISTOFFERSON, D. E., NG, A., YAO, J., DEGTEREV, A., XAVIER, R. J. & YUAN, J. 2008. Identification of a molecular signaling network that regulates a cellular necrotic cell death pathway. *Cell,* 135**,** 1311-23.

HO, P. A., ALONZO, T. A., GERBING, R. B., POLLARD, J., STIREWALT, D. L., HURWITZ, C., HEEREMA, N. A., HIRSCH, B., RAIMONDI, S. C., LANGE, B., FRANKLIN, J. L., RADICH, J. P. & MESHINCHI, S. 2009. Prevalence and prognostic implications of CEBPA mutations in pediatric acute myeloid leukemia (AML): a report from the Children's Oncology Group. *Blood,* 113**,** 6558-66.

HOESEL, B. & SCHMID, J. A. 2013. The complexity of NF-kappaB signaling in inflammation and cancer. *Mol Cancer,* 12**,** 86.

Christiana Sava

HOFFMANN, A., LEVCHENKO, A., SCOTT, M. L. & BALTIMORE, D. 2002. The IkappaB-NF-kappaB signaling module: temporal control and selective gene activation. *Science,* 298**,** 1241-5.

HOLOWIECKI, J., GROSICKI, S., GIEBEL, S., ROBAK, T., KYRCZ-KRZEMIEN, S., KULICZKOWSKI, K., SKOTNICKI, A. B., HELLMANN, A., SULEK, K., DMOSZYNSKA, A., KLOCZKO, J., JEDRZEJCZAK, W. W., ZDZIARSKA, B., WARZOCHA, K., ZAWILSKA, K., KOMARNICKI, M., KIELBINSKI, M., PIATKOWSKA-JAKUBAS, B., WIERZBOWSKA, A., WACH, M. & HAUS, O. 2012. Cladribine, but not fludarabine, added to daunorubicin and cytarabine during induction prolongs survival of patients with acute myeloid leukemia: a multicenter, randomized phase III study. *J Clin Oncol,* 30**,** 2441-8.

HORTON, T. M., SPOSTO, R., BROWN, P., REYNOLDS, C. P., HUNGER, S. P., WINICK, N. J., RAETZ, E. A., CARROLL, W. L., ARCECI, R. J., BOROWITZ, M. J., GAYNON, P. S., GORE, L., JEHA, S., MAURER, B. J., SIEGEL, S. E., BIONDI, A., KEARNS, P. R., NARENDRAN, A., SILVERMAN, L. B., SMITH, M. A., ZWAAN, C. M., WHITLOCK, J. A. & CONFERENCE, A. 2010. Toxicity assessment of molecularly targeted drugs incorporated into multiagent chemotherapy regimens for pediatric acute lymphocytic leukemia (ALL): review from an international consensus conference. *Pediatr Blood Cancer,* 54**,** 872-8.

HOSSEINI, A., ESPONA-FIEDLER, M., SOTO-CERRATO, V., QUESADA, R., PEREZ-TOMAS, R. & GUALLAR, V. 2013. Molecular interactions of prodiginines with the BH3 domain of anti-apoptotic Bcl-2 family members. *PLoS One,* 8**,** e57562.

HSI-WEN, L., JIE, L., ROBSON, N. K. B. & STEVENS, P. F. 2007. Clusiaceae (GUTTIFERAE) (Book). *Flora of China, Science Press, Beijing, and Missouri Botanical Garden Press*.

HSIAO, H. H., YANG, M. Y., LIU, Y. C., HSIAO, H. P., TSENG, S. B., CHAO, M. C., LIU, T. C. & LIN, S. F. 2005. RBM15-MKL1 (OTT-MAL) fusion transcript in an adult acute myeloid leukemia patient. *Am J Hematol,* 79**,** 43-5.

HSIEH, M. Y. & VAN ETTEN, R. A. 2014. IKK-dependent activation of NF-kappaB contributes to myeloid and lymphoid leukemogenesis by BCR-ABL1. *Blood,* 123**,** 2401-11.

HUANG, M. M. & ZHU, J. 2012. The regulation of normal and leukemic hematopoietic stem cells by niches. *Cancer Microenviron,* 5**,** 295-305.

Christiana Savva

HUANG, N., SINGH, N., YOON, K., LOIACONO, C. M., KOHUT, M. L. & BIRT, D. F. 2013. The immuno-regulatory impact of orally-administered Hypericum perforatum extract on Balb/C mice inoculated with H1n1 influenza A virus. *PLoS One,* 8**,** e76491.

HUANG, Q., DEVERAUX, Q. L., MAEDA, S., SALVESEN, G. S., STENNICKE, H. R., HAMMOCK, B. D. & REED, J. C. 2000. Evolutionary conservation of apoptosis mechanisms: lepidopteran and baculoviral inhibitor of apoptosis proteins are inhibitors of mammalian caspase-9. *Proc Natl Acad Sci U S A,* 97**,** 1427-32.

HUMMEL, J. L., ZHANG, T., WELLS, R. A. & KAMEL-REID, S. 2002. The Retinoic acid receptor alpha (RARalpha) chimeric proteins PML-, PLZF-, NPM-, and NuMA-RARalpha have distinct intracellular localization patterns. *Cell Growth Differ,* 13**,** 173-83.

HUNGER, S. P., LU, X., DEVIDAS, M., CAMITTA, B. M., GAYNON, P. S., WINICK, N. J., REAMAN, G. H. & CARROLL, W. L. 2012. Improved survival for children and adolescents with acute lymphoblastic leukemia between 1990 and 2005: a report from the children's oncology group. *J Clin Oncol,* 30**,** 1663-9.

IDRISS, H. T. & NAISMITH, J. H. 2000. TNF alpha and the TNF receptor superfamily: structure-function relationship(s). *Microsc Res Tech,* 50**,** 184-95.

JABBOUR, E. J., ESTEY, E. & KANTARJIAN, H. M. 2006. Adult acute myeloid leukemia. *Mayo Clin Proc,* 81**,** 247-60.

JACAMO, R., CHEN, Y., WANG, Z., MA, W., ZHANG, M., SPAETH, E. L., WANG, Y., BATTULA, V. L., MAK, P. Y., SCHALLMOSER, K., RUVOLO, P., SCHOBER, W. D., SHPALL, E. J., NGUYEN, M. H., STRUNK, D., BUESO-RAMOS, C. E., KONOPLEV, S., DAVIS, R. E., KONOPLEVA, M. & ANDREEFF, M. 2014. Reciprocal leukemia-stroma VCAM-1/VLA-4-dependent activation of NF-kappaB mediates chemoresistance. *Blood,* 123**,** 2691-702.

JACQUEMIN, G., GRANCI, V., GALLOUET, A. S., LALAOUI, N., MORLE, A., IESSI, E., MORIZOT, A., GARRIDO, C., GUILLAUDEUX, T. & MICHEAU, O. 2012. Quercetin-mediated Mcl-1 and survivin downregulation restores TRAIL-induced apoptosis in non-Hodgkin's lymphoma B cells. *Haematologica,* 97**,** 38-46.

Christiana Sawa

JACQUEMIN, G., SHIRLEY, S. & MICHEAU, O. 2010. Combining naturally occurring polyphenols with TNF-related apoptosis-inducing ligand: a promising approach to kill resistant cancer cells? *Cell Mol Life Sci,* 67**,** 3115-30.

JAFFE, E. S., HARRIS, N. L., DIEBOLD, J. & MULLER-HERMELINK, H. K. 1999. World Health Organization classification of neoplastic diseases of the hematopoietic and lymphoid tissues. A progress report. *Am J Clin Pathol,* 111**,** S8-12.

JANSEN, J. H. & LOWENBERG, B. 2001. Acute promyelocytic leukemia with a PLZF-RARalpha fusion protein. *Semin Hematol,* 38**,** 37-41.

JIA, M., WANG, Z. J., LI, J. Y., YANG, S. L., ZHAO, H. Z., CHENG, Y. P., LUO, Z. B. & TANG, Y. M. 2014. The impact of IKZF1 deletion on the prognosis of acute lymphoblastic leukemia: an updated meta-analysis. *Cancer Biomark,* 14**,** 493-503.

JIMENEZ FERNANDEZ, D. & LAMKANFI, M. 2015. Inflammatory caspases: key regulators of inflammation and cell death. *Biol Chem,* 396**,** 193-203.

JIN, J., CHEN, J., SUO, S., QIAN, W., MENG, H., MAI, W., TONG, H., HUANG, J., YU, W., WEI, J. & LOU, Y. 2015. Low-dose cytarabine, aclarubicin and granulocyte colony-stimulating factor priming regimen versus idarubicin plus cytarabine regimen as induction therapy for older patients with acute myeloid leukemia. *Leuk Lymphoma,* 56**,** 1691-7.

JIN, S. & LEVINE, A. J. 2001. The p53 functional circuit. *J Cell Sci,* 114**,** 4139-40.

JORDAN, C. T. & GUZMAN, M. L. 2004. Mechanisms controlling pathogenesis and survival of leukemic stem cells. *Oncogene,* 23**,** 7178-87.

KABRA, N. H., KANG, C., HSING, L. C., ZHANG, J. & WINOTO, A. 2001. T cell-specific FADD-deficient mice: FADD is required for early T cell development. *Proc Natl Acad Sci U S A,* 98**,** 6307-12.

KADIA, T. M., FADERL, S., RAVANDI, F., JABBOUR, E., GARCIA-MANERO, G., BORTHAKUR, G., FERRAJOLI, A., KONOPLEVA, M., BURGER, J., HUANG, X., WANG, X., PIERCE, S., BRANDT, M., FELIU, J., CORTES, J. & KANTARJIAN, H. 2015. Final results of a phase 2 trial of clofarabine and low-dose cytarabine alternating with decitabine in older patients with newly diagnosed acute myeloid leukemia. *Cancer,* 121**,** 2375-82.

KANNAS, C. C., KALVARI, I., LAMBRINIDIS, G., NEOPHYTOU, C. M., SAVVA, C. G., KIRMITZOGLOU, I., ANTONIOU, Z., ACHILLEOS, K. G., SCHERF,

Christiana Savva

D., PITTA, C. A., NICOLAOU, C. A., MIKROS, E., PROMPONAS, V. J., GERHAUSER, C., MEHTA, R. G., CONSTANTINOU, A. I. & PATTICHIS, C. S. 2015. LiSIs: An Online Scientific Workflow System for Virtual Screening. *Comb Chem High Throughput Screen,* 18**,** 281-95.

KANTARJIAN, H., THOMAS, D., O'BRIEN, S., CORTES, J., GILES, F., JEHA, S., BUESO-RAMOS, C. E., PIERCE, S., SHAN, J., KOLLER, C., BERAN, M., KEATING, M. & FREIREICH, E. J. 2004. Long-term follow-up results of hyperfractionated cyclophosphamide, vincristine, doxorubicin, and dexamethasone (Hyper-CVAD), a dose-intensive regimen, in adult acute lymphocytic leukemia. *Cancer,* 101**,** 2788-801.

KAPELKO-SLOWIK, K., URBANIAK-KUJDA, D., WOLOWIEC, D., JAZWIEC, B., DYBKO, J., JAKUBASZKO, J., SLOWIK, M. & KULICZKOWSKI, K. 2013. Expression of PIM-2 and NF-kappaB genes is increased in patients with acute myeloid leukemia (AML) and acute lymphoblastic leukemia (ALL) and is associated with complete remission rate and overall survival. *Postepy Hig Med Dosw (Online),* 67**,** 553-9.

KARIN, M. 1999. How NF-kappaB is activated: the role of the IkappaB kinase (IKK) complex. *Oncogene,* 18**,** 6867-74.

KASSOGUE, Y., QUACHOUH, M., DEHBI, H., QUESSAR, A., BENCHEKROUN, S. & NADIFI, S. 2014. Effect of interaction of glutathione S-transferases (T1 and M1) on the hematologic and cytogenetic responses in chronic myeloid leukemia patients treated with imatinib. *Med Oncol,* 31**,** 47.

KAUFMANN, S. H., DESNOYERS, S., OTTAVIANO, Y., DAVIDSON, N. E. & POIRIER, G. G. 1993. Specific proteolytic cleavage of poly(ADP-ribose) polymerase: an early marker of chemotherapy-induced apoptosis. *Cancer Res,* 53**,** 3976-85.

KETLEY, N. J., ALLEN, P. D., KELSEY, S. M. & NEWLAND, A. C. 2000. Mechanisms of resistance to apoptosis in human AML blasts: the role of differentiation-induced perturbations of cell-cycle checkpoints. *Leukemia,* 14**,** 620-8.

KHALIDI, H. S., CHANG, K. L., MEDEIROS, L. J., BRYNES, R. K., SLOVAK, M. L., MURATA-COLLINS, J. L. & ARBER, D. A. 1999. Acute lymphoblastic leukemia. Survey of immunophenotype, French-American-British classification, frequency of myeloid antigen expression, and karyotypic

Christiana Savva

abnormalities in 210 pediatric and adult cases. *Am J Clin Pathol,* 111**,** 467-76.

KIM, H., RAFIUDDIN-SHAH, M., TU, H. C., JEFFERS, J. R., ZAMBETTI, G. P., HSIEH, J. J. & CHENG, E. H. 2006. Hierarchical regulation of mitochondrion-dependent apoptosis by BCL-2 subfamilies. *Nat Cell Biol,* 8**,** 1348-58.

KIRSTETTER, P., SCHUSTER, M. B., BERESHCHENKO, O., MOORE, S., DVINGE, H., KURZ, E., THEILGAARD-MONCH, K., MANSSON, R., PEDERSEN, T. A., PABST, T., SCHROCK, E., PORSE, B. T., JACOBSEN, S. E., BERTONE, P., TENEN, D. G. & NERLOV, C. 2008. Modeling of C/EBPalpha mutant acute myeloid leukemia reveals a common expression signature of committed myeloid leukemia-initiating cells. *Cancer Cell,* 13**,** 299-310.

KISCHKEL, F. C., HELLBARDT, S., BEHRMANN, I., GERMER, M., PAWLITA, M., KRAMMER, P. H. & PETER, M. E. 1995. Cytotoxicity-dependent APO-1 (Fas/CD95)-associated proteins form a death-inducing signaling complex (DISC) with the receptor. *EMBO J,* 14**,** 5579-88.

KITADA, S., PEDERSEN, I. M., SCHIMMER, A. D. & REED, J. C. 2002. Dysregulation of apoptosis genes in hematopoietic malignancies. *Oncogene,* 21**,** 3459-74.

KLAMPFER, L., ZHANG, J., ZELENETZ, A. O., UCHIDA, H. & NIMER, S. D. 1996. The AML1/ETO fusion protein activates transcription of BCL-2. *Proc Natl Acad Sci U S A,* 93**,** 14059-64.

KLEIN, F., FELDHAHN, N., HARDER, L., WANG, H., WARTENBERG, M., HOFMANN, W. K., WERNET, P., SIEBERT, R. & MUSCHEN, M. 2004a. The BCR-ABL1 kinase bypasses selection for the expression of a pre-B cell receptor in pre-B acute lymphoblastic leukemia cells. *J Exp Med,* 199**,** 673-85.

KLEIN, F., FELDHAHN, N. & MUSCHEN, M. 2004b. Interference of BCR-ABL1 kinase activity with antigen receptor signaling in B cell precursor leukemia cells. *Cell Cycle,* 3**,** 858-60.

KO, H. L. & REN, E. C. 2012. Functional Aspects of PARP1 in DNA Repair and Transcription. *Biomolecules,* 2**,** 524-48.

Christiana Sawa

KOENIG, U., ECKHART, L. & TSCHACHLER, E. 2001. Evidence that caspase-13 is not a human but a bovine gene. *Biochem Biophys Res Commun,* 285**,** 1150-4.

KOJIMA, K., KONOPLEVA, M., TSAO, T., ANDREEFF, M., ISHIDA, H., SHIOTSU, Y., JIN, L., TABE, Y. & NAKAKUMA, H. 2010. Selective FLT3 inhibitor FI-700 neutralizes Mcl-1 and enhances p53-mediated apoptosis in AML cells with activating mutations of FLT3 through Mcl-1/Noxa axis. *Leukemia,* 24**,** 33-43.

KORNBLAU, S. M., QUTUB, A., YAO, H., YORK, H., QIU, Y. H., GRABER, D., RAVANDI, F., CORTES, J., ANDREEFF, M., ZHANG, N. & COOMBES, K. R. 2013. Proteomic profiling identifies distinct protein patterns in acute myelogenous leukemia CD34+CD38- stem-like cells. *PLoS One,* 8**,** e78453.

KOYAMA, D., KIKUCHI, J., HIRAOKA, N., WADA, T., KUROSAWA, H., CHIBA, S. & FURUKAWA, Y. 2014. Proteasome inhibitors exert cytotoxicity and increase chemosensitivity via transcriptional repression of Notch1 in T-cell acute lymphoblastic leukemia. *Leukemia,* 28**,** 1216-26.

KRIEGER, D., MOERICKE, A., OSCHLIES, I., ZIMMERMANN, M., SCHRAPPE, M., REITER, A. & BURKHARDT, B. 2010. Frequency and clinical relevance of DNA microsatellite alterations of the CDKN2A/B, ATM and p53 gene loci: a comparison between pediatric precursor T-cell lymphoblastic lymphoma and T-cell lymphoblastic leukemia. *Haematologica,* 95**,** 158-62.

KRUEGER, A., SCHMITZ, I., BAUMANN, S., KRAMMER, P. H. & KIRCHHOFF, S. 2001. Cellular FLICE-inhibitory protein splice variants inhibit different steps of caspase-8 activation at the CD95 death-inducing signaling complex. *J Biol Chem,* 276**,** 20633-40.

KUANG, A. A., DIEHL, G. E., ZHANG, J. & WINOTO, A. 2000. FADD is required for DR4- and DR5-mediated apoptosis: lack of trail-induced apoptosis in FADD-deficient mouse embryonic fibroblasts. *J Biol Chem,* 275**,** 25065-8.

LANGELIER, M. F., PLANCK, J. L., ROY, S. & PASCAL, J. M. 2012. Structural basis for DNA damage-dependent poly(ADP-ribosyl)ation by human PARP-1. *Science,* 336**,** 728-32.

LARSON, S. M., CAMPBELL, N. P., HUO, D., ARTZ, A., ZHANG, Y., GAJRIA, D., GREEN, M., WEINER, H., DAUGHERTY, C., ODENIKE, O., GODLEY, L. A., HYJEK, E., GURBUXANI, S., THIRMAN, M., SIPKINS, D., VAN BESIEN, K., LARSON, R. A. & STOCK, W. 2012. High dose cytarabine and

Christiana Sawa

mitoxantrone: an effective induction regimen for high-risk acute myeloid leukemia (AML). *Leuk Lymphoma,* 53**,** 445-50.

LASSUS, P., OPITZ-ARAYA, X. & LAZEBNIK, Y. 2002. Requirement for caspase-2 in stress-induced apoptosis before mitochondrial permeabilization. *Science,* 297**,** 1352-4.

LEE, E. W., KIM, J. H., AHN, Y. H., SEO, J., KO, A., JEONG, M., KIM, S. J., RO, J. Y., PARK, K. M., LEE, H. W., PARK, E. J., CHUN, K. H. & SONG, J. 2012. Ubiquitination and degradation of the FADD adaptor protein regulate death receptor-mediated apoptosis and necroptosis. *Nat Commun,* 3**,** 978.

LEE, N. K. & LEE, S. Y. 2002. Modulation of life and death by the tumor necrosis factor receptor-associated factors (TRAFs). *J Biochem Mol Biol,* 35**,** 61-6.

LEE, T. H., SHANK, J., CUSSON, N. & KELLIHER, M. A. 2004. The kinase activity of Rip1 is not required for tumor necrosis factor-alpha-induced IkappaB kinase or p38 MAP kinase activation or for the ubiquitination of Rip1 by Traf2. *J Biol Chem,* 279**,** 33185-91.

LEJEUNE, F. J., LIENARD, D., MATTER, M. & RUEGG, C. 2006. Efficiency of recombinant human TNF in human cancer therapy. *Cancer Immun,* 6**,** 6.

LI, B., GALE, R. P. & XIAO, Z. 2014. Molecular genetics of chronic neutrophilic leukemia, chronic myelomonocytic leukemia and atypical chronic myeloid leukemia. *J Hematol Oncol,* 7**,** 93.

LI, H., ZHU, H., XU, C. J. & YUAN, J. 1998. Cleavage of BID by caspase 8 mediates the mitochondrial damage in the Fas pathway of apoptosis. *Cell,* 94**,** 491-501.

LI, L. Y., LUO, X. & WANG, X. 2001. Endonuclease G is an apoptotic DNase when released from mitochondria. *Nature,* 412**,** 95-9.

LI, W. W., WANG, X. Y., ZHENG, R. L., YAN, H. X., CAO, Z. X., ZHONG, L., WANG, Z. R., JI, P., YANG, L. L., WANG, L. J., XU, Y., LIU, J. J., YANG, J., ZHANG, C. H., MA, S., FENG, S., SUN, Q. Z., WEI, Y. Q. & YANG, S. Y. 2012. Discovery of the novel potent and selective FLT3 inhibitor 1-{5-[7-(3-morpholinopropoxy)quinazolin-4-ylthio]-[1,3,4]thiadiazol-2-yl}-3-p-tolylurea and its anti-acute myeloid leukemia (AML) activities in vitro and in vivo. *J Med Chem,* 55**,** 3852-66.

LIN, R. J., NAGY, L., INOUE, S., SHAO, W., MILLER, W. H., JR. & EVANS, R. M. 1998. Role of the histone deacetylase complex in acute promyelocytic leukaemia. *Nature,* 391**,** 811-4.

Christiana Sawe

LIPINSKI, C. A. 2004. Lead- and drug-like compounds: the rule-of-five revolution. *Drug Discov Today Technol,* 1**,** 337-41.

LIU, X. S., ZHU, Y., HAN, W. N., LI, Y. N., CHEN, L. H., JIA, W., SONG, C. J., LIU, F., YANG, K., LI, Q. & JIN, B. Q. 2003. Preparation and characterization of a set of monoclonal antibodies to TRAIL and TRAIL receptors DR4, DR5, DcR1, and DcR2. *Hybrid Hybridomics,* 22**,** 121-5.

LO NIGRO, L. 2013. Biology of childhood acute lymphoblastic leukemia. *J Pediatr Hematol Oncol,* 35**,** 245-52.

LOCKSLEY, R. M., KILLEEN, N. & LENARDO, M. J. 2001. The TNF and TNF receptor superfamilies: integrating mammalian biology. *Cell,* 104**,** 487-501.

LORENZO, H. K. & SUSIN, S. A. 2007. Therapeutic potential of AIF-mediated caspase-independent programmed cell death. *Drug Resist Updat,* 10**,** 235-55.

LUCAS, C. M., HARRIS, R. J., GIANNOUDIS, A., KNIGHT, K., WATMOUGH, S. J. & CLARK, R. E. 2010. BCR-ABL1 tyrosine kinase activity at diagnosis, as determined via the pCrkL/CrkL ratio, is predictive of clinical outcome in chronic myeloid leukaemia. *Br J Haematol,* 149**,** 458-60.

LUO, X., BUDIHARDJO, I., ZOU, H., SLAUGHTER, C. & WANG, X. 1998. Bid, a Bcl2 interacting protein, mediates cytochrome c release from mitochondria in response to activation of cell surface death receptors. *Cell,* 94**,** 481-90.

MA, H. S., NGUYEN, B., DUFFIELD, A. S., LI, L., GALANIS, A., WILLIAMS, A. B., BROWN, P. A., LEVIS, M. J., LEAHY, D. J. & SMALL, D. 2014. FLT3 kinase inhibitor TTT-3002 overcomes both activating and drug resistance mutations in FLT3 in acute myeloid leukemia. *Cancer Res,* 74**,** 5206-17.

MACHNICKI, J. L. & BLOOMFIELD, C. D. 1990. Chromosomal abnormalities in myelodysplastic syndromes and acute myeloid leukemia. *Clin Lab Med,* 10**,** 755-67.

MACLACHLAN, T. K. & EL-DEIRY, W. S. 2002. Apoptotic threshold is lowered by p53 transactivation of caspase-6. *Proc Natl Acad Sci U S A,* 99**,** 9492-7.

MAHONEY, D. J., CHEUNG, H. H., MRAD, R. L., PLENCHETTE, S., SIMARD, C., ENWERE, E., ARORA, V., MAK, T. W., LACASSE, E. C., WARING, J. & KORNELUK, R. G. 2008. Both cIAP1 and cIAP2 regulate TNFalpha-mediated NF-kappaB activation. *Proc Natl Acad Sci U S A,* 105**,** 11778-83.

MAK, T. W. & YEH, W. C. 2002. Signaling for survival and apoptosis in the immune system. *Arthritis Res,* 4 Suppl 3**,** S243-52.

Christiana Savva

MANKAN, A. K., LAWLESS, M. W., GRAY, S. G., KELLEHER, D. & MCMANUS, R. 2009. NF-kappaB regulation: the nuclear response. *J Cell Mol Med,* 13**,** 631-43.

MANSSON, R., HULTQUIST, A., LUC, S., YANG, L., ANDERSON, K., KHARAZI, S., AL-HASHMI, S., LIUBA, K., THOREN, L., ADOLFSSON, J., BUZA-VIDAS, N., QIAN, H., SONEJI, S., ENVER, T., SIGVARDSSON, M. & JACOBSEN, S. E. 2007. Molecular evidence for hierarchical transcriptional lineage priming in fetal and adult stem cells and multipotent progenitors. *Immunity,* 26**,** 407-19.

MARCUCCI, G., YAN, P., MAHARRY, K., FRANKHOUSER, D., NICOLET, D., METZELER, K. H., KOHLSCHMIDT, J., MROZEK, K., WU, Y. Z., BUCCI, D., CURFMAN, J. P., WHITMAN, S. P., EISFELD, A. K., MENDLER, J. H., SCHWIND, S., BECKER, H., BAR, C., CARROLL, A. J., BAER, M. R., WETZLER, M., CARTER, T. H., POWELL, B. L., KOLITZ, J. E., BYRD, J. C., PLASS, C., GARZON, R., CALIGIURI, M. A., STONE, R. M., VOLINIA, S., BUNDSCHUH, R. & BLOOMFIELD, C. D. 2014. Epigenetics meets genetics in acute myeloid leukemia: clinical impact of a novel seven-gene score. *J Clin Oncol,* 32**,** 548-56.

MASUDA, T., INABA, Y., MAEKAWA, T., TAKEDA, Y., YAMAGUCHI, H., NAKAMOTO, K., KUNINAGA, H., NISHIZATO, S. & NONAKA, A. 2003a. Simple detection method of powerful antiradical compounds in the raw extract of plants and its application for the identification of antiradical plant constituents. *J Agric Food Chem,* 51**,** 1831-8.

MASUDA, T., OYAMA, Y., YAMAMOTO, N., UMEBAYASHI, C., NAKAO, H., TOI, Y., TAKEDA, Y., NAKAMOTO, K., KUNINAGA, H., NISHIZATO, Y. & NONAKA, A. 2003b. Cytotoxic screening of medicinal and edible plants in Okinawa, Japan, and identification of the main toxic constituent of Rhodea japonica (Omoto). *Biosci Biotechnol Biochem,* 67**,** 1401-4.

MATSUMOTO, Y., TAKI, T., FUJIMOTO, Y., TANIGUCHI, K., SHIMIZU, D., SHIMURA, K., UCHIYAMA, H., KURODA, J., NOMURA, K., INABA, T., SHIMAZAKI, C., HORIIKE, S. & TANIWAKI, M. 2009. Monosomies 7p and 12p and FLT3 internal tandem duplication: possible markers for diagnosis of T/myeloid biphenotypic acute leukemia and its clonal evolution. *Int J Hematol,* 89**,** 352-8.

Christiana Sawa

MCCOOL, K. W. & MIYAMOTO, S. 2012. DNA damage-dependent NF-kappaB activation: NEMO turns nuclear signaling inside out. *Immunol Rev,* 246**,** 311-26.

MEDINA, M. A., MARTINEZ-POVEDA, B., AMORES-SANCHEZ, M. I. & QUESADA, A. R. 2006. Hyperforin: more than an antidepressant bioactive compound? *Life Sci,* 79**,** 105-11.

MEHTA, S. V., SHUKLA, S. N. & VORA, H. H. 2013. Overexpression of Bcl2 protein predicts chemoresistance in acute myeloid leukemia: its correlation with FLT3. *Neoplasma,* 60**,** 666-75.

MEIJER, E. & CORNELISSEN, J. J. 2008. Allogeneic stem cell transplantation in acute myeloid leukemia in first or subsequent remission: weighing prognostic markers predicting relapse and risk factors for non-relapse mortality. *Semin Oncol,* 35**,** 449-57.

MELO, M. B., AHMAD, N. N., LIMA, C. S., PAGNANO, K. B., BORDIN, S., LORAND-METZE, I., SAAD, S. T. & COSTA, F. F. 2002. Mutations in the p53 gene in acute myeloid leukemia patients correlate with poor prognosis. *Hematology,* 7**,** 13-9.

MESHINCHI, S., ALONZO, T. A., STIREWALT, D. L., ZWAAN, M., ZIMMERMAN, M., REINHARDT, D., KASPERS, G. J., HEEREMA, N. A., GERBING, R., LANGE, B. J. & RADICH, J. P. 2006. Clinical implications of FLT3 mutations in pediatric AML. *Blood,* 108**,** 3654-61.

METKAR, S. S., WANG, B., EBBS, M. L., KIM, J. H., LEE, Y. J., RAJA, S. M. & FROELICH, C. J. 2003. Granzyme B activates procaspase-3 which signals a mitochondrial amplification loop for maximal apoptosis. *J Cell Biol,* 160**,** 875-85.

MICHEAU, O., LENS, S., GAIDE, O., ALEVIZOPOULOS, K. & TSCHOPP, J. 2001. NF-kappaB signals induce the expression of c-FLIP. *Mol Cell Biol,* 21**,** 5299-305.

MICHEAU, O. & TSCHOPP, J. 2003. Induction of TNF receptor I-mediated apoptosis via two sequential signaling complexes. *Cell,* 114**,** 181-90.

MIHARA, M., ERSTER, S., ZAIKA, A., PETRENKO, O., CHITTENDEN, T., PANCOSKA, P. & MOLL, U. M. 2003. p53 has a direct apoptogenic role at the mitochondria. *Mol Cell,* 11**,** 577-90.

MIKULIC, M., BATINIC, D., SUCIC, M., DAVIDOVIC-MRSIC, S., DUBRAVCIC, K., NEMET, D., SERVENTI-SEIWERTH, R., SERTIC, D. & LABAR, B. 2008.

Christiana Sawa

Biological features and outcome of biphenotypic acute leukemia: a case series. *Hematol Oncol Stem Cell Ther,* 1**,** 225-30.

MIYOSHI, H., SHIMIZU, K., KOZU, T., MASEKI, N., KANEKO, Y. & OHKI, M. 1991. t(8;21) breakpoints on chromosome 21 in acute myeloid leukemia are clustered within a limited region of a single gene, AML1. *Proc Natl Acad Sci U S A,* 88**,** 10431-4.

MIZUKI, M., FENSKI, R., HALFTER, H., MATSUMURA, I., SCHMIDT, R., MULLER, C., GRUNING, W., KRATZ-ALBERS, K., SERVE, S., STEUR, C., BUCHNER, T., KIENAST, J., KANAKURA, Y., BERDEL, W. E. & SERVE, H. 2000. Flt3 mutations from patients with acute myeloid leukemia induce transformation of 32D cells mediated by the Ras and STAT5 pathways. *Blood,* 96**,** 3907-14.

MOFFITT, K. L., MARTIN, S. L. & WALKER, B. 2010. From sentencing to execution--the processes of apoptosis. *J Pharm Pharmacol,* 62**,** 547-62.

MOLL, U. M. & PETRENKO, O. 2003. The MDM2-p53 interaction. *Mol Cancer Res,* 1**,** 1001-8.

MORA, A. L., CORN, R. A., STANIC, A. K., GOENKA, S., ARONICA, M., STANLEY, S., BALLARD, D. W., JOYCE, S. & BOOTHBY, M. 2003. Antiapoptotic function of NF-kappaB in T lymphocytes is influenced by their differentiation status: roles of Fas, c-FLIP, and Bcl-xL. *Cell Death Differ,* 10**,** 1032-44.

MORAN, A. E., KOVACSOVICS-BANKOWSKI, M. & WEINBERG, A. D. 2013. The TNFRs OX40, 4-1BB, and CD40 as targets for cancer immunotherapy. *Curr Opin Immunol,* 25**,** 230-7.

MORIZOT, A., MERINO, D., LALAOUI, N., JACQUEMIN, G., GRANCI, V., IESSI, E., LANNEAU, D., BOUYER, F., SOLARY, E., CHAUFFERT, B., SAAS, P., GARRIDO, C. & MICHEAU, O. 2011. Chemotherapy overcomes TRAIL-R4-mediated TRAIL resistance at the DISC level. *Cell Death Differ,* 18**,** 700-11.

MULLIGHAN, C. G. 2012. The molecular genetic makeup of acute lymphoblastic leukemia. *Hematology Am Soc Hematol Educ Program,* 2012**,** 389-96.

MULLIGHAN, C. G., GOORHA, S., RADTKE, I., MILLER, C. B., COUSTAN-SMITH, E., DALTON, J. D., GIRTMAN, K., MATHEW, S., MA, J., POUNDS, S. B., SU, X., PUI, C. H., RELLING, M. V., EVANS, W. E., SHURTLEFF, S. A. & DOWNING, J. R. 2007. Genome-wide analysis of genetic alterations in acute lymphoblastic leukaemia. *Nature,* 446**,** 758-64.

Christiana Savva

MULLIGHAN, C. G., MILLER, C. B., RADTKE, I., PHILLIPS, L. A., DALTON, J., MA, J., WHITE, D., HUGHES, T. P., LE BEAU, M. M., PUI, C. H., RELLING, M. V., SHURTLEFF, S. A. & DOWNING, J. R. 2008. BCR-ABL1 lymphoblastic leukaemia is characterized by the deletion of Ikaros. *Nature,* 453**,** 110-4.

MULLIGHAN, C. G., ZHANG, J., HARVEY, R. C., COLLINS-UNDERWOOD, J. R., SCHULMAN, B. A., PHILLIPS, L. A., TASIAN, S. K., LOH, M. L., SU, X., LIU, W., DEVIDAS, M., ATLAS, S. R., CHEN, I. M., CLIFFORD, R. J., GERHARD, D. S., CARROLL, W. L., REAMAN, G. H., SMITH, M., DOWNING, J. R., HUNGER, S. P. & WILLMAN, C. L. 2009. JAK mutations in high-risk childhood acute lymphoblastic leukemia. *Proc Natl Acad Sci U S A,* 106**,** 9414-8.

MURUGANANDAM, A., GHOSAL, S. & BHATTACHARYA, S. 2000. The role of xanthones in the antidepressant activity of Hypericum perforatum involving dopaminergic and serotonergic systems *Biogenic amines,* 15**,** 553-567.

NACHEVA, E. P., GRACE, C. D., BRAZMA, D., GANCHEVA, K., HOWARD-REEVES, J., RAI, L., GALE, R. E., LINCH, D. C., HILLS, R. K., RUSSELL, N., BURNETT, A. K. & KOTTARIDIS, P. D. 2013. Does BCR/ABL1 positive acute myeloid leukaemia exist? *Br J Haematol,* 161**,** 541-50.

NAGAI, M. & TADA, M. 1987. Antimicrobial Compounds, Chinesin I and II from Flowers of Hypericum chinense L. *Chemistry Letters,* 16**,** 1337-1340.

NAPETSCHNIG, J. & WU, H. 2013. Molecular basis of NF-kappaB signaling. *Annu Rev Biophys,* 42**,** 443-68.

NARITA, M., SHIMIZU, S., ITO, T., CHITTENDEN, T., LUTZ, R. J., MATSUDA, H. & TSUJIMOTO, Y. 1998. Bax interacts with the permeability transition pore to induce permeability transition and cytochrome c release in isolated mitochondria. *Proc Natl Acad Sci U S A,* 95**,** 14681-6.

NEMES, K., CSOKA, M., NAGY, N., MARK, A., VARADI, Z., DANKO, T., KOVACS, G., KOPPER, L. & SEBESTYEN, A. 2015. Expression of certain leukemia/lymphoma related microRNAs and its correlation with prognosis in childhood acute lymphoblastic leukemia. *Pathol Oncol Res,* 21**,** 597-604.

NICOLAOU, C. A. & KANNAS, C. C. 2011. Molecular library design using multi-objective optimization methods. *Methods Mol Biol,* 685**,** 53-69.

Christiana Savva

NICOLAOU, K. C. 2014. Organic synthesis: the art and science of replicating the molecules of living nature and creating others like them in the laboratory. *Proc Math Phys Eng Sci,* 470**,** 20130690.

NICOLAOU, K. C., SANCHINI, S., SARLAH, D., LU, G., WU, T. R., NOMURA, D. K., CRAVATT, B. F., CUBITT, B., DE LA TORRE, J. C., HESSELL, A. J. & BURTON, D. R. 2011. Design, synthesis, and biological evaluation of a biyouyanagin compound library. *Proc Natl Acad Sci U S A,* 108**,** 6715-20.

NICOLAOU, K. C., SANCHINI, S., WU, T. R. & SARLAH, D. 2010. Total synthesis and structural revision of biyouyanagin B. *Chemistry,* 16**,** 7678-82.

NICOLAOU, K. C., SARLAH, D. & SHAW, D. M. 2007. Total synthesis and revised structure of biyouyanagin A. *Angew Chem Int Ed Engl,* 46**,** 4708-11.

NICOLAOU, K. C., WU, T. R., SARLAH, D., SHAW, D. M., ROWCLIFFE, E. & BURTON, D. R. 2008. Total synthesis, revised structure, and biological evaluation of biyouyanagin A and analogues thereof. *J Am Chem Soc,* 130**,** 11114-21.

NIINUMA, A., HIGUCHI, M., TAKAHASHI, M., OIE, M., TANAKA, Y., GEJYO, F., TANAKA, N., SUGAMURA, K., XIE, L., GREEN, P. L. & FUJII, M. 2005. Aberrant activation of the interleukin-2 autocrine loop through the nuclear factor of activated T cells by nonleukemogenic human T-cell leukemia virus type 2 but not by leukemogenic type 1 virus. *J Virol,* 79**,** 11925-34.

NIMMANAPALLI, R., FUINO, L., STOBAUGH, C., RICHON, V. & BHALLA, K. 2003. Cotreatment with the histone deacetylase inhibitor suberoylanilide hydroxamic acid (SAHA) enhances imatinib-induced apoptosis of Bcr-Abl-positive human acute leukemia cells. *Blood,* 101**,** 3236-9.

NISHIOKA, C., IKEZOE, T., YANG, J., NOBUMOTO, A., KATAOKA, S., TSUDA, M., UDAKA, K. & YOKOYAMA, A. 2014. CD82 regulates STAT5/IL-10 and supports survival of acute myelogenous leukemia cells. *Int J Cancer,* 134**,** 55-64.

NORBERG, E., ORRENIUS, S. & ZHIVOTOVSKY, B. 2010. Mitochondrial regulation of cell death: processing of apoptosis-inducing factor (AIF). *Biochem Biophys Res Commun,* 396**,** 95-100.

NORONHA, E. J., STERLING, K. H. & CALAME, K. L. 2003. Increased expression of Bcl-xL and c-Myc is associated with transformation by Abelson murine leukemia virus. *J Biol Chem,* 278**,** 50915-22.

Christiana Savva

NUESSLER, V., STOTZER, O., GULLIS, E., PELKA-FLEISCHER, R., POGREBNIAK, A., GIESELER, F. & WILMANNS, W. 1999. Bcl-2, bax and bcl-xL expression in human sensitive and resistant leukemia cell lines. *Leukemia,* 13**,** 1864-72.

NUNEZ, G., BENEDICT, M. A., HU, Y. & INOHARA, N. 1998. Caspases: the proteases of the apoptotic pathway. *Oncogene,* 17**,** 3237-45.

O'DONNELL, M. A. & TING, A. T. 2012. NFkappaB and ubiquitination: partners in disarming RIPK1-mediated cell death. *Immunol Res,* 54**,** 214-26.

ODIATOU, E. M., SKALTSOUNIS, A. L. & CONSTANTINOU, A. I. 2013. Identification of the factors responsible for the in vitro pro-oxidant and cytotoxic activities of the olive polyphenols oleuropein and hydroxytyrosol. *Cancer Lett,* 330**,** 113-21.

OECKINGHAUS, A. & GHOSH, S. 2009. The NF-kappaB family of transcription factors and its regulation. *Cold Spring Harb Perspect Biol,* 1**,** a000034.

OH, H. & GHOSH, S. 2013. NF-kappaB: roles and regulation in different CD4(+) T-cell subsets. *Immunol Rev,* 252**,** 41-51.

OKA, D., NISHIMURA, K., SHIBA, M., NAKAI, Y., ARAI, Y., NAKAYAMA, M., TAKAYAMA, H., INOUE, H., OKUYAMA, A. & NONOMURA, N. 2007. Sesquiterpene lactone parthenolide suppresses tumor growth in a xenograft model of renal cell carcinoma by inhibiting the activation of NF-kappaB. *Int J Cancer,* 120**,** 2576-81.

OKUHASHI, Y., NARA, N. & TOHDA, S. 2010. Effects of gamma-secretase inhibitors on the growth of leukemia cells. *Anticancer Res,* 30**,** 495-8.

OLA, M. S., NAWAZ, M. & AHSAN, H. 2011. Role of Bcl-2 family proteins and caspases in the regulation of apoptosis. *Mol Cell Biochem,* 351**,** 41-58.

OUYANG, L., SHI, Z., ZHAO, S., WANG, F. T., ZHOU, T. T., LIU, B. & BAO, J. K. 2012. Programmed cell death pathways in cancer: a review of apoptosis, autophagy and programmed necrosis. *Cell Prolif,* 45**,** 487-98.

PABST, T., VELLENGA, E., VAN PUTTEN, W., SCHOUTEN, H. C., GRAUX, C., VEKEMANS, M. C., BIEMOND, B., SONNEVELD, P., PASSWEG, J., VERDONCK, L., LEGDEUR, M. C., THEOBALD, M., JACKY, E., BARGETZI, M., MAERTENS, J., OSSENKOPPELE, G. J. & LOWENBERG, B. 2012. Favorable effect of priming with granulocyte colony-stimulating factor in remission induction of acute myeloid leukemia restricted to dose escalation of cytarabine. *Blood,* 119**,** 5367-73.

Christiana Savva

PAHL, H. L. 1999. Activators and target genes of Rel/NF-kappaB transcription factors. *Oncogene,* 18**,** 6853-66.

PAN, Y., MENG, M., ZHANG, G., HAN, H. & ZHOU, Q. 2014. Oncogenic microRNAs in the genesis of leukemia and lymphoma. *Curr Pharm Des,* 20**,** 5260-7.

PANDOLFI, P. P. 2001. Oncogenes and tumor suppressors in the molecular pathogenesis of acute promyelocytic leukemia. *Hum Mol Genet,* 10**,** 769-75.

PARK, J. H. 2012. ATRA plus arsenic gets another "A" in APL. *Blood,* 120**,** 1535-6.

PASTORCZAK, A., STOLARSKA, M., TRELINSKA, J., ZAWITKOWSKA, J., KOWALCZYK, J. & MLYNARSKI, W. 2011. Nijmegen breakage syndrome (NBS) as a risk factor for CNS involvement in childhood acute lymphoblastic leukemia. *Pediatr Blood Cancer,* 57**,** 160-2.

PERKINS, N. D. 2007. Integrating cell-signalling pathways with NF-kappaB and IKK function. *Nat Rev Mol Cell Biol,* 8**,** 49-62.

PIA SCHIAVONE, B. I., VEROTTA, L., ROSATO, A., MARILENA, M., GIBBONS, S., BOMBARDELLI, E., FRANCHINI, C. & CORBO, F. 2014. Anticancer and Antibacterial Activity of Hyperforin and Its Derivatives. *Anticancer Agents Med Chem,* 14**,** 1397-1401.

PICCALUGA, P. P., PAOLINI, S. & MARTINELLI, G. 2007. Tyrosine kinase inhibitors for the treatment of Philadelphia chromosome-positive adult acute lymphoblastic leukemia. *Cancer,* 110**,** 1178-86.

PIETERS, R. & CARROLL, W. L. 2010. Biology and treatment of acute lymphoblastic leukemia. *Hematol Oncol Clin North Am,* 24**,** 1-18.

PINAROSA A. 2005. A survey on the hypericum genus: Secondary metabolites and bioactivity. *Studies in Natural Products Chemistry,* 30**,** 603-634.

POLIGONE, B. & BALDWIN, A. S. 2001. Positive and negative regulation of NF-kappaB by COX-2: roles of different prostaglandins. *J Biol Chem,* 276**,** 38658-64.

PORTER, A. G. & JANICKE, R. U. 1999. Emerging roles of caspase-3 in apoptosis. *Cell Death Differ,* 6**,** 99-104.

PRASAD, S., RAVINDRAN, J. & AGGARWAL, B. B. 2010. NF-kappaB and cancer: how intimate is this relationship. *Mol Cell Biochem,* 336**,** 25-37.

Christiana Sawa

PUCCETTI, E. & RUTHARDT, M. 2004. Acute promyelocytic leukemia: PML/RARalpha and the leukemic stem cell. *Leukemia,* 18**,** 1169-75.

PUCCI, B., KASTEN, M. & GIORDANO, A. 2000. Cell cycle and apoptosis. *Neoplasia,* 2**,** 291-9.

PUI, C. H., ROBISON, L. L. & LOOK, A. T. 2008. Acute lymphoblastic leukaemia. *Lancet,* 371**,** 1030-43.

RAVID, K. 2009. MAL: not just a leukemia inducer. *Blood,* 114**,** 3977-8.

REIKVAM, H., HAUGE, M., BRENNER, A. K., HATFIELD, K. J. & BRUSERUD, O. 2015. Emerging therapeutic targets for the treatment of human acute myeloid leukemia (part 1) - gene transcription, cell cycle regulation, metabolism and intercellular communication. *Expert Rev Hematol,* 8**,** 299-313.

REISMULLER, B., ATTARBASCHI, A., PETERS, C., DWORZAK, M. N., POTSCHGER, U., URBAN, C., FINK, F. M., MEISTER, B., SCHMITT, K., DIECKMANN, K., HENZE, G., HAAS, O. A., GADNER, H., MANN, G. & AUSTRIAN BERLIN-FRANKFURT-MUNSTER STUDY, G. 2009. Long-term outcome of initially homogenously treated and relapsed childhood acute lymphoblastic leukaemia in Austria--a population-based report of the Austrian Berlin-Frankfurt-Munster (BFM) Study Group. *Br J Haematol,* 144**,** 559-70.

RENEHAN, A. G., BOOTH, C. & POTTEN, C. S. 2001. What is apoptosis, and why is it important? *BMJ,* 322**,** 1536-8.

RICCIARDI, M. R., MIRABILII, S., ALLEGRETTI, M., LICCHETTA, R., CALARCO, A., TORRISI, M. R., FOA, R., NICOLAI, R., PELUSO, G. & TAFURI, A. 2015. Targeting the leukemia cell metabolism by the CPT1a inhibition: functional pre-clinical effects in leukemias. *Blood*.

RICCIONI, R., PASQUINI, L., MARIANI, G., SAULLE, E., ROSSINI, A., DIVERIO, D., PELOSI, E., VITALE, A., CHIERICHINI, A., CEDRONE, M., FOA, R., LO COCO, F., PESCHLE, C. & TESTA, U. 2005. TRAIL decoy receptors mediate resistance of acute myeloid leukemia cells to TRAIL. *Haematologica,* 90**,** 612-24.

RIEGER, M. A. & SCHROEDER, T. 2012. Hematopoiesis. *Cold Spring Harb Perspect Biol,* 4.

Christiana Savva

RIETHER, C., SCHURCH, C. M. & OCHSENBEIN, A. F. 2015. Regulation of hematopoietic and leukemic stem cells by the immune system. *Cell Death Differ,* 22**,** 187-98.

RIX, U., GRIDLING, M. & SUPERTI-FURGA, G. 2012. Compound immobilization and drug-affinity chromatography. *Methods Mol Biol,* 803**,** 25-38.

RIZZARDI, C., LEOCATA, P., VENTURA, L., ZWEYER, M., BROLLO, A., SCHNEIDER, M. & MELATO, M. 2009. Apoptosis-related factors (TRAIL, DR4, DR5, DcR1, DcR2, apoptotic cells) and proliferative activity in ameloblastomas. *Anticancer Res,* 29**,** 1137-42.

ROBERTS, N. J., ZHOU, S., DIAZ, L. A., JR. & HOLDHOFF, M. 2011. Systemic use of tumor necrosis factor alpha as an anticancer agent. *Oncotarget,* 2**,** 739-51.

ROBINSON, D. L. 2001. Childhood leukemia: Understanding the significance of chromosomal abnormalities. *J Pediatr Oncol Nurs,* 18**,** 111-23.

ROBINSON, L. J., XUE, J. & COREY, S. J. 2005. Src family tyrosine kinases are activated by Flt3 and are involved in the proliferative effects of leukemia-associated Flt3 mutations. *Exp Hematol,* 33**,** 469-79.

ROBOZ, G. J. & GUZMAN, M. 2009. Acute myeloid leukemia stem cells: seek and destroy. *Expert Rev Hematol,* 2**,** 663-72.

ROBSON, N. K. B. 1985. Studies in the genus Hypericum L. (Guttiferae) (Book). *Bull. Brit. Mus. (Nat. Hist.) Bot.,* 198503980 KR.

ROSS, J. A. 1998. Maternal diet and infant leukemia: a role for DNA topoisomerase II inhibitors? *Int J Cancer Suppl,* 11**,** 26-8.

ROTHBARTH, J., TOLLENAAR, R. A., SCHELLENS, J. H., NORTIER, J. W., KOOL, L. J., KUPPEN, P. J., MULDER, G. J. & VAN DE VELDE, C. J. 2004. Isolated hepatic perfusion for the treatment of colorectal metastases confined to the liver: recent trends and perspectives. *Eur J Cancer,* 40**,** 1812-24.

ROTHE, M., PAN, M. G., HENZEL, W. J., AYRES, T. M. & GOEDDEL, D. V. 1995. The TNFR2-TRAF signaling complex contains two novel proteins related to baculoviral inhibitor of apoptosis proteins. *Cell,* 83**,** 1243-52.

RUSHWORTH, S. A., ZAITSEVA, L., MURRAY, M. Y., SHAH, N. M., BOWLES, K. M. & MACEWAN, D. J. 2012. The high Nrf2 expression in human acute myeloid leukemia is driven by NF-kappaB and underlies its chemo-resistance. *Blood,* 120**,** 5188-98.

Christiana Savva

SABATTINI, E., BACCI, F., SAGRAMOSO, C. & PILERI, S. A. 2010. WHO classification of tumours of haematopoietic and lymphoid tissues in 2008: an overview. *Pathologica,* 102**,** 83-7.

SACHDEV, R., AGARWAL, N., KHAN, M. A. & KUMAR, A. 2015. Infantile Acute Monoblastic Leukemia with MLL Gene Rearrangements. *Indian J Hematol Blood Transfus,* 31**,** 146-7.

SAELENS, X., FESTJENS, N., VANDE WALLE, L., VAN GURP, M., VAN LOO, G. & VANDENABEELE, P. 2004. Toxic proteins released from mitochondria in cell death. *Oncogene,* 23**,** 2861-74.

SAFA, A. R. 2012. c-FLIP, a master anti-apoptotic regulator. *Exp Oncol,* 34**,** 176-84.

SAITO, Y., YUKI, H., KURATANI, M., HASHIZUME, Y., TAKAGI, S., HONMA, T., TANAKA, A., SHIROUZU, M., MIKUNI, J., HANDA, N., OGAHARA, I., SONE, A., NAJIMA, Y., TOMABECHI, Y., WAKIYAMA, M., UCHIDA, N., TOMIZAWA-MURASAWA, M., KANEKO, A., TANAKA, S., SUZUKI, N., KAJITA, H., AOKI, Y., OHARA, O., SHULTZ, L. D., FUKAMI, T., GOTO, T., TANIGUCHI, S., YOKOYAMA, S. & ISHIKAWA, F. 2013. A pyrrolo-pyrimidine derivative targets human primary AML stem cells in vivo. *Sci Transl Med,* 5**,** 181ra52.

SAKAHIRA, H., ENARI, M. & NAGATA, S. 1998. Cleavage of CAD inhibitor in CAD activation and DNA degradation during apoptosis. *Nature,* 391**,** 96-9.

SAKAMOTO, K. M. 2014. Letting microRNAs overcome resistance to chemotherapy in acute myeloid leukemia. *Leuk Lymphoma,* 55**,** 1449-50.

SANGHVI, V. R., MAVRAKIS, K. J., VAN DER MEULEN, J., BOICE, M., WOLFE, A. L., CARTY, M., MOHAN, P., RONDOU, P., SOCCI, N. D., BENOIT, Y., TAGHON, T., VAN VLIERBERGHE, P., LESLIE, C. S., SPELEMAN, F. & WENDEL, H. G. 2014. Characterization of a set of tumor suppressor microRNAs in T cell acute lymphoblastic leukemia. *Sci Signal,* 7**,** ra111.

SAVILL, J. & FADOK, V. 2000. Corpse clearance defines the meaning of cell death. *Nature,* 407**,** 784-8.

SCAFFIDI, C., FULDA, S., SRINIVASAN, A., FRIESEN, C., LI, F., TOMASELLI, K. J., DEBATIN, K. M., KRAMMER, P. H. & PETER, M. E. 1998. Two CD95 (APO-1/Fas) signaling pathways. *EMBO J,* 17**,** 1675-87.

SCHIMMER, A. D. 2004. Inhibitor of apoptosis proteins: translating basic knowledge into clinical practice. *Cancer Res,* 64**,** 7183-90.

Christiana Silva

SCHLETTE, E., RASSIDAKIS, G. Z., CANOZ, O. & MEDEIROS, L. J. 2005. Expression of bcl-3 in chronic lymphocytic leukemia correlates with trisomy 12 and abnormalities of chromosome 19. *Am J Clin Pathol,* 123**,** 465-71.

SCHMIEGELOW, K., LEVINSEN, M. F., ATTARBASCHI, A., BARUCHEL, A., DEVIDAS, M., ESCHERICH, G., GIBSON, B., HEYDRICH, C., HORIBE, K., ISHIDA, Y., LIANG, D. C., LOCATELLI, F., MICHEL, G., PIETERS, R., PIETTE, C., PUI, C. H., RAIMONDI, S., SILVERMAN, L., STANULLA, M., STARK, B., WINICK, N. & VALSECCHI, M. G. 2013. Second malignant neoplasms after treatment of childhood acute lymphoblastic leukemia. *J Clin Oncol,* 31**,** 2469-76.

SCHNETZKE, U., FISCHER, M., SPIES-WEISSHART, B., ZIRM, E., HOCHHAUS, A., MULLER, J. P. & SCHOLL, S. 2013. The E3 ubiquitin ligase TRAF2 can contribute to TNF-alpha resistance in FLT3-ITD-positive AML cells. *Leuk Res,* 37**,** 1557-64.

SCHROFELBAUER, B. & HOFFMANN, A. 2011. How do pleiotropic kinase hubs mediate specific signaling by TNFR superfamily members? *Immunol Rev,* 244**,** 29-43.

SCHUG, Z. T., GONZALVEZ, F., HOUTKOOPER, R. H., VAZ, F. M. & GOTTLIEB, E. 2011. BID is cleaved by caspase-8 within a native complex on the mitochondrial membrane. *Cell Death Differ,* 18**,** 538-48.

SCHULER, M. & GREEN, D. R. 2001. Mechanisms of p53-dependent apoptosis. *Biochem Soc Trans,* 29**,** 684-8.

SEBAA, A., ADES, L., BARAN-MARZACK, F., MOZZICONACCI, M. J., PENTHER, D., DOBBELSTEIN, S., STAMATOULLAS, A., RECHER, C., PREBET, T., MOULESSEHOUL, S., FENAUX, P. & ECLACHE, V. 2012. Incidence of 17p deletions and TP53 mutation in myelodysplastic syndrome and acute myeloid leukemia with 5q deletion. *Genes Chromosomes Cancer,* 51**,** 1086-92.

SENFTLEBEN, U. & KARIN, M. 2002. The IKK/NF-kappaB pathway. *Crit Care Med,* 30**,** S18-S26.

SEVAL, G. C. & OZCAN, M. 2015. Treatment of Acute Myeloid Leukemia in Adolescent and Young Adult Patients. *J Clin Med,* 4**,** 441-59.

SHAMAS-DIN, A., BRAHMBHATT, H., LEBER, B. & ANDREWS, D. W. 2011. BH3-only proteins: Orchestrators of apoptosis. *Biochim Biophys Acta,* 1813**,** 508-20.

Christina Saliva

SHANKAR, S. & SRIVASTAVA, R. K. 2004. Enhancement of therapeutic potential of TRAIL by cancer chemotherapy and irradiation: mechanisms and clinical implications. *Drug Resist Updat,* 7**,** 139-56.

SHARMA, K., D'SOUZA, R. C., TYANOVA, S., SCHAAB, C., WISNIEWSKI, J. R., COX, J. & MANN, M. 2014. Ultradeep human phosphoproteome reveals a distinct regulatory nature of Tyr and Ser/Thr-based signaling. *Cell Rep,* 8**,** 1583-94.

SHARMA, V. M., CALVO, J. A., DRAHEIM, K. M., CUNNINGHAM, L. A., HERMANCE, N., BEVERLY, L., KRISHNAMOORTHY, V., BHASIN, M., CAPOBIANCO, A. J. & KELLIHER, M. A. 2006. Notch1 contributes to mouse T-cell leukemia by directly inducing the expression of c-myc. *Mol Cell Biol,* 26**,** 8022-31.

SHEMBADE, N. & HARHAJ, E. W. 2012. Regulation of NF-kappaB signaling by the A20 deubiquitinase. *Cell Mol Immunol,* 9**,** 123-30.

SHEN, R. R., ZHOU, A. Y., KIM, E., O'CONNELL, J. T., HAGERSTRAND, D., BEROUKHIM, R. & HAHN, W. C. 2015. TRAF2 is an NF-kappaB-activating oncogene in epithelial cancers. *Oncogene,* 34**,** 209-16.

SHIH, L. Y., LIANG, D. C., HUANG, C. F., CHANG, Y. T., LAI, C. L., LIN, T. H., YANG, C. P., HUNG, I. J., LIU, H. C., JAING, T. H., WANG, L. Y. & YEH, T. C. 2008. Cooperating mutations of receptor tyrosine kinases and Ras genes in childhood core-binding factor acute myeloid leukemia and a comparative analysis on paired diagnosis and relapse samples. *Leukemia,* 22**,** 303-7.

SHIMONI, A. & NAGLER, A. 2005. Allogeneic hematopoietic stem-cell transplantation in patients with acute myeloid leukemia in first complete remission: new answers for an old question. *Leukemia,* 19**,** 891-3.

SIEDLE, B., GARCIA-PINERES, A. J., MURILLO, R., SCHULTE-MONTING, J., CASTRO, V., RUNGELER, P., KLAAS, C. A., DA COSTA, F. B., KISIEL, W. & MERFORT, I. 2004. Quantitative structure-activity relationship of sesquiterpene lactones as inhibitors of the transcription factor NF-kappaB. *J Med Chem,* 47**,** 6042-54.

SINGH, H., ASALI, S., WERNER, L. L., DEANGELO, D. J., BALLEN, K. K., AMREIN, P. C., WADLEIGH, M., GALINSKY, I., NEUBERG, D. S., FOX, E. A., STONE, R. M. & ATTAR, E. C. 2011. Outcome of older adults with

Christiana Savva

cytogenetically normal AML (CN-AML) and FLT3 mutations. *Leuk Res,* 35**,** 1611-5.

SLEE, E. A., ADRAIN, C. & MARTIN, S. J. 2001. Executioner caspase-3, -6, and -7 perform distinct, non-redundant roles during the demolition phase of apoptosis. *J Biol Chem,* 276**,** 7320-6.

SMOLEWSKI, P. & ROBAK, T. 2011. Inhibitors of apoptosis proteins (IAPs) as potential molecular targets for therapy of hematological malignancies. *Curr Mol Med,* 11**,** 633-49.

SODERSTROM, T. S., POUKKULA, M., HOLMSTROM, T. H., HEISKANEN, K. M. & ERIKSSON, J. E. 2002. Mitogen-activated protein kinase/extracellular signal-regulated kinase signaling in activated T cells abrogates TRAIL-induced apoptosis upstream of the mitochondrial amplification loop and caspase-8. *J Immunol,* 169**,** 2851-60.

SOLDANI, C. & SCOVASSI, A. I. 2002. Poly(ADP-ribose) polymerase-1 cleavage during apoptosis: an update. *Apoptosis,* 7**,** 321-8.

SONG, G., VALDEZ, B. C., LI, Y., DOMINGUEZ, J. R., CORN, P., CHAMPLIN, R. E. & ANDERSSON, B. S. 2014. The histone deacetylase inhibitor SAHA sensitizes acute myeloid leukemia cells to a combination of nucleoside analogs and the DNA-alkylating agent busulfan. *Leuk Lymphoma,* 55**,** 1625-34.

SONG, X. Y., TORPHY, T. J., GRISWOLD, D. E. & SHEALY, D. 2002. Coming of age: anti-cytokine therapies. *Mol Interv,* 2**,** 36-46.

SOROKIN, A. V., NAIR, B. C., WEI, Y., AZIZ, K. E., EVDOKIMOVA, V., HUNG, M. C. & CHEN, J. 2015. Aberrant Expression of proPTPRN2 in Cancer Cells Confers Resistance to Apoptosis. *Cancer Res,* 75**,** 1846-58.

SOROUR, A., AYAD, M. W. & KASSEM, H. 2013. The genotype distribution of the XRCC1, XRCC3, and XPD DNA repair genes and their role for the development of acute myeloblastic leukemia. *Genet Test Mol Biomarkers,* 17**,** 195-201.

SU, M., ALONSO, S., JONES, J. W., YU, J., KANE, M. A., JONES, R. J. & GHIAUR, G. 2015. All-Trans Retinoic Acid Activity in Acute Myeloid Leukemia: Role of Cytochrome P450 Enzyme Expression by the Microenvironment. *PLoS One,* 10**,** e0127790.

SUCIU, S., MANDELLI, F., DE WITTE, T., ZITTOUN, R., GALLO, E., LABAR, B., DE ROSA, G., BELHABRI, A., GIUSTOLISI, R., DELARUE, R., LISO, V.,

Christiana Saiva

MIRTO, S., LEONE, G., BOURHIS, J. H., FIORITONI, G., JEHN, U., AMADORI, S., FAZI, P., HAGEMEIJER, A. & WILLEMZE, R. 2003. Allogeneic compared with autologous stem cell transplantation in the treatment of patients younger than 46 years with acute myeloid leukemia (AML) in first complete remission (CR1): an intention-to-treat analysis of the EORTC/GIMEMAAML-10 trial. *Blood,* 102**,** 1232-40.

SUN, G. L. 1993. [Treatment of acute promyelocytic leukemia (APL) with all-trans retinoic acid (ATRA): a report of five-year experience]. *Zhonghua Zhong Liu Za Zhi,* 15**,** 125-9.

SUSIN, S. A., LORENZO, H. K., ZAMZAMI, N., MARZO, I., SNOW, B. E., BROTHERS, G. M., MANGION, J., JACOTOT, E., COSTANTINI, P., LOEFFLER, M., LAROCHETTE, N., GOODLETT, D. R., AEBERSOLD, R., SIDEROVSKI, D. P., PENNINGER, J. M. & KROEMER, G. 1999. Molecular characterization of mitochondrial apoptosis-inducing factor. *Nature,* 397**,** 441-6.

SZEGEZDI, E., FITZGERALD, U. & SAMALI, A. 2003. Caspase-12 and ER-stress-mediated apoptosis: the story so far. *Ann N Y Acad Sci,* 1010**,** 186-94.

TADA, M., NAGAI, M., OKUMURA, C., OSANO, Y. & MATSUZAKI, T. 1989. Novel Spiro-Compound, Hyperolactone from Hypericum chinense L. *Chemistry Letters,* 18**,** 683-686.

TAIT, S. W. & GREEN, D. R. 2010. Mitochondria and cell death: outer membrane permeabilization and beyond. *Nat Rev Mol Cell Biol,* 11**,** 621-32.

TAKAHASHI, A. & EARNSHAW, W. C. 1996. ICE-related proteases in apoptosis. *Curr Opin Genet Dev,* 6**,** 50-5.

TAMAI, H. & INOKUCHI, K. 2015. Molecular genetics of acute lymphoblastic leukemia. *Rinsho Ketsueki,* 56**,** 253-60.

TANAKA, N., ABE, S., HASEGAWA, K., SHIRO, M. & KOBAYASHI, J. 2011. Biyoulactones A-C, New Pentacyclic Meroterpenoids from Hypericum chinense. *Org Lett,* 13**,** 5488-5491.

TANAKA, N., KASHIWADA, Y., KIM, S. Y., HASHIDA, W., SEKIYA, M., IKESHIRO, Y. & TAKAISHI, Y. 2009a. Acylphloroglucinol, biyouyanagiol, biyouyanagin B, and related spiro-lactones from Hypericum chinense. *J Nat Prod,* 72**,** 1447-52.

Christiana Sawa

TANAKA, N., KASHIWADA, Y., KIM, S. Y., SEKIYA, M., IKESHIRO, Y. & TAKAISHI, Y. 2009b. Xanthones from Hypericum chinense and their cytotoxicity evaluation. *Phytochemistry,* 70**,** 1456-61.

TANAKA, N., OKASAKA, M., ISHIMARU, Y., TAKAISHI, Y., SATO, M., OKAMOTO, M., OSHIKAWA, T., AHMED, S. U., CONSENTINO, L. M. & LEE, K. H. 2005. Biyouyanagin A, an anti-HIV agent from Hypericum chinense L. var. salicifolium. *Org Lett,* 7**,** 2997-9.

TANAKA, N. & TAKAISHI, Y. 2006. Xanthones from Hypericum chinense. *Phytochemistry,* 67**,** 2146-51.

TANAKA, N. & TAKAISHI, Y. 2007. Xanthones from stems of Hypericum chinense. *Chem Pharm Bull (Tokyo),* 55**,** 19-21.

TANAKA N., ABE S. & KOBAYASHI J. 2012. Biyoulactones D and E, meroterpenoids from Hypericum chinense. *Tetrahedron Letters,* 53**,** 1507-1510.

TANAKA N., MAMEMURA T., ABE S., IMABAYASHI K., KASHIWADA Y., TAKAISHI Y., SUZUKI T., TAKEBE Y., KUBOTA T. & KOBAYASHI J. 2010. Biyouxanthones A - D, Prenylated Xanthones from Roots of Hypericum chinense. *Heterocycles,* 80**,** 613-621.

THOMAS, G. S., ZHANG, L., BLACKWELL, K. & HABELHAH, H. 2009. Phosphorylation of TRAF2 within its RING domain inhibits stress-induced cell death by promoting IKK and suppressing JNK activation. *Cancer Res,* 69**,** 3665-72.

THORNBERRY, N. A. 1998. Caspases: key mediators of apoptosis. *Chem Biol,* 5**,** R97-103.

THORNBERRY, N. A., RANO, T. A., PETERSON, E. P., RASPER, D. M., TIMKEY, T., GARCIA-CALVO, M., HOUTZAGER, V. M., NORDSTROM, P. A., ROY, S., VAILLANCOURT, J. P., CHAPMAN, K. T. & NICHOLSON, D. W. 1997. A combinatorial approach defines specificities of members of the caspase family and granzyme B. Functional relationships established for key mediators of apoptosis. *J Biol Chem,* 272**,** 17907-11.

TIGHE, J. E., DAGA, A. & CALABI, F. 1993. Translocation breakpoints are clustered on both chromosome 8 and chromosome 21 in the t(8;21) of acute myeloid leukemia. *Blood,* 81**,** 592-6.

TIRADO, C. A., VALDEZ, F., KLESSE, L., KARANDIKAR, N. J., UDDIN, N., ARBINI, A., FUSTINO, N., COLLINS, R., PATEL, S., SMART, R. L.,

Christiana Savva

GARCIA, R., DOOLITTLE, J. & CHEN, W. 2010. Acute myeloid leukemia with inv(16) with CBFB-MYH11, 3'CBFB deletion, variant t(9;22) with BCR-ABL1, and del(7)(q22q32) in a pediatric patient: case report and literature review. *Cancer Genet Cytogenet,* 200**,** 54-9.

TORRANO, V., PROCTER, J., CARDUS, P., GREAVES, M. & FORD, A. M. 2011. ETV6-RUNX1 promotes survival of early B lineage progenitor cells via a dysregulated erythropoietin receptor. *Blood,* 118**,** 4910-8.

TOUJANI, S., DESSEN, P., ITHZAR, N., DANGLOT, G., RICHON, C., VASSETZKY, Y., ROBERT, T., LAZAR, V., BOSQ, J., DA COSTA, L., PEROT, C., RIBRAG, V., PATTE, C., WIELS, J. & BERNHEIM, A. 2009. High resolution genome-wide analysis of chromosomal alterations in Burkitt's lymphoma. *PLoS One,* 4**,** e7089.

TOURNEUR, L. & CHIOCCHIA, G. 2010. FADD: a regulator of life and death. *Trends Immunol,* 31**,** 260-9.

TSUTSUMI, Y., TANAKA, J., MINAMI, H., MUSASHI, M., FUKUSHIMA, A., EHIRA, N., KANAMORI, H., YAMATO, H., SASAKI, J., FUNAKI, C., HASEGAWA, S., OBARA, S., OGURA, N., ASAKA, M., IMAMURA, M. & MASAUZI, N. 2005. Acute biphenotypic leukemia and an acquired X chromosome. *Cancer Genet Cytogenet,* 157**,** 94-5.

VAN DONGEN, J. J. 1995. Proposals for immunological classification of acute leukemias. *Leukemia,* 9**,** 2149-50.

VAN LOO, G., SCHOTTE, P., VAN GURP, M., DEMOL, H., HOORELBEKE, B., GEVAERT, K., RODRIGUEZ, I., RUIZ-CARRILLO, A., VANDEKERCKHOVE, J., DECLERCQ, W., BEYAERT, R. & VANDENABEELE, P. 2001. Endonuclease G: a mitochondrial protein released in apoptosis and involved in caspase-independent DNA degradation. *Cell Death Differ,* 8**,** 1136-42.

VANDEN BERGHE, T., VANLANGENAKKER, N., PARTHOENS, E., DECKERS, W., DEVOS, M., FESTJENS, N., GUERIN, C. J., BRUNK, U. T., DECLERCQ, W. & VANDENABEELE, P. 2010. Necroptosis, necrosis and secondary necrosis converge on similar cellular disintegration features. *Cell Death Differ,* 17**,** 922-30.

VANDENABEELE, P., GALLUZZI, L., VANDEN BERGHE, T. & KROEMER, G. 2010. Molecular mechanisms of necroptosis: an ordered cellular explosion. *Nat Rev Mol Cell Biol,* 11**,** 700-14.

Christiana Savva

VARDIMAN, J. W. 2010. The World Health Organization (WHO) classification of tumors of the hematopoietic and lymphoid tissues: an overview with emphasis on the myeloid neoplasms. *Chem Biol Interact,* 184**,** 16-20.

VARDIMAN, J. W., THIELE, J., ARBER, D. A., BRUNNING, R. D., BOROWITZ, M. J., PORWIT, A., HARRIS, N. L., LE BEAU, M. M., HELLSTROM-LINDBERG, E., TEFFERI, A. & BLOOMFIELD, C. D. 2009. The 2008 revision of the World Health Organization (WHO) classification of myeloid neoplasms and acute leukemia: rationale and important changes. *Blood,* 114**,** 937-51.

VARFOLOMEEV, E., GONCHAROV, T. & VUCIC, D. 2015. Roles of c-IAP proteins in TNF receptor family activation of NF-kappaB signaling. *Methods Mol Biol,* 1280**,** 269-82.

VARFOLOMEEV, E. & VUCIC, D. 2008. (Un)expected roles of c-IAPs in apoptotic and NFkappaB signaling pathways. *Cell Cycle,* 7**,** 1511-21.

VARFOLOMEEV, E. E., SCHUCHMANN, M., LURIA, V., CHIANNILKULCHAI, N., BECKMANN, J. S., METT, I. L., REBRIKOV, D., BRODIANSKI, V. M., KEMPER, O. C., KOLLET, O., LAPIDOT, T., SOFFER, D., SOBE, T., AVRAHAM, K. B., GONCHAROV, T., HOLTMANN, H., LONAI, P. & WALLACH, D. 1998. Targeted disruption of the mouse Caspase 8 gene ablates cell death induction by the TNF receptors, Fas/Apo1, and DR3 and is lethal prenatally. *Immunity,* 9**,** 267-76.

VASU, S. & BLUM, W. 2013. Emerging immunotherapies in older adults with acute myeloid leukemia. *Curr Opin Hematol,* 20**,** 107-14.

VELU, C. S., CHAUBEY, A., PHELAN, J. D., HORMAN, S. R., WUNDERLICH, M., GUZMAN, M. L., JEGGA, A. G., ZELEZNIK-LE, N. J., CHEN, J., MULLOY, J. C., CANCELAS, J. A., JORDAN, C. T., ARONOW, B. J., MARCUCCI, G., BHAT, B., GEBELEIN, B. & GRIMES, H. L. 2014. Therapeutic antagonists of microRNAs deplete leukemia-initiating cell activity. *J Clin Invest,* 124**,** 222-36.

VILLA-MORALES, M. & FERNANDEZ-PIQUERAS, J. 2012. Targeting the Fas/FasL signaling pathway in cancer therapy. *Expert Opin Ther Targets,* 16**,** 85-101.

VILLA, R., MOREY, L., RAKER, V. A., BUSCHBECK, M., GUTIERREZ, A., DE SANTIS, F., CORSARO, M., VARAS, F., BOSSI, D., MINUCCI, S., PELICCI, P. G. & DI CROCE, L. 2006. The methyl-CpG binding protein

Christiana Savva

MBD1 is required for PML-RARalpha function. *Proc Natl Acad Sci U S A,* 103**,** 1400-5.

VON HAEFEN, C., GILLISSEN, B., HEMMATI, P. G., WENDT, J., GUNER, D., MROZEK, A., BELKA, C., DORKEN, B. & DANIEL, P. T. 2004. Multidomain Bcl-2 homolog Bax but not Bak mediates synergistic induction of apoptosis by TRAIL and 5-FU through the mitochondrial apoptosis pathway. *Oncogene,* 23**,** 8320-32.

WAJANT, H. 2002. The Fas signaling pathway: more than a paradigm. *Science,* 296**,** 1635-6.

WAKEFORD, R., LITTLE, M. P. & KENDALL, G. M. 2010. Risk of childhood leukemia after low-level exposure to ionizing radiation. *Expert Rev Hematol,* 3**,** 251-4.

WALKER, A. R., KLISOVIC, R., JOHNSTON, J. S., JIANG, Y., GEYER, S., KEFAUVER, C., BINKLEY, P., BYRD, J. C., GREVER, M. R., GARZON, R., PHELPS, M. A., MARCUCCI, G., BLUM, K. A. & BLUM, W. 2013. Pharmacokinetics and dose escalation of the heat shock protein inhibitor 17-allyamino-17-demethoxygeldanamycin in combination with bortezomib in relapsed or refractory acute myeloid leukemia. *Leuk Lymphoma,* 54**,** 1996-2002.

WANG, B. H., LI, Y. H. & YU, L. 2015. Genomics-based Approach and Prognostic Stratification Significance of Gene Mutations in Intermediate-risk Acute Myeloid Leukemia. *Chin Med J (Engl),* 128**,** 2395-2403.

WANG, J., PENG, S., WANG, M., CHEN, N. & DING, L. 2002. Chemical constituents of Hyperricum monogynum. *Zhongguo Zhong Yao Za Zhi.,* 27**,** 120-122.

WANG, W., ZENG, Y. H., OSMAN, K., SHINDE, K., RAHMAN, M., GIBBONS, S. & MU, Q. 2010. Norlignans, acylphloroglucinols, and a dimeric xanthone from Hypericum chinense. *J Nat Prod,* 73**,** 1815-20.

WATTEL, E., PREUDHOMME, C., HECQUET, B., VANRUMBEKE, M., QUESNEL, B., DERVITE, I., MOREL, P. & FENAUX, P. 1994. p53 mutations are associated with resistance to chemotherapy and short survival in hematologic malignancies. *Blood,* 84**,** 3148-57.

WAWRZYNIAK, E., WIERZBOWSKA, A., KOTKOWSKA, A., SIEMIENIUK-RYS, M., ROBAK, T., KNOPINSKA-POSLUSZNY, W., KLONOWSKA, A., ILISZKO, M., WORONIECKA, R., PIENKOWSKA-GRELA, B., EJDUK, A.,

Christiana Savva

WACH, M., DUSZENKO, E., JASKOWIEC, A., JAKOBCZYK, M., MUCHA, B., KOSNY, J., PLUTA, A., GROSICKI, S., HOLOWIECKI, J. & HAUS, O. 2013. Different prognosis of acute myeloid leukemia harboring monosomal karyotype with total or partial monosomies determined by FISH: retrospective PALG study. *Leuk Res,* 37**,** 293-9.

WEINLICH, R., DILLON, C. P. & GREEN, D. R. 2011. Ripped to death. *Trends Cell Biol,* 21**,** 630-7.

WEISBERG, E. L., HALILOVIC, E., COOKE, V. G., NONAMI, A., REN, T., SANDA, T., SIMKIN, I., YUAN, J., ANTONAKOS, B., BARYS, L., ITO, M., STONE, R. M., GALINSKY, I., COWENS, K., NELSON, E., SATTLER, M., JEAY, S., WUERTHNER, J. U., MCDONOUGH, S., WIESMANN, M. & GRIFFIN, J. D. 2015. Inhibition of wild-type p53-expressing AML by novel small molecule HDM2 inhibitor, CGM097. *Mol Cancer Ther*.

WEISSMAN, I. L., ANDERSON, D. J. & GAGE, F. 2001. Stem and progenitor cells: origins, phenotypes, lineage commitments, and transdifferentiations. *Annu Rev Cell Dev Biol,* 17**,** 387-403.

WENG, A. P., FERRANDO, A. A., LEE, W., MORRIS, J. P. T., SILVERMAN, L. B., SANCHEZ-IRIZARRY, C., BLACKLOW, S. C., LOOK, A. T. & ASTER, J. C. 2004. Activating mutations of NOTCH1 in human T cell acute lymphoblastic leukemia. *Science,* 306**,** 269-71.

WENG, A. P., MILLHOLLAND, J. M., YASHIRO-OHTANI, Y., ARCANGELI, M. L., LAU, A., WAI, C., DEL BIANCO, C., RODRIGUEZ, C. G., SAI, H., TOBIAS, J., LI, Y., WOLFE, M. S., SHACHAF, C., FELSHER, D., BLACKLOW, S. C., PEAR, W. S. & ASTER, J. C. 2006. c-Myc is an important direct target of Notch1 in T-cell acute lymphoblastic leukemia/lymphoma. *Genes Dev,* 20**,** 2096-109.

WERTZ, I. E. & DIXIT, V. M. 2010. Signaling to NF-kappaB: regulation by ubiquitination. *Cold Spring Harb Perspect Biol,* 2**,** a003350.

WERTZ, I. E., O'ROURKE, K. M., ZHOU, H., EBY, M., ARAVIND, L., SESHAGIRI, S., WU, P., WIESMANN, C., BAKER, R., BOONE, D. L., MA, A., KOONIN, E. V. & DIXIT, V. M. 2004. De-ubiquitination and ubiquitin ligase domains of A20 downregulate NF-kappaB signalling. *Nature,* 430**,** 694-9.

WIENS, G. D. & GLENNEY, G. W. 2011. Origin and evolution of TNF and TNF receptor superfamilies. *Dev Comp Immunol,* 35**,** 1324-35.

Christiana Savva

WILSON, N. S., DIXIT, V. & ASHKENAZI, A. 2009. Death receptor signal transducers: nodes of coordination in immune signaling networks. *Nat Immunol,* 10**,** 348-55.

WOUTERS, B. J., JORDA, M. A., KEESHAN, K., LOUWERS, I., ERPELINCK-VERSCHUEREN, C. A., TIELEMANS, D., LANGERAK, A. W., HE, Y., YASHIRO-OHTANI, Y., ZHANG, P., HETHERINGTON, C. J., VERHAAK, R. G., VALK, P. J., LOWENBERG, B., TENEN, D. G., PEAR, W. S. & DELWEL, R. 2007. Distinct gene expression profiles of acute myeloid/T-lymphoid leukemia with silenced CEBPA and mutations in NOTCH1. *Blood,* 110**,** 3706-14.

WU, G. S., BURNS, T. F., MCDONALD, E. R., 3RD, JIANG, W., MENG, R., KRANTZ, I. D., KAO, G., GAN, D. D., ZHOU, J. Y., MUSCHEL, R., HAMILTON, S. R., SPINNER, N. B., MARKOWITZ, S., WU, G. & EL-DEIRY, W. S. 1997. KILLER/DR5 is a DNA damage-inducible p53-regulated death receptor gene. *Nat Genet,* 17**,** 141-3.

WURGLICS, M. & SCHUBERT-ZSILAVECZ, M. 2006. Hypericum perforatum: a 'modern' herbal antidepressant: pharmacokinetics of active ingredients. *Clin Pharmacokinet,* 45**,** 449-68.

XIAO, C. & GHOSH, S. 2005. NF-kappaB, an evolutionarily conserved mediator of immune and inflammatory responses. *Adv Exp Med Biol,* 560**,** 41-5.

XU, W. J., ZHU, M. D., WANG, X. B., YANG, M. H., LUO, J. & KONG, L. Y. 2015. Hypermongones A-J, Rare Methylated Polycyclic Polyprenylated Acylphloroglucinols from the Flowers of Hypericum monogynum. *J Nat Prod,* 78**,** 1093-100.

YEH, W. C., SHAHINIAN, A., SPEISER, D., KRAUNUS, J., BILLIA, F., WAKEHAM, A., DE LA POMPA, J. L., FERRICK, D., HUM, B., ISCOVE, N., OHASHI, P., ROTHE, M., GOEDDEL, D. V. & MAK, T. W. 1997. Early lethality, functional NF-kappaB activation, and increased sensitivity to TNF-induced cell death in TRAF2-deficient mice. *Immunity,* 7**,** 715-25.

YU, K. Y., KWON, B., NI, J., ZHAI, Y., EBNER, R. & KWON, B. S. 1999. A newly identified member of tumor necrosis factor receptor superfamily (TR6) suppresses LIGHT-mediated apoptosis. *J Biol Chem,* 274**,** 13733-6.

ZANGRANDO, A., DELL'ORTO, M. C., TE KRONNIE, G. & BASSO, G. 2009. MLL rearrangements in pediatric acute lymphoblastic and myeloblastic

Christiana Savva

leukemias: MLL specific and lineage specific signatures. *BMC Med Genomics,* 2**,** 36.

ZHANG, J., CADO, D., CHEN, A., KABRA, N. H. & WINOTO, A. 1998. Fas-mediated apoptosis and activation-induced T-cell proliferation are defective in mice lacking FADD/Mort1. *Nature,* 392**,** 296-300.

ZHANG, J., KABRA, N. H., CADO, D., KANG, C. & WINOTO, A. 2001. FADD-deficient T cells exhibit a disaccord in regulation of the cell cycle machinery. *J Biol Chem,* 276**,** 29815-8.

ZHANG, L., BLACKWELL, K., ALTAEVA, A., SHI, Z. & HABELHAH, H. 2011. TRAF2 phosphorylation promotes NF-kappaB-dependent gene expression and inhibits oxidative stress-induced cell death. *Mol Biol Cell,* 22**,** 128-40.

ZHANG, Y., YANG, S., WANG, J., ZHU, H., BAO, L., JIA, J., ZHAO, T., JIANG, H., LU, J., JIANG, B., HUANG, X. & JIANG, Q. 2015. [Comparison of 10 mg/m(2) or 8 mg/m(2) idarubicin plus cytarabine regimen as induction chemotherapy for adult patients with newly diagnosed acute myeloid leukemia]. *Zhonghua Xue Ye Xue Za Zhi,* 36**,** 225-9.

ZHAO, Z., ZUBER, J., DIAZ-FLORES, E., LINTAULT, L., KOGAN, S. C., SHANNON, K. & LOWE, S. W. 2010. p53 loss promotes acute myeloid leukemia by enabling aberrant self-renewal. *Genes Dev,* 24**,** 1389-402.

ZHENG, S., MA, X., ZHANG, L., GUNN, L., SMITH, M. T., WIEMELS, J. L., LEUNG, K., BUFFLER, P. A. & WIENCKE, J. K. 2004. Hypermethylation of the 5' CpG island of the FHIT gene is associated with hyperdiploid and translocation-negative subtypes of pediatric leukemia. *Cancer Res,* 64**,** 2000-6.

ZHOU, A. Y., SHEN, R. R., KIM, E., LOCK, Y. J., XU, M., CHEN, Z. J. & HAHN, W. C. 2013. IKKepsilon-mediated tumorigenesis requires K63-linked polyubiquitination by a cIAP1/cIAP2/TRAF2 E3 ubiquitin ligase complex. *Cell Rep,* 3**,** 724-33.

ZHU, J. & EMERSON, S. G. 2002. Hematopoietic cytokines, transcription factors and lineage commitment. *Oncogene,* 21**,** 3295-313.

ZONG, W. X. & THOMPSON, C. B. 2006. Necrotic death as a cell fate. *Genes Dev,* 20**,** 1-15.

Christiana Savva

Appendix I: Experimental Data

Christiana Savva

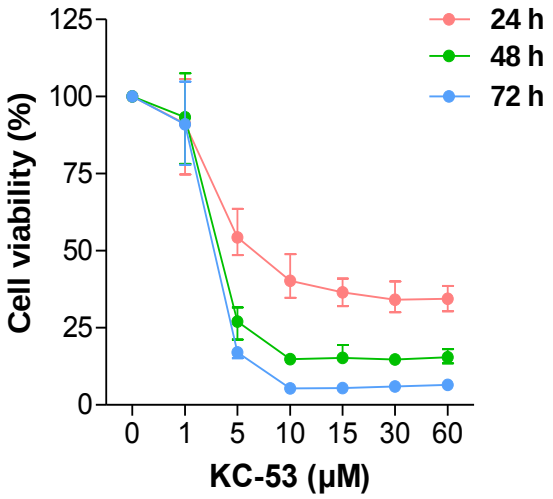

Figure S1. KC-53 inhibits Jurkat cell proliferation in a dose- and time- dependent manner. Cells were treated with increasing concentrations of KC-53 for the times indicated. Cell viability was determined by the MTT assay and is expressed as percentage of survival in untreated cells.

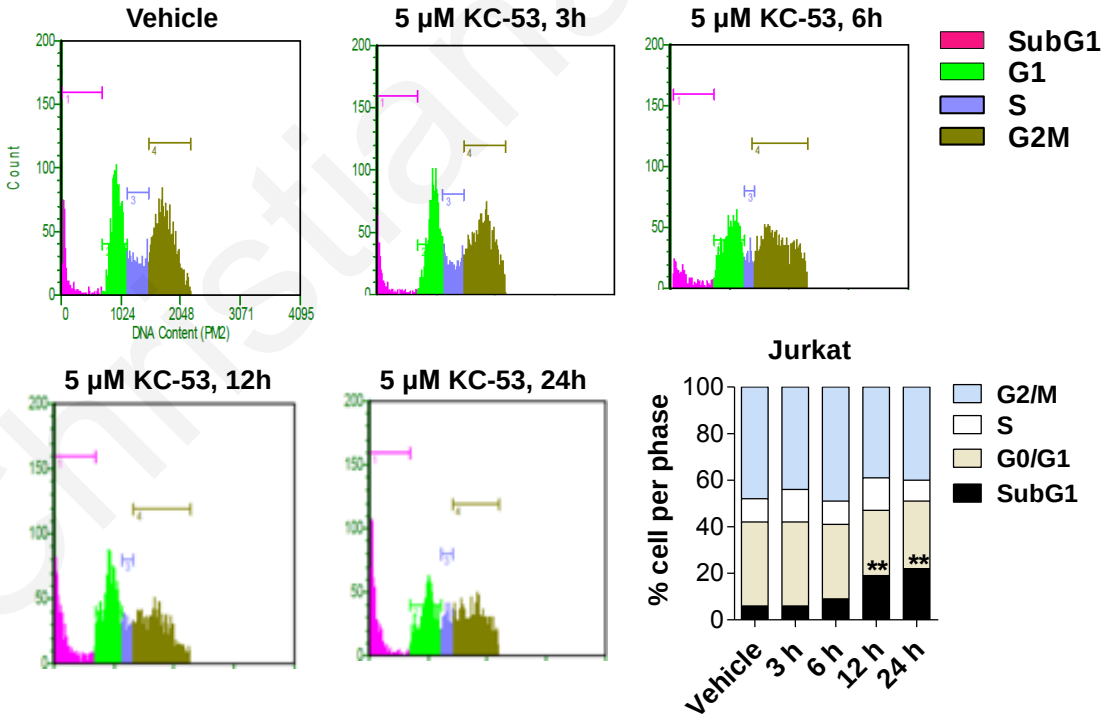

Figure S2. KC-53 increases SubG1 fraction without affecting cell cycle progression in Jurkat cells. Cells were treated with 0 or 5 µM KC-53 for 0-24 h prior to cell cycle analysis. The treatments were performed in duplicate and represent the mean ±SEM of three different experiments. (**p value < 0.01)

Cristiana Sava

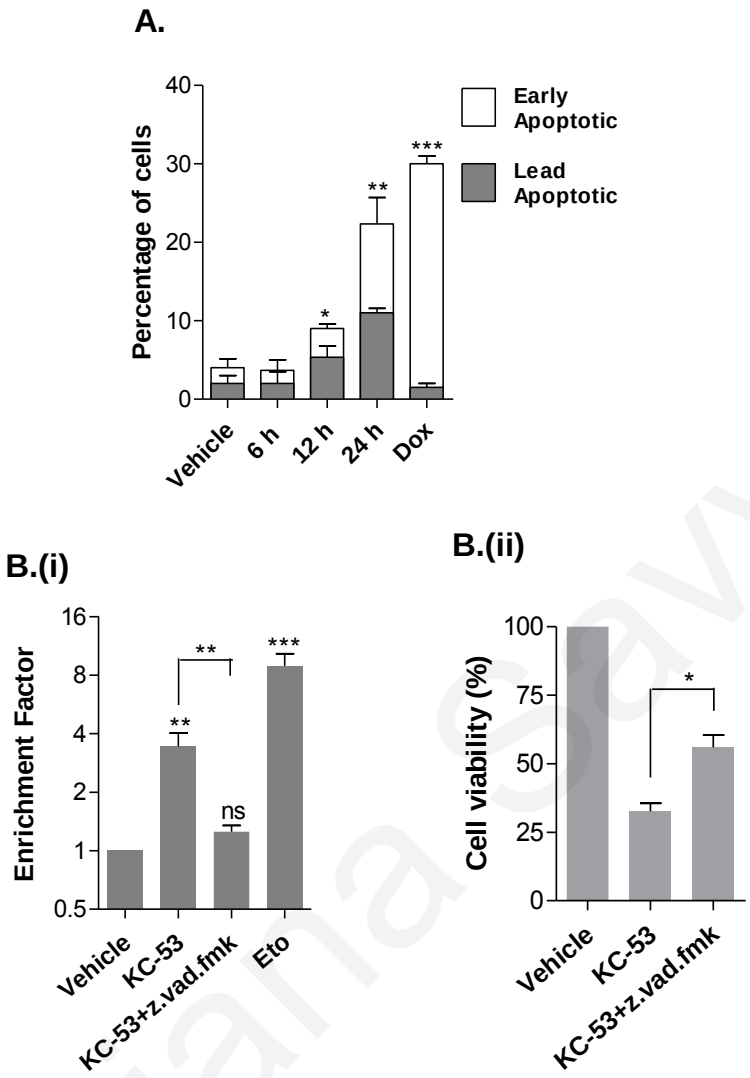

Figure S3. KC-53 induces apoptosis in Jurkat cells. (A) Cells were treated with vehicle control or 5 μM KC-53 for the indicated time points and apoptosis was assessed with Annexin-V/PI staining. Statistical significance was evaluated by comparing each cell population of the treated samples with the corresponding population of the vehicle control. Doxorubicin (Dox) at 0.5 μM was used as positive control. **(B) (i)** Cells were treated with vehicle control or 5 μM KC-53 in the presence or absence of 20 μM z.vad.fmk for 24 h. The presence of nucleosomes in the cytoplasm was determined with ELISA cell death detection kit and in expressed as Enrichment Factor. Etoposide (Eto) at 5 μM concentration was used as positive control **(ii)** Cells were treated with vehicle control or 5 μM KC-53 in the presence or absence of 20 μM z.vad.fmk as shown for 24 h. Cell viability was assessed with the MTT assay. The results represent the mean ±SEM of two different replicates and are representative of at least three independent experiments. (*p value < 0.05, **p value < 0.01, ***p value < 0.001)

Cristiana Gavva

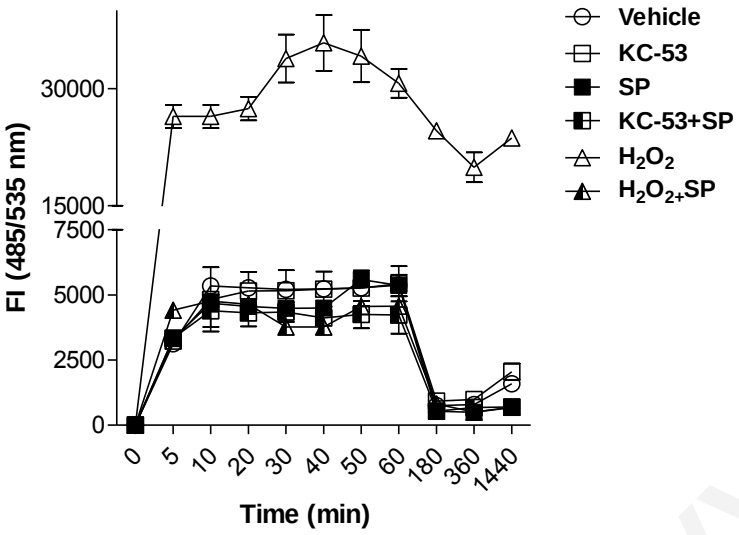

Figure S4. KC-53 does not promote the generation of ROS in Jurkat cells. Cells were treated with vehicle control or 5 µM of KC-53 in the presence or absence of 1 mM Sodium Pyruvate (SP) for the indicated time points. Cells were also treated with 100 µM Hydrogen Peroxide (H_2O_2) in the presence or absence of 1 mM SP as controls. ROS production was determined with the DCFH-DA assay. The treatments were performed in duplicate and represent the mean ±SEM of three independent experiments.

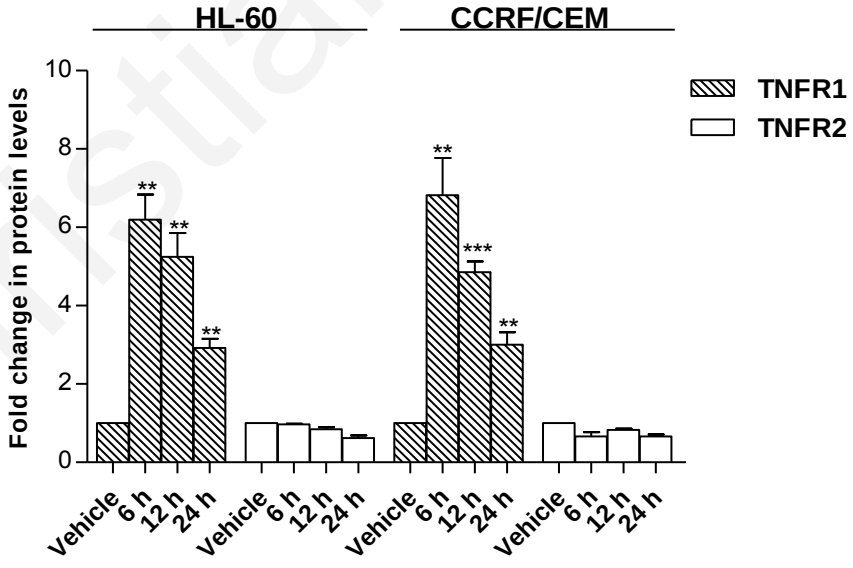

Figure S5. Representative densitometric analysis of the protein expression of membrane TNFRs in HL-60 and CCRF/CEM cells. Cells were treated as described in Figure 11A. Asterisks indicate significant increase above the value obtained in vehicle controls. (**p value < 0.01, ***p value < 0.001)

Christiana Saiva

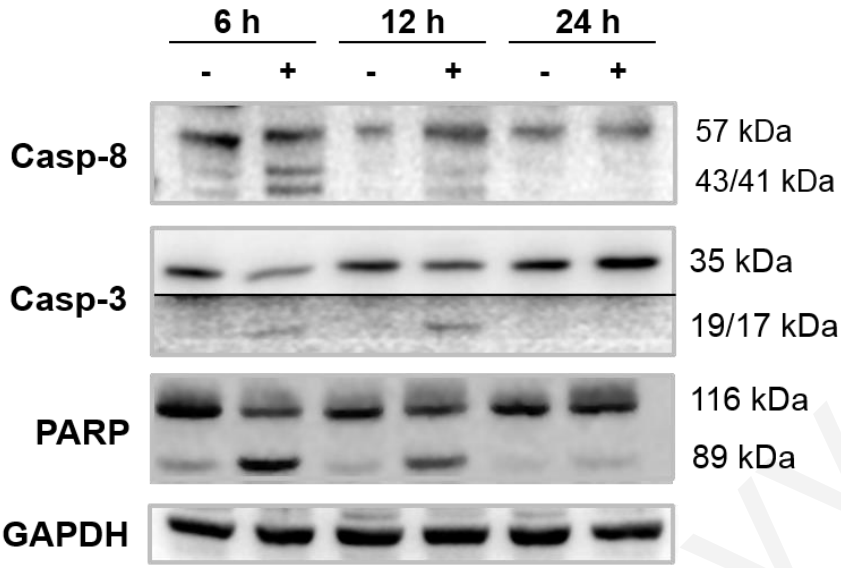

Figure S6. KC-53 induces Caspases activation and PARP1 inactivation in Jurkat cells. Cells were treated with vehicle control or 5 μM KC-53 for 6 up to 24 h and cell protein lysates were run by SDS–PAGE and immunoblotted with the indicated antibodies. The results are representative of at least three independent experiments.

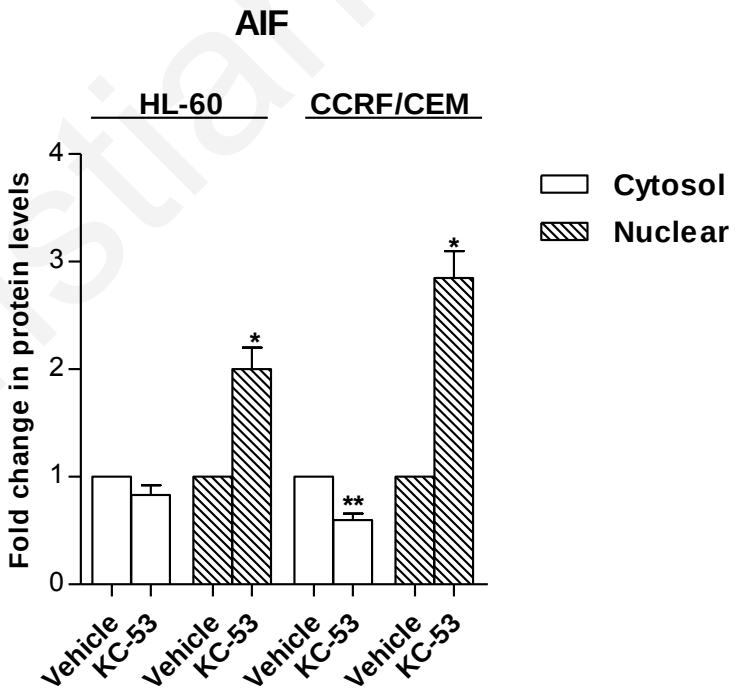

Figure S7. Representative densitometric analysis of the protein expression of AIF in HL-60 and CCRF/CEM cells. Cells were treated as described in Figure 13(ii). Asterisks indicate significant increase above or decrease below the value obtained in vehicle controls. (*p value < 0.05, **p value < 0.01)

Christiana Savva

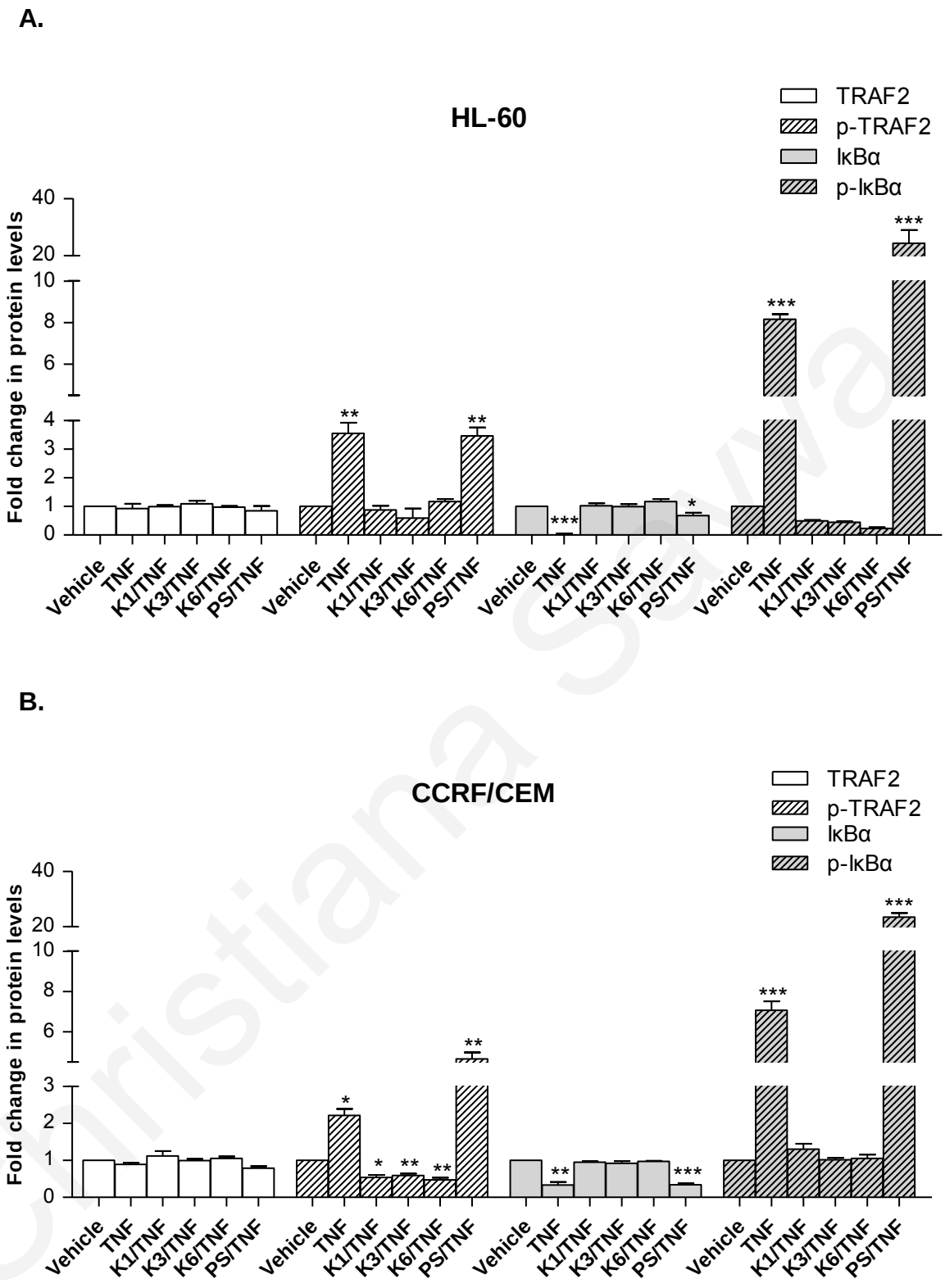

Figure S8. Representative densitometric analysis of the protein expression of total and phosphorylated TRAF2 and IκBα. (A) HL-60 and **(B)** CCRF/CEM cells were treated as described in Figure 15. Asterisks indicate significant increase above or decrease below the value obtained in vehicle controls. (*p value < 0.05, **p value < 0.01, ***p value < 0.001)

Cristiana Sousa

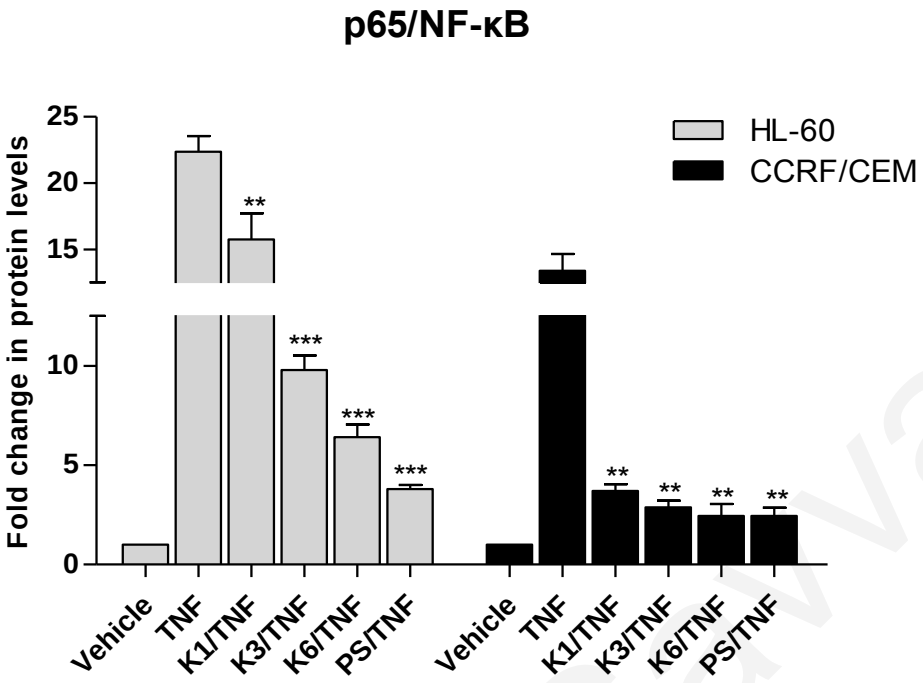

Figure S9. Representative densitometric analysis of the protein expression of nuclear p65. HL-60 and CCRF/CEM cells were treated as described in Figure 16A. Asterisks indicate significant decrease below the value obtained in TNFα-treated croups. (**p value < 0.01, ***p value < 0.001)

Christiana Saliva

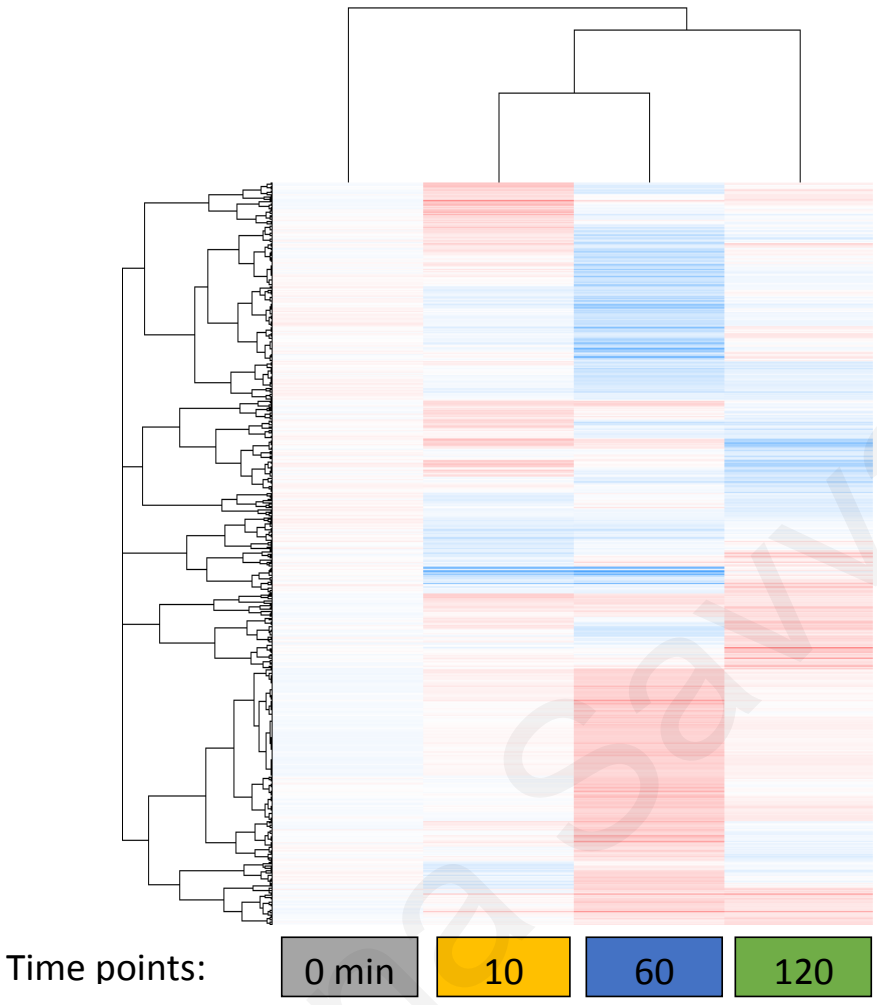

Figure S10. Heatmap of modulated proteins of KC-53 treated cells. HL-60 cells were treated with 5 µM KC-53 for 0 up to 120 min. Following incubation, aliquots of cells containing 100 µg of total protein were processed to proteolysis with trypsin and Lys-C. The phosphoproteomic analysis was performed using multidimensional liquid chromatography (LC). The separated phosphopeptides were analyzed with nano-spray ionization based ultra high-resolution mass spectrometry (nESI FTMS). The results represent the mean ± 1SD of three replicates compare to vehicle control groups. Heat map colors indicate the log2ratio for each protein expression (red=highest and blue=lowest expression).

Christiana Saiva

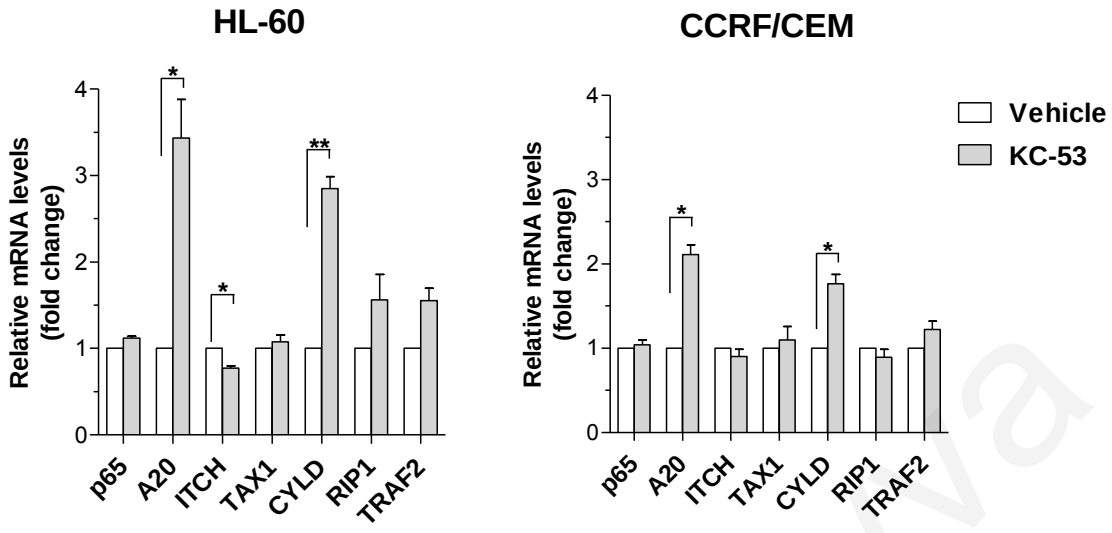

Figure S11. The effect of KC-53 on the expression of several negative regulators of the NF-κB pathway. HL-60 and CCRF/CEM cells were treated with vehicle or KC-53 (5 μM) for 6 h. The PCR products were normalized to those obtained from GAPDH mRNA amplification. The results represent the mean ± SEM of two different replicates and are representative of at least two independent experiments. (*p value < 0.05, **p value < 0.01)

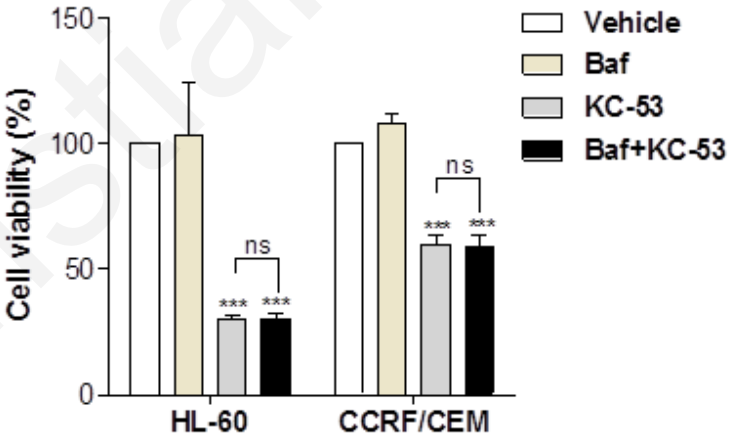

Figure S12. Bafilomycin does not prevent the antiproliferative effects of KC-53 in HL-60 and CCRF/CEM cells. Cells were subjected to either vehicle, Bafilomycin (Baf) (0.5 nM) for 1 h, KC-53 (5 μM) or Baf for 1 h prior to addition of KC-53 for 24 h. Cell viability determined by the MTT assay is expressed as percentage of survival in vehicle treated cells. The results represent the mean ±SEM of three replicates and are representative of three independent experiments. (***p value <0.001, ns; non-significant)

Christiana Sava

Appendix II: Publications

Christiana Savva

Savva et al. BMC Cancer (2016) 16:279
DOI 10.1186/s12885-016-2310-5

BMC Cancer

RESEARCH ARTICLE Open Access

Selective activation of TNFR1 and NF-κB inhibition by a novel biyouyanagin analogue promotes apoptosis in acute leukemia cells

Christiana G. Savva[1], Sotirios Totokotsopoulos[2], Kyriakos C. Nicolaou[2], Christiana M. Neophytou[1] and Andreas I. Constantinou[1*]

Abstract

Background: Acquired resistance towards apoptosis is a hallmark of cancer. Elimination of cells bearing activated oncogenes or stimulation of tumor suppressor mediators may provide a selection pressure to overcome resistance. KC-53 is a novel biyouyanagin analogue known to elicit strong anti-inflammatory and anti-viral activity. The current study was designed to evaluate the anticancer efficacy and molecular mechanisms of KC-53 against human cancer cells.

Methods: Using the MTT assay we examined initially how KC-53 affects the proliferation rates of thirteen representative human cancer cell lines in comparison to normal peripheral blood mononuclear cells (PBMCs) and immortalized cell lines. To decipher the key molecular events underlying its mode of action we selected the human promyelocytic leukemia HL-60 and the acute lymphocytic leukemia CCRF/CEM cell lines that were found to be the most sensitive to the antiproliferative effects of KC-53.

Results: KC-53 promoted rapidly and irreversibly apoptosis in both leukemia cell lines at relatively low concentrations. Apoptosis was characterized by an increase in membrane-associated TNFR1, activation of Caspase-8 and proteolytic inactivation of the death domain kinase RIP1 indicating that KC-53 induced mainly the extrinsic/death receptor apoptotic pathway. Regardless, induction of the intrinsic/mitochondrial pathway was also achieved by Caspase-8 processing of Bid, activation of Caspase-9 and increased translocation of AIF to the nucleus. FADD protein knockdown restored HL-60 and CCRF/CEM cell viability and completely blocked KC-53-induced apoptosis. Furthermore, KC-53 administration dramatically inhibited TNFα-induced serine phosphorylation on TRAF2 and on IκBα hindering therefore p65/NF-κB translocation to nucleus. Reduced transcriptional expression of pro-inflammatory and pro-survival p65 target genes, confirmed that the agent functionally inhibited the transcriptional activity of p65.

Conclusions: Our findings demonstrate, for the first time, the selective anticancer properties of KC-53 towards leukemic cell lines and provide a detailed understanding of the molecular events underlying its dual anti-proliferative and pro-apoptotic properties. These results provide new insights into the development of innovative and targeted therapies for the treatment of some forms of leukemia.

Keywords: Biyouyanagin, Leukemia, Death receptors, Tumor necrosis factor receptor 1, TNFR1, Nuclear factor κB, NF-κB, Apoptosis, Caspases

* Correspondence: andreasc@ucy.ac.cy
[1]Department of Biological Sciences, University of Cyprus, Kallipoleos 75, Nicosia 01678, Cyprus
Full list of author information is available at the end of the article

© 2016 Savva et al. **Open Access** This article is distributed under the terms of the Creative Commons Attribution 4.0 International License (http://creativecommons.org/licenses/by/4.0/), which permits unrestricted use, distribution, and reproduction in any medium, provided you give appropriate credit to the original author(s) and the source, provide a link to the Creative Commons license, and indicate if changes were made. The Creative Commons Public Domain Dedication waiver (http://creativecommons.org/publicdomain/zero/1.0/) applies to the data made available in this article, unless otherwise stated.

Background

Apoptosis deregulation occurs commonly in hematological malignancies and has been connected to cancer pathogenesis, progression and chemoresistance [1]. The two main effector cascades that are involved in apoptosis are the intrinsic (mitochondrial), and the extrinsic (death receptor) pathways [2]. Alterations affecting key molecules of these pathways such as Bcl-2, p53 and the nuclear factor κB (NF-κB) lead to accumulation of malignant cells. Among the latter, NF-κB promotes the transcription of genes encoding proteins involved in the suppression of cell death by both the intrinsic and the extrinsic pathway [3, 4]. Thus, elevation in NF-κB activity can increase cellular resistance to apoptosis.

The extrinsic pathway of apoptosis is initiated by engagement of cell surface receptors with specific ligands. The tumor necrosis factor receptor 1 (TNFR1) possesses important roles in many cellular responses. Once TNFR1 is stimulated by its ligand (TNFα), two complexes with opposing effects on cell fate can be formed: a pro-survival and a pro-apoptotic complex. In the presence of phosphorylated TNF receptor-associated factor 2 (TRAF2), pro-survival NF-κB activation dominates over pro-apoptotic Caspase-8 activation. TRAF2 phosphorylation, occurring on Ser 11, promotes receptor-interacting protein 1 (RIP1) ubiquitination, facilitating the recruitment and activation of the downstream IκB kinase complex (IKK). This leads to NF-κB activation [5, 6] and concurrently preventing RIP1 from interacting with Fas-associated death domain (FADD) protein and pro-caspase-8 [7, 8]. Under pro-apoptotic conditions, RIP1 dissociates from TRAF2 and binds to the FADD/Caspase-8 complex. Active Caspase-8 cleaves and inactivates RIP1 initiating the extrinsic pathway of apoptosis [9, 10].

Agents that trigger the extrinsic pathway are particularly intriguing, since nearly all anti-cancer drugs utilize the intrinsic pathway to induce apoptosis, and cells often become resistant by accumulating defects in this pathway (Reviewed in [11]). Consistent with this notion, deletions or mutations of *p53* [12, 13] or over-expression of *Bcl-2* [14, 15] and *NF-κB* [16] are common in acute myelocytic leukemia (AML) and acute lymphocytic leukemia (ALL) resulting in resistance to drugs that induce apoptosis through the intrinsic pathway. Consequently, the development of agents that trigger the extrinsic pathway of apoptosis is a promising approach for drug development against this disease [17–19].

Clinical trials aiming to evaluate the anticancer efficacy of TNF family members originated with the use of human TNFα mainly in advanced solid cancers [20, 21]. Recombinant human TNFα (rhTNFα) has been tested as a systemic treatment in several clinical trials and used as both a single agent and in combination with chemotherapeutics. Even though rhTNFα was proven as an effective anticancer agent in preclinical studies, these attempts were disappointing as clinical activity was rarely obtained; rhTNFα was unable to trigger apoptosis via TNFR1 unless the initial NF-κB pathway was blocked [22]. In addition, rhTNFα was highly cytotoxic towards hepatocytes causing severe side effects and lacked of evidence for therapeutic benefit [20]. Subsequently, for the development of rational death receptor-targeted therapy it is important to discover agents able to activate the death receptors without triggering the NF-κB cascade.

Biyouyanagins are sesquiterpene spiro-lactones isolated from the plant *Hypericum chinense* with selective anti-virus and anti-inflammatory properties [23–26]. Our recent research around the molecular space of biyouyanagins structure revealed a new promising lead molecule; the post-photocycloaddition modified analogue 53 (Fig. 1a) [26]. Specifically, in THP-1 human macrophage cells, KC-53 inhibited the production and secretion of cytokines IL-6, IL-1β, and TNFα without affecting the production of cytokines IL-1α no 1β and IL-8 [26].

Since KC-53 was found to possess anti-inflammatory properties, and taking into consideration the key role of NF-κB in the inflammatory response, we postulated that, KC-53 may exhibit anticancer effects mediated through its interference with the TNFR1/NF-κB pathway. Our results show that among 13 cell lines tested, HL-60 (*p53*−/−) and CCRF/CEM (*p53*mut) are especially susceptible to the KC-53 pro-apoptotic effects due to, predominantly, activation of TNFR1 and the concomitant inhibition of p65/NF-κB translocation to the nucleus. The properties of KC-53, unveiled here, are consistent with those of a promising targeted therapeutic that could be especially effective in the treatment of some forms of leukemia that do not respond to drugs inducing only the intrinsic pathway of apoptosis.

Methods

Synthesis of KC-53

KC-53 was prepared by K.C. Nicolaou laboratory as previously described [26].

Chemicals and reagents

FBS, Horse Serum, antibiotic/antimycotic, EGF, insulin, Cholera Toxin, Hydrocortizone, L-Glutamine, HEPES, Sodium Pyruvate and media used in cell culture were purchased from Gibco, Invitrogen (Carlsbad, California). Etoposide and Doxorubicin were purchased from Tocris (Bristol, UK). The pan caspase inhibitor z.vad.fmk was purchased from Sigma (St. Louis, Missouri). TNFα, and PS-341 (Bortezomib) were purchased from Merck Millipore (Darmstadt, Germany). Protease inhibitor cocktail was obtained from Roche (Indianapolis, IN).

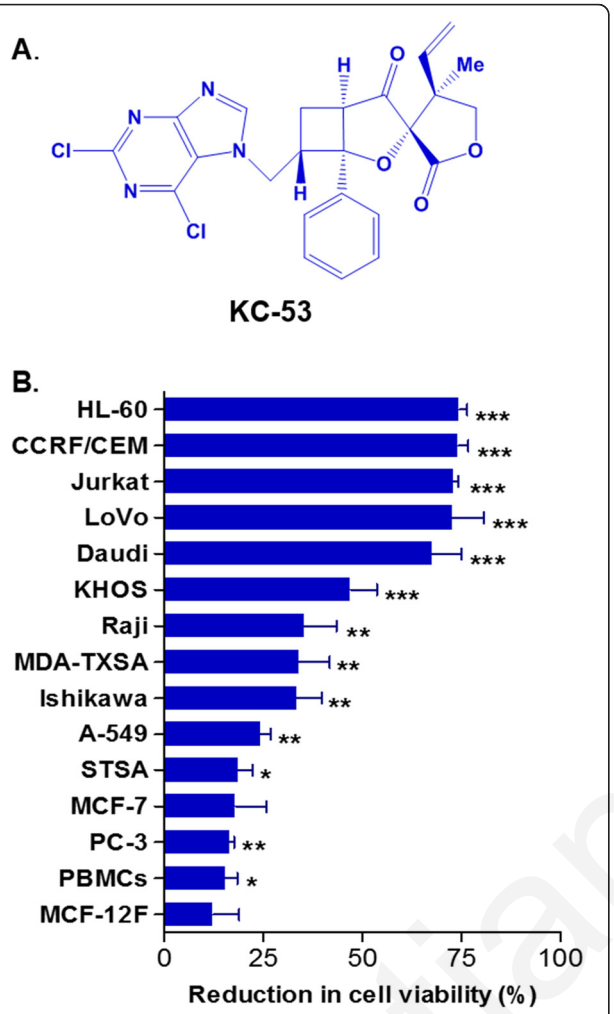

Fig. 1 KC-53 chemical structure and its antiproliferative effects on a panel of cell lines and PBMCs. **a** Chemical structure of KC-53 molecule. **b** Cells were exposed to 5 μM of KC-53 for 48 h and cell survival was determined using the MTT assay. Cell viability is expressed as percentage of survival in vehicle treated cells. The results represent the mean ± SEM of three replicates and are representative of three different experiments. (*p value <0.05, **p value <0.01, ***p value <0.001)

Caspase −3, −7, −8, −9, PARP1, RIP1, Bid, TNFR1, TNFR2, AIF, FADD, p-IκBα, p-TRAF2, p65/NF-κB and α-Tubulin antibodies were purchased from Cell Signaling Technology (Danvers, Massachusetts). Total TRAF2, total IκBα, Histone H3, EGFR, and GAPDH antibodies were obtained from Santa Cruz Biotechnology (Heidelberg, Germany). All other reagents were purchased from Sigma (St. Louis, Missouri).

Cell culture

MCF-7, MDA-MB-231-TXSA, STSA, LoVo, Ishikawa and KHOS cells were cultured in DMEM supplemented with 10 % FBS, 1 % antibiotic/antimycotic and 4 mM L-Glutamine, PC-3, A-549, Jurkat, HL-60, CCRF/CEM, Raji and Daudi in RPMI supplemented with 10 % FBS, 1 % antibiotic/antimycotic and 4 mM L-Glutamine, and MCF-12F in DMEMF12 supplemented with 20 ng/mL EGF, 100 ng/mL Cholera Toxin, 500 ng/mL Hydrocortizone, 10 μg/mL insulin, 5 % Horse Serum and 1 % antibiotic/antimycotic. All cell lines were obtained from the American Type Culture Collection (ATCC) (Manassas, VA).

Isolation of Peripheral Blood Mononuclear Cells (PBMCs)

Human normal PBMCs were isolated from heparinised venous blood samples by density gradient centrifugation method using Ficol-Histopaque (Sigma, St. Louis, Missouri). Briefly, the heparinised blood was layered on Histopaque in the ratio of 1:1 and subjected to centrifugation at 2,000 rpm for 30 min. The white layer representing PBMCs was aspirated out and transferred into sterile centrifuge tubes. The suspension of cells was then washed twice and cultured in RPMI supplemented with 10 % FBS, 1 % antibiotic/antimycotic and 4 mM L-Glutamine. After 24 h incubation at 37 °C non adherent cells (B- and T-cells) were collected for use in the experiments. Written informed consent was obtained from the donors of PBMCs and ethical approval was obtained from the Cyprus National Bioethics Committee in accordance with the Declaration of Helsinki.

Proliferation assay

A total of 1×10^4 cells were seeded per well of a 96-well plate in medium supplemented with the different concentrations of KC-53 or vehicle control, for the time periods described in the figure legends. At the end of each incubation period, MTT at a final concentration of 0.5 mg/mL was added to the medium and left to be metabolized for 3 h. Following that, plates were centrifuged at 1,500 rpm for 5 min. The medium was removed and DMSO was added in each well and incubated with gently shaking for 20 min. The absorbance measured at 570 nm, was proportional to the number of viable cells per well.

Cell cycle analysis

Cells were added at a concentration of 1×10^6 cells per a 100 mm plate and treated with KC-53 for indicated times at 37 °C. Following incubation, samples were harvested by centrifugation at 1,500 rpm for 5 min at 4 °C and washed with PBS. Cells were fixed with 70 % ethanol and stained with propidium iodide (PI) staining solution (0.2 mg/mL RNase A, 0.01 mg/mL PI). Samples were analyzed for DNA content using the Guava EasyCyte™ flow cytometer and the GuavaSoft analysis software (Millipore, Watford, UK).

Annexin-V/PI staining

Cells were seeded at a concentration of 1×10^5 cells per a 60 mm plate and treated with KC-53 or Doxorubicin (Dox) as indicated. Cells were harvested and stained using Annexin-V Alexa Fluor® 488/PI, as described by the Tali™ apoptosis kit (Life Technologies, Carlsbad, CA). Cell viability, death and apoptosis were evaluated using the Tali™ Image-based Cytometer (Life Technologies, Carlsbad, CA). The Annexin-V positive/PI negative cells were recognized as early apoptotic cells by the cytometer software whereas the Annexin-V positive/PI positive cells were identified as late apoptotic/dead cells.

Cell death detection ELISA

Cells were added at a concentration of 1×10^4 cells per well of a 96-well plate and treated with KC-53 in the present or absence of pan-caspase inhibitor, z.vad.fmk as indicated. The quantification of mono- and oligo-nucleosomes present in the cytoplasm of apoptotic cells was performed using the Cell Death ElisaPLUS Apoptosis Kit according to the manufacturer's instructions (Roche, Indianapolis, IN). The specific Enrichment Factor of mono- and oligo-nucleosomes is expressed as absorbance of treated cells to absorbance of corresponding negative control.

Caspase-8 enzymatic activity

Caspase-8 activity was measured using fluorogenic substrate IETD-AFC (KHZ0052) according to the manufacturer's instructions (Invitrogen, California, USA). In brief, PBS-washed cell pellets were resuspended in Lysis buffer and incubated on ice for 10 min. Lysate was then centrifuged at 11,000 rpm for 5 min at 4 °C and supernatant-cytosolic fraction was collected. Substrate at 50 μM final concentration was added to 50 μg of cytosolic extract in each well of a 96-well plate followed by incubation for 1 h at 37 °C. Caspase activity was measured by monitoring the release of fluorigenic AFC using an auto-microplate reader (excitation 400 nm, emission 505 nm, slit width 15). Fold-increase in Caspase-8 activity was determined by direct comparison to the level of the uninduced control.

Preparation of nuclear and cytosolic extracts

A total of 2×10^7 cells were treated as indicated. After incubation, cells were harvested by centrifugation at 1,500 rpm for 5 min at 4 °C and washed with ice cold PBS. Cells were resuspended in ice cold Lysis buffer (10 mM HEPES, 1 mM EDTA, 60 mM KCl, 0.5 % (v/v) NP-40, 1 mM DTT, 1 mM PMSF, protease inhibitors, pH 7.9) and incubated at 4 °C for 10 min. Samples were then centrifuged at 12,000 g for 10 min at 4 °C and supernatant (cytosolic extract) was collected. Cytosolic fraction was further processed by centrifugation at 14,000 g, for 10 min at 4 °C. Supernatant was recollected and stored at −80 °C. Pellet was washed twice with Washing buffer (10 mM HEPES, 1 mM EDTA, 60 mM KCl, 1 mM DTT, 1 mM PMSF, protease inhibitors, pH 7.9) and Nuclear suspension buffer (250 mM Tris-Hydrochloride, 60 mM KCl, 1 mM DTT, 1 mM PMSF, protease inhibitors, pH 7.8) was added to each sample. Nucleus lysis was achieved by sonication (4 bursts, at amplitude 4, for 4 sec with 2 min cooling between bursts) with the use of an ultrasonic microprocessor and clarified by centrifugation at 10,000 g for 15 min at 4 °C. Supernatant (nuclear extract) was collected and stored at −80 °C.

Quantitative real-time reverse transcription PCR (RT-qPCR)

Total RNA was extracted with Trizol reagent (Invitrogen, Carlsbad, CA) following the manufacturer's protocol. cDNA was synthesized with random and oligo (dT) primers using the PrimeScript Reverse Transcriptase (TaKaRa Bio. Inc, Dalian, China). Primers were designed using Primer3 and are listed in Additional file 1. Real-Time PCR was performed using the BioRad CFX96 Real-Time System and the SYBR Green PCR Master Mix (Kapa Biosystems, Massachusetts) according to the manufacturer's instructions. The PCR products were normalized to those obtained from human GAPDH mRNA amplification.

RNA interference

FADD siRNA (sc-35352) and negative control siRNA (sc-37007) were purchased from Santa Cruz Biotechnology. For the transfection procedure, HL-60 and CCRF/CEM cells were seeded at a concentration of $4x10^5$/mL per well of a 12-well plate and FADD siRNA or control siRNA were transfected with the use of LipofetamineTM 2000 (Invitrogen, Carlsbad, CA) and siTransfection Reagent (Santa Cruz Biotechnology, Heidelberg, Germany) correspondingly according to the manufacturer's instructions. The final concentration of siRNA in each well was 100 nM.

Immunoblotting

Cells were treated as indicated and lysed with RIPA buffer (10 mM Tris-Cl (pH 8.0), 1 mM EDTA, 0.5 μM EGTA, 140 mM NaCl, 1 % Triton X-100, 0.1 % SDS, protease inhibior cocktail, phosphatase inhibitors; 5 mM NaF, 1 mM Na_3VO_4). For preparation of membrane and cytosolic extracts, the Subcellular Protein Fractionation Kit for Cultured Cells (PI-78840) was used according to the manufacturer's instructions (Thermo Scientific, Rockford) with slight modifications. The total protein concentration was determined using Bradford reagent. Protein lysates were separated by electrophoresis on a 8–12 % SDS-PAGE gels and

then electrophoretically transferred to PVDF membrane. Westerns blots were probed with the specific antibodies and protein bands were detected by enhcaned chemiluminescence. Anti-GAPDH, anti-Histone H3, anti-α-Tubulin and anti-EGFR monoclonal antibodies were used as loading controls. The intensity values from the densitometry analysis of Western blots were normalized against EGFR, α-Tubulin or Histone H3 using ImageJ analysis software (NIH). Intensity values were expressed as fold change compared to control.

Statistical analysis

Results for continuous variables were presented as Mean ±Standard Error. Two- group differences in continuous variables were assessed by the unpaired T-test. *P*-values are two-tailed with confidence intervals 95 %. Statistical analysis was performed by comparing treated samples with vehicle controls. All statistical tests were conducted using Prism software version 5.0 (Graphpad, San Diego, California).

Results

KC-53 inhibits the proliferation of human cancer cell lines

The effect of KC-53 on tumor cell viability was initially determined in a series of human cancer cell lines to identify those that are the most sensitive to the agent. Thus, we have determined the effects of KC-53 on the viability of human breast (MCF-7, MDA-MB-231-TXSA), lung (A-549), prostate (PC-3), colon (LoVo), endometrial (Ishikawa), osteosarcoma (KHOS), gastric (STSA), leukemia (Jurkat, HL-60, CRF/CEM) and lymphoma (Raji, Daudi) tumorigenic cells. PBMCs and "normal" immortalized MCF-12 F breast cells were used as control cell lines. The HL-60 (AML/APL) and CCRF/CEM (ALL) cell lines were the most sensitive as determined by the IC_{50} at 48 h (Table 1). Importantly, the normal PBMCs and the immortalized MCF-12 F cells were relatively resistant to the anti-proliferative effects of the compound (Fig. 1b). KC-53 reduced cancer cell viability in a dose-depended manner in all cell lines with a maximum effect on the most sensitive cell lines ranging from 5 to 10 μM (Additional file 2). The two most sensitive cell lines were selected to further investigate the anti-proliferative mechanism of KC-53.

KC-53 was found to reduce HL-60 and CCRF/CEM cell growth in a dose- and time- depended manner producing maximum reduction in cell viability at 10 μM in HL-60 and at 5 μM in CCRF/CEM (Fig. 2a). It became apparent from these growth response curves that the effect of the agent was almost immediate. To follow-up on this observation, we examined the possibility that the effects of KC-53 were irreversible. Towards this objective, we exposed the cells to KC-53 for 1, 3, 6 and 12 h followed by a post-treatment recovery period in agent-free medium for 48 h. In both cell lines viability was only partially restored when KC-53 was removed after 1 or 3 h of treatment (Fig. 2b). Treatments for 6 and 12 h produced a similar effect to that of continuous exposure. Thus, after 6 h of treatment the compound produced an irreversible inhibition of cell growth. The observed growth inhibitory effect of KC-53 in leukemic cells was not accompanied by any significant changes in the distribution of cell cycle phases as determined by flow cytometry (Fig. 2c). However, after 12 and 24 h of treatment there was an increase in Sub-G1 phase, indicative of apoptosis.

Table 1 IC_{50} values of KC-53 in vitro antiproliferative activity in human cell lines

Cell Line	IC_{50} (μM)
HL-60	2.3 ± 1.0
CCRF/CEM	2.4 ± 1.0
LoVo	2.5 ± 1.6
Jurkat	3.4 ± 1.7
Daudi	3.8 ± 1.9
KHOS	5.0 ± 2.0
MDA-MB-231-TXSA	8.0 ± 3.5
STSA	15.4 ± 5.2
MCF-12 F	15.5 ± 5.5
MCF-7	16.0 ± 3.5
Raji	16.3 ± 6.1
A549	19.1 ± 10
Ishikawa	21.1 ± 10
PC-3	33.6 ± 9.7
PBMCs	>60

Cells were incubated with increasing concentrations of KC-53 (0–60 μM) for 48 h. The IC_{50} values were calculated from MTT viability curves. The data are expressed as the mean ± SD of three independent experiments performed in triplicate

KC-53 induces apoptosis in HL-60 and CCRF/CEM cells

The possible induction of apoptosis by KC-53 was initially evaluated with the use of Annexin-V-FITC/PI assay. As indicated in Fig. 3a, within 12 h of treatment there was a significant increase in the early apoptotic fraction of both cell lines. After 24 h of treatment, 26.5 % of HL-60 and 27.5 % of CCRF/CEM cells were characterized as early apoptotic whereas, 15 % of cells from both cell lines were in the late apoptotic stage.

Apoptotic induction was further analyzed by the ELISA cell death kit which enables the detection of mono- and oligo-released nucleosomes in the cytosol. KC-53 induced substantial DNA fragmentation in HL-60 cells (7.4 fold increase compared to the control) and in CCRF/CEM cells (6.4 fold increase compared to the control) (Fig. 3b (i)). In the presence of the pan caspase

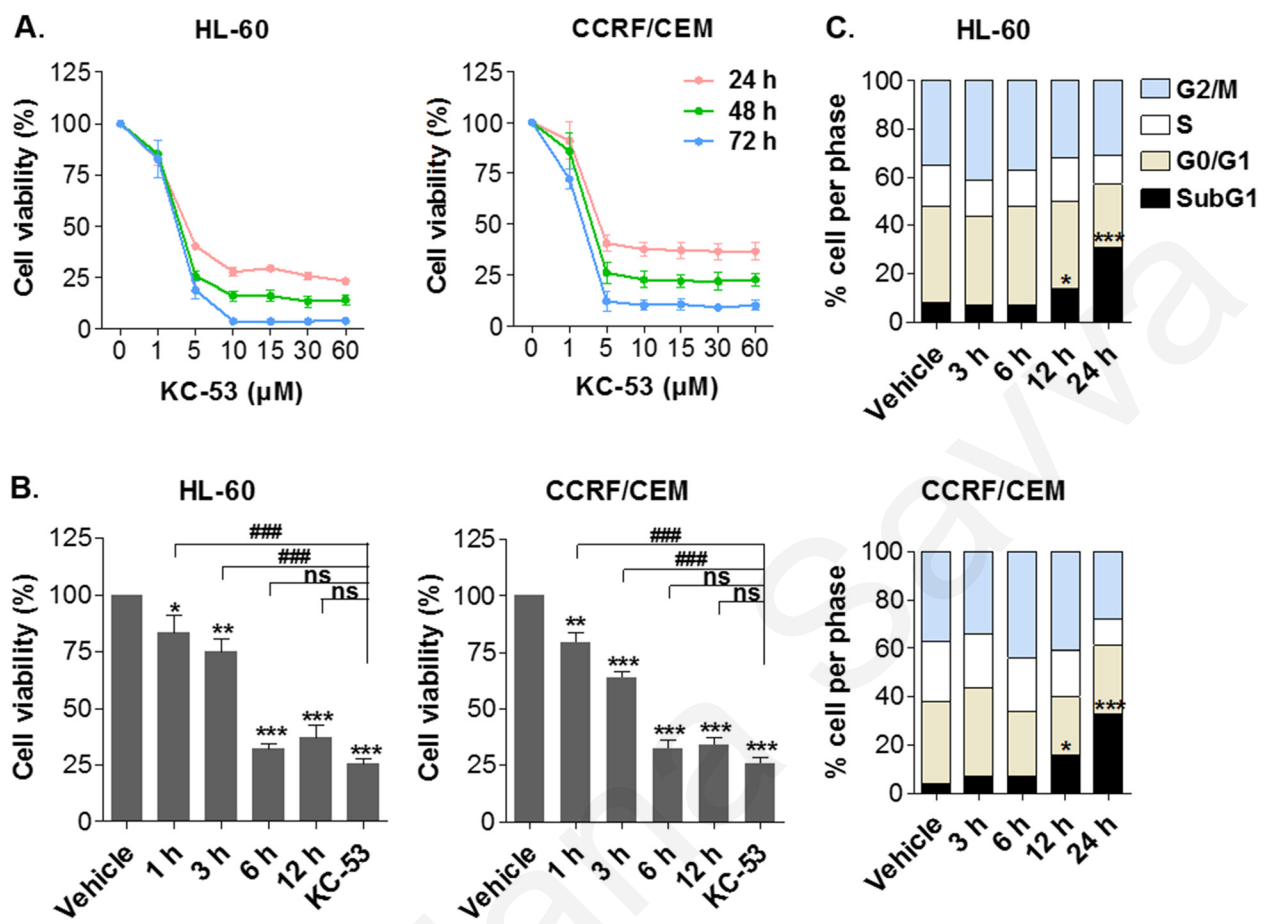

Fig. 2 Effects of KC-53 on leukemic cellular proliferation and cell cycle progression. **a** Cells were treated with increasing concentrations of KC-53 for the times indicated. Cell viability determined by the MTT assay, is expressed as percentage of survival in comparison to vehicle treated controls. **b** Cells were exposed to 0 or 5 μM of KC-53 followed by removal of the agent after 1, 3, 6 or 12 h incubation and cell viability was determined after 48 h recovery in drug-free medium. A positive control, where KC-53 was not removed, is shown for comparison. **c** Cells were treated with 0 or 5 μM KC-53 for the times indicated and cell cycle was assessed by FACS analysis. The results represent the mean ± SEM of three replicates and are representative of three different experiments. (*p value <0.05, **p value <0.01, ***p value <0.001, ###p value <0.001)

inhibitor, z.vad.fmk, DNA fragmentation was significantly reduced in HL-60 cells and it was fully abolished in CCRF/CEM cells. These data suggest that activation of caspase cascades is predominantly involved in KC-53-induced apoptosis. DNA analysis was also performed with the Comet Assay where KC-53-induced DNA damage was evident within 9 h of treatment (Additional file 3) and was exclusively attributed to apoptosis as no cellular ROS production was detected (Additional file 4).

Even though co-incubation of KC-53 with z.vad.fmk restored DNA fragmentation, it did not fully restore the viability of cells (Fig. 3b (ii)). HL-60 viability increased from 43 to 60 % in the presence of z.vad.fmk while no alterations were observed in the viability of CCRF/CEM. These findings indicate that inhibition of cell proliferation by KC-53 might be mediated by both caspase -dependent (CD) and -independent (CID) programmed cell death in a cell-context-specific manner.

KC-53 promotes apoptosis through activation of the TNFR1 signaling pathway

To fully characterize the apoptotic pathway being induced by KC-53, we monitored the potential activation of caspases and any changes in the membrane death receptor levels. In both HL-60 and CCRF/CEM cell lines an increase in membrane-associated TNFR1 was evident with KC-53 treatment for 6 up to 24 h (Fig. 4a). The corresponding protein levels of TNFR2 were not significantly affected by the treatment (Fig. 4a). The levels of death receptors FAS, DR3 and DR5, decoy receptor DcR3 as well as those of adaptor proteins FADD and TRADD remained relatively unaffected (Additional file 5).

The increase in TNFR1 levels was accompanied by strong activation and detection of the cleaved 43/41 kDa forms of Caspase-8 (C-Casp8) and proteolytic inactivation of RIP1 (C-RIP1) (Fig. 4b (i)) indicating that the

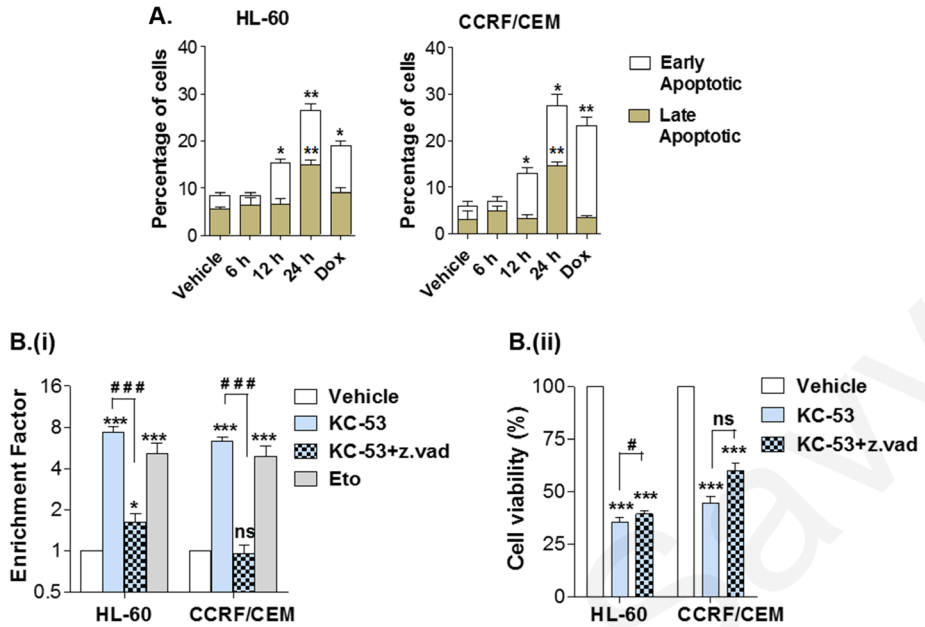

Fig. 3 Effects of KC-53 on cell apoptosis and DNA integrity. **a** Cells were treated with 0 or 5 μM KC-53 for the indicated time points and apoptosis was assessed with Annexin-V/PI staining. Statistical significance was determined by comparing treated samples with the corresponding population of the vehicle control. For comparison, Doxorubicin (Dox) at 0.5 μM was used as positive control. **b** (**i**) Cells were treated with 0 or 5 μM KC-53 in the presence or absence of 20 μM z.vad.fmk for 24 h. The presence of nucleosomes in the cytoplasm was determined with the ELISA cell death detection kit and is expressed as Enrichment Factor. Etoposide (Eto) at 5 μM was used as positive control. (**ii**) Cells were treated with vehicle control or 5 μM KC-53 in the presence or absence of 20 μM z.vad.fmk, as shown, for 24 h. Cell viability was assessed with the MTT assay. The results represent the mean ± SEM of two replicates and are representative of three independent experiments. (*p value <0.05, **p value <0.01, ***p value <0.001, #p value <0.05, ###p value <0.001)

extrinsic pathway of apoptosis is triggered. The crosstalk between the extrinsic and the intrinsic pathways is well established and occurs though Caspase-8 cleavage and activation of the pro-apoptotic protein Bid [27, 28]. To investigate this scenario we determined the expression levels of cleaved/truncated Bid (tBid). KC-53 administration resulted in the detection of the 15 kDa tBid fragment in both cell lines (Fig. 4b (i)). The cleavage of Bid occurred in the early stage of apoptosis (6 h) parallel with Caspase-8 activation. In both cell lines the amount of the 15 kDa peptide was constant during the time course of apoptosis and became undetectable after 24 h, possibly due to further degradation.

Caspase-8 enzymatic activity was verified with the use of fluorometric protease assay kit, in the presence or absence of z.vad.fmk. KC-53 produced a significant increase of Caspase-8 activity within 4 h of treatment. Specifically, after 12 h there was a 6.6 fold increase of Caspase-8 activity in HL-60 cells and an 8 fold increase in CCRF/CEM cells (Fig. 4b (ii)). The effects of KC-53 on Caspase-8 activity were fully reversed by z.vad.fmk in both cell lines.

To further evaluate the apoptotic effect of KC-53, we monitored the expression of the executor Caspases, −3 and −7 and their substrate PARP1. KC-53 markedly increased the active, cleaved forms of Caspases −3 (C-Casp3; 19/17 kDa) and −7 (C-Casp7; 20 kDa), which was evident within 6 h of treatment and persisted for 24 h post-treatment (Fig. 4c (i)). Caspase activation was accompanied by a decrease in the levels of the full length 116 kDa PARP1 and appearance of the cleaved 89 kDa form (C-PARP1) (Fig. 4c (i)). Similarly, KC-53 induced activation of the initiator Caspase-9 (C-Casp9; 37/35 kDa) (Fig. 4c (i)) and translocation of apoptosis inducing factor, AIF from the cytosol to the nucleus (Fig. 4c (ii)). In HL-60 cells, the nuclear levels of AIF increased up to two fold and in CCRF/CEM up to 2.8 fold following 6 h of treatment (Fig. 4c (ii)). Both Caspase-9 activation and AIF release are characteristics of mitochondrial outer membrane permeabilization (MOMP) apparently induced by tBid. These findings support the involvement of mitochondrial-mediated intrinsic pathway in the induction of apoptosis by KC-53. Furthermore, as AIF is a mediator of CID apoptotic mechanisms, these data provide further support to our previous observation (Fig. 3b (ii)) regarding the possible involvement of CID mechanisms by KC-53 action.

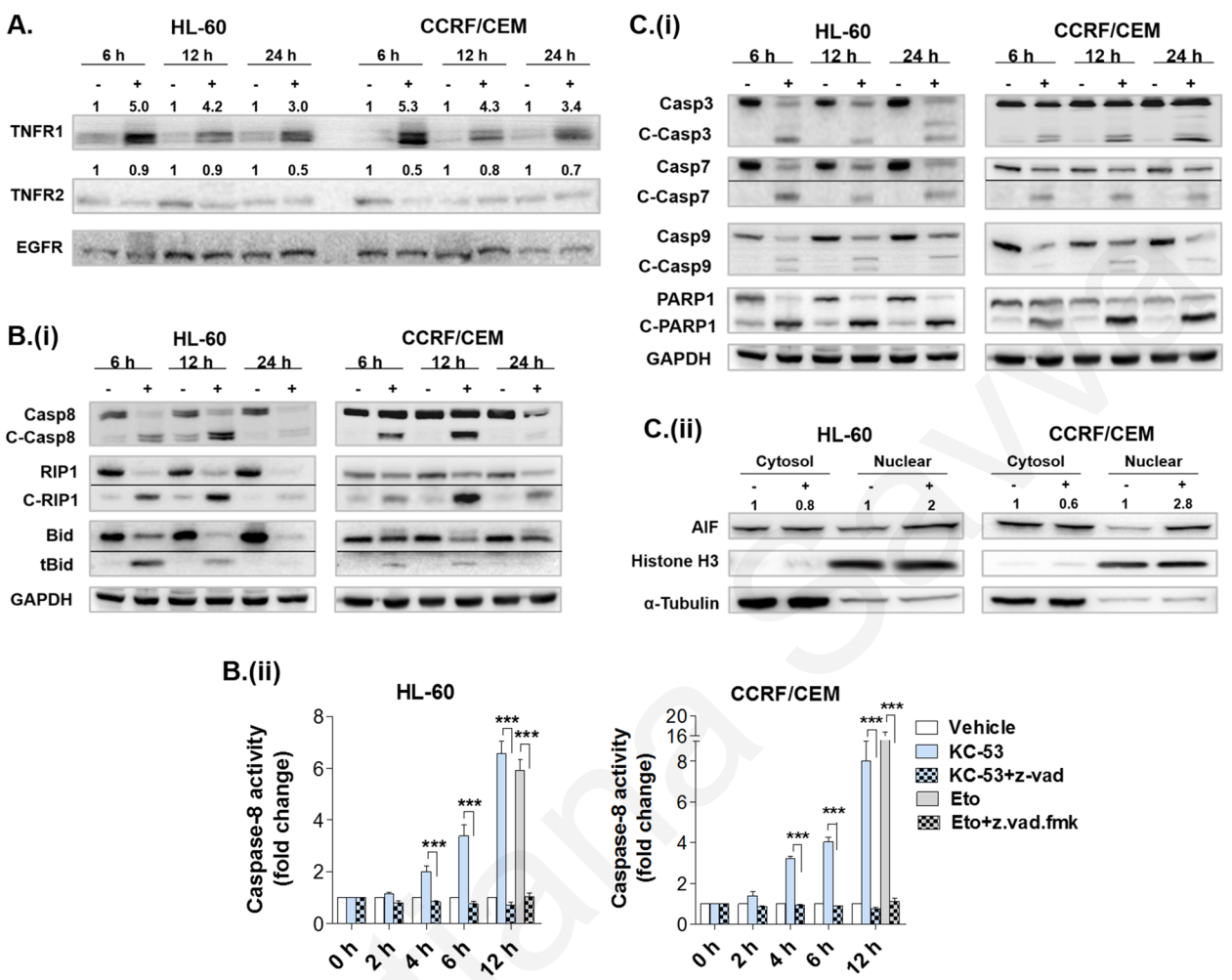

Fig. 4 Effects of KC-53 on Caspases and regulatory molecules of the apoptotic pathways in leukemia cells. **a** Cells were treated with 0 or 5 μM KC-53 for the indicated time points. TNFRs membrane expression levels were analyzed by immunoblotting. EGFR was used as a loading control and the TNFRs levels were quantified and normalized in comparison to the EGFR levels. **b** (**i**) Cells were treated with 0 or 5 μM KC-53 for the indicated time points. (**ii**) Cells were treated with 0 or 5 μM KC-53 in the presence or absence of 20 μM z.vad.fmk. Caspase-8 enzymatic activity was determined as described in Methods. Etoposide (Eto) added at 5 μM was used as a positive control. **c** (**i**) Cells were treated with 0 or 5 μM KC-53 for the indicated time points followed by immunoblotting. (**ii**) Cells were incubated with 0 or 5 μM KC-53 for 6 h and cytosolic and nuclear protein extracts were prepared. The numbers on top of each band represent intensity values and are expressed as fold change in comparison to the control. The results in panels **a**, **b** (**i**) and **c** are representative of three repetitions. The results in **b** (**ii**) panels represent the mean ± SEM of two replicates and are representative of three independent experiments. (***p value <0.001)

KC-53 inhibits the activation of IκBα and the translocation of p65/NF-κB to the nucleus

TRAF2 is required for the assembly of kinases regulating the phosphorylation and degradation of the NF-κB inhibitor, IκBα. We therefore investigated whether KC-53 treatment can affect the downstream molecular events of the TNFR1/NF-κB signalling as well as NF-κB translocation to the nucleus. This was evaluated by monitoring the phosphorylation status and protein levels of TRAF2 and IκBα following induction by TNFα in the absence or presence of KC-53.

We found that TNFα increased the phosphorylation levels of TRAF2 (Ser11) by 3.5 fold in HL-60 cells and by 2.2 fold in CCRF/CEM cells (compared to the control levels) while KC-53 fully attenuated these effects (Fig. 5a). Furthermore, in both cell lines, pretreatment with KC-53 fully abolished the TNFα-induced phosphorylation of IκBα on Ser32/36 without affecting the overall IκBα levels (Fig. 5a). Nuclear extraction and immunoblotting against the p65 subunit of NF-κB showed a time-depended decrease in the TNFα-induced nuclear translocation of p65 in response to KC-53 in both cell lines (Fig. 5b). An impressive 71 % and 82 % decrease in the p65 nuclear levels in HL-60 and CCRF/CEM cells was noted respectively, after 6 h of treatment, apparently due to decreased translocation. The above findings, clearly show that KC-53

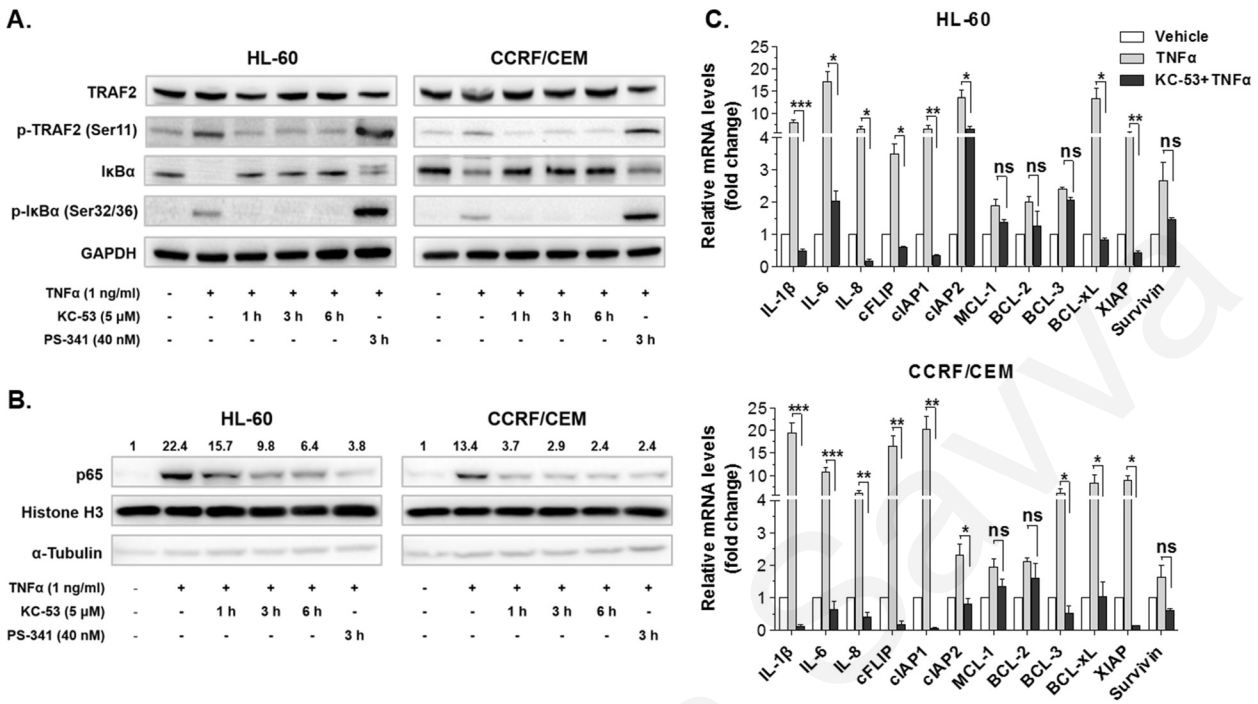

Fig. 5 Effects of KC-53 on TRAF2 and IκBα phosphorylation, and p65 translocation to the nucleus. **a** Cells were incubated with vehicle, KC-53 or PS-341 (for the times indicated) followed by incubation with TNFα for 20 min. Whole cell extracts were analyzed by immunoblotting. **b** Cells were incubated to either vehicle, KC-53 or PS-34 as indicated followed by the addition of TNFα for 20 min. The nuclear localization of p65 was examined by immunoblotting. Histone H3 levels were determined as a loading control and the α-Tubulin levels as an indicator of cytosolic contamination. Numbers signifies intensity values and are expressed as fold change compared to the control. **c** Cells were subjected to treatments either with the vehicle or TNFα (1 ng/ml) for 4 h, or KC-53 (5 μM) for 6 h plus TNFα for 4 h. The PCR products were normalized to those obtained from GAPDH mRNA amplification. The results in panels (**a**) and (**b**) are representative of three repetitions. The results in (**c**) panels represent the mean ± SEM of two replicates and are representative of three independent experiments. (*p value <0.05, **p value <0.01, ***p value <0.001)

stabilizes the p65/IκBα complex by inhibiting TNFα-induced phosphorylation on TRAF2 and IκBα, preventing in this manner p65 translocation to the nucleus.

The efficiency of KC-53 in inhibiting TRAF2 and IκBα phosphorylation and/or p65 translocation was also compared with the well-established proteasome inhibitor, Bortezomib (PS-341). As was expected, Bortezomib maintained the IκBα levels without abolishing the phosphorylation on Ser32/36 neither that of TRAF2 on Ser11 (Fig. 5a). Nonetheless Bortezomib reduced p65 nuclear levels by 83 % compared to the TNFα-treated samples (Fig. 5b). Thus, the effects of KC-53 on the nuclear levels of p65 are similar to those of Bortezomib although the mechanism by which this is achieved is different.

To further test the expectation that KC-53 hinders p65 transcriptional activity, we determined the mRNA levels of genes known to be transcriptionally activated by p65. We found that KC-53 robustly inhibited the TNFα-induced transcription of the pro-inflammatory cytokines; *IL -1β, −6 and −8* and the pro-survival mediators; *c-FLIP, cIAP-1, cIAP-2, BCL-xL* and *XIAP* whereas *BCL-2, MCL-1* and *Survivin* levels were not significantly affected (Fig. 5c). These results are consistent with the conclusion that KC-53 shifts the balance between the TNFR1-mediated pro-survival and pro-apoptotic signals in favour of the latter and thus, inhibits the activation of the NF-κB in HL-60 and CCRF/CEM cells. Therefore, the antiproliferative activity of KC-53 in leukemia cells might be also attributed in the inhibition of the NF-κB survival axis.

Silencing of FADD protects leukemic cells from KC-53 apoptotic effects

In order to investigate whether KC-53 apoptotic effects are directly linked to TNFR1 pro-apoptotic signaling axis we used siRNA for inhibiting the expression of FADD (Fig. 6a). It is known from previous reports that, FADD is a core protein of the pro-apoptotic complex facilitating Caspase-8 activation soon after TNFR1 activation thus, promoting apoptosis [29]. FADD silencing significantly restored cell viability by up to 78 and 90 % in HL-60 and CCRF/CEM respectively (Fig. 6b). These data suggest that downregulation of FADD confers resistance to KC-53 and that, the cytotoxic effects of the agent may be mediated through the formation of the pro-apoptotic complex. In agreement with this, in the absence of FADD, KC-53 was not able to activate

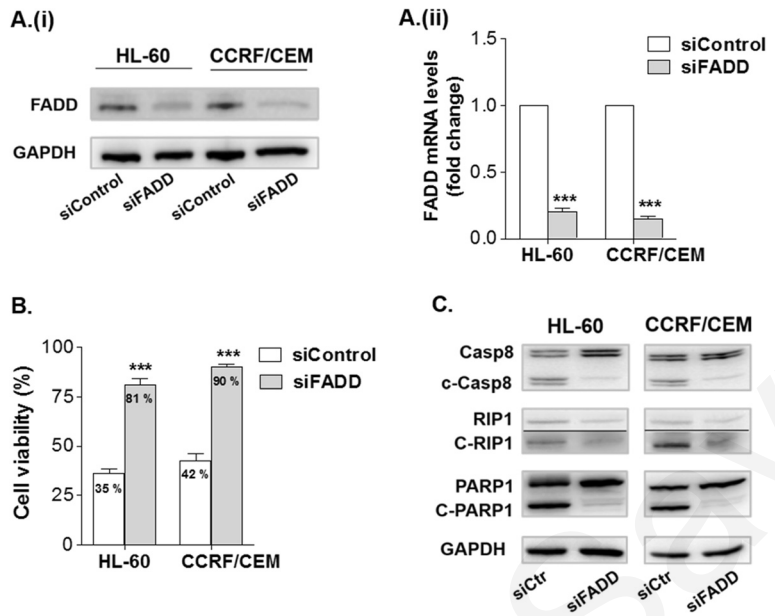

Fig. 6 Effects of FADD silencing on the antiproliferative and apoptotic properties of KC-53 in leukemic cells. **a** HL-60 and CCRF/CEM cells were transiently transfected with siRNA control or siRNA FADD followed by (**i**) immunoblotting for the detection of FADD protein levels and (**ii**) qPCR for measuring FADD mRNA levels. **b** Transfected cells were treated with 0 or 5 μM KC-53 for 24 h and cell viability was determined with the MTT assay. **c** Transfected cells were treated with 5 μM KC-53 for 6 h and protein levels were determined by immunoblotting. The results in panels **a** (**i**) and **c** are representative of three repetitions. The results in **a** (**ii**) and **b** panels represent the mean ± SEM of three replicates and are representative of three separate experiments. (***p value <0.001)

Caspase-8, nor to promote the proteolytic inactivation of RIP1 or PARP1 (Fig. 6c). Taken together, the results presented here support that the FADD/Caspase-8/RIP1 signaling axis plays a crucial role in KC-53 induced apoptosis of HL-60 and CCRF/CEM cells.

Discussion

Although the overall survival rate of leukemia patients has dramatically increased in the past decade, there is still a strong need for discovering new therapeutic agents with higher specificity and milder side-effects. In the present study we evaluated for the first time the anticancer efficacy of KC-53. Importantly, we discovered that, KC-53 reduces cancer cell viability in a dose-depended manner in all cell lines and exhibits the highest cytotoxicity towards HL-60 (AML/APL) and CCR/CEM (ALL) leukemic cell lines. Remarkably, the normal PBMCs were relatively resistant to the anti-proliferative effects of the agent, suggesting that the KC-53 inhibitory effects are selective against cancer cells. We show that KC-53 efficiently and irreversible inhibits cells growth, promoting rabidly CD and CID apoptotic cell death. The molecular events leading to reduced survival and apoptosis have been methodically unravelled in this study and are illustrated in Fig. 7.

Initially, the agent up-regulates membrane-bound TNFR1 followed by activation of Caspase-8, RIP1 proteolysis and activation of Caspases, −3, −7 and −9. The failure of restoring cell viability in the presence of the pan-caspase inhibitor, z.vad.fmk suggests that CID mechanisms may also be involved in the mode of action of KC-53 (Fig. 3b). This prediction is supported by the release and translocation of AIF from the mitochondrial to the nucleus (Fig. 4c (ii)) which is commonly induced by Calpains and Cathepsins [30]. Interestingly, it has been previously shown that when Caspase-8 activity is blocked, the cell uses necroptosis as an alternative cell death pathway (Reviewed in [31]). RIP1 and RIP3 kinase activities are crucial for this alternative CID pathway induced by death receptors, including TNFR1. Thus, activation of necroptosis by KC-53 cannot be excluded at this point.

The participation of FADD in a complex with Caspase-8 and RIP1 is known to be required for the activation of the extrinsic pathway through TNFR1 [32]. Down regulation of FADD with siRNA inhibited the formation of the pro-apoptotic complex and, consequently, the FADD-deficient HL-60 and CCRF/CEM cells developed resistance to the anti-proliferative and apoptotic effects of KC-53. These results strongly suggest that, following TNFR1 activation, one of the primary apoptotic effects of KC-53 is the formation of the FADD/Caspsase-8/RIP1 pro-apoptotic complex. Importantly, our data clearly show that KC-53 concurrently inhibits pro-survival NF-κB signaling. We determined that KC-53

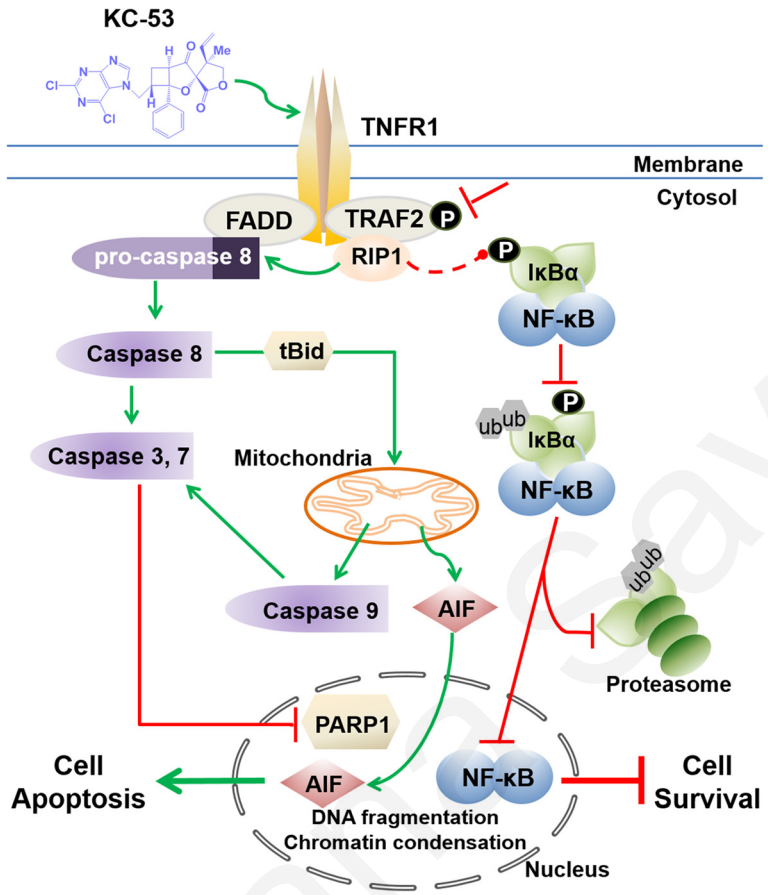

Fig. 7 Sequence of molecular events leading to anti-proliferative and pro-apoptotic effects of KC-53 in leukemic cells. KC-53 stimulates TNFR1 and inhibits TRAF2 phosphorylation. RIP1 dissociates from TRAF2 and binds to the FADD/pro-caspase 8 complex. This leads to the activation of the procaspase-8 which in turns cleaves and inactivates RIP1. Caspase-8 triggers Bid cleavage, activation of effectors Caspases, −3 and −7 and inactivation of PARP1 promoting cell apoptosis. tBid leads to Caspase-9 activation and AIF release and translocation to the nucleus. The absence of RIP1 from TRADD/TRAF2 complex diminishes the phosphorylation of IκBα by downstream kinases. As a result, IκBα is not phosphorylated and fails to be ubiquitinated and degraded by proteasome. Subsequently, NF-κB remains in complex with IκBα, fails to translocate to the nucleus and cell survival signaling is hindered. *P* phosphorylation, *ub* ubiquitination

strongly inhibited the TNFα-induced phosphorylation on Ser32/36 of IκBα. The hypo-phosphorylated form of IκBα stabilizes the cytoplasmic IκBα/p65 complex, blocking in this manner p65 translocation to the nucleus. Consequently, KC-53 TNFα-stimulated gene expression of both pro-survival and pro-inflammatory p65-mediators. This effect of KC-53 could also explain the previously reported anti-inflammatory activity of KC-53 [26].

The use of anti-TNF antibodies and specific agents to block TNFRs and NF-κB activation has been a valuable approach against inflammatory diseases [33]. Proteasome inhibitors [34] and IKK inhibitors [35, 36] have also been used to block the NF-κB pathway and to enhance the sensitivity of cancer cells to apoptosis. For instance, the proteasome inhibitor Bortezomib is currently approved for the treatment of mantle cell lymphoma [37, 38]. However, due to low specificity for cancer cells versus normal cells, it causes severe side effects [37]. The proteasome, which is responsible for IκBα degradation has many other vital cellular functions and it may also not be feasible to block it for prolonged periods. Consequently, hindering NF-κB by controlling upstream regulatory molecules such as RIP1 and TRAF2 might be a more efficient and less cytotoxic approach in comparison to Bortezomib for the treatment of blood diseases. Preclinical evidence for the importance of TRAF2 and RIP1 as targets for anticancer drugs is based on two observations: (i) that inactivating mutations of TRAF2 is a dominant-negative event, neutralizing TNFα-induced NF-κB activation [6, 39] and, (ii) RIP1-null cells or mice do not undergo TNFα-induced cell death (Reviewed in [40, 41]). Our data revealed that, KC-53 induced a robust degradation of RIP1 and dramatically inhibited the TNFα-induced phosphorylation on Ser11 of TRAF2. As such, the absence of RIP1

and phospho-TRAF2, from the pro-survival complex blocked the downstream phosphorylation events leading to NF-κB (space) activation.

Unlike most chemotherapeutic drugs, ligands of the TNF family induce apoptosis in a p53-independent manner and are promising alternatives to conventional chemotherapy. Specifically for leukemia, mutational inactivation of the *p53* gene which mainly regulates apoptosis via the DNA damage-induced intrinsic pathway, reduces cancer cell sensitivity to conventional treatments [12, 13]. In this aspect, KC-53 enables the crosstalk between the extrinsic and intrinsic pathway enabling cell lines with non-functional p53 to bypass the p53-mitochondrial block. Caspase-8-mediated cleavage of Bid provides the link between death receptor stimulation and mitochondrial apoptotic events. In both HL-60 (*p53*−/−) and CCRF/CEM (*p53*mut) KC-53 promoted the activation of Bid and the cleavage of Caspase-9. tBid has the ability to accumulate at mitochondria and to initiate MOMP [27]. MOMP in turn results in the release of pro-apoptotic factors from the mitochondrial intermembrane space, including cytochrome *c*, triggering formation of the apoptosome and activation of Caspase-9. Collectively, our data identified the key role of the TNFR1 pathway in KC-53-induced apoptosis, where the engagement of the mitochondrial system amplified cell death. This may have clinical implications, since it may critically reduce the time required for execution of the death program. This also suggests that KC-53 may find applications in the treatment of p53 mutant cancers and help to overcome resistance.

The idea to specifically target the extrinsic pathway to trigger apoptosis in malignant cells is attractive for cancer therapy since death receptors have a direct link to the death machinery. However, the clinical application of TNFα and Fas is hampered by severe toxic side effects [42, 43]. TRAIL remains promising as a cancer therapeutic, despite the fact that many tumors remain refractory towards treatment with TRAIL [44–46]. In most, if not all, clinical studies the lack of efficacy was probably attributed to their inability to overcome the mitochondrial block [47–49]. KC-53 appears to be a strong candidate for TNFR1 activation and may help to overcome TRAIL resistance and/or increase malignant cell sensitivity to chemotherapy. Our work also represents a new concept in the design of TNFR1-targeted therapies as this is the first time that an agent has been reported to stimulate efficiently TNFR1 inhibiting cancer cell growth and concurrently eliminate the activation of NF-κB.

Conclusions

Our findings show for the first time that, KC-53 effectively triggers apoptosis by facilitating both the extrinsic and intrinsic pathway, bypassing the p53-mitochondrial block and hindering the p65/NF-κB survival cascade in APL and ALL cells. Because of these qualities we anticipate that KC-53 is very likely to find applications, either as a single agent, or in combination with other conventional chemotherapeutic agents in targeted therapeutics against acute leukemias.

Additional files

Additional file 1: Nucleotide sequences of PCR primers. (PDF 186 kb)

Additional file 2: The effect of KC-53 on the survival of various human cancer cell lines, on PBMCs and on the immortalized "normal" cell line, MCF-12 F. Cells were exposed to increasing concentrations (0–60 μM) of KC-53 for 48 h. Cell survival was determined with the MTT cell viability assay and is expressed as percentage of survival compared to vehicle controls. The results represent the mean ± SEM of three replicates and are representative of at least three different experiments. (TIF 54 kb)

Additional file 3: KC-53 induces DNA damage in HL-60 and CCRF/CEM cells. HL-60 and CCRF/CEM cells were treated with vehicle control or 5 μM of KC-53 for the times indicated and DNA damage was evaluated with the Comet assay. For comparison, cell samples were treated with 100 μM H_2O_2 for 30 min which is known to produces oxidative DNA damage (positive control). (**i**) Images were obtained by fluorescence microscopy and show comet fields after SYBR Green I staining. (**ii**) The DNA damage was quantified based on the comet tail length. The results are representative of three independent experiments. (*p value <0.05, ***p value <0.001). (TIF 522 kb)

Additional file 4: KC-53 does not promote the generation of reactive oxygen species in leukemic cells. HL-60 and CCRF/CEM cells were treated with vehicle control or 5 μM of KC-53 in the presence or absence of 1 mM Sodium pyruvate (SP) for the indicated time points. Cells were also treated with 100 μM Hydrogen peroxide (H_2O_2) in the presence or absence of 1 mM SP as controls. ROS production was determined with the DCFH-DA assay. The treatments were performed in duplicate and represent the mean ± SEM of three independent experiments. (TIF 55 kb)

Additional file 5: The expression of death receptors and adaptor proteins upon KC-53 administration. HL-60 and CCRF/CEM cells were treated with 0 or 5 μM KC-53 for the indicated times prior protein extraction. Proteins were separated by SDS-PAGE and immunoblotted with the indicated antibodies. The results are representative of three repetitions. (TIF 335 kb)

Abbreviations

ALL: acute lymphocytic leukemia; AML: acute myelocytic leukemia; APL: acute promyelocytic leukemia; CD: caspase dependent; CID: caspase independent; FADD: fas-associated death domain; IKK: IκB kinase; IκBα: inhibitory protein of NF-κB; NF-κB: nuclear factor κB; PBMCs: peripheral blood mononuclear cells; rhTNFα: recombinant human TNFα; RIP1: receptor-interacting protein 1; TNFR1: tumor necrosis factor receptor 1; TNFα: tumor necrosis factor alpha; TRAF2: TNF receptor-associated factor 2.

Competing interests

The authors declare that they have no competing interests.

Authors' contributions

CGS participated in research design, conducted the experiments and performed data analysis. AIC participated in the design of the experiments and data analysis. KCN, and ST, synthesized the compound. CGS, AIC, KCN, ST and CMN all contributed to the writing of the manuscript. All authors read and approved the final manuscript.

Acknowledgements

This work was supported by funding from the Department of Biological Sciences of the University of Cyprus.

Author details
[1]Department of Biological Sciences, University of Cyprus, Kallipoleos 75, Nicosia 01678, Cyprus. [2]Department of Chemistry, BioScience Research Collaborative, Rice University, 6500 Main Street, Houston, TX 77005, USA.

Received: 4 August 2015 Accepted: 12 April 2016
Published online: 20 April 2016

References

1. Fulda S. Inhibitor of Apoptosis (IAP) proteins in hematological malignancies: molecular mechanisms and therapeutic opportunities. Leukemia. 2014;28(7):1414–22.
2. Ouyang L, Shi Z, Zhao S, Wang FT, Zhou TT, Liu B, Bao JK. Programmed cell death pathways in cancer: a review of apoptosis, autophagy and programmed necrosis. Cell Prolif. 2012;45(6):487–98.
3. Karin M, Lin A. NF-kappaB at the crossroads of life and death. Nat Immunol. 2002;3(3):221–7.
4. Gasparini C, Celeghini C, Monasta L, Zauli G. NF-kappaB pathways in hematological malignancies. Cell Mol Life Sci. 2014;71(11):2083–102.
5. Thomas GS, Zhang L, Blackwell K, Habelhah H. Phosphorylation of TRAF2 within its RING domain inhibits stress-induced cell death by promoting IKK and suppressing JNK activation. Cancer Res. 2009;69(8):3665–72.
6. Blackwell K, Zhang L, Thomas GS, Sun S, Nakano H, Habelhah H. TRAF2 phosphorylation modulates tumor necrosis factor alpha-induced gene expression and cell resistance to apoptosis. Mol Cell Biol. 2009;29(2):303–14.
7. Kanayama A, Seth RB, Sun L, Ea CK, Hong M, Shaito A, Chiu YH, Deng L, Chen ZJ. TAB2 and TAB3 activate the NF-kappaB pathway through binding to polyubiquitin chains. Mol Cell. 2004;15(4):535–48.
8. Wang C, Deng L, Hong M, Akkaraju GR, Inoue J, Chen ZJ. TAK1 is a ubiquitin-dependent kinase of MKK and IKK. Nature. 2001;412(6844):346–51.
9. Micheau O, Tschopp J. Induction of TNF receptor I-mediated apoptosis via two sequential signaling complexes. Cell. 2003;114(2):181–90.
10. Lin Y, Devin A, Rodriguez Y, Liu ZG. Cleavage of the death domain kinase RIP by caspase-8 prompts TNF-induced apoptosis. Genes Dev. 1999;13(19):2514–26.
11. Fulda S, Debatin KM. Extrinsic versus intrinsic apoptosis pathways in anticancer chemotherapy. Oncogene. 2006;25(34):4798–811.
12. Melo MB, Ahmad NN, Lima CS, Pagnano KB, Bordin S, Lorand-Metze I, SaAd ST, Costa FF. Mutations in the p53 gene in acute myeloid leukemia patients correlate with poor prognosis. Hematology. 2002;7(1):13–9.
13. Wattel E, Preudhomme C, Hecquet B, Vanrumbeke M, Quesnel B, Dervite I, Morel P, Fenaux P. p53 mutations are associated with resistance to chemotherapy and short survival in hematologic malignancies. Blood. 1994;84(9):3148–57.
14. Mehta SV, Shukla SN, Vora HH. Overexpression of Bcl2 protein predicts chemoresistance in acute myeloid leukemia: its correlation with FLT3. Neoplasma. 2013;60(6):666–75.
15. Nuessler V, Stotzer O, Gullis E, Pelka-Fleischer R, Pogrebniak A, Gieseler F, Wilmanns W. Bcl-2, bax and bcl-xL expression in human sensitive and resistant leukemia cell lines. Leukemia. 1999;13(11):1864–72.
16. Kapelko-Slowik K, Urbaniak-Kujda D, Wolowiec D, Jazwiec B, Dybko J, Jakubaszko J, Slowik M, Kuliczkowski K. Expression of PIM-2 and NF-kappaB genes is increased in patients with acute myeloid leukemia (AML) and acute lymphoblastic leukemia (ALL) and is associated with complete remission rate and overall survival. Postepy Hig Med Dosw (Online). 2013;67:553–9.
17. Droin N, Guery L, Benikhlef N, Solary E. Targeting apoptosis proteins in hematological malignancies. Cancer Lett. 2013;332(2):325–34.
18. Hegde M, Karki SS, Thomas E, Kumar S, Panjamurthy K, Ranganatha SR, Rangappa KS, Choudhary B, Raghavan SC. Novel levamisole derivative induces extrinsic pathway of apoptosis in cancer cells and inhibits tumor progression in mice. PloS One. 2012;7(9):e43632.
19. Jacquemin G, Shirley S, Micheau O. Combining naturally occurring polyphenols with TNF-related apoptosis-inducing ligand: a promising approach to kill resistant cancer cells? Cell Mol Life Sci. 2010;67(18):3115–30.
20. Roberts NJ, Zhou S, Diaz Jr LA, Holdhoff M. Systemic use of tumor necrosis factor alpha as an anticancer agent. Oncotarget. 2011;2(10):739–51.
21. Lejeune FJ, Lienard D, Matter M, Ruegg C. Efficiency of recombinant human TNF in human cancer therapy. Cancer Immun. 2006;6:6.
22. Micheau O, Lens S, Gaide O, Alevizopoulos K, Tschopp J. NF-kappaB signals induce the expression of c-FLIP. Mol Cell Biol. 2001;21(16):5299–305.
23. Tanaka N, Okasaka M, Ishimaru Y, Takaishi Y, Sato M, Okamoto M, Oshikawa T, Ahmed SU, Consentino LM, Lee KH. Biyouyanagin A, an anti-HIV agent from Hypericum chinense L. var. salicifolium. Org Lett. 2005;7(14):2997–9.
24. Nicolaou KC, Wu TR, Sarlah D, Shaw DM, Rowcliffe E, Burton DR. Total synthesis, revised structure, and biological evaluation of biyouyanagin A and analogues thereof. J Am Chem Soc. 2008;130(33):11114–21.
25. Tanaka N, Kashiwada Y, Kim SY, Hashida W, Sekiya M, Ikeshiro Y, Takaishi Y. Acylphloroglucinol, biyouyanagiol, biyouyanagin B, and related spiro-lactones from Hypericum chinense. J Nat Prod. 2009;72(8):1447–52.
26. Nicolaou KC, Sanchini S, Sarlah D, Lu G, Wu TR, Nomura DK, Cravatt BF, Cubitt B, de la Torre JC, Hessell AJ et al. Design, synthesis, and biological evaluation of a biyouyanagin compound library. Proc Natl Acad Sci U S A. 2011;108(17):6715–20.
27. Schug ZT, Gonzalvez F, Houtkooper RH, Vaz FM, Gottlieb E. BID is cleaved by caspase-8 within a native complex on the mitochondrial membrane. Cell Death Differ. 2011;18(3):538–48.
28. Luo X, Budihardjo I, Zou H, Slaughter C, Wang X. Bid, a Bcl2 interacting protein, mediates cytochrome c release from mitochondria in response to activation of cell surface death receptors. Cell. 1998;94(4):481–90.
29. Tourneur L, Chiocchia G. FADD: a regulator of life and death. Trends Immunol. 2010;31(7):260–9.
30. Norberg E, Orrenius S, Zhivotovsky B. Mitochondrial regulation of cell death: processing of apoptosis-inducing factor (AIF). Biochem Biophys Res Commun. 2010;396(1):95–100.
31. Vandenabeele P, Galluzzi L, Vanden Berghe T, Kroemer G. Molecular mechanisms of necroptosis: an ordered cellular explosion. Nat Rev Mol Cell Biol. 2010;11(10):700–14.
32. Lee EW, Kim JH, Ahn YH, Seo J, Ko A, Jeong M, Kim SJ, Ro JY, Park KM, Lee HW et al. Ubiquitination and degradation of the FADD adaptor protein regulate death receptor-mediated apoptosis and necroptosis. Nat Commun. 2012;3:978.
33. Song XY, Torphy TJ, Griswold DE, Shealy D. Coming of age: anti-cytokine therapies. Mol Interv. 2002;2(1):36–46.
34. Koyama D, Kikuchi J, Hiraoka N, Wada T, Kurosawa H, Chiba S, Furukawa Y. Proteasome inhibitors exert cytotoxicity and increase chemosensitivity via transcriptional repression of Notch1 in T-cell acute lymphoblastic leukemia. Leukemia. 2014;28(6):1216–26.
35. Carvalho G, Fabre C, Braun T, Grosjean J, Ades L, Agou F, Tasdemir E, Boehrer S, Israel A, Veron M et al. Inhibition of NEMO, the regulatory subunit of the IKK complex, induces apoptosis in high-risk myelodysplastic syndrome and acute myeloid leukemia. Oncogene. 2007;26(16):2299–307.
36. Cilloni D, Messa F, Arruga F, Defilippi I, Morotti A, Messa E, Carturan S, Giugliano E, Pautasso M, Bracco E et al. The NF-kappaB pathway blockade by the IKK inhibitor PS1145 can overcome imatinib resistance. Leukemia. 2006;20(1):61–7.
37. Blum W, Schwind S, Tarighat SS, Geyer S, Eisfeld AK, Whitman S, Walker A, Klisovic R, Byrd JC, Santhanam R et al. Clinical and pharmacodynamic activity of bortezomib and decitabine in acute myeloid leukemia. Blood. 2012;119(25):6025–31.
38. Don AS, Zheng XF. Recent clinical trials of mTOR-targeted cancer therapies. Rev Recent Clin Trials. 2011;6(1):24–35.
39. Zhang L, Blackwell K, Altaeva A, Shi Z, Habelhah H. TRAF2 phosphorylation promotes NF-kappaB-dependent gene expression and inhibits oxidative stress-induced cell death. Mol Biol Cell. 2011;22(1):128–40.
40. O'Donnell MA, Ting AT. NFkappaB and ubiquitination: partners in disarming RIPK1-mediated cell death. Immunol Res. 2012;54(1–3):214–26.
41. Weinlich R, Dillon CP, Green DR. Ripped to death. Trends Cell Biol. 2011;21(11):630–7.
42. Walczak H, Krammer PH. The CD95 (APO-1/Fas) and the TRAIL (APO-2L) apoptosis systems. Exp Cell Res. 2000;256(1):58–66.
43. Ashkenazi A, Pai RC, Fong S, Leung S, Lawrence DA, Marsters SA, Blackie C, Chang L, McMurtrey AE, Hebert A et al. Safety and antitumor activity of recombinant soluble Apo2 ligand. J Clin Invest. 1999;104(2):155–62.
44. Riccioni R, Pasquini L, Mariani G, Saulle E, Rossini A, Diverio D, Pelosi E, Vitale A, Chierichini A, Cedrone M et al. TRAIL decoy receptors mediate resistance of acute myeloid leukemia cells to TRAIL. Haematologica. 2005;90(5):612–24.
45. von Haefen C, Gillissen B, Hemmati PG, Wendt J, Guner D, Mrozek A, Belka C, Dorken B, Daniel PT. Multidomain Bcl-2 homolog Bax but not Bak mediates synergistic induction of apoptosis by TRAIL and 5-FU through the mitochondrial apoptosis pathway. Oncogene. 2004;23(50):8320–32.

46. Fulda S, Meyer E, Debatin KM. Inhibition of TRAIL-induced apoptosis by Bcl-2 overexpression. Oncogene. 2002;21(15):2283–94.
47. Jacquemin G, Granci V, Gallouet AS, Lalaoui N, Morle A, Iessi E, Morizot A, Garrido C, Guillaudeux T, Micheau O. Quercetin-mediated Mcl-1 and survivin downregulation restores TRAIL-induced apoptosis in non-Hodgkin's lymphoma B cells. Haematologica. 2012;97(1):38–46.
48. Morizot A, Merino D, Lalaoui N, Jacquemin G, Granci V, Iessi E, Lanneau D, Bouyer F, Solary E, Chauffert B et al. Chemotherapy overcomes TRAIL-R4-mediated TRAIL resistance at the DISC level. Cell Death Differ. 2011;18(4):700–11.
49. Ganten TM, Haas TL, Sykora J, Stahl H, Sprick MR, Fas SC, Krueger A, Weigand MA, Grosse-Wilde A, Stremmel W et al. Enhanced caspase-8 recruitment to and activation at the DISC is critical for sensitisation of human hepatocellular carcinoma cells to TRAIL-induced apoptosis by chemotherapeutic drugs. Cell Death Differ. 2004;11 Suppl 1:S86–96.

Christiana Savva

Submit your next manuscript to BioMed Central and we will help you at every step:

- We accept pre-submission inquiries
- Our selector tool helps you to find the most relevant journal
- We provide round the clock customer support
- Convenient online submission
- Thorough peer review
- Inclusion in PubMed and all major indexing services
- Maximum visibility for your research

Submit your manuscript at
www.biomedcentral.com/submit

Send Orders for Reprints to reprints@benthamscience.ae

LiSIs: An Online Scientific Workflow System for Virtual Screening

Christos C. Kannas[*,1], Ioanna Kalvari[2], George Lambrinidis[3], Christiana M. Neophytou[2], Christiana G. Savva[2], Ioannis Kirmitzoglou[2], Zinonas Antoniou[1], Kleo G. Achilleos[1], David Scherf[4], Chara A. Pitta[2], Christos A. Nicolaou[1], Emanuel Mikros[3], Vasilis J. Promponas[2], Clarissa Gerhauser[4], Rajendra G. Mehta[5], Andreas I. Constantinou[2] and Constantinos S. Pattichis[1]

[1]*Department of Computer Science, University of Cyprus, Nicosia, Cyprus*

[2]*Department of Biological Sciences, University of Cyprus, Nicosia Cyprus*

[3]*Department of Pharmaceutical Chemistry, Faculty of Pharmacy, National & Kapodistrian University of Athens, Athens, Greece*

[4]*Cancer Chemoprevention and Epigenomics Workgroup, German Cancer Research Center, Heidelberg, Germany*

[5]*Illinois Institute of Technology (IIT) Research Institute, Chicago, Illinois, USA*

Christos C. Kannas

Abstract: Modern methods of drug discovery and development in recent years make a wide use of computational algorithms. These methods utilise Virtual Screening (VS), which is the computational counterpart of experimental screening. In this manner the in silico models and tools initial replace the wet lab methods saving time and resources. This paper presents the overall design and implementation of a web based scientific workflow system for virtual screening called, the Life Sciences Informatics (LiSIs) platform. The LiSIs platform consists of the following layers: the input layer covering the data file input; the pre-processing layer covering the descriptors calculation, and the docking preparation components; the processing layer covering the attribute filtering, compound similarity, substructure matching, docking prediction, predictive modelling and molecular clustering; post-processing layer covering the output reformatting and binary file merging components; output layer covering the storage component. The potential of LiSIs platform has been demonstrated through two case studies designed to illustrate the preparation of tools for the identification of promising chemical structures. The first case study involved the development of a Quantitative Structure Activity Relationship (QSAR) model on a literature dataset while the second case study implemented a docking-based virtual screening experiment. Our results show that VS workflows utilizing docking, predictive models and other in silico tools as implemented in the LiSIs platform can identify compounds in line with expert expectations. We anticipate that the deployment of LiSIs, as currently implemented and available for use, can enable drug discovery researchers to more easily use state of the art computational techniques in their search for promising chemical compounds. The LiSIs platform is freely accessible (i) under the GRANATUM platform at: http://www.granatum.org and (ii) directly at: http://lisis.cs.ucy.ac.cy.

Keywords: Chemoinformatics, docking, drug discovery, predictive models, QSAR, scientific workflow, virtual screening.

INTRODUCTION

Virtual Screening (VS) can be the first step prior to biological screening. The objective of VS is to select the most promising compounds that will be subsequently scanned in a laboratory setting. In this manner a subset of a large dataset is being tested increasing the probability to identify lead compounds against specific biological targets [1, 2]. In this respect the method is related to machine learning and statistical techniques, such as classification and regression. These methods target to develop predictive models for the identification of the properties of unknown compounds based on a set of compounds with known properties. Typically, VS processes involve substantial numbers of molecules and combine a variety of computational techniques, often organized in complex computational pipelines [3].

Scientific Workflow Management Systems (SWMS) are powerful tools with immense potential to expedite the design, development and execution processes of computational experiments. SWMS can be applied by scientists for the solution of complex computational problems [4] and also to design complex *in silico* experiments [5].

In this paper we propose a VS platform based on scientific workflow modelling. A preliminary version of this study was presented in [6].

The **Li**fe **S**ciences **I**nformatic**s** (LiSIs) platform [7] is a part of GRANATUM [8], an EU FP7 project. The aim of GRANATUM [8] is to provide biomedical researchers access to state of the art computational tools to perform

*Address correspondence to this author at the Department of Computer Science, University of Cyprus, P.O. Box 20537, 1678 Nicosia, Cyprus; Tel: +357-22892685; Fax: +357-22892701; E-mail: kannas.christos@ucy.ac.cy

1386-2073/15 $58.00+.00 © 2015 Bentham Science Publishers

complex cancer chemoprevention experiments and to conduct studies on large-scale datasets.

Cancer chemoprevention is defined as the use of natural, synthetic, or biologic chemical agents to reverse, suppress, or prevent carcinogenic progression to invasive cancer [9]. The experimental approach for the discovery of cancer chemopreventive agents is similar to the typical drug discovery process (DDP) [10].

Chemoprevention research (CPR) and DDP are highly similar processes, therefore the tools used for drug discovery can also be applied to CPR. In this context, computational tools can be used to develop specific models for the needs of chemoprevention. For example, SWMS used for VS in DDP, such as Taverna [11-13], KNIME [14, 15], PipelinePilot [16] and IDBS InforSence Suite [17], can also be adapted for use in CPR. Researchers in the chemoprevention field do not generally use these computational tools. Apparently, the field of cancer chemoprevention can be advanced by customised, and easy to use *in silico* tools for data handling and analysing.

It should be emphasized that to the best of our knowledge there are no similar tools to LiSIs in cancer chemoprevention. Moreover, it is noted that the proposed platform features: (i) free and open access to the research community, (ii) it is integrated on the GALAXY platform that is familiar to molecular biologists, (iii) it aims to have a user friendly interface, (iv) it is part of a larger integrated project, GRANATUM, offering access to semantic web technologies, text mining tools, and collaborative environment for sharing data sets, models, etc. [8]. Furthermore, the paper covers two case studies that are used to evaluate and validate the system: (1) a case study on QSAR model for mutagenicity, and (2) on estrogen receptor (ER) binding.

VIRTUAL SCREENING PROCESS

VS process is carried out on libraries of real or virtual compounds and requires known measured activities of control compounds or a known structure of the biomolecular target [18]. When only measured activities of compounds are known, virtual screening uses analogue-based library design, classification and regression models or any combination of these.

Since no method is generally applicable to all cases, a VS experiment takes into account the requirements of each case. For example, if high quality ligand activity measurements are available, regression methods (Quantitative Structure Activity Relationship - QSAR modelling) can be used to extract with confidence rules predicting ligand similarity, and binding action [19].

When the structure of the target receptor is known the VS method typically relies on protein-ligand docking and small molecule modelling. Initially, it takes the advantage of the knowledge about the receptor site to model it and then perform docking from a database. A number of conformations are usually sampled for each molecule [20] and a score for every possible docking is computed [21]. Due to the computationally demanding processes computer clusters are employed by the pharmaceutical industry [20, 22]. In addition, databases of multiple conformers of compounds are prepared in advance to avoid their reproduction for every VS run [23]. Often, multi-objective methods may be used that enable the use of numerous objectives, analogue or target-based, to identify compounds that simultaneously meet multiple criteria relevant to the virtual screening experiment pursued [24].

The key measure for validating the success of VS is the achievement of high enrichment targeting in an experimental hit rate for the subset of compounds it recommends which is significantly better over that of a random compound set [22]. A successful process with high enrichment results in considerable savings in resources and time, since fewer compounds need to be physically screened while most hits present in the original large database are retrieved. In practice, to enrich the results of VS, several methods are tried and their results are combined to produce a concise, high quality virtual hit list [20, 21]. Furthermore, it is also a common practice to perform a pre-processing step where databases of molecules are cleaned by filtering out compounds with undesired properties. These properties include, a large size, high flexibility and non-compliance to Lipinski's rule of 5 [25]. During this step compounds containing known unwanted substructures, e.g. known toxicophores, may also be eliminated [22]. Although significant algorithmic improvements have been achieved in the VS process, accuracy still varies depending on the pharmaceutical target, the virtual library and the docking and scoring methods used. The last step is the evaluation of the VS experiment results typically *via* visual inspection by a human expert [26].

SCIENTIFIC WORKFLOW MANAGEMENT SYSTEMS

SWMS target in accelerating scientific discovery by incorporating in their processing steps, data management and analysis, simulation, and visualization tools into a single platform. Most importantly SWMS provide an interactive visual interface that facilitates the design and execution of workflows. A brief overview of the field is given whereas a more detailed review on SWMS can be found in [27].

Scientific workflow (SW) based platforms provide tools that automate the execution of a class of *in silico* experiments, offering significant benefits for all the phases of an experiment's life-cycle. In the context of the design and implementation phase, a repository of tried and tested workflows can be available to the scientists to choose from. During the execution phase, as experimenting is by definition a repeatable process, workflows can relieve the scientists of repetitive tasks, while at the same time enable keeping track of all the intermediary steps and data (provenance). These traces can be used at a later stage to enable the reproducibility of the experiment. Provenance information [28] is also useful during the analysis phase to see the evolution of the research, trace the origin of an error or go back to a previous stage and change the direction of research. Visualization tools are provided for this phase as well for assisting in the evaluation of the results.

Through the use of SWs, interdisciplinary teams can collaborate closely, share workflows and computational components and jointly undertake research initiatives requiring end-to-end scientific data management and

computational analysis. Moreover, recent advances in grid technologies allow workflows to exploit parallel executions enabling large-scale data processing.

MATERIALS AND METHODS

LiSIs [7] aims to provide a set of tools to create, update, store and share SWs for the discovery of active compounds for biomedical researchers. Access to LiSIs can be achieved *via* a web interface through a password protected login process either from the GRANATUM portal [8] (preferred access point) or directly from the LiSIs portal [7]. The login process provides different levels of access to platform functionality based on the user profile. The user is able to assemble SWs utilizing available *in silico* models and tools loaded into the platform. Depending on the user profile and associated permissions, users may also construct new models and tools through the development of custom workflows made available by the system for this purpose. Workflows execute on the system server. The execution results can also be stored on the user's GRANATUM workspace [8], where the user is able to access, manipulate or share them with other users.

Fig. (**1**) is an illustration of the chemoinformatics tools available on LiSIs. Below is a brief description of each tool category.

INPUT LAYER

The Input Layer consists of the following two component categories:

Data File Input: provides tools which support parsing different chemical and biological data files. File formats currently supported include Chemical Data Files, which are sdf (SDF - Structure Data File), smi (SMILES - Simplified Molecular Input Line Entry Specification), pdb (PDB - Protein Data Bank), pdbqt (AutoDock Protein and Ligand data files) and Biological Data Files which are csv (CSV - Comma Separated Values), tab (Tab Separated Values) and also text files.

These tools get as input ASCII files and create output files which are pickled Python objects, which we reference them as binary files.

GRANATUM File Input: A component which provides GRANATUM's platform users to upload on LiSIs files located at GRANATUM workspace [8].

Fig. (1). Chemoinformatics tools available on LiSIs, each tool is under a specific layer.

ChemSpider Molecule Retrieval: A component which given a file with molecules common name it uses ChemSpider API to retrieve information available for those molecules, and returns the result as a SMILES file.

PRE-PROCESSING LAYER

The Pre-Processing Layer consists of the following four component categories:

Descriptors Calculation: This component provides tools for calculating various descriptors of chemical compounds. Currently the platform enables calculation of whole-compound descriptors with the use of RDKit [29]. Example descriptors include molecular weight, number of hydrogen bond donors and acceptors, polar surface area, number of rings, calculated octanol - water partition coefficient (cLogP), molecular complexity based on the method proposed by Barone [30] and molecular flexibility, as well as molecular fingerprints which can be one of Morgan (circular) fingerprints [31], MACCS [32], Atom-Pair [33], Topological Torsion [34], and topological fingerprints, a Daylight like fingerprint based on hashing molecular sub-graphs [35].

Docking Preparation: This component provides the following tools:

- *3D Coordinate Calculator:* A tool for preparing compounds for docking experiments, by calculating their 3D coordinates and creating the appropriate files required by the docking software used by LiSIs.
- *Protein Cleaner:* A tool provided by AutoDock, which is used to automate the process of cleaning a protein to create the required files used by AutoDock Vina [36, 37].

All the tools of this layer use as input and output binary files.

PROCESSING LAYER

The Processing Layer consists of the following five component categories:

Attribute Filtering: This component provides tools for implementing compound selection filtering tuned on the compounds chemical and biological attributes. These components enable the user to pre-select ranges of acceptable values on available compound properties (including properties calculated by the Chemical Descriptors component and properties provided externally from the Data Input Layer). Three tools are available under this category, "Chemical Properties Filter", "GRANATUM Ro5 Filter" and "Lipinski Ro5 Filter".

Compound Similarity: This component provides tools for implementing filters for selecting compounds based on their chemical structure similarity to other compounds designated by the user. Two tools are available under this category, "Similarity Filter" and "Diversity Filter".

"Similarity Filter" requires two input datasets; the one is used as the reference dataset and the other as the query dataset. The results are two datasets, which are subsets of the initial reference dataset, where the first one contains the compounds that are similar to the query dataset and the second one contains those that are not similar.

"Diversity Filter" on the other and requires only one input dataset and it generates two datasets where the first contains the compounds that are not similar among them and the second contains compounds that are similar among them.

Substructure Matching: This component provides tools for implementing filters for selecting compounds based on whether they contain (or not) the chemical substructure(s) designated by the user.

This tool requires as input one dataset of compounds and at least one substructure in **SM**iles **AR**bitrary **T**arget **S**pecification (SMARTS) format.

Docking Prediction: This component provides tools for implementing filters for selecting compounds based on predicted binding affinity of a compound to a target protein using *in silico* docking prediction. The LiSIs platform currently uses AutoDock Vina, a popular docking application, freely available to the academic research community. AutoDock Vina attempts to find the best receptor-ligand docking pose by employing a scoring function that takes into consideration both intramolecular and intermolecular contributions, as well as an optimization algorithm [36].

Predictive Modelling: This component aims to provide the user with the tools to construct data-driven predictive models based on available information on a set of compounds. These models are used to predict biochemical properties of interest of new compounds and to select those with an acceptable profile. Our platform uses system's underlying R installation to support the creation and reuse of predictive models.

This component makes use of four widely used predictive modelling algorithms by the chemoinformatics community: Decision Trees (DT), Random Forests (RF), Support Vector Machines (SVM), and k-Nearest Neighbours (k-NN) [38].

Molecular Clustering: This component provides a unified interface to different molecular clustering methods such as Agglomerative Hierarchical Clustering, Divisive Hierarchical Clustering, k-Means Partitional Clustering and k-Medoids Partitional Clustering. The provided molecular clustering is based on fingerprint similarity or distance.

POST-PROCESSING LAYER

The Post-Processing Layer consists of the following two component categories:

Output Reformatting: This component provides a tool to convert results in various formats supported by OpenBabel [39].

Binary File Merging: This component provides a tool for merging binary files, containing chemical structure objects with processing component results, into one binary file.

OUTPUT LAYER

The Output Layer consists of the following component category:

Storage: This component covers the storage of results in various formats for future reuse and sharing. The tools available under this component category convert, binary files containing *in silico* molecules, to various file formats such as SMILES, SDF, CSV and Tabular.

THIRD PARTY TOOLS USED BY LISIS

The LiSIs platform uses the following 3rd party tools that are freely available:

Galaxy [40-42], a web-based platform widely used in the biomedical community for intensive data processing and analysis, used for the customized SWMS platform;

RDKit [29], an open source chemoinformatics toolkit;

Pybel [43], a Python wrapper for the OpenBabel chemoinformatics toolkit [39], used for chemical file format transformations;

R [44], a statistical environment that supports data mining, machine learning and statistics based functionalities; caret (Classification and Regression Training) package [38] is used for the generation and reuse of Predictive Models and for Molecular Clustering;

AutoDock Vina [36, 37] docking application used to support docking experiments functionality.

RESULTS

Comparison with other open source Scientific Workflow Management Systems

Taverna

Taverna is an open-source, grid-aware workflow management system [11-13]. It has found wide application in the bioinformatics, chemistry, data- and text-mining and astronomy communities although the system is domain independent. It is comprised of the Taverna Workbench graphical workflow authoring client, a workflow representation language, and an enactment engine. Taverna is implemented as a service-oriented architecture, based on web service standards. From the advent of its design Taverna was an application that applied web services technology to workflow design. That meant that tools created using different programming languages (e.g. Java, Perl, Python, etc.) or platforms (UNIX, Windows, etc.) could now be accessed *via* a web service interface eliminating any need for integration. The same applied to the databases available on the web. As a result, researchers could design and execute a pipeline of web services, with little programming knowledge. Its architecture supports parallelism, both intra-process and inter-process, asynchronous service support and separation of data and process spaces to support scaling to arbitrary data volumes.

A vital component of Taverna's open architecture is the plug-in functionality. Various plug-ins have been developed for accessing online bio-catalogues or for integrating chemoinformatics processing services. Provenance also plays an integral part in Taverna, allowing users to capture and inspect details such as who conducted the experiment, what services were used, and what results were produced. An additional strong feature of Taverna is workflow sharing. The users have direct access to the myExperiment [45] social collaboration site where they can upload or download workflows as needed.

KNIME

Konstanz Information Miner (KNIME) is a modular environment that supports operations such as data integration from various sources, processing, modelling, analysing and mining, as well as parallel execution [14,15]. KNIME is primarily used in pharmaceutical research with some applications reported in other areas like customer resource management and data analysis, business intelligence and financial data analysis. It is an open-source platform free for non-profit and academic use. It is available as a local desktop application but additional features such as user authentication, web services integration, web browser interface, remote server and cluster execution are available in (and restricted to) the professional package.

The platform enables the user to visually assemble and execute data pipelines providing an interactive view of the results. KNIME pipeline(s) consist of modular independent components that combine different projects in a single pipeline. At the same time its expandable architecture enables the easy integration of newly developed tools.

One highlight of KNIME's latest additions is the ability to support Predictive Model Markup Language (PMML) [46]. The PMML is an XML-based markup language that enables applications to define models related to predictive analytics and data mining and to share those models between PMML-compliant applications [47]. As a result a model developed by KNIME can be exported and then used in another data mining engine. Another characteristic is the addition of database ports that are JDBC-compliant that work directly in the database enabling even preview of the actual data inside the database tables [46].

Although written in Java, KNIME, permits running Python, Perl and other code fragments through the use of special scripting nodes. This is extremely useful as the majority of scientific work is currently under the form of Python or Perl scripts.

KNIME functionality is enriched by integrating functionality of different data analysis open source projects for machine learning and data mining, for statistical computations and visualizations as well as many chemoinformatics plug-ins.

Galaxy

Galaxy is a web-based platform for data intensive biomedical research [40-42]. It provides a framework for integrating computational tools and an environment for interactive data analysis, reuse and sharing. As stated in [40, 41] the primary design considerations of Galaxy were accessibility, reproducibility and transparency. Galaxy is accessible to scientists with no programming knowledge through the use of Galaxy tools. It produces reproducible

computational analysis results by generating metadata for each analysis step through the automated production of Galaxy History items. It also promotes transparency by enabling the sharing of data, tools, workflows, results and report documents.

A structured well-defined interface allows the wrapping of nearly any tool that can be run from the command-line into a Galaxy tool. The platform is open source and has been designed specifically to meet the needs of bioinformaticians supporting sequence manipulation with built in libraries. It does not support any control flow operations or remote services. Additionally it does not use a workflow language but rather a relational database. The Galaxy workflow system allows for analysis using multiple tools incorporated to the system which may be built and run or extracted from past runs, and rerun.

Pages are a unique feature to Galaxy. They are online documents used to describe the analysis performed but also to provide links to the Galaxy objects that were used in the analysis, i.e. Histories, Workflows, and Datasets. This enables the reader of the document to have direct access to the dataset used, to import the workflow and reproduce the experiment himself. It also makes it even easier for another scientist to continue and build upon reported previous work.

A recent Taverna-Galaxy integration allows the generation of Galaxy tools from Taverna 2 workflows [48]. The tools can then be installed in a Galaxy server and become part of a Galaxy pipeline. Moreover, Galaxy workflows can be directly shared through the myExperiment site [49]. Galaxy can also be instantiated on cloud computing infrastructures and interfaced with grid clusters [50].

CONCLUDING REMARKS

KNIME is considered among the top open source software for chemoinformatics. Taverna is a prominent web service oriented platform employed in more than 350 organizations around the world with frequent enhancements. Two recent ones being Taverna Mobile and Taverna On-line (under development) [51]. Galaxy is a promising platform where the online features prevail as unique among the three systems.

Galaxy offers additional benefits due to its online nature. There is no need to set up installations on local machines or remote servers, no downloads, no conflicts and no updates to worry about. All tools are available at any personal computer from anywhere in the world provided that they are connected to the internet. The same applies to data. A scientist can import data in the system and process them with the appropriate workflow or design a new one. Moreover the data and work are secure and can be backed up and protected depending on user preferences and specific system specifications. Importantly, all data and work can be shared with other collaborators in real time. Galaxy can even offer the more advanced features such as transparent access to grid services or the cloud, thus, offering speed and efficiency for scientific processes that are computationally expensive and/or data intensive.

Table **1** is a comparison of LiSIs (Galaxy) to KNIME and Taverna platforms. This comparison is focused on their system level and their deployment details.

CASE STUDY: QSAR MODEL FOR MUTAGENICITY

LiSIs was used to create a QSAR model for Mutagenicity to predict mutagenic and non-mutagenic compounds.

The process of creation and validation of QSAR models in LiSIs can be summarized in four distinct steps:

Datasets Loading on LiSIs Platform

Two datasets are needed for training a QSAR model. A dataset containing chemical information of the compounds either in SMILES or SDF format (see "SMI/SDF File Reader"), and a dataset containing the biological information of the compounds (see "Property File Reader").

Table 1. Comparison of free scientific workflow management systems used in virtual screening process.

	KNIME	Taverna	LiSIs
System Details			
Software Platform	KNIME	Taverna + myExperiment	Galaxy (Modified)
OS Requirements	Cross Platform	Cross Platform	Linux
Web based	No (Desktop based)	No (Desktop based)	Yes
Cluster deployment difficulty	Moderate (Need license)	Moderate	Moderate
Cloud deployment difficulty	High	Moderate	Low
Open Source	Yes	Yes	Yes
Tool development difficulty	Moderate	Moderate	Low
Tools Details			
Chemoinformatics Packages	CDK, RDKit, OpenBabel, Indigo, EMBL-EBI, Vernalis, Enalos, etc.	CDK	RDKit, In-house tools
Machine Learning Tools	Weka, R	R	R
Docking Tools	Available with commercial license	Not Available	AutoDock Vina
2D/3D Visualization Tools	Available	Available	Not Available
Community size	Very Large	Very Large	Large (Galaxy)

Bentham Science

Chemical and/or Structural Descriptors Calculation

Chemical and structural descriptors are the features of the compounds. LiSIs provides a tool to calculate a specific set of chemical descriptors (see "Descriptor Calculator") and a tool for calculating a specific set of structural descriptors (fingerprints) (see "Fingerprint Calculator").

1. Model(s) training and validation:

   During the training process the algorithm used strives to correlate the calculated descriptors for each compound with its biological or chemical property/activity. Training is usually followed by validation; the process by which the robustness and prediction performances of the QSAR model(s) are established. LiSIs performs those two processes in tandem, while at the same time tries to optimize the algorithm that does the prediction for its main tuning parameter. To achieve this LiSIs employs learning algorithms provided by the R environment. LiSIs currently supports four tools to create a QSAR model based on different algorithms:

   a. k-Nearest Neighbours:

   Description: A compound is classified by a majority vote of its k nearest neighbours.

   Tuning variable: Number of neighbours (k).

   b. Support Vector Machines:

   Description: An SVM model is a representation of the training data as points in space, mapped so that the different compound classes are divided by a gap that is as wide as possible. New compounds are projected into that same space and predicted to belong to a class based on which side of the gap they are placed.

   Tuning variable: Soft margin (C).

   c. item Decision Trees:

   Description: Recursive partitioning builds a decision tree that uses several dichotomous dependent variables to try and classify chemical compounds.

   Tuning variable: Complexity (cp).

   d. Random Forests:

   Description: Random forests are an ensemble method that, during training, builds a large number of decision trees that utilize a specified number of random descriptors. The final prediction is the mode of the predictions by the individual trees.

   Tuning variable: Number of variables randomly sampled as candidates at each split (mtry).

Cross-validation is a model validation technique to assess how the results of a predictive model will generalize to an independent data set. In general, cross-validation partitions the sample into training and test sets using the former to build the model and the latter to assess its performance. The procedure is performed multiple times and the final validation results are the average of the repeats. Alternatively, LiSIs offers the option to create bootstraps out of the original data as training sets while using the original data as the test set. The available algorithms provide different cross-validation options, such as:

a. Bootstrapping

b. 0.632+ bootstrapping: An improvement of the classic bootstrapping designed to correct the bias introduced by including data points of the test set into the training set.

c. k-Fold Cross-Validation

d. k-Fold Cross-Validation done multiple times

e. Leave One out Cross-Validation

f. Leave Group out Cross-Validation: This method is repeated splitting of the data into training and test sets (without replacement).

Best model selection can be performed by using one of the available tuning metrics:

a. Accuracy

b. Area Under the Curve

c. Cohen's Kappa

d. Sensitivity

e. Specificity

1. *Model(s) Annotation and Publishing*:

   Once the QSAR model is created and validated the user has the option to make it publicly available to the rest of the LiSIs' users. The model can then be utilized by the "Property Predictor" tool to filter-out compounds predicted to lack or possess specific properties. The user can mix and match several models in a side-chain fashion to substantially reduce the number of compounds that will be tested *in vitro* and to enhance the enrichment ratio of the original data set. Prior to publishing the user is encouraged to annotate the QSAR model with some essential info such as the data source, validation performance, the classifying algorithm and the value of its tuning parameter, etc.

The procedure described above was used to train and validate four QSAR models for Mutagenicity, using DT, kNN, RF and SVM algorithms respectively, from which we later selected the best.

The input dataset used was the AMES Mutagenicity dataset available at [52] that consists of 6512 molecules, out of which 3503 are mutagenic (positive) and 3009 non-mutagenic (negative).

Fig. (**2**) illustrates the workflow that has been used to train the QSAR model. This workflow creates four QSAR models using the all available algorithms. The models use the same train and test datasets, and specific configuration depending on the algorithm used in each case. At the end the workflow provides an aggregated report in order to identify the best QSAR model. When the user decides which of the four models is the best then he/she can annotate it accordingly.

Fig. (**3**) illustrates the workflow that should be used when you want to predict mutagenicity using this Mutagenicity QSAR model. The key point in this workflow is that the steps of "Descriptor Calculator" and "Fingerprint

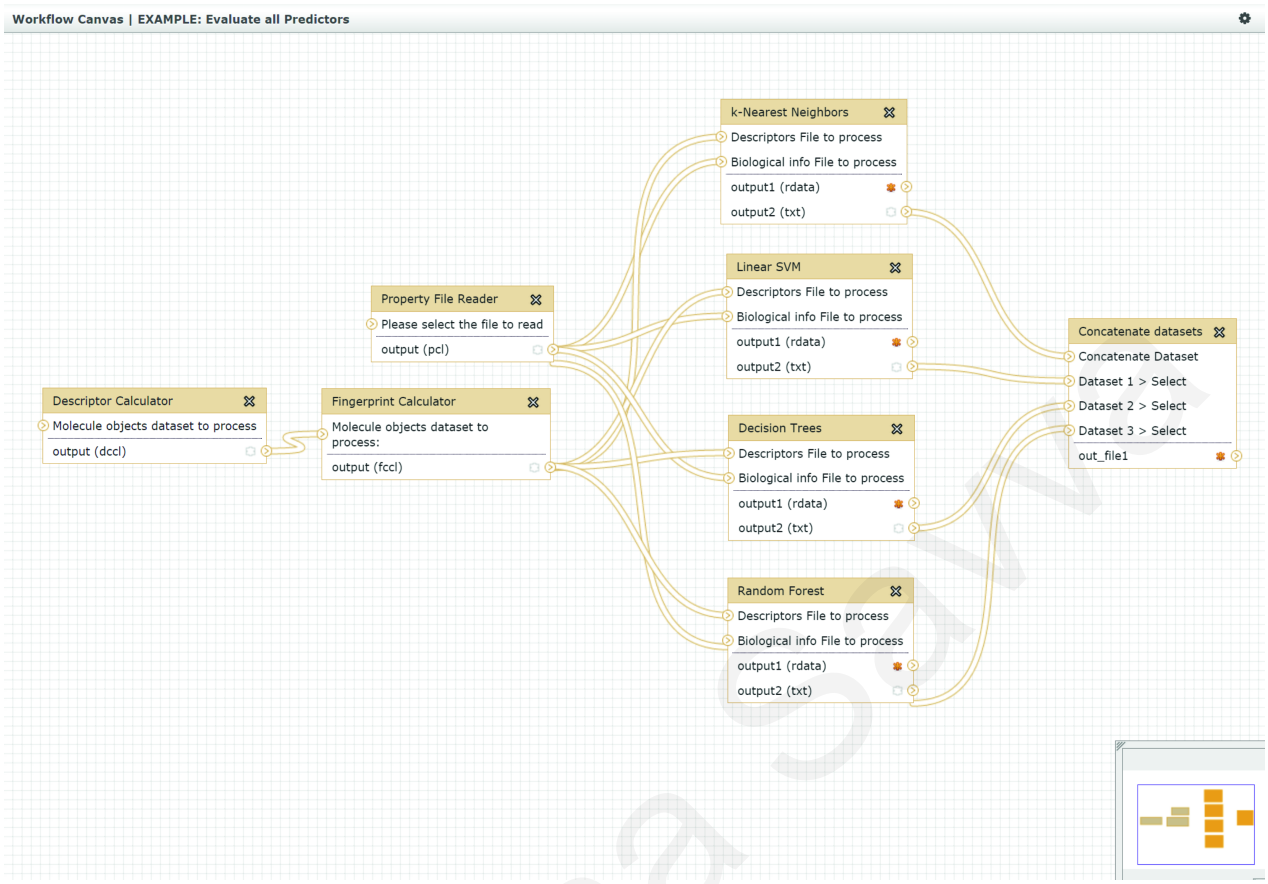

Fig. (2). LiSIs workflow for case study: "QSAR model for Mutagenicity".

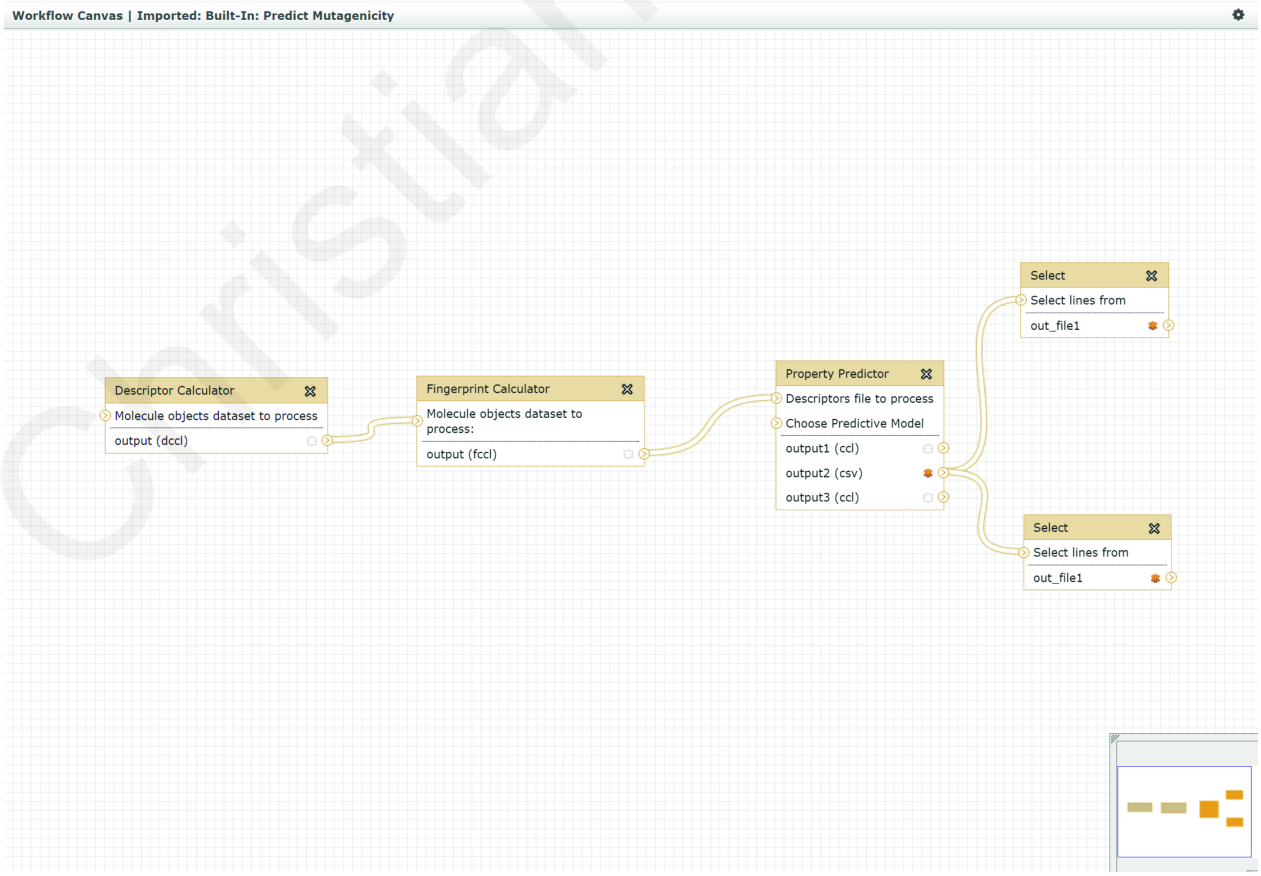

Fig. (3). LiSIs workflow for predicting mutagenicity used in case study: "QSAR model for Mutagenicity".

Calculator" must have the same input parameters as the ones used at the same steps in the QSAR model training workflow illustrated in Fig. (**2**). At the step "Property Predictor" the second input should be the previously trained QSAR model for Mutagenicity.

Table **2** shows the final details of the trained Mutagenicity QSAR model using LiSIs alongside with the details of the reference mutagenicity QSAR model by Hansen *et al.* [53].

CONCLUDING REMARKS

LiSIs provides an easy and simple way to train and validate QSAR models using the server's underlying R installation. Despite the fact that it provides a limited range of classification algorithms, the ones available are the most commonly used.

In this case study we used LiSIs to show its ability and potential in training and using QSAR models. For the purpose of this case study we used the AMES Mutagenicity dataset to train a Mutagenicity QSAR model and compare it with the one proposed by Hansen *et al.* in [53].

As shown in Table **2** the QSAR model for Mutagenicity trained with LiSIs is comparable with the one proposed by Hansen *et al.*, despite the fact that the descriptors used are obtained from different software.

Case Study: Identify Natural Compounds Able to Bind to Estrogen Receptor-α (ER-α) and/or Estrogen Receptor-β (ER-β)

LiSIs has been used for the implementation of a VS experiment in order to identify natural compounds able to bind to Estrogen Receptor-α (ER-α) and/or Estrogen Receptor-β (ER-β).

Fig. (**4**) illustrates the complete workflow used by LiSIs for the showcase described. At the Input Layer, parsing of the input datasets takes place. To start with the initial datasets in SMILES format include 2414 compounds from Indofine chemical company [56], 55 compounds characterized by Medina-Franco *et al.* [57] and 21 known ER ligands retrieved from PubChem [58], shown in Table **3**, which were used as a positive control dataset for the validation of docking tools. Tools were used to read chemical input files and create compound object structures for further processing by the Pre-Processing and Processing Layers. The total number of unique compounds pushed to the next layer were 2413 from Indofine (one was found to contain erroneous molecular information), 54 from Medina-Franco (two were found to be similar) and 21 from PubChem's ER agonists and antagonists (one was found to contain two disconnected fragments), datasets for a total of 2488 compounds.

At the Pre-Processing Layer (see Fig. **4**), a set of physiochemical molecular descriptors were calculated including Molecular Weight, Hydrogen Bond Donors, Hydrogen Bond Acceptors, Topological Polar Surface Area and Octanol - Water Partition coefficient (cLogP).

At the Processing Layer, the following tools were used:

- *GRANATUM Rule of Five (Ro5) filter (see* Fig. **4** *Processing Layer):* Molecular Weight between 160 and 700, Hydrogen Bond Donors less or equal to 5, Hydrogen Bond Acceptors less or equal to 10, Topological Polar Surface Area less than 140, and Octanol - Water Partition coefficient (cLogP) between -0.4 and 5.6.

Table 2. Mutagenicity QSAR models comparison, LiSIs versus reference.

Mutagenicity QSAR Model Properties		
Description	A model for predicting mutagenicity of compounds	
Dataset Details	6512 compounds, 3503 mutagenic, 3009 non-mutagenic	
Classes	Mutagenic (positive), Non-mutagenic (negative)	
	LiSIs	Reference QSAR Model by Hansen *et al.* A
Chemical Descriptors	Molecular Weight, Hydrogen Bond Acceptors, Hydrogen Bond Donors, cLogP, Topological Surface Area, Molecular Complexity, Number of Rings, Molecular Flexibility	Molecular descriptors were selected from blocks 1, 2, 6, 9, 12, 15, 16, 17, 18, and 20 of DragonX version 1.2 B based on a 3D structure generated by Corina version 3.4 C
Fingerprint Descriptors	Morgan (circular) Fingerprints Size: 512 bits Format: Bit-vector Radius: 3 Includes chemical features	Not Used
Algorithms Used	Support Vector Machines	Support Vector Machines
	Decision Tree	Gaussian Process
	Random Forests	Random Forests
	k-Nearest Neighbours	k-Nearest Neighbours
Algorithm with best performance	Random Forest	Support Vector Machines
Performance	Sensitivity = 0.82	Sensitivity = 0.88
	Specificity = 0.80	Specificity = 0.64

A. [53].
B. [54].
C. [55].

Criptiana Vol

Table 3. Known ER ligands used as positive controls for the validation of the *in silico* results.

A/A	Estrogen Ligand	Docking Score ER-α	Docking Score ER-β
1	Raloxifene	-11.70	-8.72
2	Lilly-117018	-11.53	-3.80
3	3-HydroxyTamoxifen	-11.02	N/A
4	Nafoxidine	-10.88	N/A
5	ICI-182780	-10.73	N/A
6	Pyrolidine	-10.04	N/A
7	Clomiphene A	-10.01	N/A
8	Nitrofinene Citrate	-9.87	N/A
9	ICI-164384	-9.82	-9.13
10	Moxestrol	-9.38	-9.77
11	Naringenine	-8.55	-7.80
12	Triphenylethylene	-8.50	N/A
13	Afema	-8.15	-7.78
14	Danazol	-6.99	N/A
15	Ethamoxytriphetol	-6.67	N/A
16	4-HydroxyTamoxifen	-6.60	N/A
17	Dioxin	-6.22	N/A
18	Estralutin	-5.86	-3.80
19	Cyclopentanone	-4.88	N/A
20	Miproxifene Phosphate	-4.48	N/A
21	EM-800	N/A	N/A

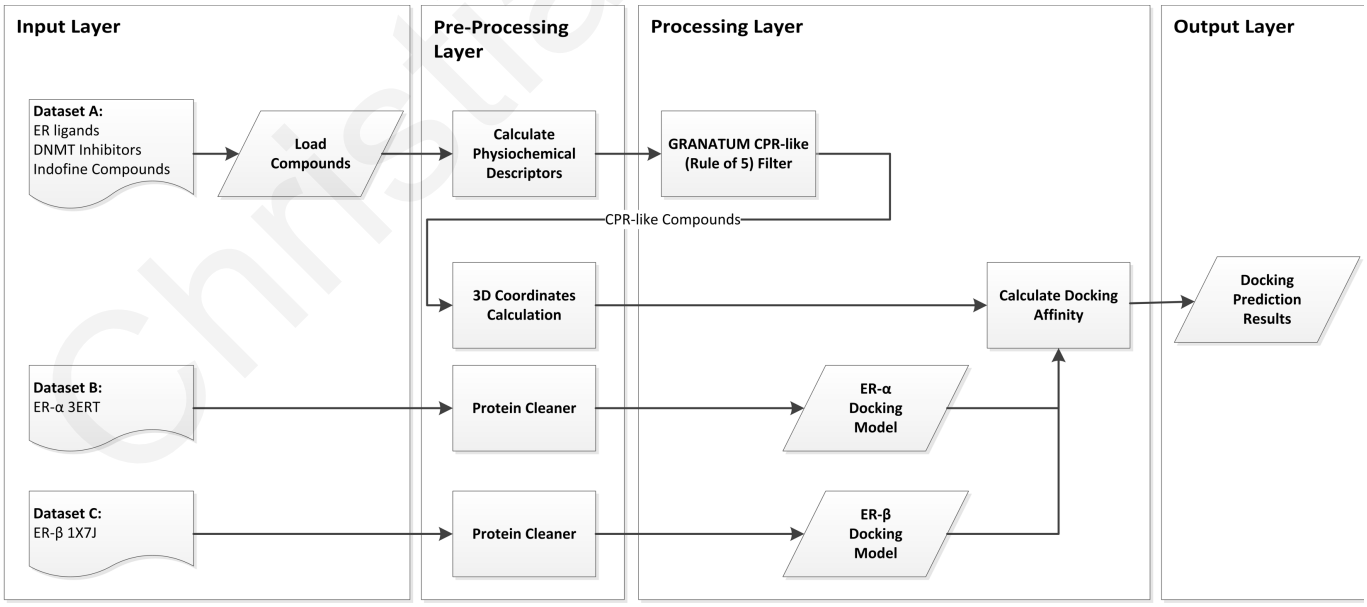

Fig. (4). LiSIs workflow for case study: "Identify natural compounds able to bind to Estrogen Receptor-α (ER-α) and/or Estrogen Receptor-β (ER-β)".

Christiana Savva

This filter was defined by CPR experts participating to the GRANATUM project [8].

The filtering resulted in 1834 compounds with CPR-like features and 654 compounds without CPR-like features. The compounds with CPR-like features were pushed for docking experiments.

- *Docking experiment against ER-α and ER-β (see* Fig. **4** *Processing Layer):*

  LiSIs uses AutoDock Vina [36, 37] and has been setup to provide us with the maximum docking affinity score. The current key aim of the GRANATUM project was to identify ER-α antagonists and ER-β agonists. Docking experiments on the filtered combined dataset have been performed by employing receptors ER-α 3ERT [PDB:3ERT] and ER-β 1X7J [PDB:1X7J]. The appropriate Docking Models were created using protein structures obtained from the PDB database [59] and related LiSIs tools for automated Protein Cleaning (see Fig. **4** Pre-Processing Layer) and Docking Model Preparation.

Fig. (**5A**) is a graphical representation of the docking affinity score predicted by LiSIs docking experiment tool for ER-α, and Fig. (**5B**) is a graphical representation of the docking affinity score predicted by LiSIs docking experiment tool for ER-β. The predicted binding affinity scores of the known ER inhibitors (see Table **3**), depicted with red colour in Fig. (**5**), indicate the validity of the docking models prepared and the ability of these models to assign a lower score to inhibitors and reproduce ground truth. The cyan dots represent DNMT inhibitors characterized in [57]. The lower (most negative) the value of the docking score is, the higher the binding affinity. Consequently, the models are applicable in a VS context, i.e. for the prioritization of unknown compounds based on their predicted binding affinity to estrogen receptors.

Finally a selection of molecules highly ranked was hand-picked; a small sample of those is shown in Table **4**. These molecules have undergone *in vitro* investigation to provide feedback for the calibration of the tools used by LiSIs platform and also to select a small set for further research.

As shown in Table **4**, three novel flavones, 3',4'-dihydroxy-a-naphthoflavone (Compound 2), 3,5,7,3',4'-pentahydroxyflavanone (Compound 5), and 4'-hydroxy-a-naphthoflavone (Compound 6) were among those with high binding scores for ER-α and ER-β as indicated from the *in silico* docking score. Flavones, a class of flavonoids, have previously been demonstrated to possess estrogenic activity in a number of hormonally responsive systems. Their estrogenic and antiestrogenic activities appear to correlate directly with their capacity to displace Estradiol from ER [60]. Our *in vitro* results showed that Compound 2 had the highest affinity for both receptors while Compound 5 also displayed similar affinity for both ER-α and ER-β. However Compound 6 was found to bind only weakly to ER according to the binding affinity assay. Furthermore, results from the *in silico* experiments showed that three previously not investigated coumarins, 3(2'-chlorophenyl)-7-hydroxy-4-phenylcoumarin (Compound 3), 3(3'-chlorophenyl)-7-hydroxy-4- phenylcoumarin (Compound 4) and 4-benzyl-7-hydroxy-3-phenylcoumarin (Compound 7) can potentially bind ER-α and ER-β based in their docking scores. Coumarins are natural or synthetic benzopyranic derivatives that form a family of active compounds with a wide range of pharmacological properties, including estrogen-like effects [61]. *In vitro* results showed that Compound 3 has greater affinity for ER-α while Compound 4 can bind with high affinity to both receptors. However, Compound 7 was not able to bind to either receptor as determined by the ER binding affinity assay.

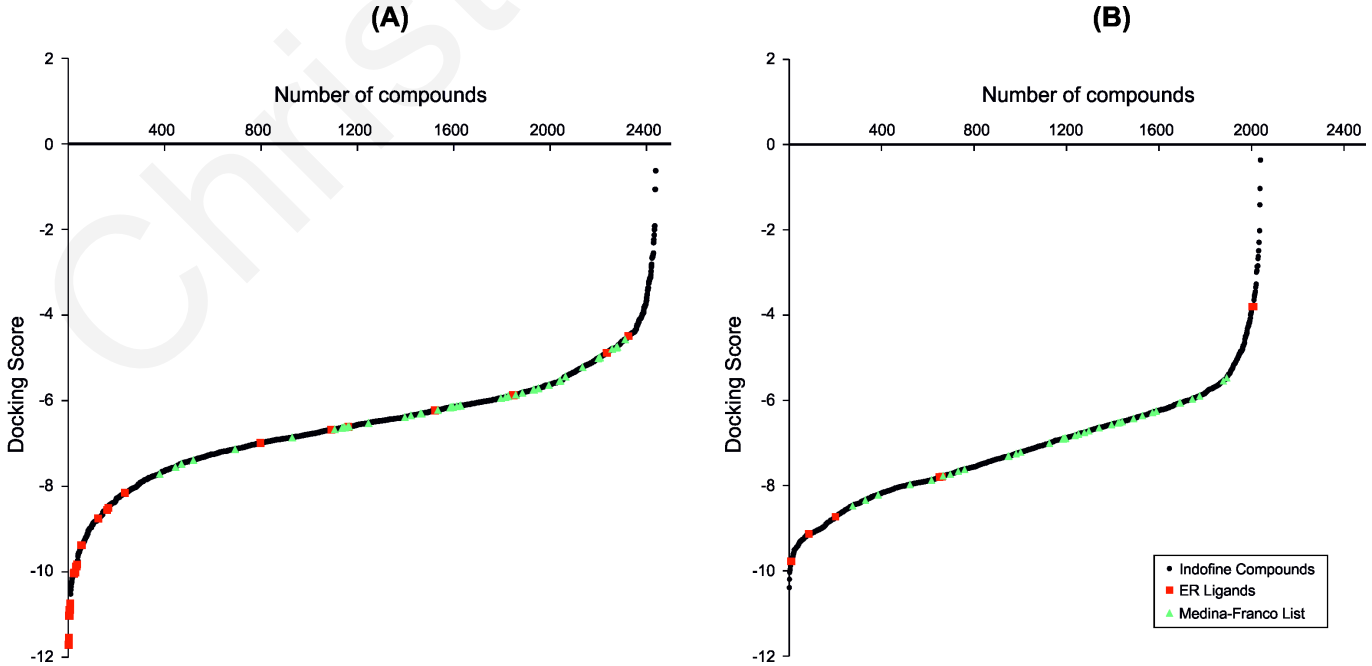

Fig. (5). Compounds were tested against ER-α (A) and ER-β (B) using *in silico* docking tools.

Table 4. Selection of highly ranked compounds from the final virtual screening results.

A/A	Chemical Structure	Molecular Weight (g/mol)	Concentration (μM)	ER-α LDB		ER-β LDB	
				Binding Affinity	Docking Score	Binding Affinity	Docking Score
1	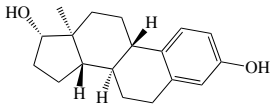 17-β Estradiol	272.38	10	1	-9.4	1	-10
2	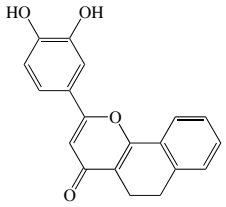 3',4'-dihydroxy-a-naphthoflavone	304.29	1 10	0.11 0.22	-7.59	0.05 0.34	-10.39
3	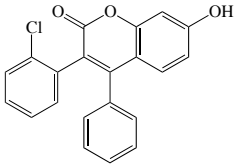 3(2'-chlorophenyl)-7-hydroxy-4-phenylcoumarin	348.78	1 10	0.21 2.71	-9.73	N/A 0.34	-10.03
4	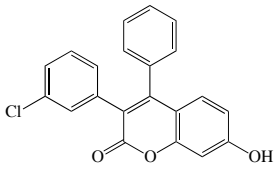 3(3'-chlorophenyl)-7-hydroxy-4-phenylcoumarin	348.78	1 10	0.24 2.23	-10.34	0.13 2.75	-9.67
5	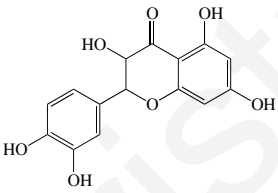 3,5,7,3',4'-pentahydroxyflavanone	304.26	1 10	N/A 0.27	-8.81	0.06 0.18	-9.61
6	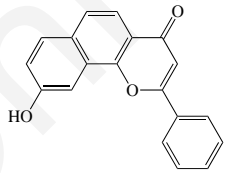 4'-hydroxy-a-naphthoflavone	228.29	1 10	N/A N/A	-8.18	0.05 N/A	-9.88
7	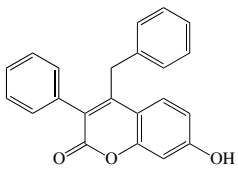 4-benzyl-7-hydroxy-3-phenylcoumarin	328.37	1 10	N/A N/A	-10.13	N/A N/A	-9.13

Christiana Savva

CONCLUDING REMARKS

In recent years, many high-throughput methods have been established in the effort to identify novel Estrogen Receptor binders with anticancer activity. However, *in vitro* assays often produce disappointing results due to the small percentage of novel active Estrogenic compounds discovered. To identify novel compounds that act as effective ER-α co-activator binding inhibitors (CBIs), Gunther *et al.* applied a time-resolved fluorescence resonance energy transfer (TR-FRET) assay developed in a 384 well format [62]. This assay measures the binding of a Cy5-labelled SRC-1 nuclear receptor interaction domain to the ligand binding domain (LBD) of labelled ER-α leading to TR-FRET signal generation. Compounds that interfere with the TR-FRET signal are identified as potential CBIs or conventional ligand antagonists. Based on this method, only 1.6% of the total compounds screened were identified as active as reported in (Pubchem ID 629).

In the present study, we used a VS workflow implemented using the LiSIs platform to screen the Indofine database of 2413 compounds. Based on their drug-like criteria and docking results we selected 18 potential ER ligands. These were further investigated *in vitro* with the ER binding assay described by Gurer-Orhan *et al.* [63] with minor modifications. In this manner it was found that five agents displayed strong affinity for ER-α, three showed selectivity for ER-β and seven were able to bind to both receptors with similar affinity. In total 15 out of 18 compounds (83.3%) were experimentally confirmed active. Therefore, the use of LiSIs system may allow researchers to execute complex biomedical studies and *in silico* experiments on largely available and high quality data repositories in order to facilitate the selection and prioritize the investigation of novel chemopreventive compounds *in vitro*.

Compounds with high binding affinity to the ERs based on the *in silico* results, display structural characteristics that are similar to Estradiol-17β (E2). All contain a phenolic ring which is indispensable for binding to the estrogen receptor [64]. The phenolic ring of Compounds 2 - 7 contains at least one hydroxyl group which mimics the 3'-OH of E2. Furthermore, all compounds have low molecular weight comparable to that of E2 (Molecular Weight equal to 272). All agents are highly hydrophobic which is required for binding in the ER binding pocket [65]. The differences observed in the binding affinities of compounds may be attributed to differences in structural characteristics. The lower ER binding affinity of Compound 5 (when compared to Compound 2) may be attributed to the hydrophilic hydroxyl group at C-11 of Compound 5 which, due to steric hindrance, lowers its binding affinity for both receptors [65].

The LiSIs platform aims to fill the current void in the application of advanced chemoinformatics and computational chemistry technology in determining efficacy and predicting possible mechanism of action or identifying a possible receptor for a chemopreventive agent in life sciences research. Its successful deployment may have a substantial impact on enabling biomedical researchers to utilize state of the art computational techniques to search for promising chemical compounds that may lead to the discovery of novel agents with chemopreventive properties. We have shown in this paper that by utilizing the LiSIs platform in conjunction to a widely used docking program we identified compounds that can bind to ER-α and/or ER-β with a high degree of success rate. This *in silico* approach is expected to facilitate the process of identification of lead compounds with estrogenic or anti-estrogenic activity and to enhance considerably the discovery process for new therapeutic agents.

CONCLUSION

In recent years, scientific workflow systems have been increasingly used by the chemoinformatics community. Several systems, both commercial and free, have been introduced with custom components catering to the needs of the drug discovery community and numerous applications have been described in the literature. In this paper we introduced LiSIs, a new SWMS platform designed and implemented to provide advanced computational chemistry and information technology tools in an online environment.

LiSIs enables the use of state of the art computational algorithms and techniques to design and implement solutions by reusing open source community tools such as RDKit [29], R [44] and AutoDock Vina [36, 37] to complement in-house code. Consequently, LiSIs users have access to numerous methods that enable operations such as molecular descriptor calculation, predictive model generation and use and docking experiments, among others. It is worth noting that, due to its online nature, LiSIs models, workflows and results can be easily shared with other platform users.

Future work will focus on current system limitations. Indicatively, LiSIs has limited visualization capabilities which need to be augmented and, certain components, such as the protein cleaner tool, need to be further expanded. System scalability is also a concern since the current infrastructure, which is limited to a single server with 12 processing cores and 16 GB of memory, will inevitably become a bottleneck as the system becomes more popular. We also intend to incorporate tools implementing multi-objective ranking and optimization methods to LiSIs in order to enable the consideration of multiple pharmaceutically important properties to VS and other library design experiments [66].

The potential of LiSIs has been highlighted through two case studies designed to illustrate the preparation of tools for the identification of promising chemical structures. The first case study involved the development of a QSAR model on a literature dataset while the second implemented a docking-based virtual screening experiment. Our results show that VS workflows utilizing docking, predictive models and other *in silico* tools as implemented in the LiSIs platform can identify compounds in line with expert expectations. For example, our experiments provided a chemical structure set that, once experimentally tested, was found to bind to ER-α and/or ER-βwith a high degree of success as computationally predicted.

Moreover, the ability to readily share knowledge between researchers in the form of models, workflows, experimental data and results was found to be an additional beneficial feature that facilitated collaboration between distributed partners and, thus, the generation of new knowledge.

In conclusion, we have shown that LiSIs facilitates the discovery of cancer chemopreventive agents. We anticipate that the deployment of LiSIs, as currently implemented and available for use, can enable drug discovery researchers to more easily use state of the art computational techniques in their search for promising chemical compounds.

LiSIs is available as a web based application, accessed directly at [7] and also under the GRANATUM platform at [8].

ABBREVIATIONS

CBIs = Co-activator Binding Inhibitors;

CPR = Chemoprevention research;

DDP = Drug Discovery Process;

DT = Decision Trees;

ER = Estrogen Receptor;

k-NN = k-Nearest Neighbours;

KNIME = Konstanz Information Miner;

LBD = Ligand Binding Domain;

LiSIs = Life Sciences Informatics;

PDB = Protein Data Bank;

PMML = Predictive Model Markup Language;

QSAR = Quantitative Structure Activity Relationship;

RF = Random Forests;

SDF = Structure Data File;

SMARTS = SMiles ARbitrary Target Specification;

SMILES = Simplified Molecular Input Line Entry Specification;

SW = Scientific Workflows;

SWMS = Scientific Workflow Management Systems;

TR-FRET = Time-Resolved Fluorescence Resonance Energy Transfer;

VS = Virtual Screening.

CONFLICT OF INTEREST

The authors confirm that this article content has no conflict of interest.

ACKNOWLEDGEMENTS

This work has been partially supported through the EU-FP7 GRANATUM project, "A Social Collaborative Working Space Semantically Interlinking Biomedical Researchers, Knowledge and data for the design and execution of *In Silico* Models and Experiments in Cancer Chemoprevention", contract number ICT-2009.5.3.

C. C. Kannas, I. Kalvari, I. Kirmitzoglou, Z. Antoniou and K. G. Achilleos developed LiSIs' tools and helped on the configuration of LiSIs server. G. Lambrinidis and E. Mikros provided valuable guidance in regards to ligand-protein docking. C. M. Neophytou, C. G. Savva, C. A. Pitta and D. Scherf were responsible for the 2nd case study and also provided valuable feedback during the development phase. V. J. Promponas, C. A. Nicolaou, C. Gerhauser, A. I. Constantinou and C. S. Pattichis are the scientific experts. All authors contributed in the writing of this article. All authors read and approved the final manuscript.

REFERENCES

[1] Reddy, A. S.; Pati, S. P.; Kumar, P. P.; Pradeep, H. N.; Sastry, G. N. Virtual Screening in Drug Discovery -- a Computational Perspective. *Curr. Protein Pept. Sci.,* **2007**, *8*, 329-351.

[2] Kar, S.; Roy, K. How Far Can Virtual Screening Take Us in Drug Discovery? *Expert Opin. Drug Discov.,* **2013**, *8*, 245-261.

[3] *Virtual Screening: Principles, Challenges, and Practical Guidelines*; Sotriffer, C., Ed.; Methods and Principles in Medicinal Chemistry; 2011.

[4] Barker, A.; Hemert, J. V. Scientific Workflow: A Survey and Research Directions. In: *Proceedings of the 7th international conference on Parallel processing and applied mathematics*; PPAM'07; Springer-Verlag: Berlin, Heidelberg, **2008**; pp. 746-753.

[5] Yang, X.; Bruin, R. P.; Dove, M. T. Developing an end-to-end scientific workflow: a case study using a comprehensive workflow platform in e-science. *Comput. Sci. Eng.,* **2010**, *12*, 52-61.

[6] Kannas, C. C.; Achilleos, K. G.; Antoniou, Z.; Nicolaou, C. A.; Pattichis, C. S.; Kalvari, I.; Kirmitzoglou, I.; Promponas, V. J. A Workflow System for Virtual Screening in Cancer Chemoprevention. In: *2012 IEEE 12th International Conference on Bioinformatics Bioengineering (BIBE)*; **2012**; pp. 439-446.

[7] LiSIs Life Sciences Informatics platform http://lisis.cs.ucy.ac.cy/ (accessed Oct 24, **2014**).

[8] GRANATUM - Project Vision http://granatum.org/ (accessed Oct 24, **2014**).

[9] Sporn, M. B. Approaches to prevention of epithelial cancer during the preneoplastic period. *Cancer Res.,* **1976**, *36*, 2699-2702.

[10] Xu, J.; Hagler, A. Chemoinformatics and Drug Discovery. *Molecules,* **2002**, *7*, 566-600.

[11] Hull, D.; Wolstencroft, K.; Stevens, R.; Goble, C. A.; Pocock, M. R.; Li, P.; Oinn, T. Taverna: A Tool for Building and Running Workflows of Services. *Nucleic Acids Res.,* **2006**, *34*, W729-W732.

[12] Oinn, T.; Greenwood, M.; Addis, M.; Alpdemir, M. N.; Ferris, J.; Glover, K.; Goble, C.; Goderis, A.; Hull, D.; Marvin, D.; Li, P.; Lord, P.; Pocock, M. R.; Senger, M.; Stevens, R.; Wipat, A.; Wroe, C. Taverna: Lessons in Creating a Workflow Environment for the Life Sciences. *Concurr. Comput. - Pract. Exp.,* **2006**, *18*, 1067-1100.

[13] Missier, P.; Soiland-Reyes, S.; Owen, S.; Tan, W.; Nenadic, A.; Dunlop, I.; Williams, A.; Oinn, T.; Goble, C. Taverna, Reloaded. In: *Scientific and Statistical Database Management*; Gertz, M.; Ludäscher, B., Eds.; Lecture Notes in Computer Science; Springer Berlin Heidelberg: Berlin, Heidelberg, **2010**; Vol. 6187, pp. 471-481.

[14] Berthold, M.; Cebron, N.; Dill, F.; Gabriel, T.; Kötter, T.; Meinl, T.; Ohl, P.; Sieb, C.; Thiel, K.; Wiswedel, B. KNIME: The Konstanz Information Miner. In: *Data Analysis, Machine Learning and Applications*; Springer Berlin Heidelberg, 2008; pp. 319-326.

[15] Berthold, M. R.; Cebron, N.; Dill, F.; Gabriel, T. R.; Kötter, T.; Meinl, T.; Ohl, P.; Thiel, K.; Wiswedel, B. KNIME - the Konstanz Information Miner: Version 2.0 and beyond. *ACM SIGKDD Explor. Newsl.* **2009**, *11*, 26-31.

[16] Pipeline Pilot is Accelrys' scientific informatics platform http://accelrys.com/products/pipeline-pilot/ (accessed Jul 16, **2012**).

[17] IDBS - InforSense Suite - analytical data management http://www.idbs.com/products-and-services/inforsense-suite/ (accessed Jul 16, **2012**).

[18] Jorgensen, W. L. The many roles of computation in drug discovery. *Science,* **2004**, *303*, 1813-1818.

[19] Dudek, A. Z.; Arodz, T.; Gálvez, J. Computational methods in developing quantitative structure-activity relationships (qsar): a review. *Comb. Chem. High Throughput Screen.,* **2006**, *9*, 213-228.

[20] Krovat, E. M.; Steindl, T.; Langer, T. Recent Advances in Docking and Scoring. *Curr. Comput. - Aided Drug Des.,* **2005**, *1*, 93-102.

[21] Bissantz, C.; Folkers, G.; Rognan, D. Protein-based virtual screening of chemical databases. 1. evaluation of different

docking/scoring combinations. *J. Med. Chem.,* **2000**, *43*, 4759-4767.

[22] Waszkowycz, B.; Perkins, T. D. J.; Sykes, R. A.; Li, J. Large-scale virtual screening for discovering leads in the postgenomic era. *IBM Syst. J.,* **2001**, *40*, 360-376.

[23] Lyne, P. Structure-based virtual screening: an overview. *Drug Discov. Today,* **2002**, *7*, 1047-1055.

[24] Nicolaou, C. A.; Brown, N. Multi-objective optimization methods in drug design. *Drug Discov. Today Technol.,* **2013**, *10*, e427–e435.

[25] Lipinski, C. A.; Lombardo, F.; Dominy, B. W.; Feeney, P. J. Experimental and computational approaches to estimate solubility and permeability in drug discovery and development settings. *Adv. Drug Deliv. Rev.*, **1997**, *46*, 3-26.

[26] Anderson, A. C.; Wright, D. L. The Design and docking of virtual compound libraries to structures of drug targets. *Curr. Comput. - Aided Drug Des.,* **2005**, *1*, 103-127.

[27] Achilleos, K. G.; Kannas, C. C.; Nicolaou, C. A.; Pattichis, C. S.; Promponas, V. J. Open Source Workflow Systems in Life Sciences Informatics. In: *2012 IEEE 12th International Conference on Bioinformatics Bioengineering (BIBE)*; **2012**; pp. 552-558.

[28] Simmhan, Y. L.; Plale, B.; Gannon, D. A survey of data provenance in e-science. *ACM SIGMOD Rec.,* **2005**, *34*, 31-36.

[29] Landrum, G. RDKit: Open-source cheminformatics http://www.rdkit.org/ (accessed Jul 17, **2012**).

[30] Barone, R.; Chanon, M. A New and Simple Approach to Chemical Complexity. Application to the Synthesis of Natural Products. *J. Chem. Inf. Comput. Sci.,* **2001**, *41*, 269-272.

[31] Morgan, H. L. The Generation of a unique machine description for chemical structures-a technique developed at chemical abstracts service. *J. Chem. Inf. Model.,* **1965**, *5*, 107-113.

[32] Durant, J. L.; Leland, B. A.; Henry, D. R.; Nourse, J. G. Reoptimization of mdl keys for use in drug discovery. *J. Chem. Inf. Comput. Sci.* **2002**, *42*, 1273-1280.

[33] Carhart, R. E.; Smith, D. H.; Venkataraghavan, R. Atom pairs as molecular features in structure-activity studies: definition and applications. *J. Chem. Inf. Comput. Sci.,* **1985**, *25*, 64-73.

[34] Nilakantan, R.; Bauman, N.; Dixon, J. S.; Venkataraghavan, R. Topological torsion: a new molecular descriptor for sar applications. comparison with other descriptors. *J. Chem. Inf. Comput. Sci.,* **1987**, *27*, 82-85.

[35] Daylight Fingerprints http://www.daylight.com/dayhtml/doc/theory/theory.finger.html.

[36] Trott, O.; Olson, A. J. AutoDock vina: improving the speed and accuracy of docking with a new scoring function, efficient optimization, and multithreading. *J. Comput. Chem.,* **2010**, *31*, 455-461.

[37] AutoDock Vina - molecular docking and virtual screening program http://vina.scripps.edu/ (accessed Jul 17, **2012**).

[38] Kuhn, M. Building predictive models in r using the caret package. *J. Stat. Softw.,* **2008**, *28*, 1-26.

[39] O'Boyle, N. M.; Banck, M.; James, C. A.; Morley, C.; Vandermeersch, T.; Hutchison, G. R. Open Babel: An open chemical toolbox. *J. Cheminformatics,* **2011**, *3*, 33.

[40] Giardine, B.; Riemer, C.; Hardison, R. C.; Burhans, R.; Elnitski, L.; Shah, P.; Zhang, Y.; Blankenberg, D.; Albert, I.; Taylor, J.; Miller, W.; Kent, W. J.; Nekrutenko, A. Galaxy: a platform for interactive large-scale genome analysis. *Genome Res.,* **2005**, *15*, 1451-1455.

[41] Goecks, J.; Nekrutenko, A.; Taylor, J.; Galaxy Team, T. Galaxy: A comprehensive approach for supporting accessible, reproducible, and transparent computational research in the life sciences. *Genome Biol.,* **2010**, *11*, R86.

[42] Blankenberg, D.; Kuster, G. V.; Coraor, N.; Ananda, G.; Lazarus, R.; Mangan, M.; Nekrutenko, A.; Taylor, J. Galaxy: a web-based genome analysis tool for experimentalists. In: *Current Protocols in Molecular Biology*; John Wiley & Sons, Inc., **2010**.

[43] O'Boyle, N. M.; Morley, C.; Hutchison, G. R. Pybel: A Python Wrapper for the OpenBabel Cheminformatics Toolkit. *Chem. Cent. J.* **2008**, *2*, 5.

[44] R. Development Core Team. *R: A Language and Environment for Statistical Computing*; R Foundation for Statistical Computing: Vienna, Austria, **2008**.

[45] De Roure, D.; Goble, C.; Bhagat, J.; Cruickshank, D.; Goderis, A.; Michaelides, D.; Newman, D. myExperiment: Defining the Social Virtual Research Environment. In *eScience, 2008. eScience '08. IEEE Fourth International Conference on*; IEEE, **2008**.

[46] KNIME | Konstanz Information Miner http://www.knime.org/ (accessed Jul 16, **2012**).

[47] Data Mining Group (DMG) http://www.dmg.org/.

[48] Abouelhoda, M.; Alaa, S.; Ghanem, M. Meta-Workflows: Pattern-Based Interoperability between Galaxy and Taverna. In *Proceedings of the 1st International Workshop on Workflow Approaches to New Data-centric Science*; Wands '10; ACM: New York, NY, USA, **2010**; pp. 2:1–2:8.

[49] myExperiment http://www.myexperiment.org/.

[50] Afgan, E.; Baker, D.; Coraor, N.; Chapman, B.; Nekrutenko, A.; Taylor, J. Galaxy Cloudman: Delivering Cloud Compute Clusters. *BMC Bioinformatics,* **2010**, *11*, S4.

[51] Taverna - open source and domain independent Workflow Management System http://www.taverna.org.uk/ (accessed Jul 16, **2012**).

[52] Benchmark Data Set for In Silico Prediction of Ames Mutagenicity http://doc.ml.tu-berlin.de/toxbenchmark/.

[53] Hansen, K.; Mika, S.; Schroeter, T.; Sutter, A.; ter Laak, A.; Steger-Hartmann, T.; Heinrich, N.; Müller, K.-R. Benchmark Data Set for in Silico Prediction of Ames Mutagenicity. *J. Chem. Inf. Model.,* **2009**, *49*, 2077-2081.

[54] Todeschini, R.; Consonni, V. *Handbook of Molecular Descriptors*; Wiley-VCH: Weinheim; New York, **2008**.

[55] Sadowski, J.; Gasteiger, J.; Klebe, G. Comparison of Automatic Three-Dimensional Model Builders Using 639 X-Ray Structures. *J. Chem. Inf. Comput. Sci.,* **1994**, *34*, 1000-1008.

[56] INDOFINE Chemical Company, Inc., NJ Chemicals, Los Angeles County Chemicals, NJ Molecules, Los Angeles County Molecules, Xian, Shijiazhuang, Shanghai, China, Call 908-359-6778 http://www.indofinechemical.com/ (accessed Jul 18, **2012**).

[57] Medina-Franco, J. L.; López-Vallejo, F.; Kuck, D.; Lyko, F. Natural Products as DNA Methyltransferase Inhibitors: A Computer-Aided Discovery Approach. *Mol. Divers.* **2010**, *15*, 293–304.

[58] The PubChem Project http://pubchem.ncbi.nlm.nih.gov/ (accessed Jul 18, **2012**).

[59] RCSB Protein Data Bank http://www.rcsb.org/pdb/home/home.do.

[60] Collins-Burow, B. M.; Burow, M. E.; Duong, B. N.; McLachlan, J. A. Estrogenic and Antiestrogenic Activities of FlavonoidPhytochemicals Through Estrogen ReceptorBinding-Dependent and -Independent Mechanisms. *Nutr. Cancer,* **2000**, *38*, 229-244.

[61] Jacquot, Y.; Laïos, I.; Cleeren, A.; Nonclercq, D.; Bermont, L.; Refouvelet, B.; Boubekeur, K.; Xicluna, A.; Leclercq, G.; Laurent, G. Synthesis, Structure, and Estrogenic Activity of 4-Amino-3-(2-Methylbenzyl)coumarins on Human Breast Carcinoma Cells. *Bioorg. Med. Chem.,* **2007**, *15*, 2269-2282.

[62] Gunther, J. R.; Du, Y.; Rhoden, E.; Lewis, I.; Revennaugh, B.; Moore, T. W.; Kim, S. H.; Dingledine, R.; Fu, H.; Katzenellenbogen, J. A. A Set of Time-Resolved Fluorescence Resonance Energy Transfer Assays for the Discovery of Inhibitors of Estrogen Receptor-Coactivator Binding. *J. Biomol. Screen.,* **2009**, *14*, 181-193.

[63] Gurer-Orhan, H.; Kool, J.; Vermeulen, N. P. E.; Meerman, J. H. N. A novel microplate reader-based high-throughput assay for estrogen receptor binding. *Int. J. Environ. Anal. Chem.,* **2005**, *85*, 149-161.

[64] Anstead, G. M.; Carlson, K. E.; Katzenellenbogen, J. A. The Estradiol Pharmacophore: Ligand structure-estrogen receptor binding affinity relationships and a model for the receptor binding site. *Steroids,* **1997**, *62*, 268-303.

[65] Agatonovic-Kustrin, S.; Turner, J. V. Molecular Structural Characteristics of Estrogen Receptor Modulators as Determinants of Estrogen Receptor Selectivity. *Mini-Rev. Med. Chem.,* **2008**, *8*, 943-951.

[66] Nicolaou, C. A.; Kannas, C. C. Molecular library design using multi-objective optimization methods. In: *Chemical Library Design*; Zhou, J. Z., Ed.; Methods in Molecular Biology; Humana Press, **2011**; pp. 53-69.

Received: July 23, 2014 **Revised: October 26, 2014** **Accepted: December 10, 2014**